Role of the ER stress and glutathione biosynthesis pathway in the anticancer activity of organometallic ruthenium-based compounds for the treatment of gastric cancer

Gilles Riegel

UNIVERSITÉ DE STRASBOURG

ÉCOLE DOCTORALE DES SCIENCES DE LA VIE ET DE LA SANTÉ

[Inserm U1113-IRFAC:

Interface de Recherche Fondamentale et Appliquée en Cancérologie]

THÈSE présentée par :

[Gilles RIEGEL]

soutenue le : 23 septembre 2019

pour obtenir le grade de : **Docteur de l'université de Strasbourg**

Discipline/ Spécialité : Sciences de la vie de la santé / Aspects Moléculaires et Cellulaires de la Biologie

Rôle de la voie du stress du réticulum et de la biosynthèse du glutathion dans l'activité anticancéreuse de composés organométalliques à base de ruthénium dans le cancer gastrique.

THÈSE dirigée par :

M MELLITZER Georg	CR, Université de Strasbourg
M GAIDDON Christian	DR, Université de Strasbourg

RAPPORTEURS :

Mme CARRIER Alice	DR, Université de Marseille
M MANIE Serge	DR, Université de Lyon

AUTRES MEMBRES DU JURY :

Mme DANTZER Françoise	DR, Université de Strasbourg
M GASSER Gilles	DR, Université de Paris

Remerciements

Je voudrais faire part de ma reconnaissance aux gens qui ont rendu possible la réalisation de ce travail.

Je tiens tout d'abord à remercier Georg et Christian d'avoir rendu ce travail possible et de m'avoir permis de me surpasser maintes et maintes fois. De plus, j'aimerai également les remercier pour toutes discussions qui ont fait aboutir mon travail à ce qu'il est devenu. Particulièrement, merci à Georg pour la rédaction et la correction de ce manuscrit pour lequel il fallait avoir beaucoup de patience. J'aimerai également remercier Jean-Noël pour sa disponibilité, son soutien et ses conseils avisés qui m'ont également permis de réussir ce travail.

Merci à Anaïs (CuiCui) d'avoir fait ce parcours avec moi. Même dans les moments difficiles on a toujours su se remonter. Merci pour ce soutien, cette aide et cette assistance tout au long de la thèse. Une belle amitié s'est formée même si tu es une wonderpfetzi

Un grand merci, tout particulier, à Christophe et Alexandre. Merci pour ces brainstorming et questions-réponses quand un problème particulier se présentait. Merci à Christophe pour ces blagues et ce bon humour tout comme ces nombreux cafés. Merci à toi Alex, avec qui nous formions un couple de travail, pour ton aide et ta compassion.

Je voudrais remercier Anaïs (Lutin), Christelle (Floflo), Susanna, Agathe, et Aïna pour leur bonne humeur et m'avoir supporté durant tout ce temps même quand je devenais insupportable. Merci à lutin d'avoir été mon souffre-douleur tout ce temps.

Merci aux étudiants du haut Marine (alias Marilde), Emilie, Benedict, d'avoir toujours été à l'écoute et de ne jamais s'être plaintes.

Je tiens également à remercier Justine (panpan) et Amandine (Dory), pour votre sympathie et de votre disponibilité ainsi que votre soutien.

Par la suite je voudrais remercier Marion, Cédric, et Andrès pour votre aide pour les manips et votre générosité dans les moments difficiles.

Merci à Isabelle G, pour la motivation que tu transmets ainsi que pour ton aide/ réponse à mes différentes questions, mais également pour ta franchise quant aux choses à améliorer.

Véronique et Elisabeth, je tiens à vous remercier pour votre aide dans les manips et également pour votre support concernant tout ce qui est en rapport avec la culture cell.

Merci à la team du CPS, Cyril, Sonia, Christine, Alain, pour leur aide et également à Laurent pour m'avoir mis en avant quand une opportunité de post-doc s'est présentée.

Particulièrement, merci à toi Léonor, Marraine la bonne fée, grâce à qui tout fonctionne comme sur des roulettes. Merci pour ton aide lors de mes nombreuses commandes et manips en collaborations ainsi que de ta bienveillance.

Merci à ma famille pour leur soutien dans les moments difficiles et leur compréhension face à mon caractère parfois difficile. C'est aussi grâce à vous que j'y suis parvenu et merci d'avoir cru en moi.

Je tiens tout particulièrement à remercier ma femme qui a su m'épauler, et m'aider à réussir ce travail. Merci d'avoir été là, d'avoir cru en moi, et de m'avoir supporté tous les jours et surtout durant les moments difficiles. Merci pour ton empathie, ta compréhension et ton encouragement.

Table des matières

Abbreviations

3-MST: 3-mercaptopyruvate sulfurtransferase

5FU: 5-Fluorouracil

ABC: ATP-binding cassette

AIF: Apoptosis inducing factor

ALT: Alanine transaminase

AML: Acute myeloid leukemia

AOAA: Aminooxyacetate

ARE: Antioxidant response element

ASK1: Apoptosis signal regulated kinase 1

AST: Aspartate transaminase

ATF4/6: Activating transcription factor

ATG5: Autophagy related 5

ATP: Adenosine triphosphate

BAX: Bcl-2-associated X

BCL-2: B-cell lymphoma 2

BER: Base excision repair

BIM: BCL-2-interacting mediator of cell death

BIP: Binding immunoglobulin protein

BPTES: Bis-2-(5-phenylacetamido-1,3,4-thiadiazol-2-yl)ethyl sulphide

BSO: Buthionine sulfoximine

bZIP: Basic leucine zipper

CA^{2+}: Calcium

CBS: Cystathionine beta synthase

C/EBP: CCAAT-enhancer-binding proteins

CHAC1: ChaC glutathione specific gamma-glutamylcyclotransferase 1

CHOP: CCAAT/-enhancer-binding protein homologous protein

CO (Carbon monoxide)

CRT-1 Copper transporter 1

CSC: cancer stem cells

CTH: Cystathionine gamma-lyase

DNA: Deoxyribonucleic acid

DP: Dipeptidase

DR5: Death receptor 5

EA: Ethacrynic acid

EIF2α: Eukaryotic initiation factor 2 alpha

EIF2AK3: Eukaryotic translation initiation factor 2 alpha kinase 3

ER: Endoplasmic reticulum

ERAD: Endoplasmic reticulum associated degradation

ERO1α: Endoplasmic Reticulum Oxidoreductase 1 Alpha

FAP: Familial adenomatous polyposis

FXR: Farnesoid X receptor

GADD34: growth arrest and DNA damage-inducible protein 34

GADD153: growth arrest- and DNA-damage inducible gene 153

GCL: Glutamate-cysteine ligase

GCN2: General control nonderepressible 2

GGT: gamma-glutamyltranspeptidase

GLs: Glutaminase

GLUT1: Glucose transporter 1

GPABR1: G protein-coupled receptors for secondary bile acids

GPCR: G protein-coupled receptors

GPx: Glutathione peroxidase

GRP78: Glucose-regulated protein of 78 kDa

GRs: Glutathione reductases

GS: Glutathione synthase

GSH: Glutathione

GSSG: Glutathione disulphide

GST: Glutathione S-transferases

H_2O_2: Hydrogen peroxide

H_2S: Hydrogen sulphide

HCC: Hepatocellular carcinoma

Hcy: Homocysteine

HDGC: Hereditary diffuse gastric cancer

HIF1: Hypoxia-inducible factor 1

HNA: 2-hydroxy-1-naphthaldehyde

HO: Heme oxygenase

HRI: Heme-regulated inhibitor kinase

HSP: Heat shock protein

IRE1α: Inositol-requiring enzyme 1 α

IRES: Internal ribosome entry site

ISR: Integrated stress response

JNK: c-Jun N terminal kinase

Keap1: Kelch-like ECH-associated protein 1

LDH: Lactate dehydrogenase

MAPK: Mitogen-activated protein kinase

MEFs: Mouse embryonic fibroblasts

MetRs: Methionyl-tRNA synthase

MMR: Mismatch repair

MRP: Multidrug resistance protein

MSD: Membrane spanning domains

mTor: Mammalian target of rapamycin

NAC: N-acetylcysteine

NADH: Nicotinamide adenine dinucleotide

NBCs: Nucleotides binding domains

NER: Nucleotide excision repair

NFE2L2: Nuclear factor erythroid-derived 2-like 2

NF-kB: Nuclear factor kappa-light-chain-enhancer of activated B cells

NO: Nitric oxide

NRF2: Nuclear factor E2-related factor 2

NSCLC: Non-small-cell lung carcinoma

Os: Osmium

PARP: Poly ADP ribose polymerase

PDI: Protein disulphide isomerase

PDT: Photodynamic therapy

PERK: Protein kinase RNA-like endoplasmic reticulum kinase

PI3KCA: Phosphatidylinositol-4,5-bisphosphate 3-kinase catalytic subunit alpha

PLP: Pyridoxal phosphate

PPG: DL-Propargylglycine

PS: Phosphatidylserine

RDC's: ruthenium-derived compounds

RIDD: regulated inositol-requiring enzyme 1-dependent decay

ROS: Reactive oxygen species

RNA: Ribonucleic acid

RNS: Reactive nitrogen species

Ru: Ruthenium

S1P/S2P: Site specific protease

SAH: S-adenosylhomocysteine

SAM: S-adenosylmethionine

SP1: Ppecific protein 1

STAT5B: Signal transducer and activator of transcription 5B

tBuOOH: Tert-Butyl hydroperoxide
TNF: Tumour necrosis factor

TDAG51: T-cell death associated gene 51

TRADD: TNFR1-associated death domain protein

TRAF2: TNF-receptor-associated factor 2

TRIB3: Tribbles homologue 3

TXNDC5: Thioredoxin Domain Containing 5

VEGF: Vascular endothelial growth factor

uORF: Upstream Open Reading Frame

UPR: Unfolded protein response

UTR: Untranslated region

XBP1: X-box binding protein 1

xCT: Cystine/glutamate antiporter

Introduction

I) Gastric cancer

I.1) Epidemiology

Gastric cancer is one of the most aggressive cancer and take the third place for cancer mortality worldwide (Globocan 2018). Each year, more than 750 000 death are recorded, and more than one million new cases are reported worldwide as it is known to be the fifth cancer in term of incidence. The predominance of this cancer is located in Asia as well as South America representing more than the half cases (World health organisation). Furthermore, the 5-year survival rate of this cancer is very low, about 20%, which can be explained by an absence of symptoms in early stages, correlating with a late diagnosis. Furthermore, this cancer type is resistances to the current therapies. All these facts show the importance of improving gastric cancer diagnosis and treatment (Karimi et al., 2014).

Gastric cancer is a multifactorial disease including a wide range of environmental and genetic risks factors. Environmental risk factors such as smoking, high salt intake, and low vegetable consumption have been identified. Furthermore, several genetic factors play a role in gastric cancer development including for example hereditary diffuse gastric cancer (HDGC), and familial adenomatous polyposis (FAP). These genetic forms of gastric cancer are very rare (between 1 and 3% of gastric cancers) but correlate with poor prognosis (Karimi et al., 2014). The major part of gastric cancer is represented by adenocarcinomas. However, following Laurén classification, gastric cancer can be divided into four groups: intestinal, diffuse, mixed and unclassified. Additionally, four molecular subgroups have been established for gastric cancer including genomically stable (20%), Epstein-Barr-Virus positive (9%), chromosomal instable (50%) and microsatellite instable (MSI) (22%) (Figure 1).

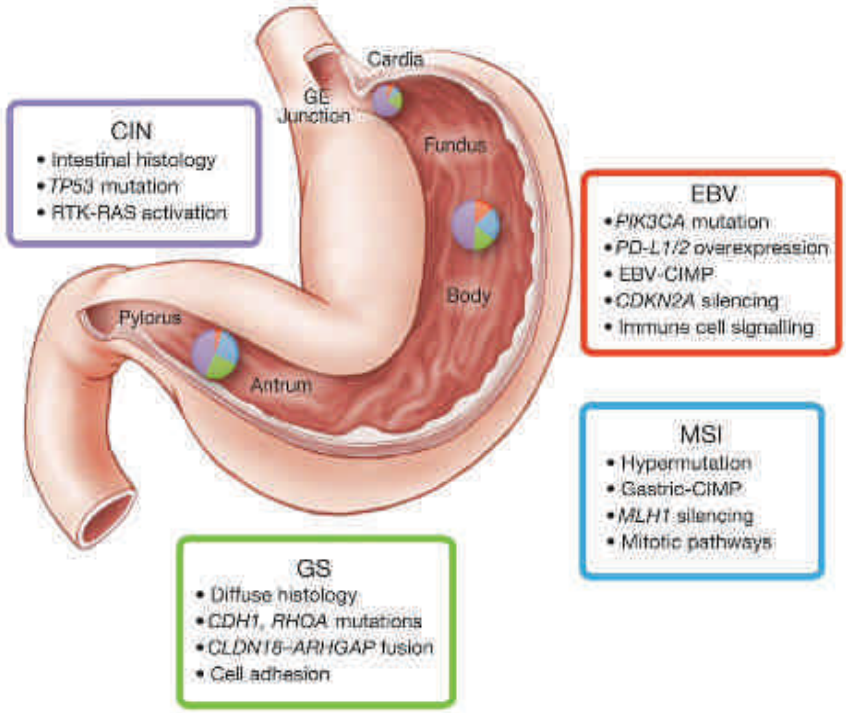

Figure 1. Tissue distribution of the four molecular subtypes of gastric cancer and some of the associated features

TCGA, nature 2014

Nevertheless, this classification is not yet used in clinic due to an absence of correlation between the subtypes and the response to the treatment and requires a further understanding of the specificities of each subtype in order to propose a better patient care. The standard treatment of gastric cancer is a perioperative chemotherapy combined with a surgical resection (Garattini et al., 2017; Röcken, 2017). The chemotherapy used is a platin-based chemotherapy which have shown good cytotoxic activity, however several problems like resistance and side effects limits the use of this type of chemotherapy.

I.2) Gold standard treatment: platinum-based compounds

Historically, the first antiproliferative discovery concerning platinum was made by Rosenberg in 1965 (Rosenberg et al., 1965). They demonstrate that a platinum electrode could inhibit Escherichia coli cell division. To explain this observation, they

hypothesized that this inhibition occurs because of the presence of a platinum salt formation in the culture medium. Encouraged by this result, they tested the effect of several platinum compounds in 1969 on sarcoma and leukaemia cells and could demonstrate the tumor growth inhibition of cisplatin (Rosenberg et al., 1969).Since these days, platinum-based compounds like cisplatin or oxaliplatin (Figure 2) enable a better patient care by displaying a high cytotoxic activity against cancer cells.

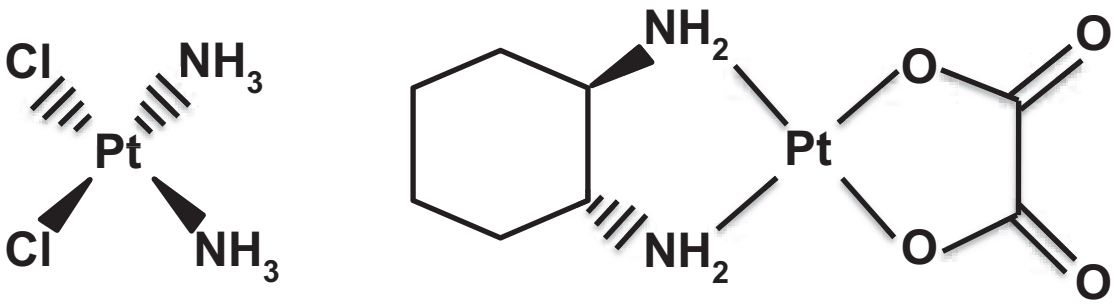

Figure 2: Chemical structures of cisplatin and oxaliplatin

This general cytotoxic activity over several cancer types was explained by their mode of action. Platinum based compounds induce intra- and inter-strand crosslinks in DNA (Figure 3). These crosslinks occur at the azote atoms on guanine in DNA and promote the development of DNA damages. These DNA damages are responsible for the induction of platin mediated cell death (Scheeff et al., 1999). However, as reviewed by Alcindor et al., platinum-based drugs can also interact with non-DNA targets (Figure 3). Indeed, platinum-based compounds are known to interact with DNA, but also RNA, proteins, glutathione, and some transcription factors. All together the damages induced by platinum-based compounds lead in a first time to a cell cycle arrest, followed commonly by the activation of caspase 3 leading to DNA cleavage and cell death (Alcindor and Beauger, 2011). Due to this general mode of action platinum-based compounds exert a general anticancer activity in several tumor types like lung, breast, and gastric cancer (Dasari and Tchounwou, 2014).

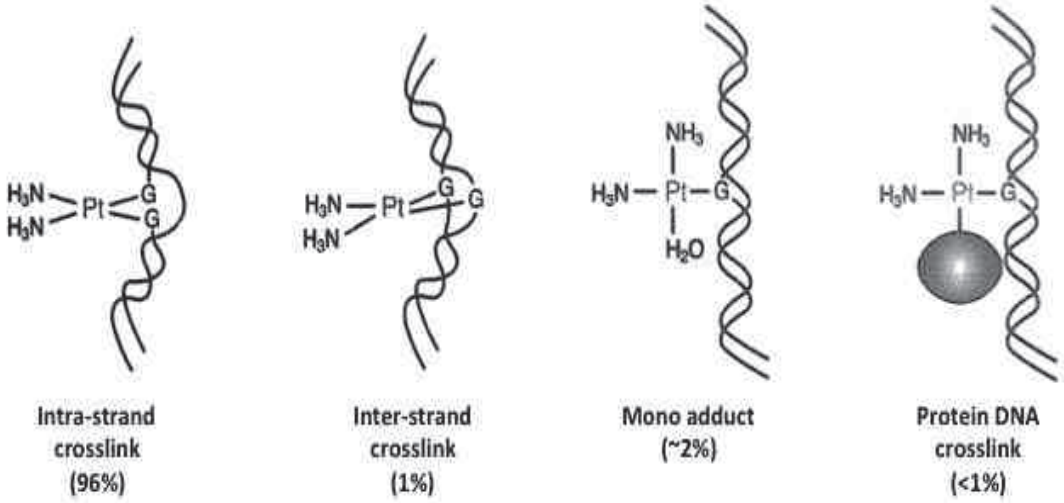

Figure 3: Cisplatin induced cytotoxicity. Schematic representation of cisplatin interaction with DNA and non-DNA targets

Two main apoptotic pathways have been described namely, the intrinsic and extrinsic pathway. Both pathways are interconnected and the actors of one pathway are implicated in the other one. The main actors of this pathway are caspases and several of these proteins have been described and classed into initiator and executioner caspases. Apoptosis lead to the activation of the executioner caspase-3 and result in endonuclease ultimately inducing DNA fragmentation. Apoptotic cells will be then phagocyted by phagocytes after phosphatidylserine (PS) externalisation which play a role in cellular recognition signal (Elmore, 2007). Extrinsic pathway involves transmembrane receptors like tumor necrosis factor (TNF). Activation of such receptors leads to the recruitment of adaptor proteins like TNFR1-associated death domain protein (TRADD) resulting in caspase activation (Figure 4). Intrinsic pathway is mediated by intracellular signals and is characterized as an event initiated in the mitochondria. Intrinsic cell death signals lead to changes in mitochondrial membrane permeability as well as mitochondrial permeability pores. Two main pro-apoptotic proteins are normally sequestrated inside the mitochondria and released after apoptosis induction. The first group is responsible of caspase mediated induction of apoptosis and is composed by proteins like cytochrome c. The second group is composed by proteins like apoptosis inducing factor (AIF) among others resulting in

caspase independent cell death (Figure 4). After apoptosis induction, AIF is released from mitochondria and translocates into the nucleus where it can cleave DNA and therefore induce cell death (Elmore, 2007).

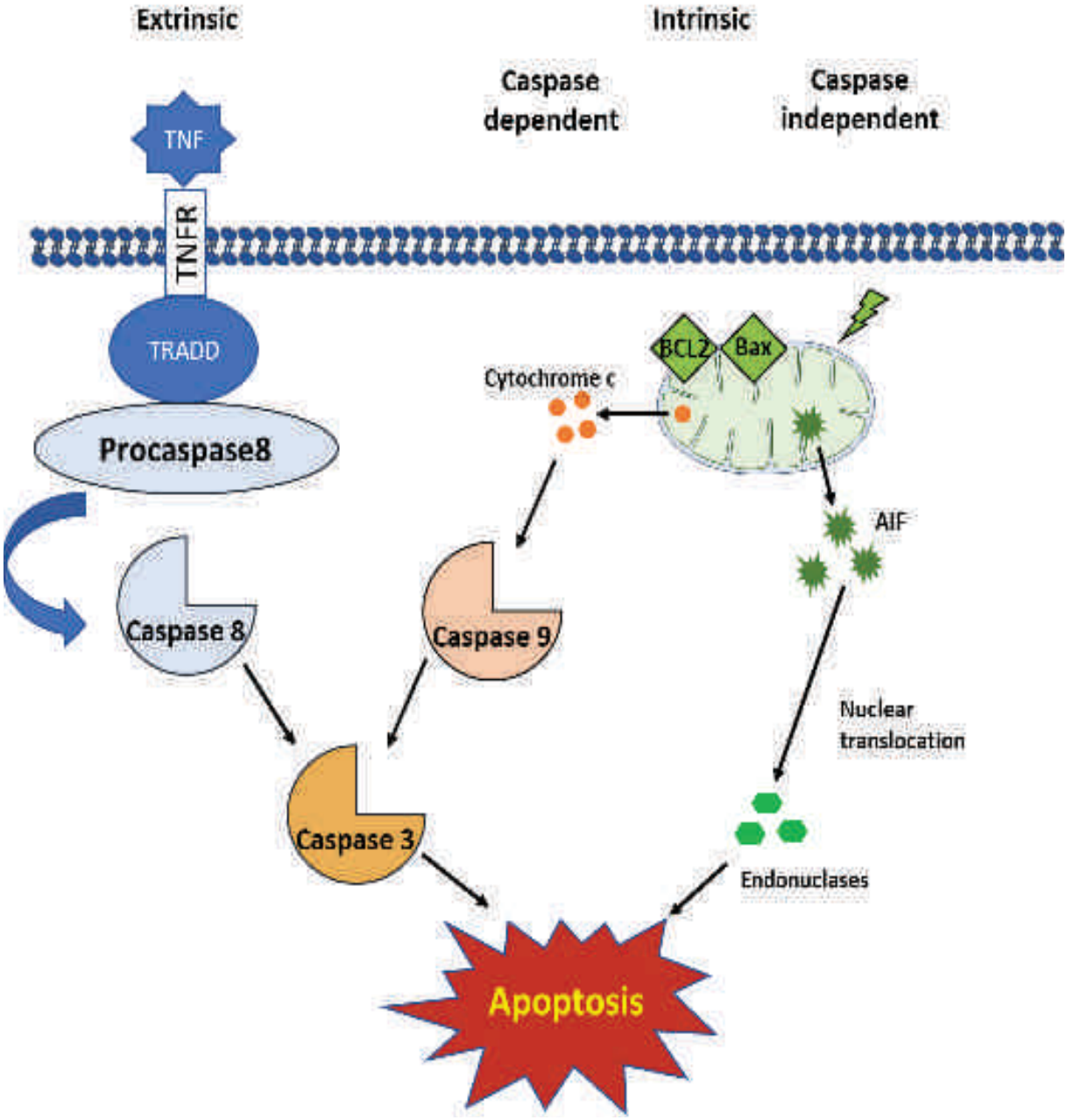

Figure 4: Schematic representation of apoptosis. Extrinsic and intrinsic pathway are represented

Unfortunately, platinum-based compounds also promote the induction of severe side effects in diverse organs like nephro-, oto-, or hepatotoxicity among others. Due to this side effects, platinum-based compounds become too deleterious for the patient

forcing the clinicians to stop the treatment. These side effects can be explained by the lack of cell type specificity of these platinum-based drugs, and also by the fact that platinum-based compounds target mostly fast-growing tissues like gastrointestinal tissue for example. In addition, the dose-limiting toxicity and the organs targeted are different for cis- and oxaliplatin further complexifying the understanding of these side effects (Oun et al., 2018). Cis- and oxaliplatin are known to damage the liver sinusoids which are blood vessels responsible of oxygen delivery for this organ. This type of damages leads to reduced hepatic function forcing the clinicians to limit the treatment duration. Nowadays, any treatment known to lower platinum mediated hepatotoxicity exists and the only way to control this side effect is the monitoring of hepatic damages markers like alanine transaminase (ALT) and aspartate transaminase (AST). These markers are induced in patient with high doses of cisplatin treatment and correlate with what is seen in mice models (Işeri et al., 2007; Sharma et al., 2014)

Furthermore, platinum-based compounds are prone to resistance mechanisms developed by cancer cells. These resistance mechanisms can be from different types, going from DNA repair mechanisms to drug efflux, and leading to an inefficient patient care.

I.3) Resistance

Cisplatin resistance is commonly described to involve several pathways and actors and therefore is known as multifactorial resistance. The resistance occurs at different levels called pre-target, on-target, post-target and off-target stages and include mechanisms like DNA repair, limiting the entry or inducing the efflux, or inhibition of pro-apoptotic cascades (Galluzzi et al., 2012).

I.3.1) DNA associated responses

Cancer cells can develop resistances through over- or underexpressing proteins involved in cell survival also called post-target resistances. More precisely,

downregulation of pro-apoptotic factors and induction of pro-survival ones is commonly described in platinum resistant cells. Indeed, platinum-based compounds are known to induce cell death through a TP53 dependent manner in response to DNA damages. Interestingly, inactivation of TP53 is commonly seen and is responsible of a strong decrease of platinum-based compounds activity leading to resistances. Moreover, B-cell lymphoma 2 (BCL-2) family members, regulating mitochondrial membrane permeability play a central role in the intrinsic apoptotic pathway. Inducing the expression of the po-survival members of this family leads to the maintaining of mitochondrial membrane potential and therefore blocking intrinsic apoptotic pathway normally induced by platinum-based compounds. Cancer cells resistant to cisplatin and oxaliplatin were described to upregulate pro-survival members of BCL-2 family, namely BCL-2 and BCL-X_l, conferring cellular resistance to cisplatin and oxaliplatin (Galluzzi et al., 2012; Martinez-Balibrea et al., 2015).

On target resistance represents mainly the regulation of DNA repair mechanism by cancer cell in order to lower the damages induces by platin compounds or also limit their recognition. ERCC1 expression is seen to be upregulated in cancer cells not mutated for kras. ERCC1 overexpression is known to correlate with cis- and oxaliplatin resistance and inversely correlate with cancer cell sensibility toward platinum-based compounds. ERCC1 like its partner ERCC4 are involved in the nucleotide excision repair (NER) mechanism known to recognize and repair DNA damages induced by cis- and oxaliplatin. NER activation leads to incision at the 5' site of the damage followed by resynthesis of DNA in order to restore genetic integrity. Higher NER activation leads to a better genetic integrity and lowers the responsiveness rate of several human neoplasms toward cis- and oxaliplatin (Galluzzi et al., 2012; Martinez-Balibrea et al., 2015). Similar role is observed for base excision repair (BER) system, due to its ability to remove the corrupt DNA base induced by platinum drugs. In the same way than for NER, higher induction rate of BER lower DNA damages caused by platinum-based drugs and therefore diminishes sensitivity toward treatments and confers resistance (Martinez-Balibrea et al., 2015).

Additionally, MSH2 and MLH1 are commonly mutated or underexpressed in cancer cells (Galluzzi et al., 2012). These genes are involved in mismatch repair (MMR) mechanism known to be decreased in resistant cancer cells. Mismatch repair (MMR) is involved in reduction of DNA damages induced by cisplatin. However, this

repair mechanism is known to fail in response to cisplatin mediated leading to higher DNA damages further leading to the activation of apoptosis. Therefore, decrease in MMR activity is seen in resistant cancer cells in order to avoid recognition by MMR and induction of apoptosis in response to these damages. However, oxaliplatin DNA adducts are not recognized by this mechanism and therefore oxaliplatin resistance is not seen in MMR deficient cells (Martinez-Balibrea et al., 2015).

Off target resistances is mediated by up or downregulation of general cellular pathways. For example, autophagy related 5 (ATG5) and beclin-1 are overexpressed in several cancer cell lines including ovarian, non-small-cell lung carcinoma (NSCLC) and colon cancer cells (Galluzzi et al., 2012; Martinez-Balibrea et al., 2015). This leads to autophagy induction in order to survive to stressful conditions ultimately leading to chemoresistance. However further understanding will be needed to target these pathways possibly resulting in an enhancement of platinum-based compound activity (Galluzzi et al., 2012). Additionally, glutathione (GSH) content and antioxidant defence play an important role for platin-based compounds resistance and will be discussed in a latter section.

I.3.2) Entry limiting and efflux of the chemotherapeutic agent

Limiting the entry or inducing the efflux of the drugs represent the pre-target resistance. Especially for platin-based compounds, cisplatin and oxaliplatin resistance takes place by limiting the entry of the drugs in the cells. Cisplatin, as well as oxaliplatin are thought to enter the cells through passive diffusion (Figure 5). However, several studies demonstrate the role of Copper transporter 1 (CRT-1) in active transport of platinum-based compounds in the cells (Figure 5). Lowering the expression of CRT-1 leads to acquisition of cis- and oxaliplatin resistance (Galluzzi et al., 2012; Martinez-Balibrea et al., 2015). Several studies provided the evidence of differential expression of CRT-1 in patient with stage III/IV ovarian, stage III endometrial as well as NSCLC cancer. Interestingly, patient with high expression were responsive to the platinum-based treatment, with a higher drugs uptake correlating with long disease-free survival and overall survival. Unfortunately, patients with low CRT-1 expression display refractory and resistant tumors (Kilari et al., 2016). Interestingly, the copper mediated

transport for oxaliplatin is less important than in the case of cisplatin showing differences in mechanism involved in resistance acquisition. Furthermore, p-type ATPase called ATP7a and ATP7b have been related to cis- and oxaliplatin sequestration and efflux (Figure 5). Avoiding correct cellular localisation of these drugs thanks to sequestration strongly decrease their cytotoxicity as well as efflux decreases the drug amount inside the cells. However, low level of ATP7b is associated with better outcome for patient treated with oxaliplatin showing the role of this family in platinum-based response. In addition, over expression of these two proteins (ATP7a and b) were shown to mediate cisplatin resistances (Galluzzi et al., 2012; Martinez-Balibrea et al., 2015).

More importantly, the ATP-binding cassette (ABC) transporter superfamily is known to dictate drug efflux and cancer cell responsiveness. The ABCC subfamily which includes the MRP (multidrug resistance protein) is involved in resistance to cisplatin and oxaliplatin. This subfamily is characterised by a hydrophobic polytopic membrane spanning domain (MSD) and hydrophilic cytosolic nucleotides binding domains (NBDs) resulting in drug efflux (Perek and Denoyer, 2002). More precisely, MRP1, MRP2, MRP3 and MRP5 can be correlated to cis- and oxaliplatin resistance due to induce drug export. Deeley and co-workers already demonstrate in 1997, that MRP expression is high in cell lines derived from human resistant tumors. Furthermore, several studies found a strong expression of this protein in lung as well as neuroblastoma cancer (Deeley and Cole, 1997). In addition, the MRP subfamily requires a higher GSH content in order to facilitates this anticancer agent efflux. Interestingly, coordinated overexpression of glutathione related enzyme and MRP expression are seen in different cancer types like colorectal cancer, leading to cellular resistance (Traverso et al., 2013). Other members of the ABC family were described as lowering platin-based toxicity like ABCB1. This pump was seen to be overexpressed in several cancer cell lines and confer resistance to chemotherapeutic agents through inducing the efflux of these drugs (Figure 5) (Galluzzi et al., 2012; Martinez-Balibrea et al., 2015; Perek and Denoyer, 2002).

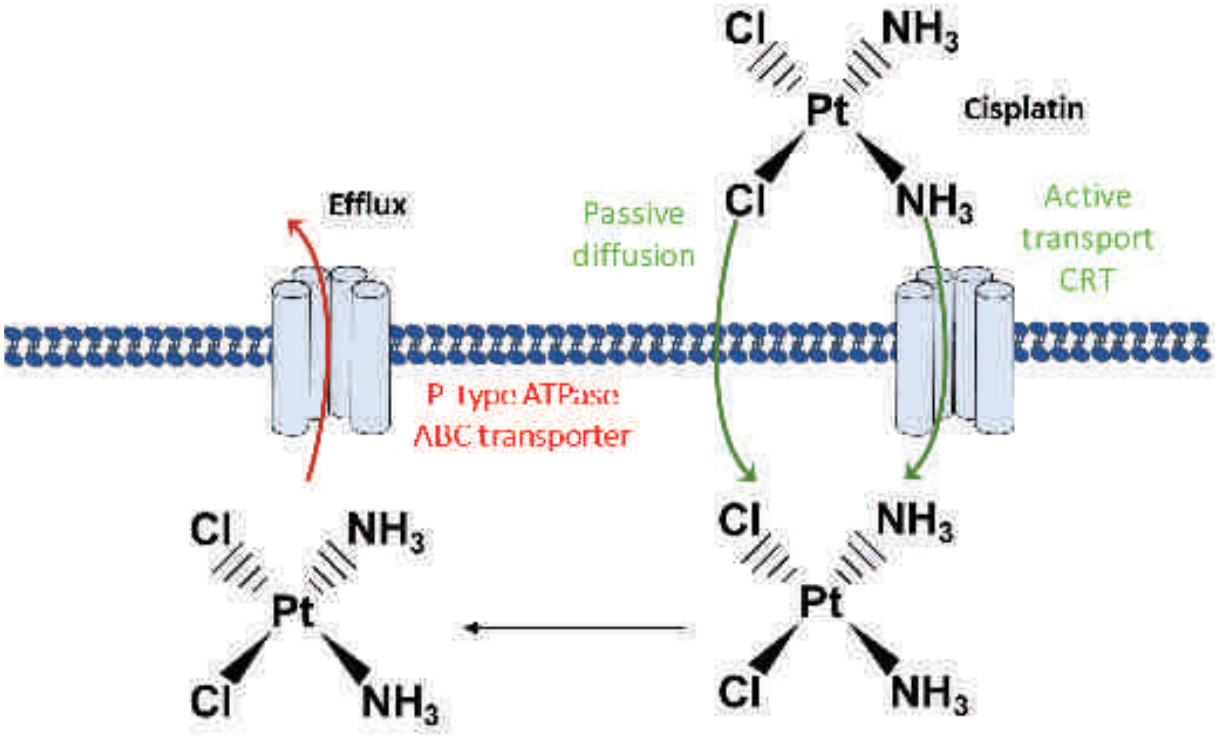

Figure 5: Dynamic regulation of platinum-based compounds entry and efflux

II) Metal-based compounds

II.1) Generalities

In order to overcome platinum limitations, other metal-based compounds have been synthetized and investigated. Several metals were studied for their anticancer activities including for example iron and titanium compounds. However, due to too low cytotoxicity, other metals have taken over and are much more studied. Under these families of compounds, the osmium and ruthenium compounds have obtained a special interest.

II.1.1) Osmium

Osmium-based compounds revealed a special interest as anticancer treatment due to a high stability of the complexes and also an overall good solubility. Several types of osmium families were developed and some compounds shows a good cytotoxic activity.

First osmium-based compounds attending interest in anticancer therapy where the osmium arene complexes. These complexes were described to interact in vitro with DNA by a direct interaction with guanine nucleobase but also cytosine showing different DNA targeting properties than platinum. However, these complexes do not have cytotoxic activities on breast cancer cells despite their DNA binding capacity (Konkankit et al., 2018). However, osmium (II) arene complexes display good cytotoxic activities toward several cancer cells including colon prostate and breast cancer cells (Hanif et al., 2014). Mononuclear or trinuclear osmium complexes bearing either pyridyl-imine or phenoxy-imine ligands present high cytotoxic activity toward osteosarcoma cells. Furthermore, this family of osmium-based drugs inhibits topoisomerase I activity. Some of these compounds are known to induce reactive oxygen species (ROS) production and oxidize NADH (Nicotinamide adenine dinucleotide) in order to promote cell death. However, this mode of action is highly dependent on the cellular GSH content. Changing the ligand of these osmium arene to flavonoid-based ligands display extremely high anticancer activity with IC_{50} in the nanomolar range. The type of ligand attached to the osmium center play a very important role for the activity of these osmium complexes (Konkankit et al., 2018). Depending on the ligand attached to the osmium center, the cytotoxic activity and the pathway regulated by the compounds can be strikingly different. Binding protein kinase inhibitor or glutathione S-transferases (GST) inhibitors on osmium center display cytotoxic activities towards cancer cells. Nevertheless, these complexes display no real advantage compared to the use of the ligands alone (Konkankit et al., 2018). In vivo studies of indolo[3,2-c]quinoline osmium complexes give insight on the tumour growth reduction capacity of these compounds. Interestingly, the activity of the osmium compounds is more important than this of the ruthenium counterparts. Interestingly, in vitro assay showed the ruthenium counterparts seems to be more effective suggesting different behaviour of these compounds in vitro and in vivo (Konkankit et al., 2018).

Other family of osmium complexes known to release CO (Carbon monoxide) or NO (Nitric oxide) were investigated and exhibit anticancer activity on xenograft mouse models. Nitridoosmium (VI) complexes were demonstrated to significantly reduce tumor growth without any effect on mice survival and their possible main target was shown to be DNA (Hanif et al., 2014). Osmium nitrosyl and carbonyl complexes can release NO and CO inside the cells, however, due to a strong covalent bound with osmium, the rate of CO and NO released is low. Furthermore, low entry of these compounds in the cells also explain in part the low cytotoxicity of these last ones (Hanif et al., 2014; Konkankit et al., 2018)

Some osmium-based compounds induce cell death through the induction of DNA damages. These osmium-based clusters were described to be cytotoxic on breast cancer cells and can target oestrogen receptor + or – cells depending on their ligand type but also their solubility. Compounds with labile ligands, can undergo hydrolysis further improving cytotoxicity compared to compounds displaying stable ones. These compounds have a cytotoxic activity in the low micromolar range and selectivity towards cancer cells. They induce DNA damages resulting in TP53 expression. Furthermore, they are also able to target microtubule and increase their polymerisation rates leading to morphological abnormalities and cell death (Hanif et al., 2014; Hartinger et al., 2011). In addition, some osmium polypyridyl complexes can inhibit STAT5B (Signal transducer and activator of transcription 5B), a transcription factor favourable for cancer progression as well as HIF1 (Hypoxia-inducible factor 1) showing that different cellular pathways can be regulated by these compounds (Konkankit et al., 2018). Specific interest for Os(iV) nitrido complexes arises from the diversity of cellular pathways that they can target. Depending on the ligand attached to the osmium metal center, compounds of similar structure can induce or not the same pathway. Changing just one part of the ligand results in a switch from DNA targeting mechanisms, to cytoplasmic accumulation followed by ER stress induction (Johnstone et al., 2015). Interestingly, other osmium (IV) complexes can specifically induce toxicity towards cancer stem cells (CSC). Osmium (IV) nitride compounds inhibit the formation of CSC breast mammospheres in a similar way than the well-known CSC targeting compound salinomycin. This demonstrate the utility of osmium-based compound in chemotherapy that could target primary cancer cells but also cancer stem cells (Johnstone et al., 2015).

A novel type of cyclometaled osmium (II) compounds possessing a C-Os bound was synthetized by Boff and co-workers in 2013. These complexes are much more effective on glioblastoma cell lines than the temozolimide, the current drug used for the treatment of this pathology. They wanted to determine if a correlation between structure and cytotoxic activity exists for these compounds. Unfortunately, any correlation could be observed between the structure of these compounds and their cytotoxic activity. Interstingly, they could correlate redox potential of these compounds to their cytotoxic activity. More precisely, the compounds with a redox potential between 0,3V-0,6V was seen to be the ones presenting the lowest cytotoxic activity. Furthermore, lipophilicity of this family of organometallic compounds is a good indicator of cytotoxicity as it was seen that the compounds presenting a high lipophilicity ($LogP_{o/w}$ >2) corresponds to the compounds with the highest cytotoxic effects (Boff et al., 2013; Hanif et al., 2014).

One of the most studied type of osmium-based compounds is the family of osmium analogous of ruthenium-based drugs. These osmium compounds which are analogues of effective and promising ruthenium-based compounds were tested in order to assess if osmium substitution of the ruthenium center in drugs like NAMI-A, KP1019, RAPTA-C would lead to a better cytotoxic activity (Figure 6). Even if these osmium compounds display cytotoxic activities towards human cancer cell lines and are able to limit in vivo tumor growth, for all the compounds the ruthenium counterpart seems to be the most active. Therefore ruthenium-based compounds have obtained a growing interest for the anticancer field (Hanif et al., 2014; Konkankit et al., 2018).

II.1.1) Ruthenium

Several interesting ruthenium drugs have demonstrated promising anticancer properties. NAMI-A is a ruthenium compound displaying no direct cytotoxic effect on primary tumor cells; however, this compound displays strong anti-metastatic effects (Figure 6) (Bergamo et al., 2012; Zeng et al., 2017). This effect was higher than that of cisplatin in lung cancer models but was also stage dependent. NAMI-A was seen to block cell cycle in phase G2-S and more importantly target actin dependent adhesion as well as cytoskeletal remodelling. It also exhibits antiangiogenic characteristics seen

in vascular endothelial growth factor (VEGF) induced neo-angiogenic models. Furthermore, it can change mitochondrial membrane shape suggesting mitochondrial damages (Bergamo et al., 2012). Additionally, NAMI-A can be used synergistically with cisplatin and other anticancer drugs. This characteristic leads to the entry of the first ruthenium-based compound into clinical trial. Nevertheless, the clinical development of this compound was stopped in early stages because the disease still progresses in phase I and due to a partial response in phase I/II (Zeng et al., 2017). Interestingly, another anti-metastatic family of ruthenium compound called RAPTA became a growing interest (Figure 6). One member of this family, RAPTA-T, was seen to be active only in cancerous cells strongly limiting the development of side effects. This result was also seen in In vivo experiments. This compound was seen to present the same mode of action than NAMI-A, more precisely it was seen to bind cytoskeleton and limiting the invasion and metastasis rates. Unfortunately, the antimetastatic effect of this drug was still too weak strongly limiting the development of this drugs. (Bergamo et al., 2012). Other family members were showed similar results like RAPTA-C compound (Figure 6). However, in order to improve the cytotoxic activity of these compounds, nanostructure complexed with the compound are investigated (Lu et al., 2016). RAPTA-C conjugated water-soluble micelle were synthesized and demonstrated a stronger antiproliferative effect than the compound alone, suggesting a better entry of the drugs when conjugated with these micelles. Interestingly, they also demonstrated that the antiproliferative effect was more pronounced on cancer cells than on non-cancerous ~~cells~~ CHO cells showing a possible clinical use of nanostructure enhancing drugs delivery and activity (Lu et al., 2016).

Another ruthenium compound, KP1019, displays antiproliferative characteristics on colorectal cancer cells in vitro and is still active on chemoresistant colorectal carcinoma cells (Figure 6). This cytotoxic activity can be explained by the ability of the compound to induce mitochondrial damages and ROS production. Additionally, it was also seen that KP1019 can induce DNA damages, but in a lower extend than cisplatin suggesting that these damages are not the principal mode of action of this compound (Bergamo et al., 2012). KP1019 entered clinical trial, however, due to too low solubility its clinical use can not be followed. Therefore, a more soluble salt based on KP1019 was synthetized, called KP1339, which is currently in clinical trial (Zeng et al., 2017).

Some ruthenium compounds were described as strong DNA damages inducers. This is the case of RM175 (Figure 6). RM175 was able to induce more pronounced DNA damages than cisplatin due to its ability to target, guanines of DNA like cisplatin, but also to act as an intercalating agent thanks to its arene ligand. The main mode of action of this compound is to induce apoptosis through TP53-P21-Bax pathway. Moreover, in vivo, cisplatin resistant ovarian cancer models display no cross resistance with this compound showing interesting anticancer properties. However, a better understanding about the DNA independent mode of action is required (Bergamo et al., 2012).

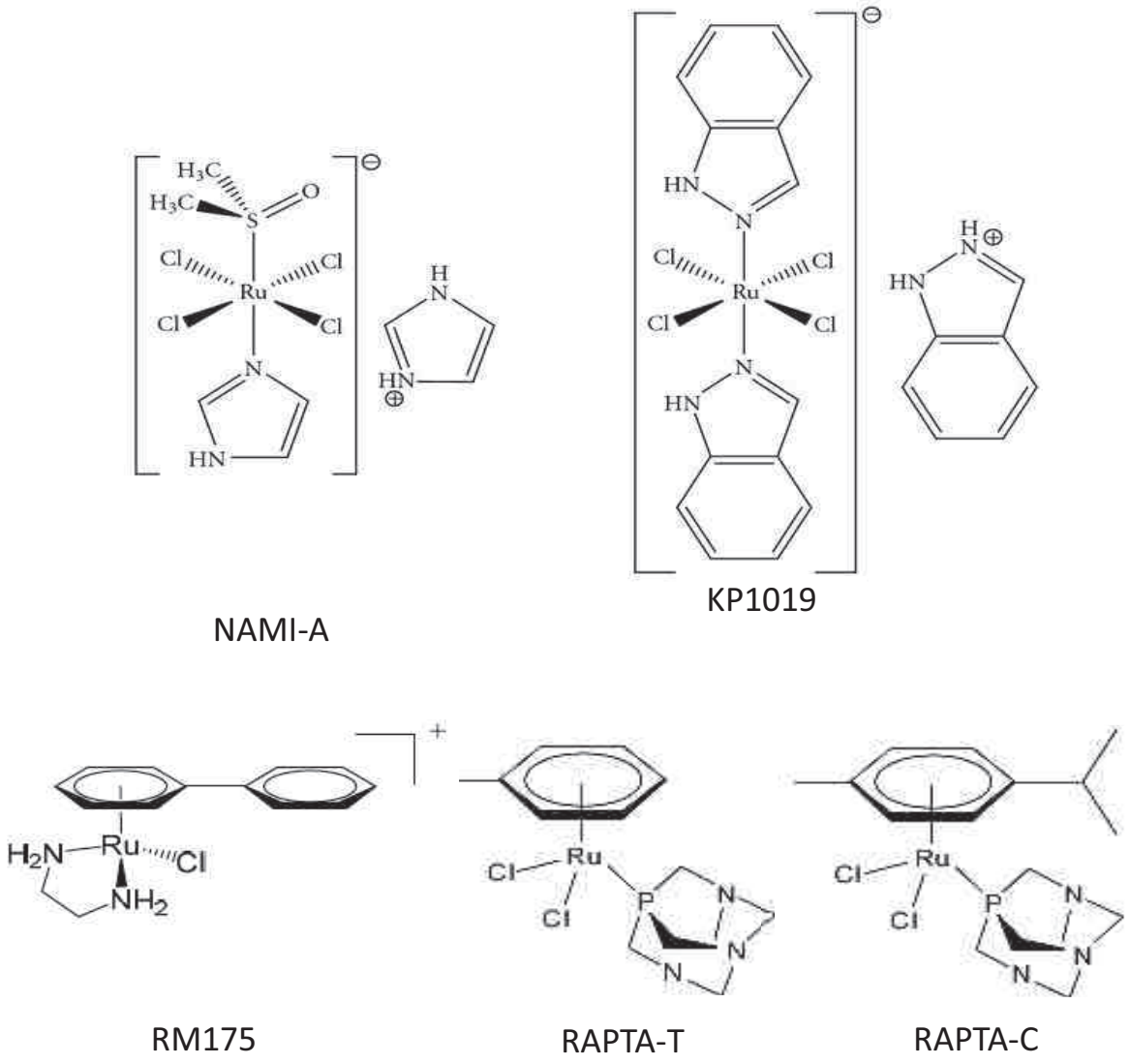

Figure 6: Schematic representation of the structure of ruthneium-based compounds

Kljun et al., 2010 / Ndagi et al., 2017 / Coverdale et al., 2019

Besides the ability of targeting DNA, ruthenium-based compounds were developed in order to trigger mitochondrial stress. Ruthenium nistrosyl-based compounds containing NO and their osmium counterparts have been synthesized. They display cytotoxic activity towards several human cancer cell lines (A549, CH1/PA-1 and SW480). Interestingly the ruthenium complexes presents a much more important cytotoxic activity then their osmium counterparts. This can be explained by the fact that ruthenium-based compounds are reduction prone, suggesting a possible cellular activation of these complexes in comparison to the osmium-based ones which are more stable. (Novak et al., 2016). The presence of NO molecule in these compounds is responsible for the cytotoxic activity which can be explained by the fact that NO can induce several types of mitochondrial damages. The ruthenium compounds induce an important mitochondrial membrane depolarisation about 60% after 48h seen by the use of the JC-1 dye. The same but weaker observation was made for osmium complexes (about 4-20% of mitochondrial depolarisation) (Novak et al., 2016). Correlating with these mitochondrial damages, the apoptosis induction was in similar proportions, meaning approximatively 80% for the ruthenium compounds and up to 5% for osmium ones. Explanation of differences between RU (ruthenium) and OS (osmium) can be made by the fact that osmium stabilises the link to NO whereas ruthenium bound is much weaker and can release NO inside the cells (Novak et al., 2016). Furthermore, other group have also synthetized ruthenium-based compounds able to directly target mitochondria. The Gasser group demonstrates that their Ru compound $[Ru(dppz)_2(CppH)]^{2+}$ (1a,(2'-CppH = 2-pyridyl)pyrimidine-4-carboxylic acid) localises in the mitochondria suggesting an oxidative stress induction. Interestingly, this compounds displays similar a cytotoxic activitiy than cisplatin while displaying no cross resistance (Zeng et al., 2017).

Combining ruthenium with gold in a same compound also represents a novel way to induce cancer cell death due to the capacity of the two metals. Massai and co-workers developed a bimetallic compound displaying lower IC_{50} than the ruthenium containing compound. In order to assess if the presence of gold-phosphane in the bimetallic compound also affects healthy cells, non-cancerous L929 mouse fibroblasts were used. They demonstrate a lower cytotoxic activity in healthy cells than tumoral cells for their bimetallic complexes which was not the case for the gold compound used as a control (Massai et al., 2015). This demonstrates that the addition of ruthenium on

the gold compound (bimetallic) enhances the selectivity toward cancer cells. In addition, the bimetallic compound was not able to interact with DNA however, they were able to inhibit cathepsin activity. Inhibition of cathepsin (implicated in tumor proliferation and metastasis) leads to lower tumor proliferation and aggressiveness. Moreover, thioredoxin reductase, known to regulate cellular redox homeostasis, was also inhibited by the bimetallic compound showing the range of cellular targets for this compound explaining the high cytotoxic activity (Massai et al., 2015).

Another way to target specifically the tumor and avoiding the development of side effects is to target directly the tumor mass by activating the compound by light specifically in the target zone, and therefore, photodynamic therapy (PDT) is considered as a main therapeutical option that needs to be developed. Cloonan and co-workers synthetized several RU(II) polypyridyl complexes and demonstrated that one of their compounds (number 5) displays a high switch in IC_{50} in light irradiation conditions compared to dark conditions. Furthermore, those complexes display an important DNA binding capacity and perinuclear localisation suggesting a DNA dependent mode of action. Interestingly, in isolated nuclei, they achieve to interact with DNA, however, in whole cells nuclear entry failed (Cloonan et al., 2015). Other intracellular localisations were seen including mitochondria, lysosomes and endoplasmic reticulum. In addition, the compound was seen to decrease the mitochondrial membrane potential leading to mitochondrial defects. The photoactivated cell death was demonstrated to be time dependent and dose dependent. Previously, other Ru(II) complexes have also shown to exhibit light sensible activation like Ru(II) phthalocyanine, Ru(II) 2,3-naphthalocyanines. In the case of this photoactivable RU(II) polypyridyl compound, photoactivation results in an increase of DNA damages as well as single stranded DNA content. It is well known that photoactivable compounds often strongly induce oxidative stress. The authors described classical PDT characteristics as the pre-treatment with the antioxidant, n-acetylcysteine (NAC), showed a rescue of cell death. Furthermore, they also described an induction of cell death mediated by caspases as the use of caspase inhibitor limited strongly cell death induction. All together the development of such type of drugs could largely inhibit side effects because the compound will be active only in cancer cells specifically irradiated with light (Cloonan et al., 2015). In a similar manner, Sainuddin and co-workers also developed 3 Ru(II) metal-organic dyads with photoactivable

characteristics. Photoactivation of their compounds enable a dose dependent effect on DNA by producing even a more pronounced interaction with DNA than cisplatin. One of their compounds, compound 3, displays good photoactivable characteristics by inducing a strong DNA cleavage after light activation (Sainuddin et al., 2016). All three compounds present production of singlet oxygen molecules. For compound 3, the longer the complex is pre-exposed to light, the more this compound will then accumulate in the cells, explaining the low dark cytotoxicity due to low cellular accumulation (Sainuddin et al., 2016). Nowadays, the leading compound in PDT is the Ru(II)-polypyridyl compound (TLD-1433) recently entered in phase IB clinical trial as PDT agent for patients with bladder cancer in 2015 (Zeng et al., 2017). Altogether, PDT is a promising strategy for cancer treatment thanks to a cytotoxic activation in the targeted zone after light irradiation

In our lab, in collaboration with co-workers from Singapore, two interesting Ru(II) arene Schiff-base (RAS) compounds were developed. These Ras complexes, RAS-1T and RAS-1H, display cytotoxic activities against a panel of human cancer cell lines with IC_{50} lower than those seen for cisplatin (Figure 7). The cytotoxic activity of these compounds could be attributed to P53 independent effects (Chow et al., 2014). Further work on RAS-1T and RAS-1H also characterized that the cytotoxic activity of these complexes is stronger on gastric cancer cells than this of cisplatin (Figure 7). Both compounds are able to induce ROS production in a dose and time dependent manner, correlating with nuclear factor E2-related factor 2 (NRF2) activation (also known as nuclear factor erythroid-derived 2-like 2 NFE2L2). RAS-1T was also more potent to induce ROS production than RAS-1H, however caspase inhibition did not significantly change cell death induction suggesting a non-apoptotic programmed cell death activation (Chow et al., 2016). Furthermore, on cisplatin-resistant colorectal cells (null-P53 status as well as higher level of BCL-2 and lower levels of Bax (Bcl-2-associated X protein)), these complexes displays the same cytotoxic activity than on cisplatin-sensible ones suggesting an absence of cross resistance of these RAS complexes and cisplatin. The two ruthenium drugs still display in this cell line the lowest IC_{50} and also the lowest resistant factor when compared to cisplatin, oxaliplatin, doxorubicin, 5FU (5-Fluorouracil) or etoposide again demonstrating the possible therapeutic use of those compounds.

Another important aspect of our work in the lab is the development of a family of ruthenium compounds harbouring a direct C-Ru covalent bond (Figure 7). Those compounds like for example RDC34, RDC44 and RDC11 are intensively studied in our lab. Klajner and co-workers demonstrated that RDC34 and 44, Ru(II) complexes harbouring aromatic ligands, display more important cytotoxic activities on cancerous cells than on healthy cell lines. When incubated in vitro with DNA, RNA and protein, those complexes emit a more important luminescence suggesting a possible interaction with those macromolecules. Those two compounds are also self-luminescent which allow to follow their cellular localisation and interactions (Klajner et al., 2014). In cell culture, the import of RDC34 is more important than for RDC44, however, both compounds were found to be localized near the nucleus. The perinuclear localisation correlates with ER-tracker green dye and with the induction of CHOP protein and CHAC1 mRNA levels after treatment with RDC34 and 44 suggesting the induction of the ER stress pathway. Furthermore, RDC34 was described to localise in the nucleus and inducing the expression of the DNA damage marker p-γH2AX suggesting a DNA dependent mode of action. Additionally, RDC34 also localize in the mitochondria and induce the expression of SATB2 and its target gene HSP60 (heat shock protein 60) demonstrating mitochondrial stress induction. This study shows the complexity of pathways regulated by this family of compounds. In order to better understand their mode of action, the import of those complexes inside the cells has also been studied. Confocal microscopic observation demonstrates that the entry of those complexes is dependent on the initial amount of the drug. Another level of complexity was also added when cancerous and healthy cell lines were compared. The import rate of those RDC's (ruthenium-derived compounds) was lower in healthy glial cells than in cancerous glioblastoma cells A172. The kinetics analysis suggested several mechanisms implicated in RDC34 import including facilitated, and active transport. The use of 2-Deoxy-D-glucose, known to block ATP mediated active transport, demonstrates that under low concentrations of RDC34, the active transport is needed to import the drug inside the cell. Under high concentration of drug, the active transport is not needed and passive diffusion is used to import RDC34. Similar results for amino acid transporter SLC7A5 by the use of D-phenylalanine, known to block SLC7A5-dependent import. Pre-treatment with D-phenylalanine also reduces the accumulation of RDC34 inside the cells showing another active import (Klajner et al., 2014). Furthermore, RDC34 induces also the expression of transferrin receptor and

ferritin suggesting an iron mediated active transport. Pre-treatment of cells with deferoxamine (iron chelator) induces about 25% the accumulation of RDC34 in cells suggesting that in iron missing conditions, more RDC34 can be uptaken by iron transporter. Another member of the RDC family, RDC11, displays promising anticancer activities and is the lead compound of this family (Figure 7). This compound was able to inhibit proliferation and tumor growth of many solid tumors causing at the same time any side effects like damages to liver, kidney, and nervous system (Bergamo et al., 2012; Meng et al., 2009). This compound was seen to weakly interact with DNA and therefore inducing DNA damages. However, the DNA damages induced by RDC11 are very weak suggesting the induction of DNA independent pathways. The most important pathway induced by RDC11 further leading to cell death was characterized as ER stress activation (Bergamo et al., 2012; Meng et al., 2009).

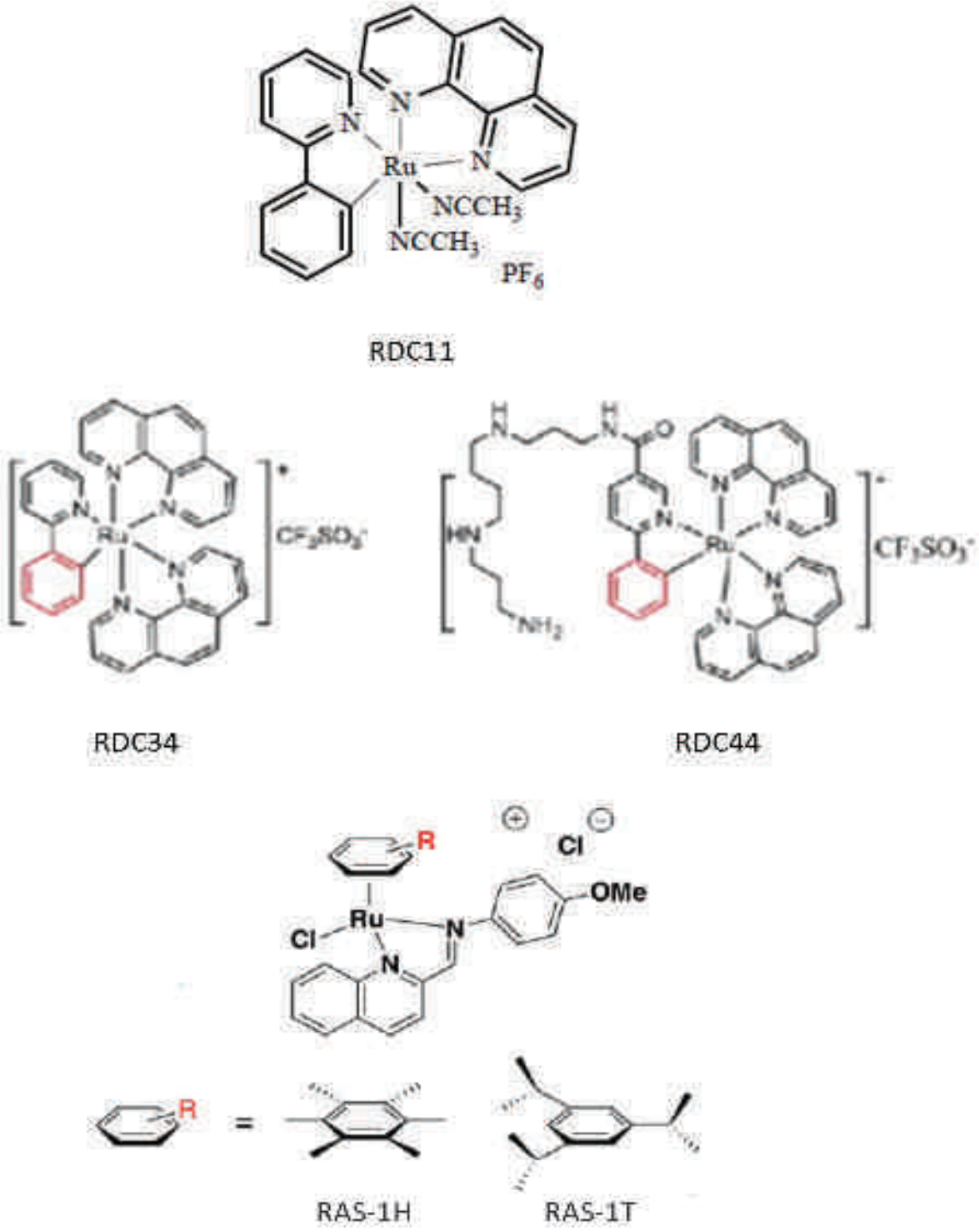

Figure 7: Schematic representation of the structure of ruthenium-based compounds under investigation in our laboratory
Leyva et al., 2008 / Vidimar et al., 2012 / Chow et al., 2016

III) ER stress pathway

III.1) Description

The endoplasmic reticulum is a cellular organelle where proteins are synthetized, properly folded, and where CA^{2+} is stored. Accumulation of misfolded proteins is known to induce a reticulum stress called UPR (unfolded protein response) pathway (Alasiri et al., 2018). Different stimuli including hypoxia, nutrient deprivation and amino acid starvation among others, can promote an accumulation of misfolded proteins and lead to ER stress induction. The ER stress pathway is activated in order to limit protein synthesis and refold misfolded ones. In the presence of un-refoldable proteins, ER stress can induce protein degradation through endoplasmic reticulum associated degradation (ERAD) pathway, however, if too many un-refoldable proteins are present in the cell, ER stress activation leads to the induction of apoptotic pathway. Protein folding is orchestrated by ER resident chaperone, foldase or protein disulphide isomerase (PDI). The ER chaperones are known to bind to newly synthetized protein and recruit the folding enzymes in order to fold correctly them. The general chaperone GRP78/BiP (glucose-regulated protein of 78 kDa/immunoglobulin heavy-chain-binding protein) is the most abundant chaperone in the ER and its expression is induced by the accumulation of misfolded proteins. GRP78 has a high affinity for misfolded protein, enabling their recognition, and facilitates their refolding. However, if the proteins cannot be folded properly, GRP78 can induce their translocation into the cytosol where they undergo ERAD. ERAD represents the proteasomal degradation of misfolded proteins. Other proteins like the oxidoreductase Ero-1, and by the PDI family are also implicated in the refolding of misfolded proteins. In the presence of misfolded proteins, GRP78 dissociates from the central ER sensor protein namely inositol-requiring enzyme 1 α (IRE1α), activating transcription factor 6 (ATF6), and protein kinase RNA-like endoplasmic reticulum kinase (PERK) (Figure 8), leading to the induction of the ER stress pathway. The activation of those three ER sensors promotes the induction of adaptative cellular responses or cell death (Alasiri et al., 2018).

IRE1α pathway: Due to the presence of misfolded proteins, IRE1α is released from GRP78 leading to its dimerization and autophosphorylation. Active form of IRE1α

presents an endonuclease and a RNAse activity and leads to the splicing of XBP1 (X-box binding protein 1) by excision of 26bp intron. XBP1s is the active form and can regulate the expression of genes involved in protein folding as well as ERAD. Furthermore, this RNAse activity also enables the cleavage of several mRNA in order to diminish their amount in the reticulum in a pathway called RIDD (regulated inositol-requiring enzyme 1-dependent decay) (Alasiri et al., 2018; Binet and Sapieha, 2015; Hetz, 2012; McConkey, 2017; Oakes, 2017; Verfaillie et al., 2013). If the ER stress is not resolved, IRE1α activation can lead to the induction of apoptosis by interacting with specific partners like TRAF2 (TNF-receptor-associated factor 2). After the binding to TRAF2, this complex promotes the recruitment of ASK1 (Apoptosis signal regulated kinase 1), leading to ER stress-induced c-Jun N terminal kinase (JNK) activation (Figure 8). JNK activation induces caspase-12 activation promoting ER stress dependent apoptosis. Additionally, several Bcl-2 family members including Bax or Bak can interact with IRE1α and regulate its pro-survival or pro-apoptotic activity. Regulation of IRE1α activity is also mediated by post-translational modifications like phosphorylation known to decrease its activity in order to resolve ER stress after homeostasis restoration.

ATF6 pathway: ATF6 is a transmembrane protein known to display transcription factor function upon activation. Loss of GRP78/ATF6 interaction in response to ER stress promotes ATF6 translocation into the Golgi apparatus where it can be processed by 2 site specific proteases (S1P and S2P) (Figure 8) (Alasiri et al., 2018; Binet and Sapieha, 2015; Hetz, 2012; McConkey, 2017; Oakes, 2017; Verfaillie et al., 2013). The released fragment called ATF6f are cytosolic amino terminal fragments which display bZIP (basic leucine zipper) transcription factor function. The ATF6f are then translocated into the nucleus where they activate the transcription of genes involved in protein folding, ERAD and XBP1.

PERK pathway: eukaryotic translation initiation factor 2 alpha kinase 3 (EIF2AK3) also called PERK is a type 1 transmembrane protein resident in the endoplasmic reticulum. Under normal conditions, PERK is associated to GRP78 and is non active. Ones dissociated from GRP78 due to accumulation of misfolded proteins, PERK is activated and phosphorylates EIF2α (eukaryotic initiation factor 2A) in order to stop general protein synthesis or induces NRF2 expression in order to restore cellular redox homeostasis. In addition, the phosphorylation of EIF2α promotes the

translation of specific mRNA displaying specific 5'UTR like it is the case for activating transcription factor 4 (ATF4) (Figure 8) (Alasiri et al., 2018; Binet and Sapieha, 2015; Hetz, 2012; McConkey, 2017; Oakes, 2017; Verfaillie et al., 2013). ATF4 is a 351 amino acid containing protein and its mRNA displays in the 5' untranslated region (5'UTR) several uORFs (upstream Open Reading Frame). Under basal conditions, these uORFs are arranged in order to inhibit its translation (Harding et al., 2000a). However, after the phosphorylation of EIF2α, these uORFs are rearranged in a specific way in order to re-initiate the translation of ATF4 mRNA (Harding et al., 2000a). Harding and co-workers provide the evidence that under this unstressed conditions, ATF4 is associated with low molecular weight ribosomes and switch to a fraction of higher molecular weight under stress conditions demonstrating the stress activated characteristic of ATF4 (Harding et al., 2000a). The ATF4 protein presents several homo/heterodimerization domains known to regulate its activity, affinity for targets and is also regulated at the post-translational level. The dimerization of ATF4 can include several partners like, for example, Fos, Jun or several C/EBP proteins (CCAAT-enhancer-binding proteins). Post-translational modifications can also regulate ATF4 activity like phosphorylation known to promote its degradation, contrary to acetylation known to induce its stability (Ameri and Harris, 2008). ATF4 can induce the expression of pro-survival but also pro-apoptotic genes showing its dual role in cell survival. Interestingly, ATF4 expression leads to the transcription of several genes involved in protein synthesis and amino acid metabolism promoting cellular homeostasis. However, ATF4 can also induce the expression of CHOP (CCAAT/-enhancer-binding protein homologous protein), a transcription factor inducing pro-apoptotic target genes like the p53-upregulated modulator of apoptosis (also called BBC3), tribbles homologue 3 (TRIB3), the B-cell lymphoma 2 (BCL-2) family of apoptotic regulators and death receptor 5 (DR5 or TNFRSF10B) (Alasiri et al., 2018). Interestingly, ChaC glutathione specific gamma-glutamylcyclotransferase 1 (CHAC1) expression was also seen to be ATF4 dependent. CHAC1 was seen to be involved in ATF4 mediated apoptosis induction by cleavage of Parp, and nuclear relocalisation of AIF1 (Mungrue et al., 2009). Furthermore, ATF4 can regulate autophagy through translational regulation of ATG5/7/10 and p62 protein expression also impacting cell survival. Additionally, ATF4 and CHOP promote the expression of growth arrest and DNA damage-inducible protein 34 (GADD34) which is the regulatory subunit of protein phosphatase 1c (PP1c), responsible of EIF2α dephosphorylation and therefore

promoting a regulatory feedback loop on ER stress activation (Alasiri et al., 2018; Hetz, 2012). In addition, the PERK branch can also regulate Akt expression on one hand by directly phosphorylating the Ser473 leading to Akt activation and on the other hand by ATF4 known to induce Akt under hypoxia or nutrient deprivation (Alasiri et al., 2018).

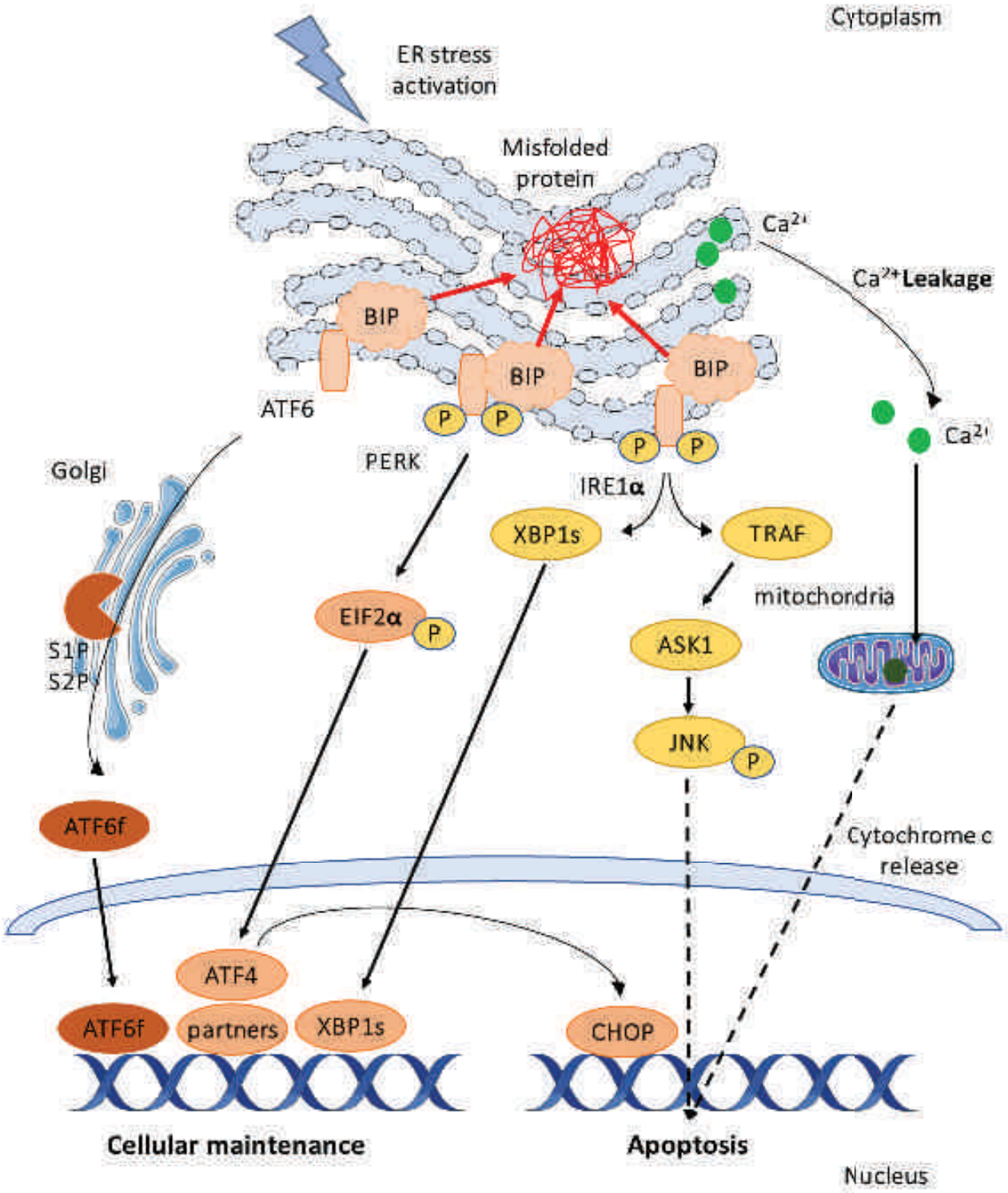

Figure 8: Schematic represntation of the ER stress pathway and its implication in cell death/survival
Inspired by Inagi et *al.*, 2014. Nat Rev Nephrol

The cellular characterisation of this PERK-ATF4 axis of ER stress pathway was performed by Harding and co-workers at the beginning of the 2000s.

Embryonic stem cells KO for PERK expression display no changes in general translation in response to ER stress activation. ER stress induction (thapsigargin, tunicamycin) induces a dissociation of polysomes and accumulation of monosomes and ribosomal subunits in wild type cells. In contrast, PERK-/- cells display intact polysomes showing the loss of control over protein synthesis during ER stress (Harding et al., 2000b). Loss of PERK expression leads to lack of response after ER stress induction. Interestingly, loss of ATF4 expression blocks the activation of genes involved in amino acid transport and metabolism as well as oxidative stress resistance (Figure 8) (Harding et al., 2003). Functional role of this ATF4 signature was further assessed by knocking down ATF4 expression in mouse embryonic fibroblasts (MEFs). Wild-type MEFs were able to grow in DMEM normal culture conditions, which is not the case for MEF explanted from ATF4 KO MEFs. Those KO need a supplementation of culture medium with 7 non-essential amino acids in order to survive suggesting an implication of the response to amino acid starvation.

Different stimuli can induce EIF2α phosphorylation but it needs the presence of specific kinase. In response to ER stress, EIF2α phosphorylation is mediated by PERK, however, in response to amino acid starvation the phosphorylation occurs through general control nonderepressible 2 (GCN2) activated by the presence of uncharged tRNA (Harding et al., 2000a). The induction of ATF4 target genes are seen impaired in response to amino acid starvation and ER stress in GCN2-/- and PERK-/- cells respectively demonstrating the protective role of ATF4 in these stress conditions (Harding et al., 2003). Pushing further the investigation, Harding and co-workers demonstrate that basal expression level of genes involved in sulfur-containing amino acid synthesis are normal in PERK-/- cells but can not be induced under ER stress This data demonstrate that under stress conditions, ATF4 expression is increased in order to induce amino acid metabolism in order to overcome this stress condition.

Beside the ability to regulate amino acid metabolism, the PERK-ATF4 axis is to regulate genes involved into oxidative damage protection. PERK-/- cells are apoptosis prone under ER stress conditions due to an endogenous peroxide production resulting in a cytochrome c leakage and caspase-9 (intrinsic signal dependent) activation.

CHOP expression was also impaired in those KO cell lines. Under amino acid starvation conditions, CHOP was unimpaired in PERK-/- cells. However, CHOP expression was not induced by ER stress activation in PERK-/- cells, showing that CHOP activation in response to ER stress is highly PERK dependent. Those results provide the evidence of a fine tune regulation of CHOP expression in response to several stimuli. Nevertheless, under ER stress conditions, CHOP expression was impaired in ATF4 mutated cells. Furthermore, introducing ATF4 expression in PERK-/- ER stressed cells induces CHOP expression (Harding et al., 2000a, 2003).

Restoration of protein homeostasis after ER stress induction is characterized by the reversal of IRE1α activation. In order to test if this restoration occurs in PERK-/- cells, Harding and co-workers tested the reversal of IRE1α activation after exposure to ER stress inducers, and observed that IRE1α was still activated in response to ER stress in those cells. They observed a sustain activation of IRE1α in PERK-/- in comparison to a fast reversal of IRE1α activation in wild-type cells showing an unresolved ER stress in those KO cells. The unresolved ER stress cleavage of caspase-12 further leading to apoptosis. Interestingly, the apoptosis was seen to be more important for the PERK-/- cells than in wild type ones. This result demonstrates a higher sensibility of the PERK-/- cells to ER stress inducers and a lower ability to resolve ER stress. This phenotype can be rescued by reintroduction of PERK in those cells demonstrating the protective effect that PERK activation can play in stressed cells (Harding et al., 2000b, 2000a).

Two temporal induction waves are induced in response to ER stress activation. PERK activation occurs immediately after accumulation of misfolded proteins in order to inhibit cap dependent translation. In addition, IRE1α is also directly activated and RIDD activity allows the degradation of misfolded proteins. The second wave of ER stress activation leads to the expression of several classes of target genes involved in protein refolding, amino acid synthesis and metabolism among others. The expression of those genes is mediated by the activation of XBP1s, ATF4 and ATF6f, and their target genes are partially the same in order to restore cellular homeostasis (Hetz, 2012). Nevertheless, under unresolved ER stress, a switch from pro-survival to pro-apoptotic conditions is seen.

How this switch can occur in cells is not fully understood but several hypotheses are proposed like interaction partners of ER stress sensors and the type or intensity of ER stress activation.

One possible sign of ER stress switch from pro-survival to pro-apoptotic activation can be the interaction partners of ER stress sensors. Changes in the cytosolic domains of ER stress sensor allows its interaction with activator or inhibitor of their functions. This dynamic platform can regulate the signalling outputs of ER stress activation and is known as UPRosome (Hetz, 2012).

IRE1α regulator Bak is known to induce IRE1α activation and to trigger apoptosis induction due to Bim (BCL-2-interacting mediator of cell death) and NOXA expression. In contrast, IRE1α interaction with Bax inhibitor 1 (BI-1) lowers IRE1α activation. Furthermore, mammalian target of rapamycin (mTor) can also regulate IRE1α activity through a yet unknown mechanism showing the range of pathways regulating the activity of this ER stress sensor. These cofactors are known to regulate the output of IRE1α activation and therefore can act as sentinels regulating apoptosis and pro-survival pathway activation (Hetz, 2012). For the ER stress sensor PERK, the kinase $P58^{IPK}$ is upregulated by ATF6f and XBP1s and can inhibit PERK activity in order to lower pro-apoptotic side of PERK activation and sustain pro-survival UPR activity. However, ER stress pathway can also induce the expression of a BiP splicing variant known to induce PERK signalling possibly due to $P58^{IPK}$ antagonism demonstrating the complexity of the autoregulatory loops activated under stress conditions (Hetz, 2012). ATF6 activity is also regulated by interaction partners including the transmembrane protein Wolframin inducing ER stress dependent degradation of ATF6 and lower this branch of the UPR. The intensity of ER stress activation also plays a role in cell survival. Under weak ER stress activation, IRE1α can splice XBP1s but does not induce RIDD. Interestingly, under the same conditions, PERK activation does not result in activation of pro-apoptotic factor CHOP.

Another sign for the ER stress switch from pro-survival to pro-apoptotic activation can be made by the different stimuli activating ER stress, changing the kinetics of ER stress sensors activation. IRE1α and PERK are preferentially activated by changes in ER calcium load as well as the presence of reducing agents for IRE1α. In contrast, ATF6 is preferentially activated in response to a high misfolded protein

load or alteration in redox homeostasis. These kinetic could explain how the ER stress activation can switch from pro-survival signal to pro-apoptotic one. For example, under prolonged ER stress activation, IRE1α activity is decreased after time, in contrast to PERK, probably explaining the transition from a pro-survival to a pro-apoptotic pathway. The explanation would be a decrease of pro-survival characteristics of XBP1s, whereas PERK expression induces pro-apoptotic factors. Furthermore, after prolonged ER stress activation, calcium release is seen and sensitizes mitochondria to apoptosis (Hetz, 2012).

III.2) ER Stress and cancer

Cancer cells display high proliferation rates suggesting a high protein synthesis and high energy/nutrient demands, and therefore, ER stress pathway plays a central role for cancer survival due to its role in protein folding and stress adaptative response initiation. Several cancer cell characteristics leads to the induction of ER stress pathway in order to support the harsh conditions and promote cell survival. More precisely, insufficient vascularisation promotes nutrients and oxygen deprivation leading to oxidative stress and ER stress induction in cancer cells (Alasiri et al., 2018; Binet and Sapieha, 2015). Furthermore, oncogene activation can also induce ER stress pathway like it is the case for c-Myc, which induces general protein synthesis leading to accumulation of misfolded proteins and so to ER stress activation. Additionally, mutant B-raf can directly binds to GRP78/BiP, resulting in a release of the three ER sensors and activation of ER stress (Alasiri et al., 2018).

For many cancers, ER stress pathway was seen to promote cancer initiation, progression as well as resistance against chemotherapeutic agents (Figure 9) (Alasiri et al., 2018). ER stress pathway can regulate important pathways including Akt, mTor and NF-kB (nuclear factor kappa-light-chain-enhancer of activated B cells) among others leading to cancer cell survival. In addition, BiP was shown to induce prostate cancer cell survival through mitogen-activated protein kinase (MAPK) and PI3K/Akt pathways. This induction of Akt results in mTor activation leading to higher survival and proliferation rates of cancer cells (Ojha and Amaravadi, 2017). Cancer cell survival can also be promoted through PERK mediated JNK regulation (Alasiri et al., 2018). NF-kB

pathway is also induced in response to ER stress promoting tumorigenesis (Figure 9). Due to the ER stress mediated stop of cap dependent protein synthesis, the NF-kB inhibitor, IkB expression is also decreased leading to NF-kB activation and cancer progression. (Oakes, 2017). ER stress can also promote resistance to anticancer agents due to its ability to inhibit P53 accumulation in nucleus and therefore blocks P53 mediated apoptosis while it enhances cancer cell survival (Figure 9) (Moenner et al., 2007).

Activation of ER stress under hypoxic conditions help tumor cells to adapt to stress conditions through induction of antioxidant capacity. All three ER stress branches were shown to induce the expression of VEGF in order to restore the O_2 needs of cancer cells thanks to neovascularization, further promoting their survival and dissemination (Figure 9) (Alasiri et al., 2018; Moenner et al., 2007; Verfaillie et al., 2013). PERK can induce VEGF expression through ATF4 mediated transcription but also independent of ATF4 expression through enhancing the internal ribosome entry site (IRES) dependent translation (Binet and Sapieha, 2015; Oakes, 2017; Philippe et al., 2016). The ATF6 transcription factor was also shown to induce directly VEGF expression. Furthermore, in vivo studies provided the evidence of IRE1α mediated VEGF upregulation. More precisely, less IRE1α activation leads to less XBP1s expression. XBP1s can interact with HIF1α in order to promote tumor growth by regulating genes like VEGF and glucose transporter 1 (GLUT1) leading to a better neovascularization. These data demonstrate impairing IRE1α expression leads to less VEGF expression resulting in lower angiogenesis in several cancer xenograft models including lung carcinomas and gliomas (Binet and Sapieha, 2015). (Figure 9) (Binet and Sapieha, 2015; Moenner et al., 2007; Oakes, 2017).

Interestingly, deficiency of the ER chaperone BiP/GRP78 correlates with lower tumor growth and angiogenesis contrary to BiP overexpression which promotes tumor aggressiveness and recurrence for a number of tumors including gastric and liver ones. This effect can be explained by the fact that, in response to VEGF signalling, the chaperone GRP78 can bind to plasma membrane and induces the PI3Kinase/Akt pathways leading to pro-survival signals (Figure 9) (Binet and Sapieha, 2015). To summarize the role of ER stress activation for cancer cell survival, PERK can help cancer cells to resist to hypoxia and nutrient deprivation (Alasiri et al., 2018), but also

under strong ER stress induction those proangiogenic capacities of UPR can be reversed (Binet and Sapieha, 2015).

ER stress can also promote tumor growth and survival by inducing autophagy in order to support and adapt to the harsh environmental conditions as well as chemotherapeutic agents (Figure 9). ATF4 mediated TRIB3 expression can act as an Akt-mTor inhibitor and therefore promotes autophagy (Alasiri et al., 2018). Autophagy is necessary for misfolded aggregates degradation but can be taken as a potential target. This protective autophagy is induced in cancer cells through ATF6 and IRE1α mediated JNK regulation (Alasiri et al., 2018; Kania et al., 2015). However, a too important need of autophagy in order to resolve ER stress results in a lower capacity of preventing mitochondrial damages. Lowering mitophagy results in mitochondrial damages, ROS production, cytochrome c release and cell death (McConkey, 2017).

ER stress has a direct effect on cancer cells survival and proliferation and is commonly seen to be upregulated (seen by higher PERK, IRE1α and ATF6 levels) in many cancers like stomach and oesophagus cancers (Oakes, 2017). In order to characterize more precisely the role of each ER stress arm, several studies modulate the expression of each ER stress sensor and characterize the phenotypical outcomes.

PERK-/- xenograft models display higher sensibility to hypoxic conditions. These PERK -/- cells displays less ER-mitochondria sites, known to paly a role in oxidative stress protection, and therefore rendering the cells more sensitive to ROS mediated apoptosis. More precisely, it was shown that kras transduced MEF also KO for PERK are more sensible to oxidative stress than PERK +/+ ones (Verfaillie et al., 2013). Furthermore, PERK inhibition decreases mammary tumor development as well as lung metastasis (Oakes, 2017; Ojha and Amaravadi, 2017). Those results suggest that PERK supports tumoral growth and survival by limiting oxidative damages (Figure 9) (Moenner et al., 2007).

IRE1α activation is important for several cancers due to its role in resistance to hypoxia and regulation of proliferation (Figure 9). IRE1α is often mutated in cancer cells which allows an impairment in the terminal UPR in order to promote cell survival and decreases apoptosis induction (Hetz et al., 2013; Oakes, 2017). Hypoxia induces IRE1α expression in a pro-survival way (Ojha and Amaravadi, 2017). In human prostate cancer cells as well as breast cancer and hepatocellular carcinomas, IRE1α

promotes cell proliferation via XBP1 splicing, important for cancer cells survival under hypoxic conditions, and glucose starvation due to the adaptative stress responses driven by this transcription factor (Alasiri et al., 2018). Additionally, for glioma cells, suppression of IRE1α expression leads to a decrease angiogenesis potential. This is supported by the fact that after injection to mice limit tumor growth and neovascularisation. This effect can be explained by the RIDD mediated decay induced by IRE1α (Oakes, 2017), the pro-inflammatory, and pro-angiogenic effect of IRE1α (Hetz et al., 2013). Furthermore, it was described that XBP1s deficient cells have reduced abilities to form solid tumors in mice and that high XBP1s expression correlates with poor prognosis in triple negative breast cancer and glioblastoma demonstrating the important role of XBP1s in cancer cell survival and adaptation (Hetz et al., 2013; Ojha and Amaravadi, 2017).

ATF6, BiP and other ER chaperones are also implicated in cancer cells survival and dormancy. ATF6 was seen to play a central role in cell dormancy, resistance to chemotherapeutic agents and nutritional stress in dormant cell through mTor regulation (Figure 9) (Ojha and Amaravadi, 2017; Hetz et al., 2013). In contrast, other chaperones like GRP78 allows cancer to resist to pro-apoptotic challenge and are seen overexpressed in at least 10 types of cancer including colon and breast cancer (Moenner et al., 2007).

Altogether, ER stress is induced in cancer cells through different activators such as hypoxia or low glucose levels. Under low ER stress induction or in response to several anticancer agents, the pro-survival side of the UPR is activated and promotes cell survival through different mechanisms (Moenner et al., 2007). However, under strong ER stress activation, the pro-apoptotic side of the ER stress pathway is activated, rendering the ER stress pathway a good therapeutical target. Under basal conditions, for normal as well as for cancer cells, survival requires the continual expression of pro-survival proteins, however under ER stress, the cap dependent translation is inhibited lowering the amount of pro-survival proteins while inducing the expression of pro-apoptotic ones (McConkey, 2017). In several cancer cell lines, like human carcinoma cell line (KB cells), ER stress can also directly activate caspase cleavage and cell death through multiple pathways like Ca^{2+} leakage from ER to mitochondria or cytochrome c release (Figure 8) (McConkey, 2017; Verfaillie et al., 2013).

In conclusion, ER stress pathway is a central actor of cancer cells homeostasis regulating several aspects of cancer cell survival/death balance. Therefore, the ER stress pathway is seen as a good therapeutical target in order to induce cancer cell death. Many small molecules and inhibitors of the ER stress pathway have been developed in order to lower the pro-survival side of the UPR and to induce the pro-apoptotic one.

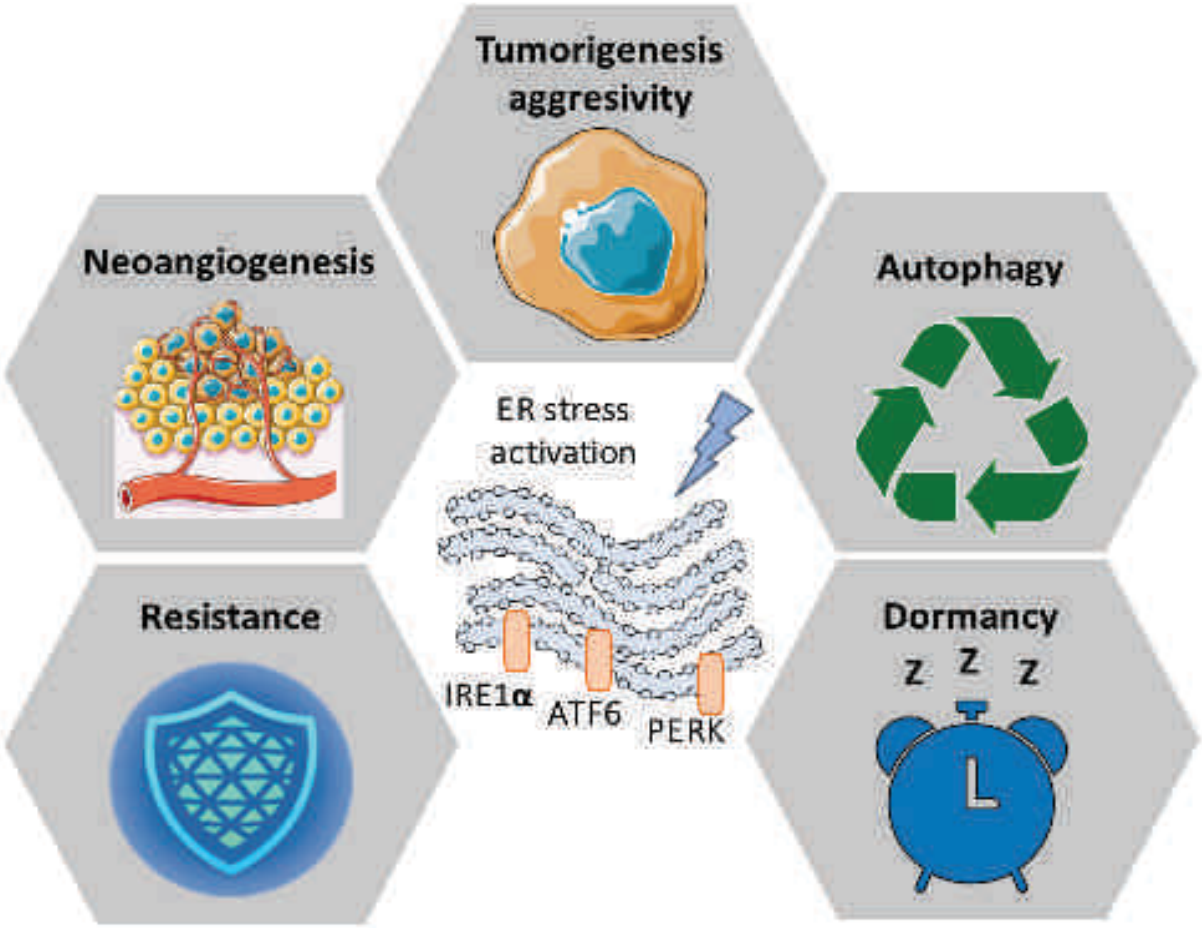

Figure 9: Roles of the ER stress for cancer biology

III.3) ER stress and anticancer therapies

Targeting ER stress pathway as anticancer therapy has received many attentions during the last decade. Several inhibitors like chemical chaperones, ERAD, PDI, PERK, IRE1α and proteasome inhibitors have been synthetized and tested for their anticancer activity (Binet and Sapieha, 2015). The desired rendering was to inhibit the pro-survival part while inducing the pro-apoptotic one of the ER stress pathway.

Further, inducing ER stress is an approach for cancer treatment consisting in increasing the misfolded protein load leading to cell death. That's why, ERAD inhibitors including proteasome inhibitors and ATPase inhibitors, are under investigation (Hetz et al., 2013). Proteasome inhibition by treatment, such as bortezomib, promotes ER stress mediated apoptosis and has revealed interesting properties for treatment of a variety of malignancies such as several myelomas (Alasiri et al., 2018; Ojha and Amaravadi, 2017; Verfaillie et al., 2013). Additionally, targeting the membrane bound GRP78/BiP using a mouse monoclonal antibody provides impairment of glioma cell survival and further sensitizes cancer cell to gold standard chemotherapeutic agents like cisplatin in vivo (Binet and Sapieha, 2015; Ojha and Amaravadi, 2017; Verfaillie et al., 2013). Several reviews refere that inhibition of BiP by specific inhibitors also display a great cytotoxic potential by lowering the ER folding capacity of cancer cells in vitro (Hetz et al., 2013).

Curcumin derivate B19 can induce cancer cell apoptosis through an ER stress dependent manner in vitro. Treatment of gastric cancer cells SGC-7901 leads to changes of ER morphology as well as induction of specific ER stress markers p-EIF2α, CHOP and ATF4. The ER stress induction mediated by B19 is totally ROS dependent and can be totally reversed by cotreatment with NAC (Chen et al., 2016).

Many inhibitors of the ER stress sensors have been synthetized like PERK and IRE1α inhibitors. PERK inhibitor like GSK2656157 and GSK2606414 among others, inhibits tumor growth of several xenograft models like pancreatic xenograft models (Hetz et al., 2013; Oakes, 2017). This family of molecules also presents the ability of lowering angiogenesis and tumoral activity (Binet and Sapieha, 2015). IRE1α can also be inhibited by targeting the catalytic core of its RNAse domain or the ATP-pocket of its kinase domain. For example, the IRE1α inhibitor MKC-3946, inhibiting the RNAse

domain blocks XBP1 splicing as well as RIDD activation. MKC-3946 mediated inhibition of IRE1α activity results in lower tumor growth, reduced tumour formation and was shown to potentiate proteasome inhibitor Bortezomib antitumor activity (Hetz et al., 2013). MKC-3946 is fastly hydrolysed, into A-106 (2-hydroxy-1-naphthaldehyde, HNA) which has gain great interest. HNA was shown to induce acute myeloid leukaemia (AML) cell death in vitro by inducing Parp and caspase-3 cleavage, cell cycle arrest and pro-apoptotic factors such as Bim (Sun et al., 2016).

All those therapeutic strategies underline the anticancer effect of targeting ER stress pathway in cancer cells in order to promote induction of pro-apoptotic factors and in the meantime lowering the pro-survival ones. However, further research need to be done allowing the development of more potent inhibitors which could be used in clinic.

III.4) Role of ER stress for gold standard treatment and metallic compounds

III.4.1) Platin-based compounds

The induction of ER stress by platinum-based compounds and its role in the cytotoxicity of those compounds is still contested. On one hand, platinum-based compounds display an ER Stress dependent cytotoxicity in several cancer cell lines. On the other hand, the induction of ER Stress mediates platinum resistance.

The first evidence of platinum-based compounds, more precisely cisplatin, and ER Stress dependent cell death was provided by Mandic and co-workers (Mandic et al., 2003). A DNA independent cell death was highlighted in enucleated melanoma cells as well as in HCT116 colon cancer cells. Furthermore, ER stress specific caspase (caspase-12) was seen to be cleaved in response to cisplatin. In addition, cisplatin was reported to induce a calcium dependent apoptosis in Hela cells (Shen et al., 2016). Cleavage of caspase-3 level is induced by cisplatin and it was lowered by the addition of a calcium chelator. As it is known that the endoplasmic reticulum is the principal

calcium storage in cell, the implication of ER Stress was tested. They observed a GRP78 accumulation as well as a CHOP activation suggesting an ER stress activation (Shen et al., 2016; Xu et al., 2015). Other types of platinum-based compounds were also seen to be able to induce ER stress pathway. Wang and co-workers developed two platin-based compounds called Mon-pt-1 and Mon-pt-2 and showed their ability to induce ER stress pathway (Wang et al., 2018a). Those two compounds display a higher cytotoxic activity compared to cisplatin and are able to strongly induce ROS production which will further localize within the ER. Furthermore, those compounds induce the expression of ER stress markers like PERK, p-EIF2α and CHOP demonstrating ER Stress activation in A549 lung carcinoma cell line. All together these data show a platin mediated ER stress induction. However, in those studies, they never demonstrate if the induction of ER stress they have seen was a consequence of DNA damages induced by platinum-based compounds or was specifically induced by there compounds. Furthermore, they never directly correlate the functional role of these ER stress markers and the cytotoxicity of the platin-based compounds.

Several studies demonstrate the opposite effect, meaning that platinum-based compounds do not induce ER stress in order to induce apoptosis, but that ER stress induction lowers the cytotoxic activity of platinum-based compounds. Jiang and co-workers demonstrate that treatment of melanoma cell lines (Mel-RM and MM200) with platinum compounds promote the induction of GRP78 further resulting in resistance against cisplatin treatment (Jiang et al., 2009). For lung cancer cell lines A549 and H460, cisplatin treatment induces GRP78, PERK and IRE1α expression demonstrating an ER stress induction after cisplatin treatment (Shi et al., 2016). Nevertheless, blocking ER stress activation by the use of 4-PBA, further induces the cytotoxic activity of cisplatin demonstrating the protective role of ER Stress in response to cisplatin. In addition, the cytotoxicity of cisplatin was unchanged when used on cells transfected with a siRNA against CHOP showing that, in head and neck cancer cells SQ20B, cisplatin displays cytotoxicity fully independent of the ER Stress activation (Rabik et al., 2008). Moreover, Tian and co-workers demonstrate that pre-treatment of SKOV-3x ovarian cancer cell line with an ER Stress inducer, Saquinavir, results in lower cytotoxic effect of cisplatin (Tian et al., 2017). Interestingly, the ER stress activation in response to cisplatin treatment is responsible of the induction of the protein TXNDC5 (Thioredoxin Domain Containing 5) known to regulate the intracellular antioxidant

content and so cell resistance to oxidative stress and drugs in LSCC cells (Lung squamous cell carcinoma) (Peng et al., 2018). Feng and co-workers support the fact that ER Stress induction promotes resistance against chemotherapeutic agent like cisplatin (Feng et al., 2011). More precisely, they demonstrate that pre-treatment with tunicamycin lowers the cell death induction mediated by cisplatin in gastric cancer cell line (BGC823 and SGC7901). Another level of complexity is added when sensible or tolerant/resistant cells are used to describe the role of ER Stress for the cytotoxic activity of platinum-based compounds. In 2011, Lin and co-workers established ER Stress tolerant cells derived from the parental lung cancer cell line A549 and H460 by several tunicamycin treatments. On those new ER tolerant cells, cisplatin treatment was shown to be less active due to higher levels of GRP78 leading to platinum resistance (Lin et al., 2011). Taken together, those results demonstrate a cisplatin dependent induction of ER Stress markers. However, in this case, the ER Stress is responsible of a lower cytotoxic activity of cisplatin, and also participating to cisplatin resistance.

To conclude, the ER Stress induction mediated by platinum-based compounds is found in several cancer cell lines. Nevertheless, its role in cell survival is still controversial due to, on one hand, the induction of pro-survival proteins and pathways playing a role in cancer cells resistance. On the other hand, platinum-based compounds can also in some cases, induce pro-apoptotic factors such as CHOP which can, in part, play a role in the cytotoxic activity of the compounds. Those studies demonstrate the complexity of the ER Stress activation in response to platinum-based compounds and show the need to understand more deeply the real role of this pathway in response to platinum-based therapies.

III.4.2) Ruthenium-based compounds

In the case of ruthenium-based compounds, a novel unconventional target was discovered for the first time by our team. We showed that one of our ruthenium-based compounds called RDC11 (Figure 7) is able to induce the endoplasmic reticulum stress pathway (ER Stress). Meng and co-workers provide the evidence that RDC11 displays a greater cytotoxic effect on human glioblastoma cell line (U87), but also in mice skin

melanoma cells (B16F10) than cisplatin (Meng et al., 2009). This higher cytotoxic activity is further linked to fewer side effects mainly on the nervous system, and liver damages. Interestingly, in order to understand how our compound could present better characteristics than commonly used platinum-based drugs, ER stress pathway has been investigated. Our lab proves that, contrary to cisplatin, RDC11 was able to strongly induce markers of the ER stress pathway mainly BiP, XBP1, PDI or CHOP in TK6 and NH32 cells (lymphoblastoid cell lines). To further explain the role of this ER stress in the cytotoxic activity of RDC11, our lab shows that blocking its activation strongly reduces the ability of our compound to induce cell death in U87 cells underlining the importance of this pathway for the anticancer activity of RDC11. To support the role of ER Stress activation for the cytotoxic activity of this compound, the silencing of a proapoptotic key marker of this pathway, CHOP, significantly increases cell survival of U87 cell line when treated with RDC11. In a same manner, Xu and co-workers demonstrate the importance of CHOP for the cytotoxic activity of their RU(II) compounds on HeLa cells (Xu et al., 2019).

Similar results were obtained for other type of compounds like RDC34, RAS-1T or RAS-1H, but this time in other type of cancer cells (Figure 7) (Chow et al., 2016; Vidimar et al., 2012). Indeed, the activation of the ER stress pathway by ruthenium-based compounds is seen in colorectal cancer cells (HCT116) and in gastric cancer cells (AGS). Chow and colleagues also demonstrate that depending on the type of ruthenium-based compounds, the induction of ER stress pathway can be dependent or not on the ROS production (Chow et al., 2018). RAS-1T, compound 2 and 4 are able to promote the disruption of ER homeostasis that can be restored with cotreatment with NAC, an antioxidant molecule. However, the cotreatment does not impact on the ability of compound 3 to induce ER Stress pathway showing multiple ways to induce ER Stress pathway through ruthenium-based compounds.

All together our lab showed the role of the reticulum stress pathway in the mode of action of those ruthenium-based compounds displaying a great cytotoxic effect on several types of cancer cell lines than platinum-based ones. Thus, compounds like RDC11 are promising candidates for the development of future drugs because of their unconventional mode of action, but also due to a similar activity on several cancers. Other teams obtained similar results, namely the induction of several ER Stress markers (BiP, pEIF2α,...) in response other types of ruthenium-based compounds like

(NKP-1339 or (salen)ruthenium(III) complexes) (Flocke et al., 2016; Li et al., 2017). Interestingly, the ER Stress induction seen with a majority of ruthenium-based compounds is not cell type specific, like it was seen for colon, but also breast tumors cell lines. All those studies show the importance of the ER Stress pathway for the cytotoxic activities of many ruthenium-based compounds, which therefore present DNA independent mode of action. Some ruthenium-based compounds are also used in order to induce cell death by inhibiting ER stress induction. KP1339, in phase I of clinical trials, is a known inhibitor of the ER Stress protein GRP78, which is required to induce an ER Stress. KP1339 displays a good cytotoxic activity towards several cancer cell lines (CAPAN-1, HCT116, SW480, or KB-3-1) derived from pancreas, colon or cervix respectively (Schoenhacker-Alte et al., 2017). Schoenhacker-Alte and co-workers could demonstrate the ability of this compound to reduce protein expression of several ER Stress markers, like PERK, IRE1α and ERO1α (Endoplasmic Reticulum Oxidoreductase 1 Alpha). Cotreating cells with KP1339 and an ER stress inhibitor 4-PBA leads to a synergistic activity underlining the implication of lowering ER Stress for the cytotoxic activity of this compound.

III.4.3) Osmium-based compounds

Most of the studies reveal DNA dependent cytotoxic activity for osmium-based compounds. However, Suntharalingam and co-workers described also ER stress mediated cytotoxicity for one osmium-based compound (Suntharalingam et al., 2013). They studied the mode of action of osmium (VI) nitride complexes and discovered a DNA independent mode of action for their complex 4. This complex was more localized in the cytoplasm than in the nucleus and co-treatment of complex 4 with the ER stress inhibitor salubrinal, lowered the cytotoxic activity of complex 4. Furthermore, they proved that in ovarian cancer cell (A2780), treatement with this complex induce the expression of several markers of ER stress like p-EIF2α and CHOP (Suntharalingam et al., 2013). This work demonstrates that osmium compounds can also induce ER stress pathway in order to induce cell death activation. Nevertheless, osmium compound mediated induction of the ER stress pathway is largely understudied and

therefore should be investigated to characterize more precisely their mode of action further leading to the development of more potent anticancer agents.

III.5) ATF4 and metabolism regulations

As described in the section III.1, ATF4 is known to regulate several genes involved in amino acid transport and metabolism in order to induce the integrated stress response (ISR) (Harding et al., 2003). Harding and co-workers demonstrate that mouse embryonic fibroblasts lacking ATF4 display lower overall glutathione (GSH) content. Interestingly, supplementation of culture medium with non-essential amino acids rescued the low level of GSH in the ATF4 lacking fibroblasts showing an impairment in amino acid metabolism. Interestingly, Dickhout and co-workers also showed in this study that the level of CBS (cystathionine beta synthase) and CTH (cystathionine gamma-lyase) were deregulated in ATF4-/- cells in comparison to wild-type cells. Those two enzymes belong to the transsulfuration pathway implicated in cysteine production further promoting GSH synthesis (Figure 10). More precisely, in these ATF4-/- cells, CBS protein level were higher and CTH lower showing the regulatory role of ATF4 on this pathway (Combs and DeNicola, 2019; Dickhout et al., 2012). In accordance to those results, CTH expression was induced in HEK293 and HeLa cells after treatment with the ER stress inducer thapsigargin (Dickhout et al., 2012). To assess whether the transsulfuration pathway can functionally supply the cells in cysteine and regulate glutathione production, Dickhout and co-workers used a chemical inhibitor of the CTH in order to test GSH content in absence of transsulfuration. They showed that treatment of MEFs by PPG (DL-Propargylglycine, a CTH inhibitor) leads to a significant decrease in glutathione content showing the implication of the transsulfuration pathway on glutathione production. In the same time, ROS production was seen to be increased in the ATF4-/- MEFs correlating with a higher apoptosis rate as seen by Tunnel and LDH (Lactate dehydrogenase) release experiments (Dickhout et al., 2012). The role of CTH induction under those conditions is to support GSH production by cysteine production as well as avoiding accumulation of toxic metabolites like homocysteine (Dickhout et al., 2012; Kabil et al., 2016). Furthermore, it was seen that cells lacking CTH expression are more sensible to ER stress mediated apoptosis (Kabil et al., 2016).

The direct regulation of the CTH mediated by ATF4 was described by Mistry and co-workers in 2015. They demonstrate that ATF4 can directly bind to CTH, however not in the promoter region, but by direct binding in the first intron of CTH. They create a specific construct containing the promoter region of CTH plus region from the first intron directly attached to luciferase and demonstrate that co-transfection of this construct and ATF4 leads to a high induction of luciferase activity compared with transfection of the construct alone in HEK cells (Mistry et al., 2016). Other types of cellular stress like nutrient deprivation or hypoxic conditions can also induce ATF4 mediated activation of CTH independently of PERK activation. Other kinases like GCN2 or Heme-regulated inhibitor kinase (HRI) known to induce phosphorylation of EIF2α can also induce ATF4 expression and further regulate the transsulfuration pathway (Mistry et al., 2016; Ojha and Amaravadi, 2017).

All together those studies provide the evidence of an ER stress mediated regulation of the transsulfuration pathway. This pathway is important for cellular supply in cysteine in order to promote GSH biosynthesis and resist to cellular stress.

IV) Transsulfuration pathway

IV.1) Description and regulation

IV.1.1 Description

Transsulfuration pathway is dependent on methionine pathway due to its ability to provide cellular homocysteine (Figure 10). Methionine is obtained by the diet and is firstly transformed by the methionine adenosyltransferase into s-adenosylmethionine (SAM). SAM is then used as a major donor for DNA methylation and this DNA methylation reaction produces s-adenosylhomocysteine (SAH). SAH is then hydrolysed by SAH hydrolase promoting synthesis of homocysteine (Hcy) which is the entry point for the transsulfuration pathway (Combs and DeNicola, 2019). Transsulfuration is the only way for de novo cysteine synthesis in mammals. Cysteine produced by this pathway has an essential role in protein synthesis but can also be

used to form the major antioxidant molecule GSH (Kim et al., 2018; Maclean et al., 2012; Mosharov et al., 2000; Sbodio et al., 2019; Zhu et al., 2018). Transsulfuration pathway is an irreversible transformation of homocysteine into cysteine and is composed by two PLP (Pyridoxal phosphate) dependent enzymes called CBS (cystathionine beta synthase) and CTH (cystathionine gamma-lyase). CBS catalyzes the formation of cystathionine by the condensation of homocysteine and serine (Figure 10). The first step of this pathway is known to be rate limiting, however, normally only a portion of this homocysteine is used by the transsulfuration pathway. Cystathionine is then cleaved into cysteine, α-ketobutyrate and ammonia by CTH (Figure 10).

Those two reactions of the transsulfuration pathway are responsible of the formation of the gaseous transmitter H_2S (Hydrogen sulphide) known particpates in several biological processes like neoangiogenesis, stimulation of the mitochondrial electron transport chain or act as a direct antioxidant molecule, as well as regulate cell proliferation and survival (Hellmich and Szabo, 2015; Zhu et al., 2018). Complexity of H_2S responses can be explained due to different effect of low and high doses of this gaseous transmitter. H_2S can modify cysteine on proteins in a reaction called sulfhydration or persulfidation, which can be reversed by cellular reductants. Sulfhydration can regulate several biological processes like vasodilatation, oxidative or inflammatory stimuli. H_2S can also control mitochondrial ATP synthesis by regulating the electron transport chain in a dose dependent manner. Low level of H_2S is known to act as electron donor at complex II enhancing mitochondrial bioenergetics. High levels of H_2S inhibit cytochrome c oxidase blocking ATP production (Sbodio et al., 2019). Furthermore, H_2S can stimulate kinases like MAPK and PI3K/Akt in order to promote cell proliferation (Zhu et al., 2018).

Interestingly, CBS and CTH are present in almost all non-neoplastic tissue with a predominant expression in liver and kidney. Nevertheless, 20 to 50% of cysteine is produced in the liver by the transsulfuration pathway (Combs and DeNicola, 2019).

CBS is a 551 amino acids long protein predominantly expressed in the brain, liver, kidney, pancreas. The active form of human CBS is composed by 4 63kDa subunits binding 2 PLP (pyridoxal 5'-phosphate) as cofactors. Two CBS motifs (CBS1 and CBS2) are located in the c-terminal region of the enzyme and are responsible of dimerization, leading to the formation of Bateman domain containing binding sites for

SAM, the allosteric activator. Binding of SAM to CBS promotes the use of Hcy for the transsulfuration pathway reactions. CBS can also be cleaved in the C-terminal region at R413 in order to generate a shorter monomer (45kDa), two times more active protein which is refractory to SAM mediated activation. This CBS cleavage was observed for example after TNF-α induction promoting a higher GSH production due to inducing flux through transsulfuration pathway in order to respond to higher ROS insult. This more active form of CBS can therefore play a role in cell survival and proliferation by producing more cysteine and GSH leading to a better resistance to different cellular stress conditions (Combs and DeNicola, 2019; Sbodio et al., 2019; Zhu et al., 2018). N-terminal region of CBS is known to interact with the cofactor heme in order to allow a proper protein folding. However, this cofactor is not required directly for the activity of the enzyme. CBS is most commonly found in the cytosol, but recent studies provided the evidence of other cellular localisations including mitochondria and the nucleus in specific cell types (Zhu et al., 2018).

CTH is the second enzyme of the pathway and is found as an homotetramer composed by units of 45kDa each binding to PLP cofactors by the carboxylate of Asp^{187}. Mutation of this amino acid results in a total abolishment of CTH activity promoting deleterious effects because it is the only enzyme producing cysteine. CTH level can be regulated by various molecular signals ranging from cellular stress to nutrient deprivation (Sbodio et al., 2019).

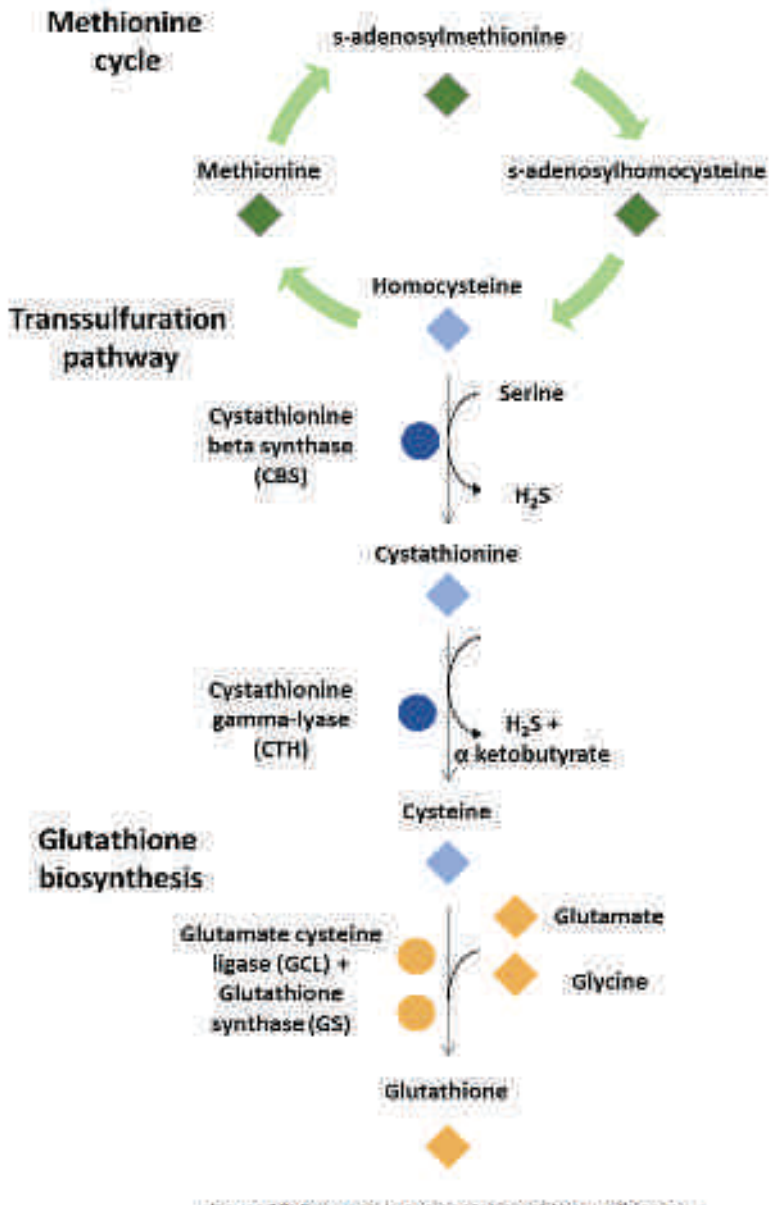

Figure 10: Schematic representation of the methionine cycle, the transsulfuration pathway and its link to glutathione biosynthesis

IV.1.2 Regulation

Transsulfuration can be regulated at different levels including cofactors, epigenetic, stress responses and posttranslational regulations. For instance, it is known that CBS can be regulated directly by the presence of carbon monoxide (CO). CO is a gaseous transmitter produced by heme oxygenase (HO) known to inhibit CBS

activity. In response to inhibition of CBS activity, more homocysteine is used for remethylation, other methionine related pathways and polyamine (Hishiki et al., 2012).

At the transcriptional level, several mechanisms are known to regulate transsulfuration. Zhao and co-workers suggest that CBS promoter is commonly methylated in some colorectal and gastric cancer cell lines. This methylation should lead to the silencing of CBS expression. However, CBS expression was found to be relatively high in normal gastric tissue suggesting a role for this pathway in this tissue (Zhao et al., 2012; Zhu et al., 2018). Furthermore, many stress stimuli are known to regulate the expression of this enzyme. Hypoxic condition was seen to regulate CBS expression by enhancing its expression through the hypoxia inducible factor 1 (HIF1) and by limiting its degradation in the mitochondria. In addition, oxidative stress can induce the flux through the transsulfuration pathway increasing cystathionine, cysteine and glutathione levels. Cystathionine beta synthase is known to be a redox sensible enzyme as demonstrated by Mosharov and co-workers (Mosharov et al., 2000). They use PPG treatment (CTH inhibitor) of HepG2 cells in order to determine the flux through transsulfuration by measuring the relative level of cystathionine level as well as [^{14}C] incorporation into cystathionine after 100µM H_2O_2 (Hydrogen peroxide) treatment. In response to oxidative insult, the flux through the transsulfuration pathway is 1,6 fold increased as well as the level of CBS about 1,7fold. Similar results were obtained with another oxidant molecule (tBuOOH, tert-Butyl hydroperoxide) but in a stronger extend. To further confirm the redox sensible characteristic of CBS, the use of methionine by the transsulfuration pathway has been tested by measuring incorporation of [^{35}S] methionine into glutathione (Figure 10). The only way of incorporating methionine into glutathione occurs through transsulfuration mediated cysteine production using methionine and therefore assess the flux through the transsulfuration pathway. Mosharov and co-workers exposed HepG2 to tBuOOH 200µM and showed a 1.5 fold increase in glutathione labelling suggesting that more methionine is used by the transsulfuration pathway (Mosharov et al., 2000). Moreover, the sensitivity of CBS to increasing homocysteine concentrations and under oxidative conditions, enabling a higher rate of GSH production due to higher cysteine availability. They validate these characteristics in HepG2 cells by treatment with PPG, providing the evidence of a lower cysteine concentration leading to a decrease about 1,5 fold of the GSH:GSSG (Glutathione disulphide) ratio in absence of transsulfuration.

Regulation by oxidative stress was seen to be mediated by the stress response gene NRF2. NRF2 is known to promote CTH but also CBS expression leading to synthesis of glutathione in order to respond to oxidative stress conditions. This regulation is induced by a direct NRF2 binding on CBS and CTH promoters (Sbodio et al., 2019). CTH can be induced by ER stress, oxidative stress, inflammation, starvation and many other stimuli. CTH expression is, under basal conditions regulated by specific protein 1 (Sp1). However, it was seen that other proteins can regulate CTH expression like FXR (Farnesoid X receptor) in the liver to promote hepatic microcirculation, as well as GPCR (G protein-coupled receptors) for secondary bile acids, GPABR1, activating cAMP response element which then bind to CTH promoter (Combs and DeNicola, 2019; Sbodio et al., 2019).

At the posttranslational level, CBS is sensible to phosphorylation at the serine 227 in order to produce more H_2S, as well as to glutathionylation and to sumoylation respectively responsible of an increase and a decrease of its activity (Sbodio et al., 2019; Zhu et al., 2018). CTH can also be regulated at the posttranslational level by Akt mediated phosphorylation in order to enhance its activity. Additionally, it was reported that CTH can have different cellular localisation including nucleus in response to sumoylation but also mitochondria under stress conditions (Sbodio et al., 2019). All those regulations underline the sensibility of the transsulfuration pathway in response to several stress stimuli as well as the important role of this pathway in cellular adaption.

IV.2) Transsulfuration and disease

Given its important role in cysteine, glutathione and H_2S production transsulfuration pathway participates in several biological process. Therefore, modifications or changes in the activity of this pathway are responsible of several health problems.

Several diseases like cardiovascular, neurological and Alzheimer's disease can be induced by a too high level of cellular homocysteine. High level of homocysteine is

called hyperhomocysteinemia and is directly correlated with CBS deficiency. The most common reason for hyperhomocysteinemia is an inefficiency of CBS activity mostly due to mutations in the CBS gene. Nowadays, more than 150 mutations have been described for CBS and all of those ultimately lead to CBS deficiency (Mosharov et al., 2000; Sbodio et al., 2019; Zhu et al., 2018). These too high levels of homocysteine are toxic and disturb the SAM/SAH ratio leading to DNA hypomethylation and abnormal gene expression (Kim et al., 2018). Furthermore, high level of Hcy promotes the production of homocysteine thiolactone produced by methionyl-tRNA synthase (MetRS) misactivation. The thioester group of thiolactone can avidly bind to lysine residues on proteins in a process called N-homocysteinylation. The N-homocysteinylated proteins are prone to aggregate which can explain the ER stress induction by a too high level of homocysteine. Unresolved ER stress is known to induce pro apoptotic genes like CHOP/GADD153 (growth arrest- and DNA-damage inducible gene 153) and TDAG51 (T-cell death associated gene 51) relying the toxic role of too high levels of homocysteine (Jakubowski, 2006; Lai and Kan, 2015; Zhu et al., 2018). Additionally, lack of CBS activity also results in lack of cystathionine production known to have ER stress lowering effects. Maclean and co-workers demonstrate that an induced accumulation of cystathionine by PPG treatment of WT C57/BL6 mice can have a protective role on response to the ER stress inducer tunicamycin (Maclean et al., 2012). Furthermore, preincubation of HepG2 and human embryonic kidney AD290 cells prevent damages induced by tunicamycin demonstrating the protective effect of cystathionine in ER stress conditions.

In vivo experiments were performed in order to determine the phenotypical impact of the transsulfuration pathway. Mice lacking CBS generally die postnatally within the 4 first weeks due to severe hepatic dysfunction, vascular and skeletal abnormalities and display very high level of circulating Hcy. Additionally, CBS mutation leads to several problems ranging from cardiovascular disease to skeletal problems and are further lethal. CSE (mouse homologue of human CTH) KO mice display no severe phenotypical modifications as long as they are supplied by dietary cysteine. Nevertheless, after cysteine starvation, they display the same phenotypical syndrome than CBS KO ones (Combs and DeNicola, 2019; Maclean et al., 2012; Sbodio et al., 2019; Zhu et al., 2018).

IV.3 Transsulfuration and cancer

Glutathione production and changes in DNA methylation are very important for cancer biology. Transsulfuration pathway, which is the edge of that, is deregulated in several cancers and can lead to cancer survival/death. Zhang and co-workers but also Hellmich described an increase in transsulfuration for gastric, colon and ovarian cancer tissue by observing a CBS and/or a CTH overexpression in tumoral tissue when compared to adjacent non tumoral one (Hellmich and Szabo, 2015; Zhang et al., 2015). Furthermore, promoter methylation resulting in CBS silencing and transsulfuration decrease was described for many gastric, colon and hepatocellular cancer cell lines (Combs and DeNicola, 2019; Zhu et al., 2018). Interestingly, Zhu and co-workers described similar results in cancer cell lines and more precisely, a CBS overexpression in cancer cell lines including colon, ovarian, prostate and breast cancer cells (Zhu et al., 2018). Biological roles of CBS and CTH expression for several cancer types have been investigated and show the potential therapeutic role of targeting this pathway.

Some cancer cells are unable to take cysteine from the extracellular environment, like for example breast cancer cells harboring oncogenic PI3KCA (phosphatidylinositol-4,5-bisphosphate 3-kinase catalytic subunit alpha) mutations (E545K or H1047R). Those cells require the activation of the transsulfuration pathway in order to restore intracellular cysteine levels, sustain survival and higher proliferation rates. In physiological conditions, transsulfuration pathway is not sufficient alone to supply the total cysteine needs. However, in some pathological conditions like cancers, the transsulfuration pathway is upregulated, leading to a transsulfuration pathway dependency. Nevertheless, many cancers are supposed to be unable to use the transsulfuration pathway due to a hypermethylation of the CBS promoter (Combs and DeNicola, 2019). The up or down regulation of this pathway is cancer type dependent but, even in the same cancer type, it remains controversial.

In most of the case, transsulfuration pathway helps cancer cells to support their high proliferation rate and oxidative stress conditions. Several studies silenced CBS expression in order to determine its beneficial role for cancer biology. In colon cancer (HCT-116) or ovarian cancer cell line (A2780, SKOV-3), silencing of CBS diminishes cell proliferation, migration, invasion as well as survival. Silencing of CTH expression

leads to similar effects in colon cancer cells (SW480), namely a decrease in cancer cells (Hellmich and Szabo, 2015). In vivo experiments support this result and more precisely, silencing, as well as pharmacological inhibition of CBS, result in reduced tumor growth, reduced proliferation and enhanced sensitivity toward cisplatin treatment of patient derived xenograft (Hellmich and Szabo, 2015).Treatment of mouse xenograft models derivated from breast and colon cancer with Aminooxyacetate (AOAA), a common but not specific inhibitor of CBS (also impacts CTH, 3-MST (3-mercaptopyruvate sulfurtransferase)), was found to exert antitumoral actions (Zhu et al., 2018). In order to determine the real impact of CBS inhibition in tumor survival, Wang and co-workers developed a specific CBS inhibitor called CH004 which has an IC_{50} about 1µM for the hCBS and about 0,6µM for the truncated hCBS (Wang et al., 2018b). Thanks to mutational assay, they could see a total abolishment of CH004 inhibitory effect when CBS is mutated from gln22 to ala22 (mutation Q22A) which cause an increase about 23-fold for CH004 IC_{50}. In vivo experiments demonstrate a 2-fold induction in Hcy in rat haemorrhagic shock models at a dose of 3mg/kg without affecting mean arterial pressure commonly used as CTH indicator demonstrating the possibility of in vivo applications. In vitro, CH004 was able to lower cell proliferation in different cancer cell lines including HepG2 and HEK293T cells as well as colon cancer HCT116 and breast cancer MDA-MB-231 among others. Flow cytometry assay provides the evidence of induction of apoptosis, cell cycle arrest as well as increased levels of ROS for HepG2 and HEK293T treated with CH004. Interestingly, cotreatment with ferroptosis inhibitor, ferrostatin, reversed those effects, demonstrating the induction of ferroptosis by CBS inhibition in liver and kidney cancer cells. For tumor growth experiment, CH004 showed similar results than anticancer drugs Cytoxan with a decrease of 2 times of liver xenograft models without affecting mice weight after 21 days of experiment with treatment at 10mg/kg/day during 12 days showing the therapeutic benefits of CBS inhibition for cancer treatment (Wang et al., 2018b).

To conclude, silencing of enzymes of the transsulfuration pathway leads to a decrease of H_2S production as well as lowering cysteine production resulting in lower mitochondrial activity and more sensibility toward oxidative stress respectively (Hellmich and Szabo, 2015; Zhu et al., 2018). More precisely, lack of transsulfuration activity leads to a decrease in H_2S production which is important for mitochondrial membrane potential and activity. Low H_2S amount results in cytochrome c release and

ultimately to cell death pathway activation (Zhu et al., 2018). Furthermore, decrease in transsulfuration mediated cysteine production also lead to lower GSH and GSSG content as well as ATP production further sensitizes cancer cells toward oxidative stress (Hellmich and Szabo, 2015). Therefore, in response to stress conditions, cancer cells overexpress CBS, like colon cancer cells (HCT-116, HT29, LoVo) and also display a mitochondrial localisation of this enzyme correlated with a higher H_2S production allowing a better stress resistance (Hellmich and Szabo, 2015). Those data are demonstrating that induction of transsulfuration correlates with tumor proliferation, metastasis and resistances suggesting that blocking transsulfuration pathway can be a therapeutic option.

In contrast, some studies support that transsulfuration pathway activation results in anticancer effects and induces apoptosis. Treatment of gastric and colon cancer cells by NaHS (H_2S donor) or inducing CBS activity in order to increase H_2S production were shown to induce cancer cell death. Inversely, lowering H_2S production by inhibiting CTH mediated H_2S production enhances cancer cell viability. The proapoptotic effect of high level of H_2S can be explained by enhancing Bax protein expression as well as decreasing expression of P21, P27 and cyclin D1 (Zhang et al., 2015; Zhu et al., 2018). Another antiapoptotic effect of the transsulfuration pathway is mediated by the use of homocysteine for transsulfuration and not for remethylation. Several cancer cells induce HO/CO dependent CBS inhibition in order to promote remethylation metabolites and promote cancer metastasis (Hishiki et al., 2012). Furthermore, several publications show the role of PI3K/Akt/mTor mediated autophagy and apoptosis induction in response to CBS in HCC (Hepatocellular carcinoma) (Zhu et al., 2018). Those data suggest that inducing transsulfuration pathway could enhance cell death through a too high H_2S production but also a lower flux through remethylation and PI3K/Akt/mTor pathway.

Adding another level of complexity, some cancer cell lines are not sensible to changes in transsulfuration pathway. This is the case for melanoma cells presenting no CBS but a CTH upregulation. However, silencing of CBS or CTH does not affect cellular proliferation of melanoma cancer cell lines (Hellmich and Szabo, 2015; Zhu et al., 2018). Moreover, transsulfuration pathway was shown to be implicated in acquired resistance to doxorubicin in breast cancer cells (MCF-7). Those resistant cells display some changes in sulfur amino acid metabolism, and furthermore, a lower efflux of

homocysteine suggesting a higher consumption of this metabolite. CBS mRNA and protein levels are induced in comparison to the non-resistant counterparts suggesting a higher transsulfuration activity in resistant cells. Ryu and co-workers demonstrate that under amino acid starvation, the treatment of resistant cells with PPG decreases cell viability correlating with the need of a functional transsulfuration pathway for the acquirement of resistant phenotype (Ryu et al., 2011, 2013). However, further understanding of the role of transsulfuration pathway in resistance development needs to be developed.

V) Glutathione metabolism

V.1) Biosynthesis and ROS detoxification

Glutathione (GSH) is a natural tripeptide found at a high level in cells and contributes to the major part of antioxidant defence. This tripeptide is composed by 3 amino acids: glutamate, cysteine and glycine. GSH is synthetized by two successive ATP dependent steps. Glutamate-cysteine ligase (GLC, composed by two subunits: GCLC and GCLM) is the rate limiting enzyme creating a γ-glutamylcysteine group. Then glutathione synthase (GS) links this γ -glutamylcysteine group to glycine to create GSH (Figure 11) (Liu et al., 2014; Traverso et al., 2013). Activity of the rate limiting enzyme GCL is modulated by several cellular stress signals like oxidative stress activation as well as the presence of lipid peroxides. Glutathione is mostly cytoplasmic but is present in all cellular compartments at a lower level (Liu et al., 2014). Cysteine, which is the rate limiting amino acid for GSH synthesis, can be supplied in cells thanks to the diet or protein breakdown in the liver. In case of cysteine restriction, another source can be used by the use of the xCT antiporter or by the transsulfuration as described in the upper section (Hatem et al., 2017).

The major role of GSH is to detoxify reactive oxygen species (ROS) or reactive nitrogen species (RNS) produced by the normal cellular metabolism. Those reactive species are produced in mitochondria during ATP production and are known to induce

damages to several cellular components like lipids, DNA and proteins. GSH can buffer the cellular redox system and is able to detoxify ROS/RNS. Glutathione peroxidases (GPx) are responsible for this detoxification, by catalysing the conjugation of GSH to ROS creating less harmful fatty acids, water and GSH disulphide (GSSG) (Figure 11) (Balendiran et al., 2004; Hatem et al., 2017; Jefferies et al., 2003). Additionally, the glutathione s-transferase family (GST) is known to be implicated in the glutathione mediated detoxification of xenobiotics (Hatem et al., 2017; Jefferies et al., 2003). The GST family members are known to act as homo-, hetero- and less commonly as trimer when activated (Perek and Denoyer, 2002). Glutathione-S-transferase (GST) promote the conjugation of GSH with electrophilic compounds like chemotherapeutic agents (Figure 11) (Hatem et al., 2017; Jefferies et al., 2003). In response to this detoxification metabolism, the total cellular pool of GSH decreases while the GSSG pool increases. However, glutathione reductases (GRs) promote the inverse effect by using NADPH as an electron donor, leading to GSSG consumption to reform active GSH available for other detoxification reactions (Figure 11) (Hatem et al., 2017; Jefferies et al., 2003; Liu et al., 2014). This equilibrium is responsible for the maintenance of the GSH:GSSG ratio which is in favour of GSH. Due to this ability of lowering ROS production and preventing mitochondrial and other types of damages, GSH can prevent cytochrome c leakage from the mitochondria known to induce apoptosis. Furthermore, GSH is known to maintain mitochondrial cytochrome c in a reduced and inactive state further inhibiting apoptosis induction (Jefferies et al., 2003).

Another important way used by the cell to maintain a good GSH biosynthesis is mediated by the glutathione scavenger pathway. This pathway is able to recycle extracellular glutathione into primary amino acids, which are then imported in the cells in order to induce GSH de novo synthesis. Extracellular GSH is degraded by the membrane bound gamma-glutamyltranspeptidase (GGT) responsible of the cleavage of the γ-glutamyl peptide bound, leading to the release of γ-glutamyl and cysteinylglycine moieties (Figure 11). The cysteinylglycine is then cleaved by a dipeptidase (DP) leading to basic amino acid formation which will be imported in the cells. The γ-glutamyl group is then used by γ-glutamylcyclotransferase to produce 5-oxoproline which will be used for the cellular supply in glutamate (Liu et al., 2014).

Almost all genes implicated in glutathione biosynthesis are regulated in response to oxidative stress. This regulation is mediated by the transcription factor NRF2 which is a major regulator of antioxidant defences. NRF2 can bind directly and enhance the expression of GCLC, GCLM, GS and SLC7A11 (Figure 12). SLC7A11 is a cystine/glutamate antiporter (xCT) induced in response to oxidative stress (Figure 13). Under normal conditions, NRF2 is inhibited by Kelch-like ECH-associated protein 1 (Keap1) by direct protein-protein interaction. Under oxidative stress, NRF2-Keap1 binding is blocked, releasing NRF2 which can heterodimerize and become active. This NRF2 heterodimers can enter the nucleus and bind to antioxidant response elements (ARE) present in the promoter region of genes implicated in glutathione metabolism.

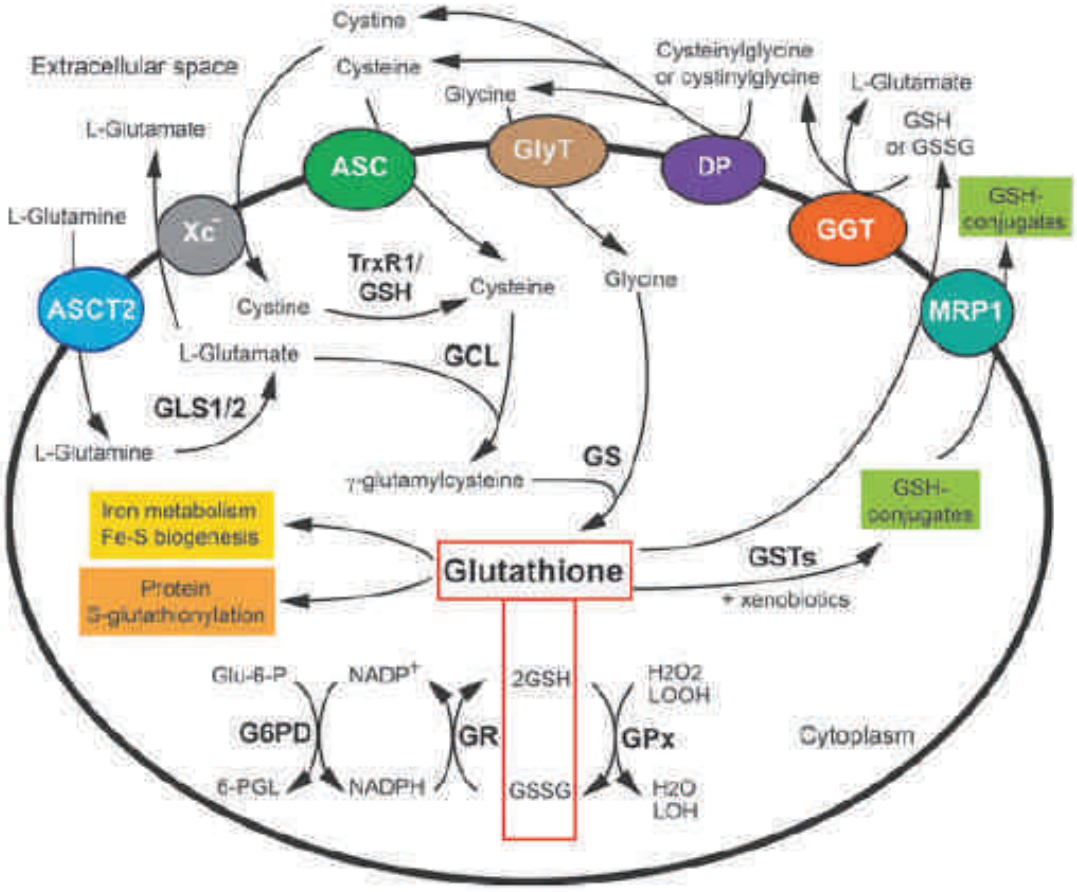

Figure 11: Schematic representation of the glutathione homeostasis
Hatem et al., 2017

V.2) Glutathione and cancer

Nowadays, glutathione is known to play a central role in cancer metabolism due to its multiple roles in detoxification, stress resistance. Cancer cells are also known to produce higher levels of GSH like it's the case for colorectal, lung or head and neck cancer (Liu et al., 2014). More importantly, GSH plays a central role in drug detoxification and participates to resistance mechanisms. Glutathione can be conjugated to several types of anticancer drugs including doxorubicin, cisplatin and oxaliplatin among others. Those S-conjugates can then be exported out of the cell through ATP dependent transporter for detoxification called GS-X pump like MRP1 (multidrug resistance protein 1) (Balendiran et al., 2004; Jefferies et al., 2003; Liu et al., 2014). This mechanism is the major one for drugs detoxification and requires the presence of GSH transferase (GST). This underlines the importance of GSH investigation for drug studies. Those GST are commonly found to be upregulated in several tumoral cell lines with a more important role for some specific members of this family (Hatem et al., 2017).

GST upregulation and polymorphisms are known to be risk factors for several cancers and are further found to be overexpressed in a large panel of cancer cell lines. More precisely, in those cancer cell lines overexpressing GST, polymorphisms in the isoform GSTP1 was the most important one found, for example, in lung, colorectal and gastric cancer. This higher GST expression combined with higher GSH level leads to a more important drug GSH conjugation. Those GSH conjugates can be exported out of the cells through MRP1 (multidrug resistance protein 1) allowing their clearance out of the cells participating to cancer cells resistances (Balendiran et al., 2004; Hatem et al., 2017; Jefferies et al., 2003; Perek and Denoyer, 2002; Tew, 2016; Traverso et al., 2013). Furthermore, resistant cancer cells are also known to display even higher GSH and GSH related enzymes like GCL, GGT and GSH exporting pumps (Perek and Denoyer, 2002; Traverso et al., 2013). Moreover, cancer stem cells are also known to display higher levels of GCL and GS expression resulting in a lower oxidative insult (Liu et al., 2014). As it was described in the upper section, the transcription factor NRF2 can regulate glutathione related enzymes in response to cellular stress. Under basal conditions, the direct binding of NRF2 with Keap1 results in NRF2 inhibition (Figure 12). However, many tumors present NRF2 mutations responsible of preventing

NRF2/Keap1 binding and therefore the NRF2 inhibition leading to constitutive activation of NRF2. In response to NRF2 activation, several glutathione related target genes, like GCL and GS, are overexpressed which are known to favour resistances for cancer cells (Traverso et al., 2013).

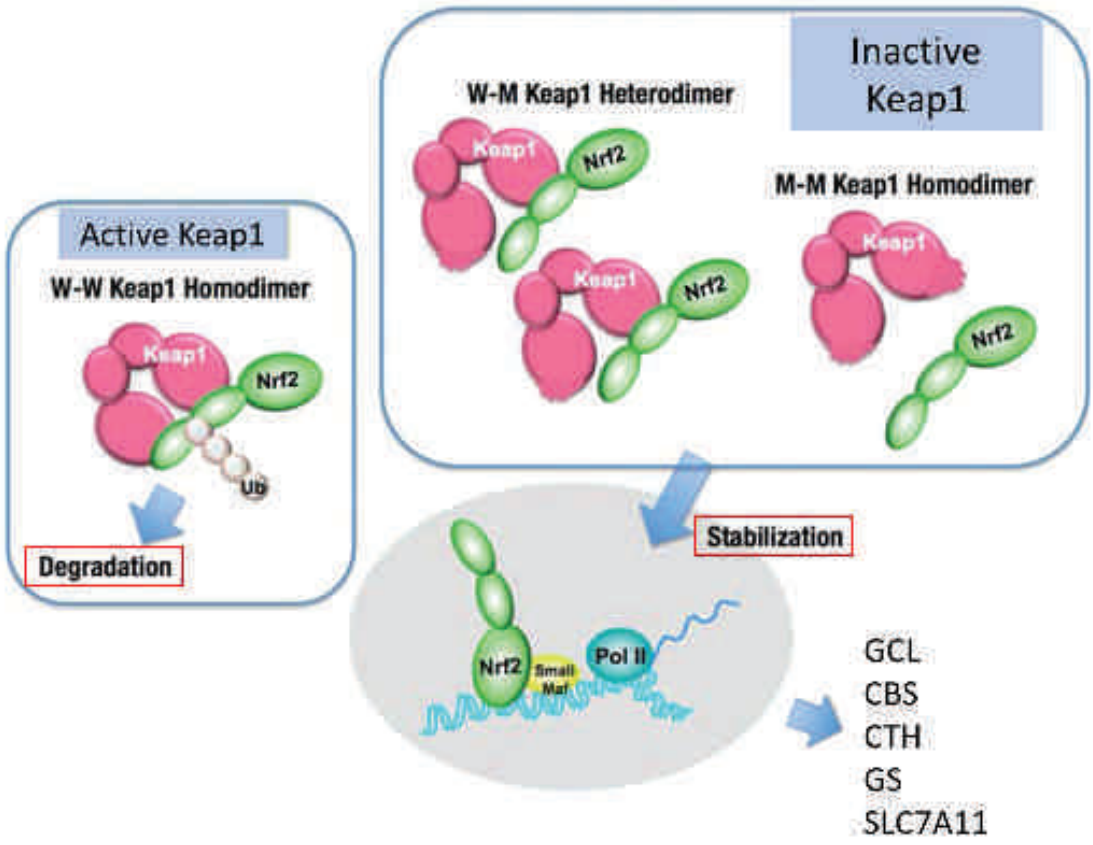

Figure 12: Schematic representation of the NRF2/Keap1 homeostasis. Mitsuishi et al., 2012

That is why lowering GSH levels or inhibiting GST activity before treatment with cytotoxic agent is investigated to sensitize cells to treatment. This would result in decreasing cellular antioxidant defence mechanisms and further increase the oxidative damages induced by anticancer agent in cancer cells. Furthermore, this would lead lowering the export of anticancer drugs resulting in an enhancement of the treatment efficacity. Specific glutathione targeting molecules will be presented in a next section. The use of glutathione for GSH conjugated export is a limiting point for cancer cells due to an important use of the tripeptide for this reaction. Therefore, cancer cells overexpress membrane bound γ-glutamyltranspeptidase (GGT) to release the basic amino acids which are then available for replenishment (Figure 11). It was also seen

that during treatment, cancer cells increase the expression of GGT to enhance their detoxification metabolism linking GGT expression with poor prognosis. Several resistant cancer cell lines display higher level of glutamate/cystine antiporter (xCT) suggesting the importance of GSH mediated detoxification for their survival (Hatem et al., 2017).

Beside this antixenobiotics properties, GST can interact with specific proteins like c-Jun N terminal kinase (JNK). Several anticancer agents induce JNK expression in order to induce apoptosis. However, due to the specific interaction of GSTπ with JNK, JNK is kept in an inactive state rendering cancer cell resistant to JNK activating anticancer agents (Traverso et al., 2013). Another important aspect of glutathione metabolism in cancer is linked to protein regulation and post translational modifications. S-glutathionylation is known to be one of the major posttranslational modification in cells and can regulate kinases and phosphatases activity known to play a central role in redox dependent signalling and therefore important for cancer cells (Tew, 2016). Tew and co-workers provided the evidence of all proteins that can be targeted by s-glutathionylation and further summarize the effect of s-glutathionylation of these prroteins (Tew et al., 2011). Velu and co-workers already demonstrate in cancer cells U87 and HCT116 that s-glutathionylation of P53 leads to lower DNA binding of P53 (Velu et al., 2007). Therefore, GSH levels and protein s-glutathionylation could impact cancer cells response toward platinum-based drugs and leads to resistances (Tew et al., 2011; Traverso et al., 2013; Velu et al., 2007).

V.3) Anticancer therapies targeting metabolic pathways

V.3.1) Therapies

Targeting glutathione metabolism is a central field for the development of new anticancer molecules. Several compounds targeting all the major actors of the glutathione biosynthesis were synthetized with some interesting properties.

Historically, the γ-glutamylcysteine synthase inhibitor BSO (Buthionine sulfoximine) strongly decreasing GSH levels was well studied for the potentiation of

cancer cells to chemotherapeutic agents. BSO is widely used as a selective inhibitor of γ-glutamylcysteine synthase and furthermore is so far the only one tested in clinical trial. In vitro treatment with BSO potentiates the effect of azathioprine, used for the treatment of acute lymphoblastic leukemia, due to mitochondrial deregulation and higher cytochrome c release in hepatocellular carcinoma (Hernández-Breijo et al., 2011). Interestingly, BSO in combination with melphalan showed promising results in clinical trials for neuroblastoma in children and phase III malignant melanoma. It is also described that BSO can enhance the sensitivity of cancer cells to chemotherapeutic agents like doxorubicin. However, the development of such types of cotreatment were stopped due to the short half-life of BSO and it was shown that prolonged infusion results in non-targeted effects of healthy tissue (Balendiran et al., 2004; Hatem et al., 2017; Liu et al., 2014; Townsend et al., 2005; Traverso et al., 2013). Other compounds targeting directly cellular GSH were also under investigation like disulfiram which causes a shift in the GSH:GSSG ratio in favour of GSSG. This leads to a lower GSH content available for drugs detoxification and efflux ultimately leading to less resistance toward chemotherapeutic agents. Phase II clinical trial in patient with metastatic melanoma showed promising effects and was completed in 2016 (clinical trials.gouv, (Traverso et al., 2013)). Moreover, several ongoing studies for the treatment of metastatic breast cancer or refractory tumoral germ cells show the interesting properties of this type of therapies.

Targeting glutathione metabolism can also include other stages of this metabolic pathway like, for example NRF2, glutathione salvage pathway or GST targeting.

NRF2 inhibition leads to cancer sensitization of several cancer cells due to a lower antioxidant response. It was shown that inhibition of the NRF2/HO-1 axis leads to a higher sensibility of neuroblastoma cells to etoposide. Moreover, inhibition of NRF2 by ascorbic acid shows a restored sensitivity of imatinib-resistant cell line KCL22 to this compound. Generally, it is also known that NRF2 depletion by butrasol inhibits tumor growth both in vitro and in vivo (Hatem et al., 2017; Traverso et al., 2013).

Researchers are also looking to target the cystine/glutamate antiporter (xCT) in order to lower cysteine cell supply and glutathione production were studied. For example, Sulfasalazine that inhibits xCT expression was shown to be synergistic with many anticancer drugs to decrease the growth of several tumors in vitro and in vivo (Figure 13).

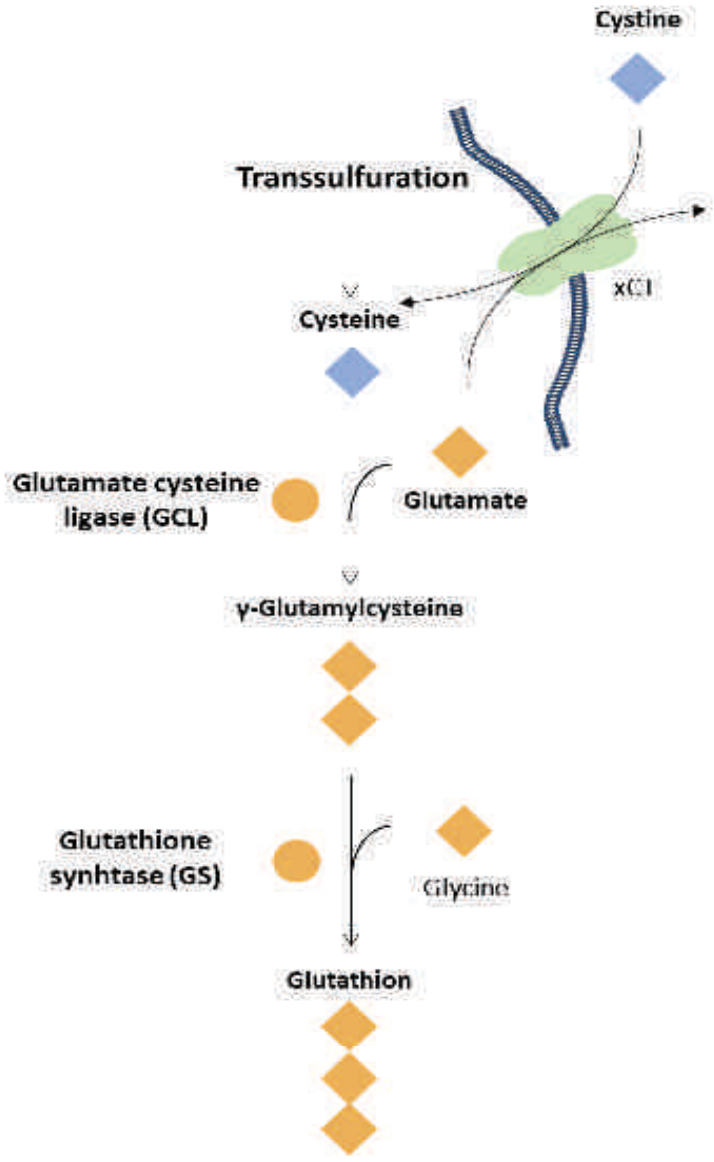

Figure 13: Schematic representation of the cysteine and glutamate homeostasis

Lowering the level of precursor amino acids can also be a therapeutic option like it was shown for glutamate targeting. Glutamine to glutamate transformation is mediated by glutaminase (GLs) which can be inhibited by Bis-2-(5-phenylacetamido-1,3,4-thiadiazol-2-yl)ethyl sulphide (BPTES). This drug was shown to decrease proliferation rates of several cancer cells in vitro and in xenograft models (Hatem et al.,

2017). The role of GGT overexpression in cancer aggressiveness and resistance is well established. For melanoma cells, blocking GGT expression combined with GSH diminution is known to increase oxidative stress mediated cytotoxicity induced by chemotherapies such as doxorubicin, cisplatin, 5FU (Traverso et al., 2013).

One of the most studied aspect of cancer resistances for the last decades was the investigation of drugs targeting GST.

On one hand, the approach is to inhibit GST activity in order to induce chemosensibility. Therefore, ethacrynic acid (EA) is a well-studied compound known to inhibit GST family activity due to a covalent binding to those enzymes. This compound was seen to potentiate cytotoxic effect of anticancer agent in resistant cells by diminishing the impact of GST mediated detoxification. However, EA induces strong side effects and in addition presents diuretic properties limiting clinical applications (Hatem et al., 2017; Townsend et al., 2005). Encouraged by those in vitro results other GST inhibitors have been developed including TER199. This small molecule is known to inhibit GST family and was seen to be a more potent inhibitor of GSTP1-1 frequently overexpressed in cancers. TER199 is more effective than ethacrynic acid and can sensitize cancer cells to chemotherapeutic agents. However, its further development in clinical trial was stopped due to a JNK mediated induction of proliferation in myeloid cells (Kauvar et al., 1998; Townsend et al., 2005).

On the other hand, another approach is to use this GST overexpression in order to activate prodrugs in cancer cells overexpressing these GST. TLK286 is a cytotoxin only activated during GST overexpression. In non-cancerous cells, TLK286 can not be activated due to a too low GST level and is therefore non-toxic and does not induce any side effects. In cancer cells overexpressing GST, the GST mediated prodrugs activation results in the release of more active subparts. Those subparts, analogues of cyclophosphamide, can target several nucleophile moieties by their alkylating properties but also MRP1 for example to sensitize cancer cells to common chemotherapeutic namely platinum-, taxanes- or anthracycline-based therapies. Its sensitizing capacity was proven on several cancer cell lines (Kauvar et al., 1998; Townsend et al., 2005).

V.3.2) Platinum and metallic based therapies targeting glutathione

Platinum-based therapies have proven their efficacy as potent anticancer treatment. New types of platinum-based compounds have been developed in order to induce well described DNA damages and, in addition, to target also glutathione metabolism. NOV-002 is a coordination complex composed by platinum and glutathione tested for sensibilization of cancer cells by diminishing GSH levels and GST activities. More precisely, NOV-002 leads to GSSG stabilization and therefore lowering the GSH level and inducing s-glutathionylation (Hatem et al., 2017; Townsend et al., 2005; Traverso et al., 2013). This s-glutathionylation is able to decrease cell proliferation and invasion in myeloid cell lines and was able to potentiate the anticancer activity of cyclophosphamide in murine colon cancer models. Beside the preclinical investigations, multiple clinical trials were performed showing the interesting properties of this compound like a promising phase III study is completed for advanced NSCLC as well as a phase II for patients with stage IIIb/IV NSCLC (Traverso et al., 2013). Phase II trials showing synergistic effects of NOV-002 with carboplatin were also conducted for breast and ovarian cancer. Those results encourage further studies on NOV-002 but also the development of new platinum-based anticancer molecules with not only a DNA dependant activity, but also with the ability of targeting the glutathione metabolism.

V) Objectives

One of the major challenges remains the development and characterization of new anticancer compounds displaying strong cytotoxic activities without side effects induction. Our group is investigating the mode of action of a specific family of ruthenium-based compounds called RDCs (ruthenium derivate compounds), which display a C-metal covalent bond. RDC11, the lead compound of this family, was shown to induce the ER stress pathway in several cancer cell lines. However, ER stress activation gives not account for the whole cytotoxic potential of our compound. Therefore, the goal of my thesis was to understand more precisely the mode of action of RDC11 and its osmium counterpart ODC2 by investigating several points:

1) To characterize the role of the transsulfuration pathway and determine if it plays a role for RDC11 mediated cytotoxicity.

2) To identify the how RDC11 can regulate metabolic pathways. Therefore, we want to assess the role of the ER stress pathway in RDC11 mediated metabolic regulation.

3) To understand how RDC11 can induce the ER stress pathway.

4) To determine the molecular mechanism giving account for RDC11 mediated cytotoxicity by investigating several cell death pathways including ferroptosis and caspase independent apoptosis.

5) To determine the role of ABCB1 mediated efflux in cancer cell sensitivity towards ruthenium and osmium-based compounds.

Résumé de thèse

Le cancer gastrique reste un problème de santé publique majeur car il possède une forte mortalité (supérieure à 80%) s'expliquant par le diagnostic tardif et de nombreux mécanismes de résistances développés par les cellules cancéreuses. Le traitement de référence est une résection chirurgicale précédée et suivie d'une radiothérapie ou chimiothérapie aux sels de platine (oxaliplatine, cisplatine). Ces composés cytotoxiques exercent leur activité anti-cancéreuse en induisant des dommages à l'ADN. Malheureusement, ces composés génèrent des effets secondaires importants (ex. neurotoxicité). Par ailleurs, l'efficacité de ces thérapies est limitée par le développement de résistances, telles que des mutations de TP53 ou l'amplification de ERCC1 qui altèrent la réponse aux dommages à l'ADN. Malgré ces limites, les sels de Pt restent largement utilisés et sont même associés à des thérapies récentes comme les thérapies ciblées et l'immunothérapie. Toutefois, les résultats de ces combinaisons sont décevants car 1) les thérapies ciblées sont particulièrement sensibles au développement de mécanismes de résistance, 2) la combinaison augmente les effets secondaires, 3) l'efficacité des thérapies ciblées et de l'immunothérapie est conditionnée par les caractéristiques moléculaires de la tumeur, ce qui correspond à un groupe restreint de patients dans le cas des cancers gastriques. Cet échec thérapeutique souligne la nécessité de développer des alternatives thérapeutiques.

Dans ce contexte, une des stratégies poursuivies est la recherche de drogues anticancéreuses avec des métaux autres que le platine. En particulier, le ruthénium (Ru) fait l'objet d'une recherche intensive reposant sur des propriétés physico-chimiques intéressantes comme : 1) une capacité à effectuer jusqu'à 6 liaisons, ouvrant des possibilités de structures spatiales nouvelles, et 2) une large gamme de potentiels redox. Ces propriétés redox, c'est-à-dire la capacité d'échanger des électrons avec son environnement, notamment des composants biologiques, leur permet d'interférer avec des processus biologiques redox de même que produire des radicaux oxygénés réactifs (ROS). Trois complexes de ruthénium (NAMI-A, RM175, KP1019…) ont été testés en phase d'essais cliniques (Bergamo et al., 2012) mais leur développement a été arrêté pour plusieurs raisons : une efficacité insuffisante (in vitro

un IC_{50} > 25µM), une stabilité faible et l'absence de marqueur de stratification permettant de choisir les patients les plus susceptibles de répondre. Ce constat souligne la nécessité d'approfondir nos connaissances concernant les déterminants physico-chimiques et le mode d'action cellulaire des complexes de ruthénium de manière à améliorer leur efficacité et leur donner un statut d'alternatives thérapeutiques crédibles.

Au laboratoire, en collaboration avec M. PFEFFER, une famille de dérivés de ruthénium appelé les RDC (Ruthenium Derived Compounds) et une famille de dérivés d'osmium appelé les ODC (Osmium Derived Compounds) sont en développement préclinique. Ces familles de complexes ont la particularité de présenter une liaison carbone-métal conférant ***une stabilité chimique supérieure*** qui corrèle avec ***une cytotoxicité plus élevée*** (IC_{50}<2µM). Le laboratoire étudie les propriétés biologiques de ces composés intéressants, en particulier au travers d'un complexe représentatif de chaque famille, le RDC11 et l'ODC2. Le RDC11 possède une plus forte cytotoxicité que les dérivés de platine tout en provoquant moins d'effets secondaires chez la souris. Contrairement aux dérivés de platine, le RDC11 induit également certains marqueurs (CHOP, XBP1) de la voie du stress du réticulum (Meng et al., 2009; Vidimar et al., 2012). La voie du stress du RE est normalement activée par un mauvais repliement protéique et conduit, en réponse, à un rétablissement de l'homéostasie protéique intracellulaire, ou alors, à la mort cellulaire (Alasiri et al., 2018). Cette particularité des RDC permet d'expliquer pourquoi ces complexes sont actifs sur des cellules résistantes aux dérivés de platine. Des travaux du laboratoire montrent que l'activation de marqueurs de la voie du stress du RE est également causée par des complexes de ruthénium et d'osmium ayant une structure chimique différente démontrant ainsi que l'activation de la voie du stress du réticulum (SRE) représente un des modes d'action général de ces familles de composés. Par ailleurs, un autre aspect étudié au laboratoire est l'implication de l'efflux de ces composés et le rôle de cet efflux dans la sensibilité de cellules cancéreuses envers ces composés. Cela nous a mené à l'étude de la famille de pompes à ATP, les ABC (ATP-binding cassette) et leur rôle dans l'efflux des composés de ruthénium et d'osmium.

Ces résultats sont très intéressants car ils permettent de mieux appréhender les mécanismes moléculaires sous-jacents aux activités anticancéreuses des

complexes de ruthénium et d'osmium de différentes natures, mais de nombreuses questions restent encore posées. En particulier, il reste à comprendre comment ces complexes induisent les marqueurs de la voie du SRE et quelles sont les conséquences exactes de l'activation de cette voie. En effet, la voie du stress du RE a été également décrite comme régulant l'autophagie et le métabolisme cellulaire.

Le but de ma thèse est d'essayer d'apporter des réponses à ces questions en abordant quatre aspects :

1) Caractériser le rôle d'une voie métabolique, la voie de transsulfuration, dans l'activité cytotoxique des complexes de ruthénium. En effet, une analyse transcriptomique effectuée par le laboratoire indique que certaines enzymes de cette voie sont dérégulées par le RDC11 et le cisplatine de manière différente. Or, cette voie est impliquée dans la synthèse de cystéine et de glutathion et joue donc un rôle important dans la balance survie/mort cellulaire.
2) Identifier les mécanismes moléculaires précis permettant aux dérivés de ruthénium et de platine de réguler l'expression des enzymes de la voie de transsulfuration. De façon intéressante, la voie du SRE, et plus précisément, le facteur de transcription ATF4 a été démontré comme étant capable de réguler l'expression de la CTH, une enzyme de la voie de transsulfuration.
3) Déterminer par quels mécanismes le RDC11 est capable d'induire la voie du stress du réticulum.
4) Déterminer quels sont les mécanismes expliquant l'activité cytotoxique du RDC11
5) Comprendre le rôle des transporteur ABC dans la cytotoxicité des composés de ruthénium et d'osmium.

Les résultats obtenus sur ces différents points nous permettrons de mieux comprendre les propriétés biologiques des complexes de ruthénium et d'osmium ce qui nous permettra d'améliorer ces composés mais également d'identifier des marqueurs prédictifs afin de sélectionner le sous type de patients susceptibles de répondre à ce type de traitement et plus largement aux dérivés de ruthénium et d'osmium.

Implication de la voie de transsulfuration dans l'activité du RDC11

Des résultats du laboratoire ont permis d'observer des dérégulations de voies métaboliques telles que la transsulfuration en réponse au RDC11. L'ensemble des résultats que j'ai obtenu connectent pour la première fois l'activité cytotoxique d'un dérivé de Ru à la dérégulation de la voie de transsulfuration qui est cruciale pour la production de GSH et la survie des cellules tumorales.

En effet, j'ai montré que le RDC11 diminue la synthèse du glutathion (GSH) intracellulaire en réprimant l'expression de la CBS (cystathionine bêta synthase), l'enzyme limitante de la voie de transsulfuration. Pour essayer de compenser cet effet, l'expression de la CTH (cystathionine gamma lyase) est augmentée. Cette activité du RDC11 est opposée à celle des sels de Pt.

De façon intéressante, l'utilisation du BSO (un inhibiteur chimique de la synthèse de glutathion) m'a permis de mettre en évidence que le co-traitement au RDC11 et au BSO, ou à l'oxaliplatine et au BSO, augmente de façon significative l'activité de ces composés, soulignant le rôle du glutathion dans la réponse aux drogues et démontrant ainsi le rôle de la diminution du GSH pour l'activité cytotoxique du RDC11.

Ces résultats ont été démontrés par le biais de plusieurs tests de survie, comme les MTT ou encore le test clonogénique, ce qui renforce d'autant plus la pertinence de ce résultat. Ces résultats prouvent que la diminution de la synthèse de glutathion médiée par le RDC11 participe activement à son activité cytotoxique et que l'augmentation de la production de glutathion par l'oxaliplatine représenterait plus un mécanisme de résistance. Cette première partie a également pu être mise en évidence dans 2 autres lignées de cancer gastrique qui sont les MKN45 (type diffus) et les KATO3 (type intestinal et P53 KO).

Mécanismes de régulation de la voie de transsulfuration par les dérivés de ruthénium et de platine

Je me suis par la suite intéressé aux mécanismes mis en place par le RDC11 et l'oxaliplatine pour réguler la voie de transsulfuration. Le facteur de transcription ATF4, acteur central de la voie du SRE, a été démontré comme capable de réguler

l'expression de la CTH, une enzyme de la voie de transsulfuration (Dickhout et al., 2012; Mistry et al., 2016). C'est pourquoi, nous nous sommes intéressés au rôle d'ATF4 dans la régulation des enzymes de la voie de transsulfuration médiée par le RDC11. En réduisant l'expression d'ATF4 à l'aide d'un ARN interférent, la répression de la CBS médiée par le RDC11 est totalement abolie, alors que l'induction de la CTH médiée par le RDC11 est réprimée ce qui démontre l'implication d'ATF4 dans cette régulation. De façon intéressante, l'absence d'ATF4 n'impacte pas la régulation de ces enzymes médiée par l'oxaliplatine. Sachant que les dérivés de platine présentent des modes d'action P53 dépendent, je me suis également intéressé au rôle de P53 dans la régulation de la transsulfuration. L'augmentation de la CBS par l'oxaliplatine est totalement réprimée lorsque l'on utilise un siRNA dirigé contre P53, alors qu'il n'impacte pas les effets du RDC11 sur cette voie. Dans leur globalité, ces résultats démontrent une disparité des voies de signalisation mises en jeu par le RDC11 et l'oxaliplatine. Dans cette optique, j'ai également voulu confirmer le rôle de P53 dans la régulation de la CBS et mettre en évidence un lien entre l'expression de P53 et de la CBS. C'est pourquoi, je me suis intéressé tout particulièrement à la lignée KATO3 qui est KO pour P53, dans laquelle j'ai pu mettre en évidence que l'expression de la CBS est fortement diminuée en comparaison aux cellules AGS (P53 sauvage) en raison de l'absence de P53. Cependant, je n'ai pas encore pu établir comment ces facteurs de transcription interviennent précisément, et notamment s'ils se fixent directement sur les promoteurs de la CTH et de la CBS.

Mécanismes expliquant l'activité cytotoxique du RDC11 dans les cellules de cancer gastrique

1) Mécanismes responsables de l'activation du SRE : rôle des PDI

L'induction de la voie du SRE en réponse aux dérivés de ruthénium est bien décrite dans la littérature (Chow et al., 2016, 2018; Meng et al., 2009; Xu et al., 2015), cependant les cibles directes de ces composés permettant d'expliquer comment ils induisent la voie du SRE ne sont pas connues. Dans l'optique de trouver des cibles directes du RDC11 permettant d'expliquer ce mode d'action, nous avons réalisé une analyse par chromatographie d'affinité en utilisant une matrice de RDC11, suivie d'une

analyse par spectrométrie de masse qui nous a permis de mettre en évidence une interaction entre le RDC11 et 2 protéines disulfide isomérase (PDI) ERdj5 et ERp57. Les PDIs sont des protéines impliquées dans le contrôle du repliement protéique et pouvant ainsi limiter l'agrégation de protéines mal repliées. L'inhibition de ces protéines est connue pour induire un mauvais repliement protéique conduisant à l'activation de la voie du stress du réticulum (Lee and Lee, 2017).

Les premiers résultats que j'ai obtenus suggèrent que le RDC11 diminue de façon générale l'expression d'ERDJ5 et ERp57. De plus, nous avons pu déterminer qu'en absence d'ERDJ5, l'induction d'ATF4 et de la CTH médiée par le RDC11 est légèrement diminuée, ce qui suggère qu'ERDJ5 participe à l'activité de notre composé. Les dérivés de platine répriment de façon similaire l'expression de ces PDI, alors que la tunicamycine augmente leur expression. Ces résultats sont intéressants car ils nous ont permis de mettre en évidence une différence entre l'effet du RDC11 et de la tunicamycine qui est un inducteur classique de la voie du stress du réticulum. Ceci suggère que le RDC11, bien qu'induisant certains marqueurs de la voie de réponse au stress du réticulum endoplasmique, n'induit pas exactement les mêmes mécanismes qu'un activateur classique de cette voie, soulignant son potentiel bénéfice thérapeutique. Cependant, il reste à identifier précisément ces différences.

2) Activation de la production de ROS et rôle d'AIF

Du fait de la diminution du glutathion dans les cellules de cancer gastrique, nous nous sommes focalisés sur la possibilité d'induction d'un stress oxydant en réponse au RDC11. Nous avons pu déterminer que le RDC11 est capable d'induire une importante production de radicaux oxygénés réactifs (ROS) reflétant un fort stress oxydant. Les niveaux d'induction retrouvés sont similaires aux conditions de traitement à l'H_2O_2 (utilisé comme contrôle positif). De façon intéressante, ni la tunicamycine, ni les dérivés de platines ne sont capables d'induire un tel stress, montrant la spécificité du RDC11 pour l'induction d'un tel stress dans les cellules de cancer gastrique. Par ailleurs, une diminution du glutathion cellulaire plus importante par l'utilisation du BSO ne provoque aucune augmentation du niveau de radicaux libres produits, démontrant une induction de ROS indépendant du niveau de glutathion cellulaire. Cependant, il

est probable que la diminution de la GSH favorise la toxicité des ROS produits par le RDC11, mais ceci reste encore à démontrer.

Pour déterminer quel type de mort cellulaire est induite par le RDC11, nous avons réalisé une analyse par cytométrie en flux, qui nous a permis de mettre en évidence une mort cellulaire par apoptose en réponse au RDC11 tout comme aux dérivés de platines. Cependant, la faible induction du clivage de la caspase-3 ainsi que la forte production de ROS et la forte baisse du glutathion, nous a amené à déterminer que les facteurs responsables de l'apoptose caspase indépendante et de la ferroptose sont présents en réponse au RDC11. L'apoptose caspase indépendante est caractérisée par la translocation nucléaire d'une protéine mitochondriale qui est appelée AIF (Apoptosis-inducing factor). Nous avons pu observer que le traitement des cellules AGS au RDC11 est responsable d'une induction de l'expression, mais aussi d'une translocation nucléaire d'AIF. Par ailleurs, cette translocation d'AIF est corrélée avec une augmentation d'un marqueur de dommage à l'ADN qui est la phosphorylation de l'histone γH2AX. Ces résultats prouvent que le RDC11, par son induction de stress oxydant et la diminution de glutathion, permet une translocation nucléaire d'AIF, conduisant au clivage de l'ADN et ainsi à une apoptose majoritairement caspase indépendante. Au niveau de l'induction de la ferroptose, malgré l'induction de ROS et la réduction de GSH cellulaire, l'inhibition de cette voie de mort cellulaire ne modifie pas la cytotoxicité du RDC11 suggérant une absence d'induction de cette voie en réponse au RDC11. La ferroptose nécessitant également une présence de fer, une étude plus approfondie de l'effet du RDC11 sur le métabolisme du fer nous permettrait de mettre en évidence la cause de l'absence de l'induction de cette voie en réponse au RDC11.

Dans leur ensemble, mes travaux ont permis de mieux caractériser le potentiel thérapeutique des composés de ruthénium pour le cancer gastrique et d'améliorer nos connaissances du mode d'action de ce type de composé. Plus précisément, ces travaux mettent en avant l'importance de voies métaboliques telles que la transsulfuration, le taux de glutathion ou le stress du réticulum, dans l'activité de composés organométalliques à base de ruthénium. Ces résultats mettent en évidence une meilleure activité cytotoxique du RDC11 en combinaison avec le BSO (inhibiteur de la synthèse du glutathion) sur des cellules de cancer gastrique. Ainsi, ce type de traitement semble présenter un avantage clinique par rapport aux traitements de

référence à base de dérivés de platine et pourrait de ce fait mener à une meilleure prise en charge des patients.

Importance du métal pour l'activité de composés organométalliques

Une autre partie de mon projet visait à étudier les différences entre les composés d'osmium et de ruthénium et l'implication de l'efflux de ces drogues pour la sensibilité des cellules de cancer du côlon à ceux-ci. Dans un premier temps, nous nous sommes intéressés à l'effet d'un « switch » de métal pour déterminer quel est l'impact du métal sur l'activité de ces composés. Nous avons pu mettre en évidence une activité cytotoxique plus forte pour les dérivés d'osmium (ODC2 et ODC3) en comparaison avec leurs homologues de ruthénium (RDC11 et RDC34) possédant les mêmes ligands. Cette plus forte cytotoxicité a été confirmée par une induction de marqueurs d'apoptose, comme le clivage de la PARP ou encore de la caspase-3, plus important pour les dérivés d'osmium. Appuyant ces résultats, des analyses par cytométrie en flux ont prouvé que le traitement de cellules de cancer du côlon (HCT116) par nos dérivés d'osmium et de ruthénium augmente la population cellulaire en phase G0/G1 témoignant d'un arrêt du cycle cellulaire et de l'induction d'apoptose.

Indépendance à P53 et induction de la voie du stress du réticulum par l'ODC2

Certains composés d'osmium cyclométallés ont été décrits comme incapables d'induire la voie du stress du réticulum, comme le composé que nous allons appeler CL2 (Suntharalingam et al., 2013). De ce fait, nous avons évaluer la capacité de notre composé d'osmium (ODC2) à induire la voie du stress du réticulum. Nous avons mis en évidence une induction de certains marqueurs comme p-EIF2α et CHOP. En revanche, en accord avec la littérature, le traitement avec le composé CL2 ne permet pas d'induire les marqueurs de cette voie, démontrant ainsi la particularité des dérivés d'osmium en cours de développement dans notre laboratoire (Suntharalingam et al., 2013). Par ailleurs, nous avons mis en évidence que l'ODC2, comme le RDC11 ne requiert pas la présence de P53 pour induire ces effets cytotoxiques. Plus précisément, nous avons observé que la mutation de P53 n'impacte pas l'activité de l'ODC2 dans

les lignées de cancer du NCI. De plus, le co-traitement à la pifithrine, un inhibiteur de P53, ne provoque pas de changement dans l'activité de l'ODC2 confirmant ainsi le caractère indépendant de P53 de l'ODC2.

Rôle d'ABCB1 dans la sensibilité des cellules de cancer du côlon aux RDC et ODC

Dans le but de comprendre pourquoi l'ODC2 est plus cytotoxique que le RDC11, nous avons analysé les lignées de cancer du NCI (National Cancer Institut) et comparé quels sont les gènes qui permettaient de discriminer les cellules sensibles et les cellules résistantes à nos composés. Nous avons mis en évidence que le taux d'expression de la pompe ABCB1 permettait de discriminer les cellules sensibles des cellules résistantes ce qui suggère pour la première fois l'implication de l'efflux dans l'activité de composés organométalliques à base d'osmium et de ruthénium. ABCB1 est un transporteur de la famille ABC (ATP-binding cassette) connu pour être impliqué dans l'efflux de drogues anticancéreuses telles que les platines et ainsi dans la participation à la mise en place de résistance aux platines. L'efflux de composés organométalliques est de nos jours faiblement connu, alors qu'il est connu que l'efflux représente un des mécanismes principaux de résistance aux dérivés de platine (Galluzzi et al., 2012; Martinez-Balibrea et al., 2015; Perek and Denoyer, 2002).
Nous avons observé que la différence de sensibilité entre les cellules résistantes et sensibles, est plus importante pour les dérivés de ruthénium que les dérivés d'osmium suggérant que le RDC11 est plus sensible à la présence d'ABCB1 que ne l'est son homologue l'ODC2. Nous avons pu mettre en évidence par l'utilisation de Vérapamil, un inhibiteur des ABCs, que l'activité de nos composés est augmentée quand ce transporteur est inhibé démontrant pour la première fois le rôle de l'efflux pour ce type de drogue. En corrélation avec les résultats du NCI, nous avons observé une augmentation de l'activité plus importante lors de l'utilisation du Vérapamil pour le RDC11 que pour l'ODC2, confirmant une sensibilité à l'efflux accrue pour le RDC11 que pour l'ODC2. Ces résultats démontrent pour la première fois que des dérivés d'osmium ou de ruthénium peuvent être expulsés hors de la cellule par des transporteurs de type ABCB1 et ouvrent la voie à des études plus approfondies sur la corrélation entre l'efflux d'une drogue organométallique et son activité biologique.

Dans son ensemble, cette deuxième étude a démontré l'importance du métal pour l'activité biologique de composés organométalliques. L'utilisation d'osmium à la place de ruthénium nous a permis d'obtenir des composés anticancéreux possédant une plus forte activité cytotoxique. En corrélation avec une activité cytotoxique plus élevée, nous avons démontré que les dérivés d'osmium sont moins sensibles à l'efflux par les transporteurs ABCs que les dérivés de ruthénium permettant d'obtenir la première explication de ce changement de cytotoxicité. Par ailleurs, cette étude a démontré pour la première fois le rôle des transporteurs ABC dans l'efflux de composés d'osmium et de ruthénium ouvrant un nouveau domaine d'étude pour comprendre l'activité biologique de ce genre de composés.

Durant ma thèse j'ai pu mettre en évidence une dérégulation de la voie de transsulfuration en réponse au RDC11 dans les cellules de cancer gastrique. J'ai pu identifier le rôle de la voie du stress du réticulum et plus précisément d'ATF4 dans ces régulations. Les dérégulations de la voie de transsulfuration induisent par la suite une diminution du taux de glutamate cellulaire liée à une forte baisse de la production de glutathion. Par ailleurs, en parallèle de cette baisse de glutathion, j'ai pu mettre en évidence une forte induction de stress oxydant conduisant à une translocation nucléaire du facteur AIF reflétant l'induction d'une mort cellulaire par apoptose caspase indépendante. J'ai également mis en évidence pour la première fois que les dérivés organométalliques sont sujets à l'efflux par le transporteur ABCB1. L'efflux de ces composés reflète les différences obtenues pour les activités cytotoxiques de ces composés démontrant l'importance de ce mécanisme dans la sensibilité envers ce type de drogue.

Results (Objectives 1, 2 and 3)

Targeting glutathione metabolism in gastric cancer: A non-conventional target for ruthenium-based compounds.

Contexte et apport scientifique de l'article

La prise en charge standard des patients atteints de cancer est basée sur une chirurgie associée à une chimiothérapie néoadjuvante. Cette chimiothérapie, à base de dérivés de platine, a pour but de cibler l'ADN pour conduire les cellules cancéreuses à la mort. Depuis plus de 50 ans, ce type de chimiothérapie est considéré comme « gold-standard » du fait de sa bonne cytotoxicité. Cependant, de part ce mode d'action non-spécifique, les dérivés de platine induisent des effets secondaires très importants conduisant, dans les cas les plus prononcés, à l'arrêt du traitement. Un autre aspect négatif associé à ces dérivés de platines est la mise en place de nombreux mécanismes de résistance limitant leur efficacité.

Dans l'optique de développer des composés anticancéreux présentant une activité au moins similaire aux dérivés de platine, tout en limitant les effets secondaires et la mise en place de mécanismes de résistance, d'autres organométalliques sont en cours d'investigation, parmi lesquels les dérivés de ruthénium.

Ces dérivés présentent des caractéristiques intéressantes telles que i) la possibilité de créer 6 liaisons autour de l'atome de ruthénium, ii) avoir une large gamme de potentiels redox, iii) une charge variable (de 0 à +3), iv) la possibilité de créer des prodrogues et v) leur capacité à être importés dans les cellules par les transporteurs du fer (Bergamo *et al.,* 2011, Klajner *et al.,* 2014). Certains composés comme le KP1019 a montré une activité anticancéreuse intéressante en phase II d'essai clinique, cependant leur développement est ralenti par un manque de connaissance sur leur mode d'action.

C'est dans ce but que nous avons, au laboratoire, développé et caractérisé une famille de dérivés de ruthénium particulière appelée RDC qui est caractérisée par une liaison C-Ru. Le composé phare de cette famille, le RDC11, présente une activité cytotoxique supérieure aux dérivés de platine dans de nombreuses cellules cancéreuses notamment corrélée avec l'induction de la voie du stress du réticulum (SRE). Cette activation de la voie SRE a été observée par l'induction de plusieurs marqueurs de cette voie comme XBP1s et CHOP. De plus, nous avons démontré que le RDC11 est également capable de générer un stress oxydant participant également à l'induction de la mort cellulaire. Cependant, ces modes d'actions ne permettent pas

d'expliquer en totalité l'activité cytotoxique de notre composé c'est pourquoi nous nous sommes intéressés davantage au mode d'action du RDC11 afin de lui permettre d'entrer en essai clinique et améliorer la prise en charge des patients.

Pour approfondir nos connaissances sur le mode d'action du RDC11, nous avons réalisé une analyse transcriptomique qui nous a permis d'identifier des voies cellulaires dérégulées par le RDC11 (et non par le cisplatine), parmi lesquelles nous avons retrouvé des voies du métabolisme cellulaire. Parmi ces voies dérégulées, la voie de transsulfuration a particulièrement retenu notre attention de par son implication dans la survie et la mort cellulaire, mais également de par son implication dans la biosynthèse du glutathion qui est un antioxydant majeur connu pour induire des mécanismes de résistance envers les chimiothérapies dites classiques.

Le but de ce projet était de déterminer le rôle du métabolisme cellulaire dans l'activité anticancéreuse du RDC11 en se focalisant sur la voie de transsulfuration et de biosynthèse du glutathion. Ceci permettra d'améliorer notre compréhension du mode d'action de ce type de dérivés conduisant, à plus long terme, à améliorer la prise en charge des patients.

Ce projet a permis de mettre en évidence pour la première fois des dérégulations métaboliques induites par un dérivé de ruthénium (RDC11) sur des cellules de cancer gastrique. J'ai mis un évidence une répression spécifique de la CBS médiée par la voie du SRE notamment par l'action répressive d'ATF4 sur cette enzyme. Cette répression conduit à une diminution du flux à travers la voie de transsulfuration, conduisant à une forte diminution de la biosynthèse du glutathion. J'ai également pu valider que, dans les cellules de cancer gastrique, le RDC11 est capable d'induire un fort stress oxydant. J'ai également mis en évidence que ces forts taux de stress oxydant, associés à de faibles taux cellulaires de glutathion, conduisent à l'induction de l'apoptose caspase indépendante représentant un nouveau versant de l'activité cytotoxique de ce composé. Cette étude est la première décrivant le rôle du métabolisme cellulaire dans l'activité anticancéreuse de dérivés organométalliques à base de ruthénium et, de ce fait, à améliorer notre compréhension du mode d'action du RDC11. Par ailleurs, cette étude démontre également que ces résultats peuvent être extrapoler à d'autres dérivés de ruthénium présentant des structures tout à fait différentes démontrant la relevance de ces régulations décrites.

Targeting glutathione metabolism in gastric cancer: A non-conventional target for ruthenium-based compounds.

Riegel G.,[1] Orvain C.,[1] Barthe A.,[1] Schleiss C.,[1] Venkatasamy A.,[1] Poschet G.,[2] Yamamoto M.,[3] Nomura S.,[4] Tetsuya T.,[5] Pfeffer M.,[6] Mellitzer G.,[1$] Gaiddon Christian.,[1$]

[1] Université de Strasbourg, Inserm, UMR_S1113 IRFAC, Laboratory "Streinth" (Stress Response and Innovative Therapies), Strasbourg, France

[2] Centre for Organismal Studies (COS), University of Heidelberg, Heidelberg, Germany

[3] Department of Pathology, Nippon Veterinary and Life Science University, Tokyo, Japan

[4] Department of Gastrointestinal Surgery, Graduate School of Medicine, The University of Tokyo, Tokyo, Japan

[5] Department of Pathology, Graduate School of Medicine, Fujita Health University, Toyoake, Japan

[6] Institut de Chimie, UMR7177, Laboratoire de Synthèses Métallo-Induites, Strasbourg, France

Keywords: RDC11, ER stress, Transsulfuration, Glutathione, Caspase-independent apoptosis, Metabolism

[$]Corresponding authors: Christian Gaiddon, gaiddon@unistra.fr; Georg Mellitzer, mellitzer@unistra.fr

The authors declare no potential conflicts of interest

Abstract

Ruthenium-based compounds are considered as promising candidates to replace gold standard platinum-based drugs known to be resistant prone and to induce strong side effects. Unfortunately, their clinical development is slowed down due to a still poorly characterized mode of action. The lead compound of the RDC family, RDC11 was demonstrated to induce stronger cytotoxic activity than platinum-based drugs while inducing lower or no side effects in mice. In addition, previous studies provided the evidence that RDC11 display different mode of action than classical platinum-based compounds. RDC11 displays a P53 independent mode of action and interacts with other targets than DNA like PHD2 and histones. Furthermore, RDC11 induces its cytotoxic activity through the induction of the ER stress pathway. However, it has not been demonstrated yet through which type of cell death RDC11 displays its cytotoxic activity. In this study we could confirm that RDC11 mediates ER stress induction in gastric cancer cells and further characterize an ER stress dependent effect on cancer metabolism. Here, we highlighted an RDC11 mediated ATF4 induction resulting in a CBS repression, which is the rate limiting enzyme of the transsulfuration pathway. In addition, RDC11 strongly decrease glutamate levels further leading to a drastic decrease of GSH production. RDC11 was also able to induces an important oxidative stress in gastric cancer cells and further leads to nuclear AIF translocation demonstrating the induction of caspase independent apoptosis in response to RDC11. Interestingly, we provided the evidence of similar effects mediated by structurally different ruthenium-based compounds suggesting that those regulations could be a more general mode of action for other ruthenium-based compounds. This study provides a more precise understanding about RDC11 mode of action regarding its effect on central metabolic pathways namely transsulfuration and GSH biosynthesis.

Introduction

For several years, the implication of transition metal in the development of anticancer compounds prepared the way for the development of a whole new generation of drugs. The most well-known are cisplatin and oxaliplatin use for the treatment of many different cancer including lung, breast, colon, and gastric cancers. The principal mode of action of the platinum-based compounds is to target DNA inducing cell cycle arrest and apoptosis (Puigvert et al., 2016). However, although this mode of action is frequently very efficient in killing cancer cells it is flawed by its mode of action as it is not specific for cancer cells targeting also normal healthy tissues. Consequently, platinum base anti-cancer drugs are known to induce strong side effects, like neuro- and/or renal-toxicity or bone marrow-suppression, forcing sometimes clinicians to stop the treatment. Another drawback of platin-anti-cancer drug is that their efficacy is often defied by cancer cells through intrinsic or acquired resistance. These resistances can be due to several mechanism including reduce cellular drug uptake, enhance DNA damage repair mechanism, or overproduction of glutathione for detoxification (Galluzzi et al., 2012; Hatem et al., 2017). To overcome these flaws of platinum-based anti-cancer drugs other transition-metals like gold, osmium, or ruthenium are investigated (Bergamo et al., 2012) and have entered clinical trials. For example, the ruthenium-based compounds NAMI-A, KP1019 or RM175 have entered phase I/II clinical trials, showing high anti metastatic activity, and a high cytotoxic effect against different cancers (Bergamo et al., 2012, Zeng et al., 2017). When compared to platinum ruthenium-based compounds have completely different characteristics i) they can hold 6 covalent bonds giving the possibilities to attach a multitude of ligands increasing the library that can be synthetized, ii) they have a wide range of redox states, iii) they can be under different charges (from 0 to +3), iv) and can form prodrugs according to their capacity to exchange ligands, v) and they can be transported into cancer cells through iron transportation mechanism (Bergamo et al., 2012; Klajner et al., 2014). Nevertheless, the progression of new ruthenium-based anti-cancer drugs into clinal trials has been slowed down mainly due to their still poorly characterized mode of action. In this respect, over the past years we have developed and studied in our lab a new family of ruthenium compounds called RDCs, which are characterised by a C-RU (Leyva et al., 2007). These compounds also display the ability to interact with some redox enzymes impacting on cellular metabolism (Meng et al., 2009; Ryabov et al., 2005). One of our lead compound RDC11 displays a greater cytotoxicity in comparison to cisplatin (IC_{50} between 1 and 5µM), does not generate cross resistance with platinum compounds and diminished tumour growth in a xenograft mouse model, without inducing liver, or neurologic side effects (Bergamo et al., 2012; Meng et al., 2009; Vidimar et al., 2019). Our subsequent studies to characterise its mode of action showed that RDC11 can in U87 (glioblastoma cells), TK6 and NH32 (lymphoblastoid cells) (Meng et al., 2009) induces some markers of the endoplasmic reticulum (ER) stress pathway like BiP, XBP1s and Chop (Meng et al., 2009), which correlated with the cytotoxicity of the compound. Additionally, we also have shown than RDC11 induces the production of oxygen reactive species, which participates to its cytotoxic

effect (Vidimar et al., 2019). However, this mode of actions cannot totally give account for the cytotoxic activity of the compound. To get further into the mode of action of RDC11 we have recently performed on RDC11 treated U87 cells a transcriptomic analysis revealing the ability of RDC11 to regulate the transsulfuration pathways, a metabolic pathway implicated in the synthesis of cysteine and glutathione (Licona et al., 2017; Sbodio et al., 2019). In this study we provide the evidence that RDC11 and Oxaliplatin differently impact on the transsulfuration pathway regulating glutathione production. We demonstrate that the impact of RDC11 on the transsulfuration pathway is specifically mediated by the repressive effect of the transcription factor ATF4 (ER stress pathway) on CBS resulting in low cellular glutathione levels, increased ROS production and induction of an AIF linked caspase independent apoptosis.

Materials and Methods

Chemicals

RDC11 was synthesized and purified according to a previously described technique (Gaiddon et al., 2005). Tunicamycin was purchased from Santa Cruz Biotechnology. Cisplatin and oxaliplatin were purchased from Accord Healthcare France SAS and Hospira France respectively.

Cell cultures

Both intestinal types of gastric cancer cells AGS and KATOIII cells were obtained from ATCC. The diffuse type cells MKN45 were acquired by Riken® (RCB1001). The cells were cultured in RPMI medium with 10% FBS (Dominique Dutcher^{TM}) and 1% Penicillin + Streptomycin (Sigma) at 37°C with 5% CO2 atmosphere. YTN16 cells were obtained from Dr Tsukamoto in Japan. The cells were cultured in DMEM medium with 10% FBS, 1% Penicillin + Streptomycin, 1% Glutamine and MITO+ on collagen coated culture dishes. All experiments were conducted by comparing the treatment (RDC11, tunicamycin, oxaliplatin, cisplatin) to non-treated cells.

In vivo tumor growth

C57BL/6 mice (6-weeks old) were injected subcutaneously with 15 x 10^6 YTN16 cells and matrigel solution. After tumor formation, tumors were harvested and reinjected into a new group of mice. Injections of RDC11 (8µmole/kg), Oxa+5FU (10mg/kg) and RDC11+BSO (8µmole/kg and 600mg/kg) started when tumors were palpable (100 mm3) and were performed intraperitoneally once a week. Tumor volumes were measured using caliper. Solutions were prepared in PBS/5% Cremophore. Data are representing the difference between the beginning and the end of the experiment in percentage. Control group was injected only with vehicle (PBS/5% Cremophore). Drugs effect was statistically different ($p < 0.05$) compared to the control, as calculated by a student t-test. Animal experiments have been approved by the regional ethic and animal welfare committee, are performed by authorized and trained personnel and

hosted in an animal facility with the necessary mandatory administrative authorizations.

siRNA silencing

ATF4 and P53 siRNAs against human ATF4 and P53 were purchased form Invitrogen ID n°122372 and designed from Eurogenetec respectively. SiRNAs were transfected in cells using Lipofectamine RNAimax (Invitrogen) as described by invitrogen.

MTT cell survival assay

1.10^4 cells were seeded per well in 96-well microplates (Falcon Multiwell) 24h prior to any treatment. RDC11, tunicamycin, oxaliplatin, and cisplatin were applied for 48h in fresh medium. MTT assay was performed as previously described by replacing medium with fresh one for 2h supplemented with 5 mg/mL MTT (Sigma). MTT medium was removed and the formazan crystal was then dissolved with an adjunction of 100µl of DMSO (dimethyl sulphoxide VWR Chemicals) per well. Measurements were performed at 590 nm with Tristar² Multimode Reader LB942 (Berthold Technologies®).

Clonogenic assay

AGS cells were plated in 6-well plates 24h prior to any treatment. RDC11, tunicamycin, oxaliplatin, and cisplatin were applied for 24h in fresh medium. After the treatment, cells in every condition are counted and 1.10^3 cells were seeded in 3004 plates for 8 days. After this delay, cells were fixed with 4% PFA during 20 min. After one PBS wash, cells were incubated with violet crystal (0,1% filtered) during 20 min. Colonies were counted manually and reported to the control condition.

Flow cytometry of cell death

Cell apoptosis was evaluated using FITC annexin-V Apoptosis detection kit and propidium iodide (PI) (both from BD Pharmingen, BD Bioscience, San Jose, CA, USA). Cells (10^6) were washed in phosphate-buffered saline (PBS) and re-suspended in annexin buffer before the addition of FITC annexin-V and incubated for 20 min on ice in the dark. PI was then added for 5 min before flow cytometry analysis. DAPI (Sigma-Aldrich; Missouri, USA) was also used to analyse cell viability.

Quantitative reverse transcription PCR

Cultured cells were lysed with 1ml of TRIzol (Invitrogen) and RNA was extracted according to the manufacturer's instructions. RNA samples were isopropanol-precipitated and ethanol-washed twice. 2 µg was used for reverse transcription (High-Capacity cDNA Reverse Transcription Kit, Applied Biosystems). qPCR was performed with cDNA previously diluted 10 times SYBR Green mix (SYBR Green PCR Master Mix, Applied Biosystems) and with 500nM of each primer according to the manufacturer's instructions. The relative expression was calculated using the ΔΔCt method. Expression levels were normalized using average of TBP.

Western blotting

Cells were lysed with NP40 Lysis Buffer (50mM TrisHCl pH 7,5, NaCl 150 mM, NP40 1%). 30µg of proteins were denatured and deposited into a SDS-PAGE gel. Western blotting was performed using antibodies against CTH (clone F-1, Santa Cruz Biotechnology®, 1/1000), ATF4 (clone W16016A, BioLegend ®, 1/500), CHOP (L63F7, Cell Signaling, 1/1000), XBP1s (Clone 143F BioLegend) P53 (DO-1 sc-126 Santa Cruz ®), cleaved caspase-3 (D175 Cell Signaling ®) and CBS (G1 sc-271886 Santa Cruz ®). Secondary antibodies (anti-rabbit, anti-rat, anti-mouse: Sigma, MA) were incubated at 1:1000 or 1:5000 depending on the primary antibody. Loading was controlled with GAPDH (purified in the lab).

Glutathione production measurement

AGS cells were seeded in 6-well plates and treated for 24h. After the treatment, cells were harvested and the glutathione production was measured with the glutathione detection kit provided by Enzo life sciences. The experiment was performed as described by the provider.

Ros production measurement

AGS cells were seeded in black 96-well plates and treated for 6h. After the treatment, cells were incubated with a solution of PBS, 10% FBS and 50µM of dihydroethidium for 30min. Photos are taken with a fluorescent microscope and positive cells were counted.

Immunofluorescent staining

Cells were seeded in 6-well plates and treated the day after with the indicated agents for 6h. Cells were stained with a rabbit anti-AIF (H-300 sc-5586 Santa Cruz) antibody 1:1000 and a mouse anti-phospho-Histone-H2AX (05-636 Merck) 1:250. Cells were stained with secondary antibodies goat anti-rabbit Alexa 488 and with a goat anti-mouse Alexa 565 1:1000. Nuclei were labelled with a DAPI solution (1/40000) for 10 min. Pictures of cells were taken with a Zeiss Axio Imager M2-Apotome2 fluorescence microscope coupled to a Hamamatsu's camera Orca Flash 4v3.

Analysis of metabolites

Free amino acids and thiols were extracted from 4 x 10^6 cells starting material with 0.35 ml of 0.1 M HCl in an ultrasonic ice-bath for 10 min. The resulting extracts were centrifuged twice for 10 min at 4°C at 16.400 g to remove cell debris. Amino acids were derivatized with AccQ-Tag reagent (Waters) and determined as described in Weger et al., 2016. Free Cys was quantified by reducing disulfides with DTT followed by thiol derivatization with the fluorescent dye monobromobimane (Thiolyte, Calbiochem). Derivatization was performed as described in Wirtz et al., 2004. UPLC-FLR analysis was carried out using an Acquity H-class UPLC system. Separation was achieved with

a binary gradient of buffer A (100 mM potassium acetate, pH 5.3) and solvent B (acetonitrile) with the following gradient: 0 min 2.3 % buffer B; 0.99 min 2.3 %, 1 min 70 %, 1.45 min 70 %, and re-equilibration to 2.3 % B in 1.05 min at a flow rate of 0.85 ml min^{-1}. The column (Acquity BEH Shield RP18 column, 50 mm x 2.1 mm, 1.7 µm, Waters) was maintained at 45°C and sample temperature was kept constant at 14 °C. Monobromobimane conjugates were detected by fluorescence at 480 nm after excitation at 380 nm and quantified using ultrapure standards (Sigma). Data acquisition and processing was performed with the Empower3 software suite (Waters).

Statistical analysis

All statistical analyses were performed by using Prism 6 (GraphPad Software). Statistical significance was determined by the Student t test and the minimal level of significance was $P < 0.05$.

Results

1) RDC11 induces cell death in a p53 and caspase 3 independent manner in gastric cancer cells.

Previous results of our lab suggested that RDC11 induces the ER-stress pathway but the underlying mechanism and its importance in the cytotoxicity has not been studied. To address these questions, we first tested the cytotoxicity of RDC11 on different human gastric cancer cells lines and compared it to tunicamycin and oxaliplatin (Fig. 1A). The latter is frequently used in clinics for the treatment of gastric cancer patients. In general, in all three tested cells lines the IC_{50} of RDC11 was lower than the IC_{50} of oxaliplatin. In addition, in MKN45 and KATOIII its IC_{50} was similar to that of tunicamycin whereas it was higher in AGS cells (Fig 1A). Interestingly, in a clonogenic survival assay RDC11 was as efficient as oxaliplatin in inhibiting colony formation whereas tunicamycin only let to a decrease in colony size (Fig 1B). To test it in vivo anti-cancer activity we used a syngeneic gastric cancer mouse model (Fig 1D), namely YTN16 cell line, which was derived from a mouse gastric tumour (Yamamoto et al., 2018). We firstly assess the cytotoxic potential of RDC11 and oxaliplatin on the YTN16 cell line. RDC11 displays again a lower IC_{50} than oxaliplatin (Fig 1C). YTN16 cells were injected subcutaneously and when tumours reached $50mm^3$ mice were treated with RDC11, the standard treatment protocol for gastric cancer oxaliplatin together with 5FU. When tumours of the untreated control group reached a tumour volume of around $500mm^3$ the experiment was stopped, and tumour volume compared in the three groups. This showed that RDC11 drastically inhibited tumour growth, with even a complete disappearance of the tumour in two cases (Fig 1D). We performed then FACS (Fig 1E) and Western blot analyses for the expression of cleaved caspase 3 (Fig 1F) to further pinpoint down the cell death pathway induced by RDC11. RDC11 and tunicamycin treatment induced a strong accumulation of cells being in an early apoptotic phase

(annexin V positive) when compared to oxaliplatin (Fig 1E). Interestingly, whereas tunicamycin and cisplatin induced cleaved caspase 3 expression already after 24h and more strongly after 48h of treatment, cleaved caspase 3 expression was almost undetectable in RDC11 treated cells even after a high concentration (IC_{75}) after 48h (Fig 1F). In addition, RDC11 induce cell death seemed to be independently of p53 induction (Fig 1G). Taken together, these results suggest that RDC11 mostly induces a p53 – caspase 3 independent cell death pathway.

2) RDC11 induces the expression of ATF4

We have previously shown that RDC11 induces the expression of components of the ER stress pathway IRE1α, XBP1 and CHOP respectively, in the mouse melanoma cell line B16F10 similarly to tunicamycin a known induction of ER stress (Chow et al., 2018; Licona et al., 2017; Meng et al., 2009). In the human gastric cancer cell line AGS RDC11 strongly induced the expression of XBP1s and CHOP whereas oxaliplatin and cisplatin had no effect (Fig 2A). Importantly, RDC11, like the ER stress inducer tunicamycin, strongly induced the expression of ATF4 (Fig 2B, C), which regulates the expression of CHOP, whereas oxaliplatin and cisplatin again failed to do so.

Taken together, these data confirming our previous observation that RDC11 is a strong inducer of the different components of the ER stress pathway.

3) RDC11 inversely regulates the expression of CBS and CTH two enzymes in the transsulfuration pathway.

ATF4 is known to regulate several genes involved in amino acid transport and metabolism in order to induce the integrated stress response (ISR). Notably, ATF4 was shown to directly regulate the expression of the cystathionine γ-lyase (CTH) linking the activation of the ER-stress pathway to the transsulfuration pathway responsible for the de-novo production of cysteine and glutathione production.

To investigate if RDC11 via the activation of ATF4 impacts on the transsulfuration pathway we first analysed for the expression of CTH by RT-qPCR and Western blot in AGS cell which were treated with different concentrations of RDC11, tunicamycin, oxaliplatin and cisplatin for 6h or 24h (Fig 3B, C). This showed that RDC11, like tunicamycin, strongly increased the expression of CTH at the RNA and protein level, whereas oxaliplatin and cisplatin had only a very minor (6h) or even repressive (24h) effect (Fig 3B, C). These results suggest that RDC11 via the activation of ATF4 impacts on the expression of CTH and consequently increasing glutathione production (Fig 3A). However, in the transsulfuration pathway the “rate limiting step” is the conversion of homocysteine to cystathionine by the cystathionine beta synthase (CBS) (Fig 3A).

AGS cells were treated with RDC11, tunicamycin, oxaliplatin and cisplatin at the indicated concentrations for 6h or 24h and expression of CBS was then analysed by RT-QPCR and Western blot. Interestingly, in contrast to CTH expression, CBS protein expression was completely lost after 6h of RDC11 treatment and maintained to be undetectable after 24h (Fig 3D, E). In contrast CBS expression was induced by tunicamycin, oxaliplatin and cisplatin at the RNA and protein level (Fig 3D, E). Taken together, this suggests that also RDC11 increases the level of CTH expression it at the same time represses the expression of CBS, which is the “rate limiting” enzyme in the transsulfuration pathway.

4) ATF4 and p53 are differently involved in the regulation of CTH and CBS mRNA expression

To further study the role of ATF4 in the transsulfuration pathway, AGS cells were transfected with a siRNA targeting ATF4 and then treated with RDC11, tunicamycin or oxaliplatin for 24h at the IC_{50} (Fig 4A), and CTH and CBS expression analysed by RT-QPCR (Fig 4B, C). The loss of ATF4 expression in AGS cells clearly reduced the capacity of RDC11 and tunicamycin to induce CTH mRNA expression (Fig 4C). Interestingly, loss of ATF4 rescued the repressive effect of RDC11 on CBS mRNA expression and let also to a weak increase of its expression induced by oxaliplatin. In contrast, tunicamycin slightly lost its capacity to induce CBS mRNA expression in ATF4 negative AGS cells (Fig 4C). Taken together, these data supporting published data showing CTH to be a direct target gene of ATF4, but they also suggest that ATF4 might also be directly involved, also differently, in the transcriptional regulation of CBS in response to RDC11, tunicamycin and oxaliplatin.

Although oxaliplatin does not induce ER stress pathways markers like XBP1s, CHOP (Fig 2A) and ATF4 (Fig 2B, C) it induced the expression of the CBS (Fig 3D, E) the rate limiting enzyme of the transsulfuration pathway. In contrast to RDC11, oxaliplatin strongly induces the expression of p53 (Fig 1G and Fig 4D) and as p53 is also implicated in the regulation of different metabolic pathways we investigated its role in the expressional regulation of CTH and CBS mRNA expression in response to the different drug treatments (Fig 4E, F). Inhibition of p53 expression, using a specific siRNA, slightly reduced the capacity of tunicamycin to induced mRNA expression of CTH, whereas it did not alter the inductive or repressive effect of RDC11 and oxaliplatin, respectively (Fig 4E). Interestingly, loss of p53 clearly diminished oxaliplatin induced expression of CBS mRNA, whereas it did not alter the effect of RDC11 or tunicamycin (Fig 4F).

5) RDC11 lowers glutathione production possibly via enhanced cellular glutamate expulsion.

Our results show that RDC11 specifically down regulated the expression of CBS, the "rate limiting" enzyme in the transsulfuration pathway (Fig 3D, E), which should consequently lead to a reduction in cellular glutathione levels (Fig 5 A) the end-point product of this pathway. To investigate this, we treated AGS cells with RDC11, tunicamycin or oxaliplatin at the indicated concentrations and times and measured the cellular concentration of glutathione but also of Glutamate and Cysteine, two amino acids upstream necessary for its production (Fig 5B – D). As expected RDC11 lead to a strong reduction in the cellular glutathione concentration (Fig 5B). In contrast, tunicamycin and oxaliplatin treatment slightly increased cellular glutathione concentration, which is consistent with their positive effect on CBS expression (Fig 3D, E). In addition, inhibition of ATF4 rescued the repressive effect of RDC11 on cellular glutathione concentration and further stimulated it in the case of tunicamycin (Suppl Fig 1), whereas inhibition of p53 had no effect except for oxaliplatin (Suppl Fig 1). Furthermore, RDC11 treatment led also to a strong reduction in Glutamate levels where as tunicamycin and oxaliplatin had no effect (Fig 5C). Likewise, tunicamycin and oxaliplatin had no effect on cysteine levels (Fig 5D). But surprisingly, RDC11 treatment did also not reduce the cellular cysteine levels, which we would have expected as it strongly reduces CBS expression (Fig 5D). It is well known that cellular cysteine levels can be replenished from outside the cells via expulsion of glutamate through the anti-porter xCT, which is encoded by the SLC7A11 gene (Fig 5A). To investigate this, we analysed the expression of SLC7A11 mRNA by RT-qPCR after treatment of AGS cells with RDC11, tunicamycin or oxaliplatin (Fig 5E). This showed that RDC11 and tunicamycin treatment increases the expression of SLC7A11 (Fig 5E) in AGS cells. This suggest, that although RDC11 decreases the expression of CBS, the rate limiting enzyme in the transsulfuration pathway, cellular homeostasis of cysteine is established by the up-regulation of the anti-porter xCT, which however leads to a decrease of glutamate concentration resulting in a decrease in glutathione. In addition, we also analysed the expression of Glutamate Cysteine Ligase (GCL), which ligates glutamate to cysteine to produce γ-glutamylcysteine (Fig 5A). This showed that RDC11 and tunicamycin treatment increases the expression of GCL whereas oxaliplatin decreased it.

6) RDC11 treatment leads to a strong increase in Ros production

It is well known that increased glutathione levels serve to lower oxidative stress. To investigate if RDC11 increases Ros concentrations AGS cells were treated with either RDC11, tunicamycin, oxaliplatin at the indicated concentration or with H_2O_2 know to strongly induce Ros production. Ros production was then analysed by dihydroethidium staining and positive cells counted. This showed that RDC11 strongly induced the percentage of Ros positive cells whereas tunicamycin and oxaliplatin had no effect (Fig 6A B). This strong increase in Ros positive cells is specific to RDC11 as BSO, an inhibitor of GCL, did not significantly increase Ros positive staining in tunicamycin and oxaliplatin treated AGS cells (Fig 6C).

7) Inhibiting the negative effect of RDC11 on the transsulfuration pathway partially blocks its cytotoxic effect.

The strong effect of RDC11 on the transsulfuration pathway prompted us to investigate its contribution in its cytotoxicity we performed a series of clonogenic assays. In the first assay, we transfected AGS with an ATF4 specific or control siRNA and then treated cells prior to the clonogenic assay with RDC11 or oxaliplatin (Fig 7A). As expected, in the siCTL transfected cells RDC11 drastically decreased colony formation even stronger than oxaliplatin. Inhibition of ATF4 expression significantly increased colony formation of the RDC11 treated AGS whereas it did not alter the cytotoxicity of oxaliplatin. Similarly, supplementing the cell culture medium with glutathione rescued colony formation of RDC11 treated AGS cells (Fig 7B). Furthermore, co-treatment of AGS cells with the glutamate-cysteine-ligase (GCL) inhibitor BSO further increased the cytotoxicity of RDC11 (Fig 7C). In contrast, inhibition of p53 expression did not alter the cytotoxicity of RDC11 but decreased the efficiency of oxaliplatin (Fig 7D).

8) RDC11 does not induce ferroptosis but caspase independent apoptosis.

Our observations that RDC11 does not induce cleaved caspase 3 expression (Fig 1F) but induces ER stress, as well as strong reduction of intracellular GSH concentrations and an increase in ROS production suggests that it might either induce cell death through ferroptosis or caspase independent apoptosis. To address the first possibility, we treated AGS cells with increasing doses of RDC11 with or without ferrostatin-1 a known inhibitor of ferroptosis and performed MTT survival assay (Fig 8A). Co-treatment of RDC11 with ferrostatin-1 did not diminish the cytotoxic effect of RDC11 at all concentration tested. This data suggests that RDC11 does not induce ferroptosis but rather caspase independent apoptosis.

Induction of caspase independent apoptosis is marked by the nuclear translocation of AIF leading to DNA damage. To address this, AGS cells were treated with RDC11 or H_2O_2, a known strong inducer of nuclear translocation of AIF, and analysed by immunofluorescence staining for the nuclear translocation of AIF and the expression of p-γH2AX a marker for DNA damage (Fig 8B). As seen in immunofluorescence staining (Fig 8B) and confirmed by our cell counts (Fig 8C) RDC11 treatment led to a marked increase in cells showing a nuclear expression of AIF and p-γH2AX staining. Taken together, these results suggest that RDC11 induces cell death via caspase independent apoptosis.

9) Other ruthenium-based compounds also impact on the transsulfuration pathway.

To investigate if only RDC11 impacts on the transsulfuration pathway or if it might also hold true for other ruthenium-based compounds (RDC) we treated cells with structurally different RDCs compounds and analysed by RT-QPCR and Western blot for their impact on the expression of ATF4, CBS and CTH. When compared to RDC11, from the 3 tested ruthenium compounds 2 showed a similar effect on the transsulfuration pathway. For example, similar to RDC11 treatment of AGS cells with RDC60 (Fig 8A) led to an increase in ATF4 and CTH but a decrease in CBS expression at the mRNA and protein level (Fig 9B, C).

Conclusion

Here we demonstrate that the ruthenium-based anti-cancer compound RDC11 displays a higher cytotoxicity in gastric cancer cells than classical gold-standard chemotherapeutic agents like oxaliplatin. We show that it induces a strong ER stress response and that via induction of ATF4 expression it impacts negatively on one of the key enzymes of the transsulfuration pathway. Furthermore, we demonstrate that RDC11 strongly up-regulates the expression of cystine/glutamate exchanger (xCT) correlating with reduction of cellular glutamate concentrations. The loss of glutamate, a precursor of glutathione (GSH) synthesis, results in a strong reduction of GSH production. Importantly, the negative effect of RDC11 on cell survival can be rescued with the supplementation of glutathione showing that the negative impact of RDC11 on the transsulfuration pathway is one of its principle mode of action. Moreover, RDC11 was able to induce strong levels of ROS correlating with a strong nuclear translocation of AIF. This leads to the activation of DNA cleavage correlating with DNA damage observed by phosphorylation of the histone γH2AX. Altogether, this work highlights the role of ER stress pathway and its interconnection with cellular metabolism for the cytotoxic activity of the RDC11.

Discussion

Unravelling the mode of action of anticancer drugs still represents a great challenge in oncology. Platinum-based gold standard treatment displays good anticancer activity against several cancer types, including gastric cancer. Unfortunately, due to side effects, and frequent resistance mechanism, they do not completely fulfil the needs of clinicians for save and efficient anti-cancer drug. However, their long-lasting success encourages the development new metal-based

anticancer drugs with the aim of avoiding side effects induction and resistances. In this respect, ruthenium- and osmium-based compounds are good candidates due to their interesting cytotoxic capacities and the variety of compounds that can be synthetized. Some ruthenium-based compounds enter clinical trials like NAMI-A and KP1019 (Bergamo et al., 2012; Zeng et al., 2017), however, their clinical development was stopped due to lack of knowledge about their mode of action. A better understanding of their mode of action and the chemical structure responsible for it would ultimately lead to the development of more active and supportable anticancer drugs. In this study we demonstrate the impact of RDC11 on metabolic pathways including transsulfuration and GSH biosynthesis and describe their role for RDC11 mediated cytotoxicity. The repression of these two metabolic pathways observed in response to RDC11 leads to a mitochondrial-dependent induction of apoptosis in gastric cancer.

RDC11 induces a strong ER stress response in gastric cancer cells

We firstly demonstrate that RDC11 displays higher cytotoxic potential in gastric cancer cells correlating with a higher apoptosis induction when compared to oxaliplatin. More importantly, RDC11 decreases more strongly the tumour volume in syngenic gastric xenograft models as oxaliplatin/5FU demonstrating the potential application benefits provided by RDC11. Interestingly, in contrast to classical anticancer drugs like cisplatin and oxaliplatin, RDC11 doesn't induces strong cleavage of caspase-3 nor strong P53 expression suggesting that the classical DNA/P53 dependent mechanism is not its principal mode of action. However, and in contrast to oxaliplatin, RDC11 was seen to induce another pathway important for cell survival called ER stress pathway. We could demonstrate that RDC11 induces the expression of XBP1s and CHOP, which are central actors and markers of ER stress activation. This result is in line with previous work of our group demonstrating an induction of ER stress pathway in response to RDC11 in other cancer cell lines including colon cancer, glioblastoma, and lymphoblastoma (Licona et al., 2017; Meng et al., 2009). This highlights the important role of ER stress induction for the mode of action of RDC11, and an ER stress induction mediated by RDC11 in cancer cell lines of different origin. Together with published data showing the activation of the ER stress pathway by structurally different ruthenium compounds clearly suggest that induce of the ER stress pathway (Chow et al., 2016, 2018; Meng et al., 2009; Xu et al., 2019) might be a general mode of action of these type of anti-cancer drugs. More importantly, we could also validate that RDC11 can induce the expression of the transcription factor ATF4 the upstream regulator of CHOP expression suggesting that the Perk-ATF4 axis is an important branch of ER stress pathway induced by RDC11. Moreover, platinum-based compounds did not induce the ER stress pathway but required the presence of a functional P53 for their cytotoxic activity confirming data published by others (Dasari and Tchounwou, 2014). In contrast, RDC11 did not induce P53 and further P53 silencing didn't impact on the cytotoxic activity of RDC11 confirming the P53 independent mode of action of RDC11. Interestingly, in contrast to RDC11, the activity of platinum-based compound is dictated

by the presence of P53 as well as most of the resistance mechanisms implicate DNA repair mechanisms (Galluzzi et al., 2012; Martinez-Balibrea et al., 2015). Furthermore, it is important to note that RDC11 can induce the expression of CHOP, XBP1s as strongly as tunicamycin a known strong inducer of ER stress markers. However, even if both drugs are able to induce apparently the same type of ER stress, they don't have the same effect on metabolism. According to the literature, the outcome of ER stress activation can differ strongly due to differences in kinetics, and branche(s) of ER stress activated (Hetz, 2012). The ER stress pathway is tightly regulated by the interaction partners of the ER stress sensor. The cytosolic domains of the sensors enable interaction with several activator or inhibitor leading to the formation of a regulation platform called UPRosome. This platform can differ from one situation to another leading to differences in the effects observed by the ER stress induction. In addition, the way of activation of ER stress including misfolded protein accumulation or changes in ER calcium loads can also determine which sensor will be preferentially activated and further decide the cellular outcome (Hetz, 2012). However, how RDC11 induces ER stress has still to be elucidated and knowledge of it would help to dictate the further development of these type of anti-cancer compounds.

RDC11 impacts on cellular metabolism

Our results show that RDC11 induce strong expression of ATF4, a transcription factor known to be implicated in amino acids import and synthesis including cystathionine gamma-lyase, a central actor of the transsulfuration pathway (Dickhout et al., 2012; Mistry et al., 2016). This suggests that RDC11 might impact via ATF4 on the transsulfuration and indeed found that RDC11 increases CTH and represses CBS expression, two key enzymes of the transsulfuration pathway, whereas oxaliplatin showed an opposite effect. Importantly we could demonstrate that ATF4 silencing rescued the repressive effect of RDC11 on CBS expression. Although ATF4 is most commonly known as a transcriptional activator Horiguchi and coworkers demonstrate that when ATF4 interacts with C/EBPα it has a transrepresionnal activity (Horiguchi et al., 2012). Furthermore, the homologous form of ATF4 found in california sea hare, Aplysia CREB2, was also described to have a rather transcriptional repressor function in the nervous system (Bartsch et al., 1995). These published data suggest that in our condition where RDC11 induces ATF4 expression and represses CBS expression in an ATF4 dependent many, ATF4 functions as a transcriptional repressor. Despite the repressionnal activity on CBS, the induction of ATF4 by RDC11 results in an upregulation of CTH expression, as it was shown that ATF4 silencing reduces RDC11 mediated CTH induction. This result is in line with the literature as CTH is known to be a transcriptional target gene of ATF4 (Dickhout et al., 2012; Mistry et al., 2016), and further suggest that depending on the interaction partners of ATF4, the target genes can be upregulated or repressed. In addition, these results demonstrate the importance of ATF4 in RDC11 mediated regulation of the transsulfuration pathway.

CBS is the limiting enzyme of the transsulfuration pathway, and repression of it leads to a lower flux through this pathway (Zhu et al., 2018). Furthermore, transsulfuration is the only way for de novo cysteine production (Combs and DeNicola, 2019; Sbodio et al., 2019) suggesting that RDC11 treatment result in a lower cysteine production. However, metabolomic analysis of AGS cells treated with RDC11 and oxaliplatin didn't confirm this as we found no change in cellular cysteine content after RDC11 treatment. However, this could be explained by our finding that RDC11 increased the expression of xCT antiporter. This antiporter is known to be responsible for cysteine supply, by continuously importing this amino acid from the culture medium while exporting glutamate (Hatem et al., 2017). Interestingly, we demonstrate that RDC11 induces the level of this anti-porter correlating with a strong decrease in glutamate content in gastric cancer cells. Importantly, low levels of glutamate are known to reduce glutathione (GSH) production (Hatem et al., 2017). It is exactly what we see, RDC11 treatment not only reduces glutamate concentrations in the gastric cancer cells but also leads to a dramatic decrease in GSH production. In addition, oxaliplatin induces the GSH production in the same cells. It is well known that high levels of GSH results in a more efficient drug detoxification (Balendiran et al., 2004; Traverso et al., 2013) correlating with the resistance of cancer cells to the treatment with platinum drugs. Therefore, the differences observed for GSH production between RDC11 and oxaliplatin could explain the difference observed in the cytotoxic effect of these two drugs.

Importantly, we could demonstrate that reintroduction of synthetic GSH in the culture medium reduced the cytotoxicity of RDC11 whereas inhibition of CBS activity with BSO increased it. Altogether, the functional analysis demonstrates that the reduction of GSH by RDC11 participates to its cytotoxic activity and the induction mediated by oxaliplatin represents a resistance mechanism toward this drug.

Reduction of GSH production is known to correlated with a Ros insults. Indeed, RDC11 induces high levels of Ros suggesting that due to its ability to decrease GSH production, RDC11, in contrast to oxaliplatin, is able to induce a strong oxidative stress. This result is in line with previous studies demonstrating that oxidative stress is induced by different ruthenium-based compounds like RDC34, RAS-1T, and RAS-1H (Chow et al., 2016; Vidimar et al., 2019). Ros production is an early process already induced at 6h by RDC11 whereas the decrease in glutathione production is only observed after 24h. Several studies, as reviewed by (Hatem et al., 2017; Liu et al., 2014), demonstrate that GSH homeostasis is also controlled by Ros levels due to the detoxification role of GSH. More precisely, GSH in consumed by the cells in order to lower oxidative stress and avoid cell death induction, resulting in lower GSH levels. This might also give account for the GSH reduction mediated by RDC11 as Ros induction is already observed after 6h inducing GSH consumption resulting in GSH reduction later on. The absence of Ros induction by oxaliplatin in AGS cells could be explained by the higher GSH levels induction. However, cotreatment of AGS cells with oxaliplatin and the GSH inhibitor buthionine sulfoximine (BSO) didn't results in a higher Ros production further

suggesting an absence of Ros induction by platinum-based drugs in gastric cancer cells. Interestingly, we could confirm the same type of regulation of ATF4, CBS and CTH expression by structurally different ruthenium-based compounds suggesting that it might be a more general mode of action of these types of drugs further demonstrating the strength of our findings.

RDC11 induces caspase independent cell death

The ability of RDC11 to impact on the transsulfuration pathway and to induce high levels of Ros suggested that it might induce cell death known as ferroptosis (Dixon et al., 2012; Yang et al., 2014). However, when we cotreated AGS cells with RDC11 and ferrostatin-1, a ferroptosis inhibitor, we didn't observe changes in its cytotoxicity. This suggested RDC11 does not induce cell death via induction of ferroptosis. Interestingly, ferroptosis depends on iron and some links between iron and ruthenium import have already been described as it was shown that ruthenium interacts with the transferrin system. For example, Klajner and co-workers (Klajner et al., 2014) demonstrated that RDC34 lowers the expression of transferrin and induces the expression of ferritin, an iron packaging protein. This suggests that RDC34 can impact directly on the iron metabolism. Furthermore, RDC34 was shown to be imported inside the cells through iron transporter and probably taking over the place of normal iron. The effect of RDC11 on iron metabolism should therefore be further investigated in order to understand why RDC11 did not induce ferroptosis and its difference to RDC34.

Importantly, in contrast to cisplatin and oxaliplatin RDC11 didn't induce caspase-3 cleavage prompting us to the investigation caspase independent apoptosis, a cell death pathway characterized by the nuclear translocation of the mitochondrial factor AIF (apoptosis inducing factor) (Bano and Prehn, 2018). Indeed, treatment of AGS cells with RDC11 promoted nuclear translocation of AIF suggesting that this cell death pathway is implicated in RDC11 cytotoxic activity. In addition, we could observe in the same conditions, the phosphorylation of the histone γH2AX known to be a DNA damage marker. In accordance with the literature, when AIF is imported in the nucleus it activates non-specific endonucleases leading to DNA condensation and fragmentation (Bano and Prehn, 2018; Elmore, 2007). It is noteworthy that RDC11 did not induce strong P53 levels suggesting that DNA damage is not the principal mode of action of RDC11. However, in our case where RDC11 treatment leads to AIF nuclear translocation, DNA damage seems more to be the outcome of apoptosis induction. Despite the fact that induction of DNA damage is known to correlate in some cases with induced cell death, more precise analysis are required in order to determine if RDC11 induces, in a AIF dependent manner, endonuclease and if this results in DNA fragmentation contributing to its mode of action or not.

Altogether, this study provides new insides into the mode of action of RDC11 anticancer compound. We highlighted the higher cytotoxic potential of RDC11, correlating with lower side effect as described in previous studies (Meng et al., 2009),

demonstrating the potential benefits of RDC11 over platinum-based compounds. Through the ER stress induction and more precisely through ATF4, RDC11 is able to regulate the transsulfuration pathways leading to amino acids deregulation in glutamate content. Therefore, RDC11 was seen to decrease strongly glutathione levels and induce strong Ros levels participating in its cytotoxic activity. Furthermore, we provided the evidence of caspase independent apoptosis induction showing unconventional cell death pathway activation for RDC11.

Acknowledgements

We are thanking L. Mathern for her administrative support. We want also to thank Metabolomics Core Technology Platform of the Excellence cluster “CellNetworks” (University of Heidelberg) and the Deutsche Forschungsgemeinschaft (grant ZUK 40/2010-3009262) for support with metabolite quantification.

References

Balendiran, G.K., Dabur, R., and Fraser, D. (2004). The role of glutathione in cancer. Cell Biochem. Funct. *22*, 343–352.

Bano, D., and Prehn, J.H.M. (2018). Apoptosis-Inducing Factor (AIF) in Physiology and Disease: The Tale of a Repented Natural Born Killer. EBioMedicine *30*, 29–37.

Bartsch, D., Ghirardi, M., Skehel, P.A., Karl, K.A., Herder, S.P., Chen, M., Bailey, C.H., and Kandel, E.R. (1995). Aplysia CREB2 represses long-term facilitation: relief of repression converts transient facilitation into long-term functional and structural change. Cell *83*, 979–992.

Bergamo, A., Gaiddon, C., Schellens, J.H.M., Beijnen, J.H., and Sava, G. (2012). Approaching tumour therapy beyond platinum drugs: status of the art and perspectives of ruthenium drug candidates. J. Inorg. Biochem. *106*, 90–99.

Chow, M.J., Licona, C., Pastorin, G., Mellitzer, G., Ang, W.H., and Gaiddon, C. (2016). Structural tuning of organoruthenium compounds allows oxidative switch to control ER stress pathways and bypass multidrug resistance. Chem Sci *7*, 4117–4124.

Chow, M.J., Babak, M.V., Tan, K.W., Cheong, M.C., Pastorin, G., Gaiddon, C., and Ang, W.H. (2018). Induction of the Endoplasmic Reticulum Stress Pathway by Highly Cytotoxic Organoruthenium Schiff-Base Complexes. Mol. Pharm. *15*, 3020–3031.

Combs, J.A., and DeNicola, G.M. (2019). The Non-Essential Amino Acid Cysteine Becomes Essential for Tumor Proliferation and Survival. Cancers (Basel) *11*.

Dasari, S., and Tchounwou, P.B. (2014). Cisplatin in cancer therapy: molecular mechanisms of action. Eur. J. Pharmacol. *740*, 364–378.

Dickhout, J.G., Carlisle, R.E., Jerome, D.E., Mohammed-Ali, Z., Jiang, H., Yang, G., Mani, S., Garg, S.K., Banerjee, R., Kaufman, R.J., et al. (2012). Integrated stress response modulates cellular redox state via induction of cystathionine γ-lyase: cross-talk between integrated stress response and thiol metabolism. J. Biol. Chem. *287*, 7603–7614.

Dixon, S.J., Lemberg, K.M., Lamprecht, M.R., Skouta, R., Zaitsev, E.M., Gleason, C.E., Patel, D.N., Bauer, A.J., Cantley, A.M., Yang, W.S., et al. (2012). Ferroptosis: an iron-dependent form of nonapoptotic cell death. Cell *149*, 1060–1072.

Elmore, S. (2007). Apoptosis: a review of programmed cell death. Toxicol Pathol *35*, 495–516.

Gaiddon, C., Jeannequin, P., Bischoff, P., Pfeffer, M., Sirlin, C., and Loeffler, J.P. (2005). Ruthenium (II)-derived organometallic compounds induce cytostatic and cytotoxic effects on mammalian cancer cell lines through p53-dependent and p53-independent mechanisms. J. Pharmacol. Exp. Ther. *315*, 1403–1411.

Galluzzi, L., Senovilla, L., Vitale, I., Michels, J., Martins, I., Kepp, O., Castedo, M., and Kroemer, G. (2012). Molecular mechanisms of cisplatin resistance. Oncogene *31*, 1869–1883.

Hatem, E., El Banna, N., and Huang, M.-E. (2017). Multifaceted Roles of Glutathione and Glutathione-Based Systems in Carcinogenesis and Anticancer Drug Resistance. Antioxid. Redox Signal. *27*, 1217–1234.

Hetz, C. (2012). The unfolded protein response: controlling cell fate decisions under ER stress and beyond. Nat. Rev. Mol. Cell Biol. *13*, 89–102.

Horiguchi, M., Koyanagi, S., Okamoto, A., Suzuki, S.O., Matsunaga, N., and Ohdo, S. (2012). Stress-Regulated Transcription Factor ATF4 Promotes Neoplastic Transformation by Suppressing Expression of the INK4a/ARF Cell Senescence Factors. Cancer Res *72*, 395–401.

Klajner, M., Licona, C., Fetzer, L., Hebraud, P., Mellitzer, G., Pfeffer, M., Harlepp, S., and Gaiddon, C. (2014). Subcellular localization and transport kinetics of ruthenium organometallic anticancer compounds in living cells: a dose-dependent role for amino acid and iron transporters. Inorg Chem *53*, 5150–5158.

Leyva, L., Sirlin, C., Rubio, L., Franco, C., Lagadec, R.L., Spencer, J., Bischoff, P., Gaiddon, C., Loeffler, J.-P., and Pfeffer, M. (2007). Synthesis of Cycloruthenated Compounds as Potential Anticancer Agents.

Licona, C., Spaety, M.-E., Capuozzo, A., Ali, M., Santamaria, R., Armant, O., Delalande, F., Van Dorsselaer, A., Cianferani, S., Spencer, J., et al. (2017). A ruthenium anticancer compound interacts with histones and impacts differently on epigenetic and death pathways compared to cisplatin. Oncotarget *8*, 2568–2584.

Liu, Y., Hyde, A.S., Simpson, M.A., and Barycki, J.J. (2014). Emerging regulatory paradigms in glutathione metabolism. Adv. Cancer Res. *122*, 69–101.

Martinez-Balibrea, E., Martínez-Cardús, A., Ginés, A., Ruiz de Porras, V., Moutinho, C., Layos, L., Manzano, J.L., Bugés, C., Bystrup, S., Esteller, M., et al. (2015). Tumor-Related Molecular Mechanisms of Oxaliplatin Resistance. Mol. Cancer Ther. *14*, 1767–1776.

Meng, X., Leyva, M.L., Jenny, M., Gross, I., Benosman, S., Fricker, B., Harlepp, S., Hébraud, P., Boos, A., Wlosik, P., et al. (2009). A ruthenium-containing organometallic compound reduces tumor growth through induction of the endoplasmic reticulum stress gene CHOP. Cancer Res. *69*, 5458–5466.

Mistry, R.K., Murray, T.V.A., Prysyazhna, O., Martin, D., Burgoyne, J.R., Santos, C., Eaton, P., Shah, A.M., and Brewer, A.C. (2016). Transcriptional Regulation of Cystathionine-γ-Lyase in Endothelial Cells by NADPH Oxidase 4-Dependent Signaling. J. Biol. Chem. *291*, 1774–1788.

Puigvert, J.C., Sanjiv, K., and Helleday, T. (2016). Targeting DNA repair, DNA metabolism and replication stress as anti-cancer strategies. FEBS J. *283*, 232–245.

Ryabov, A.D., Kurova, V.S., Ivanova, E.V., Le Lagadec, R., and Alexandrova, L. (2005). Redox Mediation and Photomechanical Oscillations Involving Photosensitive Cyclometalated Ru(II) Complexes, Glucose Oxidase, and Peroxidase. Anal. Chem. *77*, 1132–1139.

Sbodio, J.I., Snyder, S.H., and Paul, B.D. (2019). Regulators of the transsulfuration pathway. Br. J. Pharmacol. *176*, 583–593.

Traverso, N., Ricciarelli, R., Nitti, M., Marengo, B., Furfaro, A.L., Pronzato, M.A., Marinari, U.M., and Domenicotti, C. (2013). Role of glutathione in cancer progression and chemoresistance. Oxid Med Cell Longev *2013*, 972913.

Vidimar, V., Licona, C., Cerón-Camacho, R., Guerin, E., Coliat, P., Venkatasamy, A., Ali, M., Guenot, D., Le Lagadec, R., Jung, A.C., et al. (2019). A redox ruthenium compound directly targets PHD2 and inhibits the HIF1 pathway to reduce tumor angiogenesis independently of p53. Cancer Letters *440–441*, 145–155.

Weger, B.D., Weger, M., Görling, B., Schink, A., Gobet, C., Keime, C., Poschet, G., Jost, B., Krone, N., Hell, R., et al. (2016). Extensive Regulation of Diurnal Transcription and Metabolism by Glucocorticoids. PLOS Genetics *12*, e1006512.

Wirtz, M., Droux, M., and Hell, R. (2004). O-acetylserine (thiol) lyase: an enigmatic enzyme of plant cysteine biosynthesis revisited in Arabidopsis thaliana. J. Exp. Bot. *55*, 1785–1798.

Xu, L., Zhang, P.-P., Fang, X.-Q., Liu, Y., Wang, J.-Q., Zhou, H.-Z., Chen, S.-T., and Chao, H. (2019). A ruthenium(II) complex containing a p-cresol group induces apoptosis in human cervical carcinoma cells through endoplasmic reticulum stress and reactive oxygen species production. J. Inorg. Biochem. *191*, 126–134.

Yamamoto, M., Nomura, S., Hosoi, A., Nagaoka, K., Iino, T., Yasuda, T., Saito, T., Matsushita, H., Uchida, E., Seto, Y., et al. (2018). Established gastric cancer cell lines transplantable into C57BL/6 mice show fibroblast growth factor receptor 4 promotion of tumor growth. Cancer Sci. *109*, 1480–1492.

Yang, W.S., SriRamaratnam, R., Welsch, M.E., Shimada, K., Skouta, R., Viswanathan, V.S., Cheah, J.H., Clemons, P.A., Shamji, A.F., Clish, C.B., et al. (2014). Regulation of ferroptotic cancer cell death by GPX4. Cell *156*, 317–331.

Zeng, L., Gupta, P., Chen, Y., Wang, E., Ji, L., Chao, H., and Chen, Z.-S. (2017). The development of anticancer ruthenium(ii) complexes: from single molecule compounds to nanomaterials. Chem Soc Rev *46*, 5771–5804.

Zhu, H., Blake, S., Chan, K.T., Pearson, R.B., and Kang, J. (2018). Cystathionine β-Synthase in Physiology and Cancer. Biomed Res Int *2018*, 3205125.

Figure 1

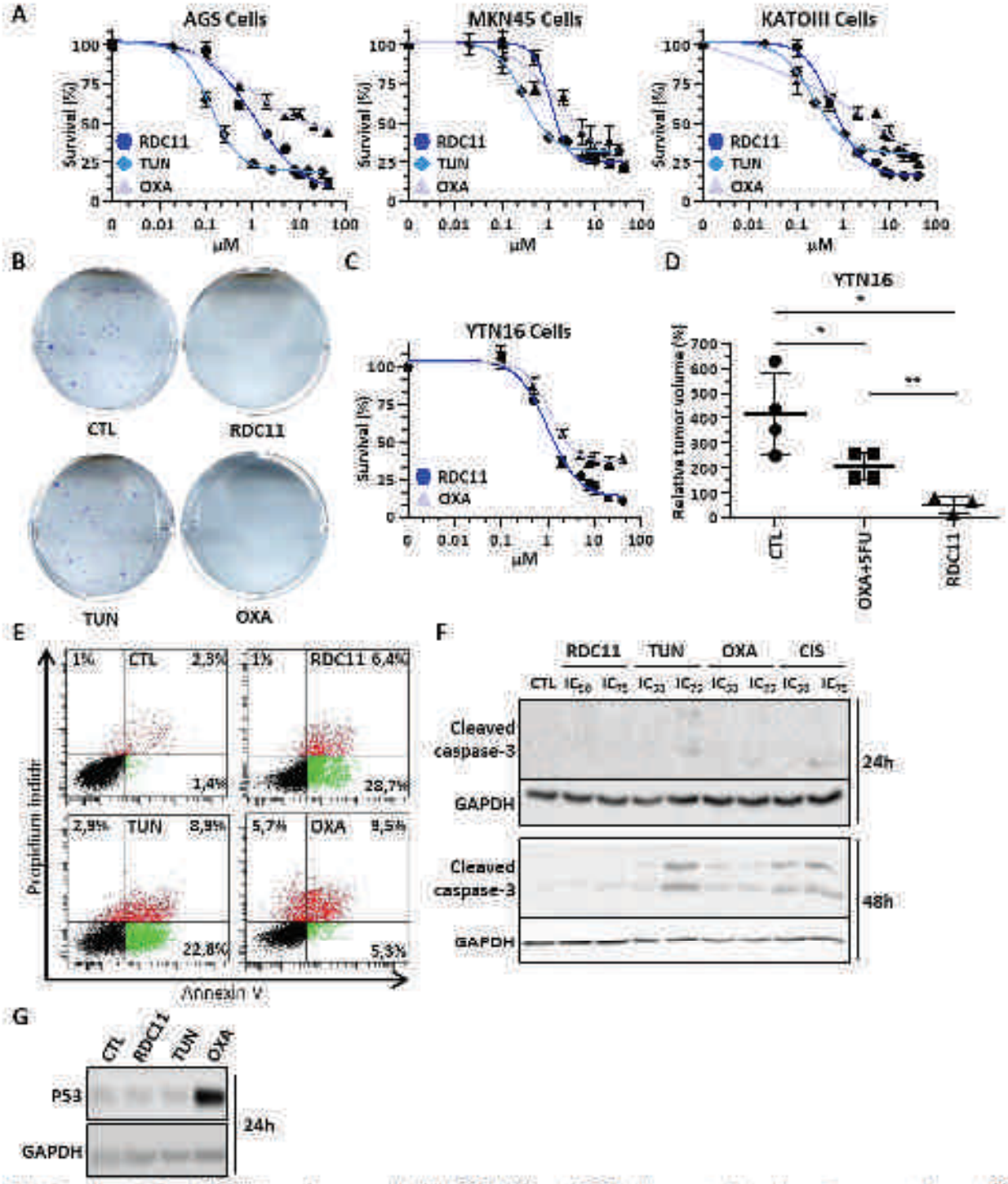

Cytotoxic characteristics of RDC11 in gastric cancer cells: (A) AGS, MKN45 and KATOIII cells were treated with growing concentrations of RDC11, tunicamycin (TUN) and oxaliplatin (OXA) for 48h and cell survival was assessed by a MTT assay in each cell line. (B) AGS cells were treated with RDC11, TUN and OXA at the IC_{50} for 24h or non treated (CTL) and survival was assessed by clonogenic assay 8 days after plating. (C) YTN16 cells were treated with growing concentrations of RDC11 and Oxaliplatin (OXA) for 48h and cell survival was assessed by MTT. (D) YTN16 syngenic xenograft mouse models treated once per week with vehicule (CTL), oxaliplatin + 5-fluorouracile (OXA+5FU) and RDC11 for 4 weeks. Tumor volumes after the 4 weeks are represented. (E) AGS cells were treated with RDC11, TUN and OXA at the IC_{50} for 48h or non treated (CTL) and apoptosis was assessed by flow cytometry. (F) AGS cells were treated for 24h and 48h with RDC11, TUN and OXA at the IC_{50} and IC_{75} or non treated (CTL) and western blot analysis revealed the caspase-3 cleavage. (G) AGS cells were treated for 24h with RDC11, TUN, and OXA at the IC_{50} or non treated (CTL) and western blot analysis revealed P53 expression. Representative experiments are shown and statistics were performed on technical replicates. Student t-test are considered as significative with α=0,5. *=0,05; **=0,01; ***=0,001.

Figure 2

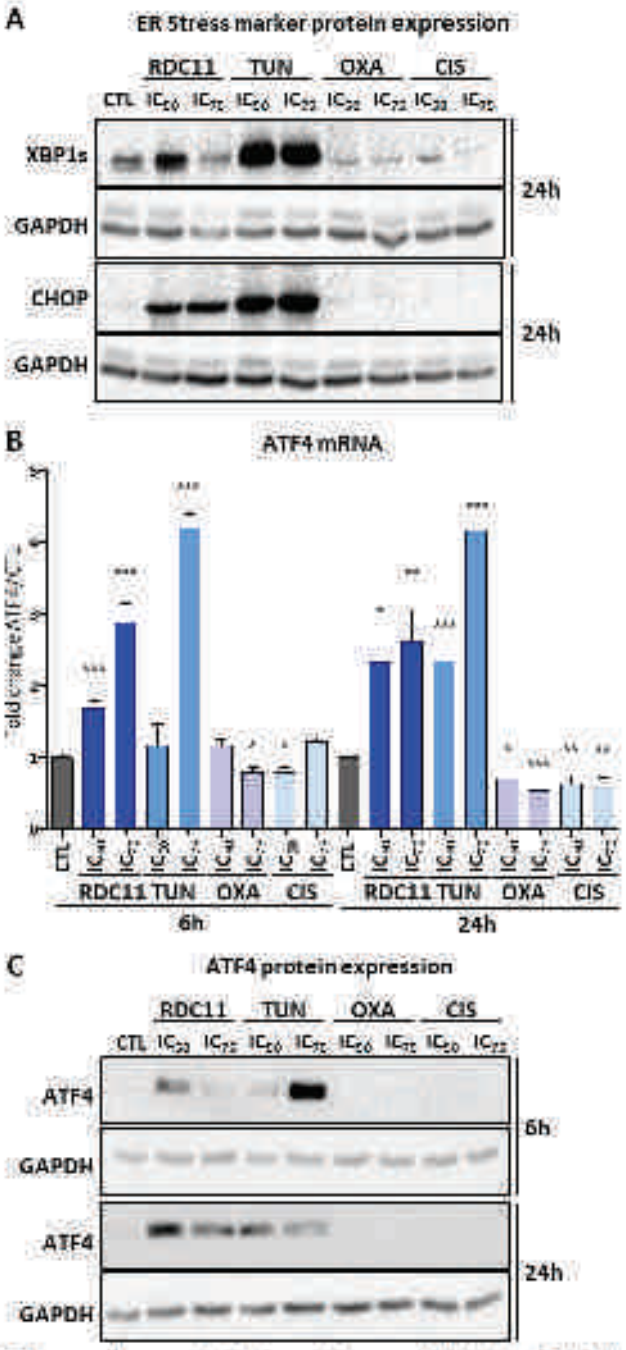

ER Stress pathway activation in gastric cancer: (A) Protein of Kis5 cells treated with RDC11, tunicamycin (TUN), oxaliplatin (OXA) and cisplatin (CIS) at the IC_{20} and IC_{72} for 6h and 24h or non treated (Ctl) were obtained and western blot analysis revealed XBP1s, CHOP and GAPDH protein expression level. (B,C) Protein and RNA were extracted from Kis5 cells treated with the same conditions and RT qPCR analysis revealed the relative mRNA expression level of ATF4 (B) and Western Blot analysis revealed ATF4 protein expression (C). Representative experiments are shown and statistics were performed on technical replicates. Student *t* test are considered as significative with $^{*}p<0.05$, $^{**}p<0.01$, $^{***}p<0.001$.

Figure 3

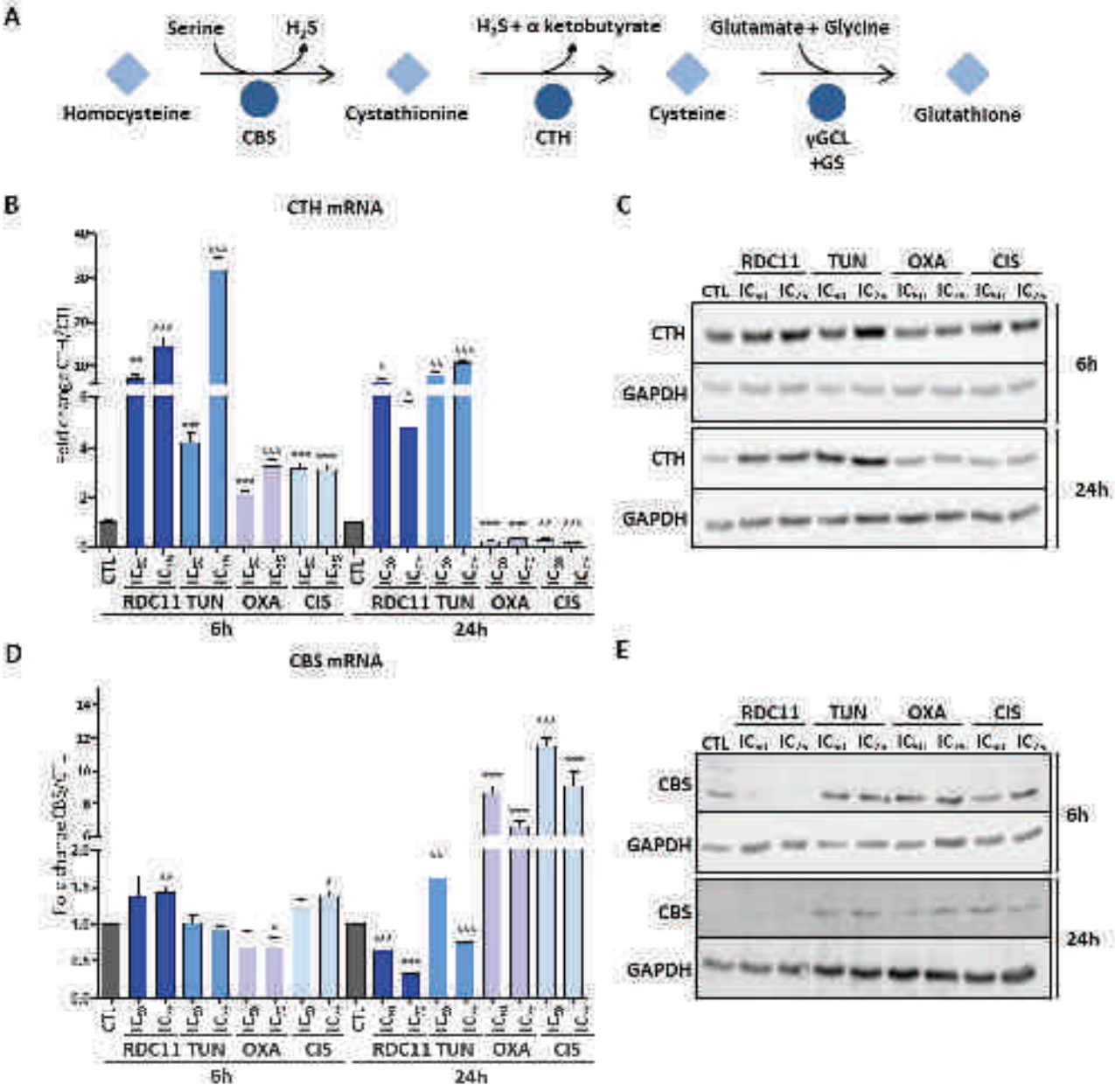

Regulation of the transulfuration pathway by the RDC11: (A) Schematic representation of the transsulfuration and glutathione biosynthetic pathway. (B&D) RNA of A549 cells treated with RDC11, tunicamycine (TUN), oxaliplatin (OXA) and cisplatin (CIS) at the IC_{50} and IC_{75} for 6h and 24h or non treated (CTL) were obtained and RT-qPCR analysis revealed CTH (B) and CBS (D) expression. (C&E) Protein extraction of A549 cells in the same conditions were obtained and western blot analysis revealed the protein expression of CTH (C) and CBS (E). Representative experiments are shown and statistics were performed on technical replicates. Student *t* test are considered as significative with *=0,05; **=0,01; ***=0,001

Figure 4

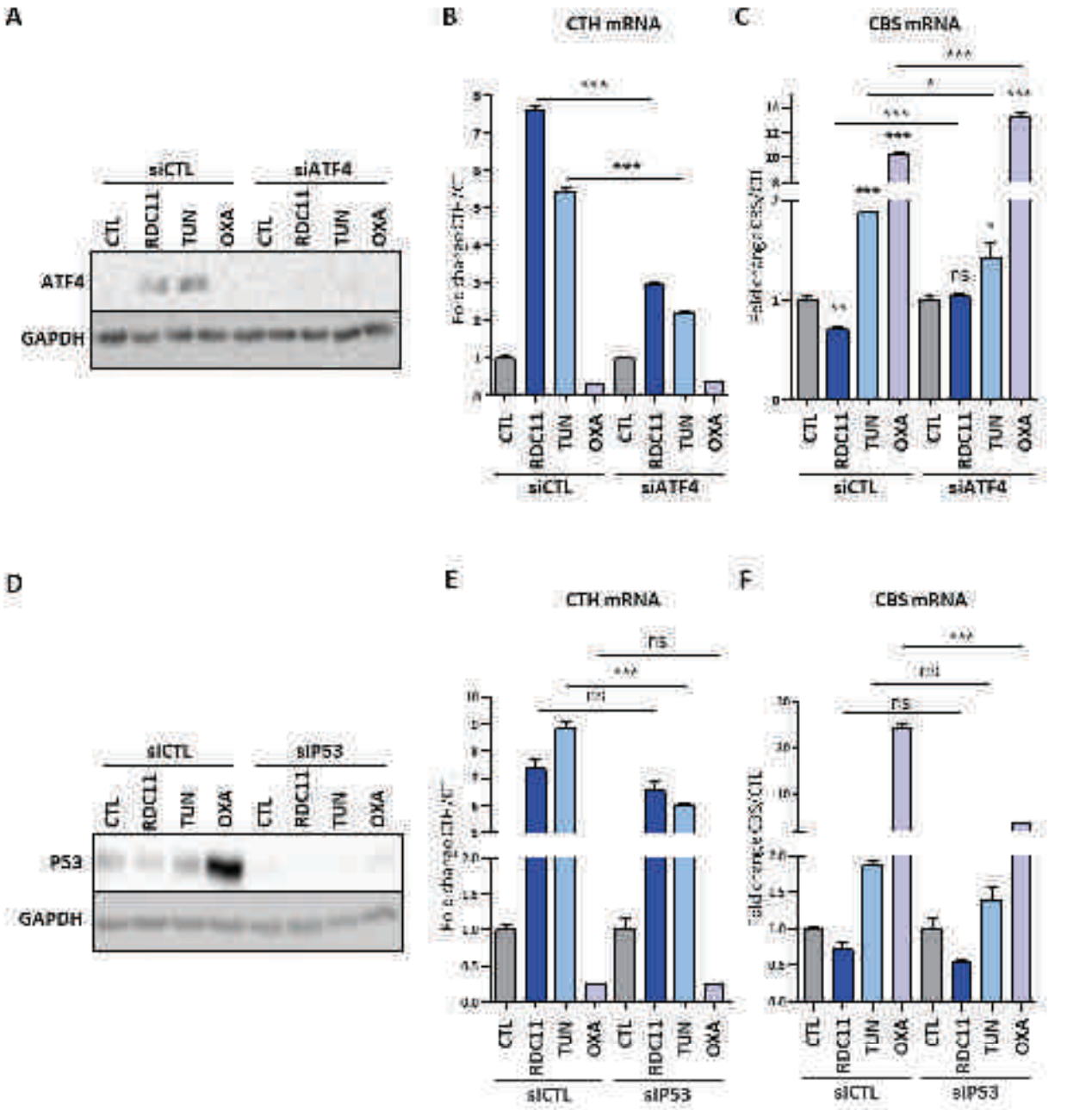

Implication of ATF4 and P53 in the regulation of the transsulfuration pathway: (A&D) Proteins were extracted from AGS cells transfected with a silencer RNA control (siCTL) or a specific siRNA against ATF4 (siATF4) or P53 (siP53) for 48h and then treated with RDC11, tunicamycin (TUN) and oxaliplatin (OXA) at the IC_{50} or non treated (CTL) for 24h. Western Blot analysis revealed the efficient silencing of ATF4 and P53 in these conditions. (B,C,E,F) RNA were extracted from AGS cells in the same conditions and RT-qPCR analysis showed the expression of CTH (B&E) and CBS (C&F). Representative experiments are shown and statistics were performed on technical replicates. Student t-test are considered as significative with α=0,5. *=0,05, **=0,01, ***=0,001

Figure 5

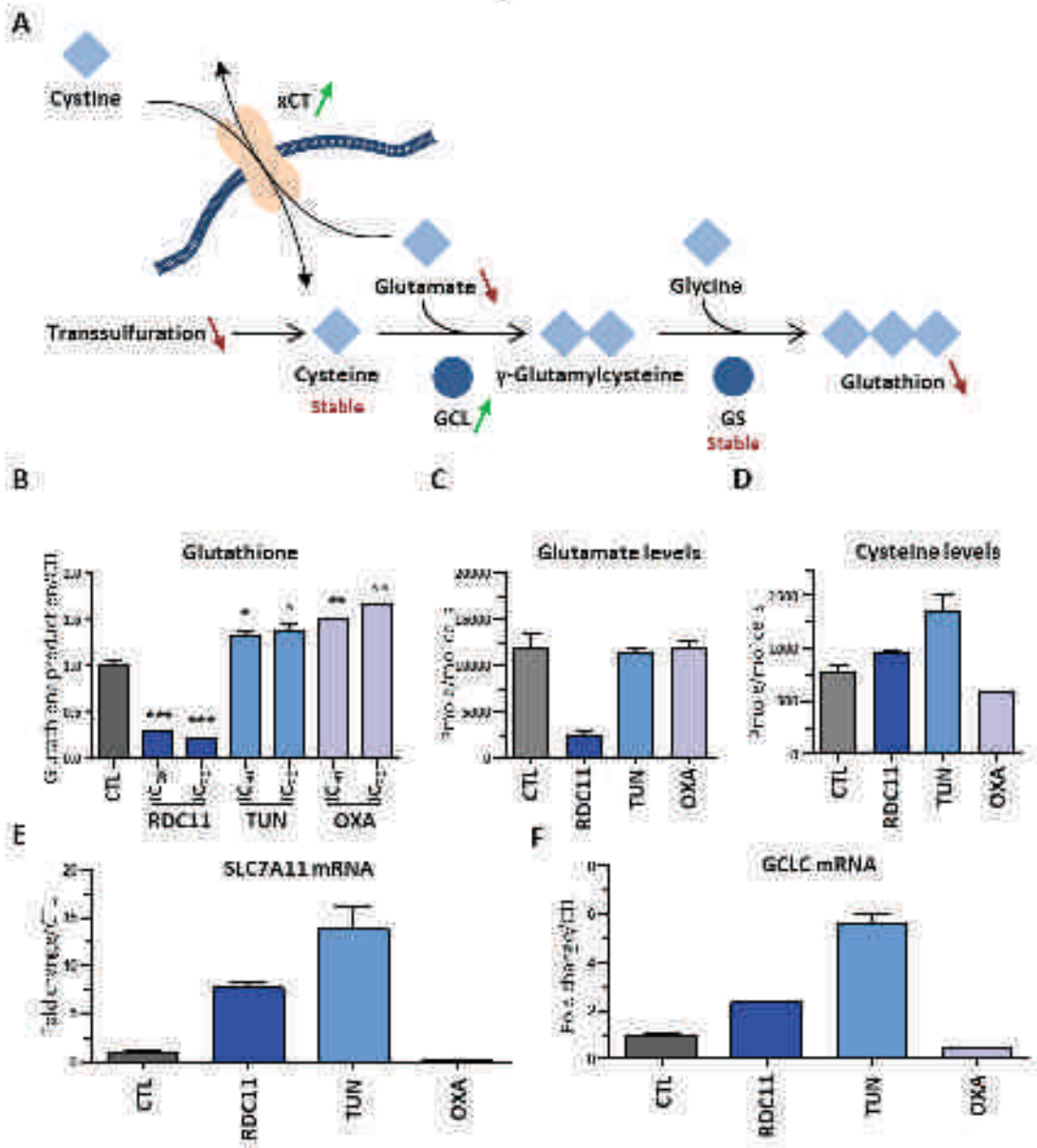

Metabolic changes induced by RDC11 in gastric cancer: (A) Schematic representation of glutathione biosynthetic pathway. Modulations induced by RDC11 are represented with green arrows for the upregulations and in red for the repressions. (B) AGS cells were treated with RDC11, tunicamycin (TUN) and oxaliplatin (OXA) at the IC_{50} and IC_{75} for 24h or non treated (CTL) and glutathione production was measured using a glutathione kit (Enzo lifesciences). (C&D) AGS cells were treated with RDC11, tunicamycin (TUN) and oxaliplatin (OXA) at the IC_{50} for 0h and 24h or non treated (CTL) and metabolomic analysis revealed the cellular content of glutamate (C) and cysteine (D). (E&F) AGS cells were treated with the same conditions and RT-qPCR analysis showed the expression level of SLC7A11 (E) and GCLC (F). Representative experiments are shown and statistics were performed on technical replicates. Student t-test are considered as significative with α<0,5, *=0,05, **=0,01, ***=0,001

Figure 6

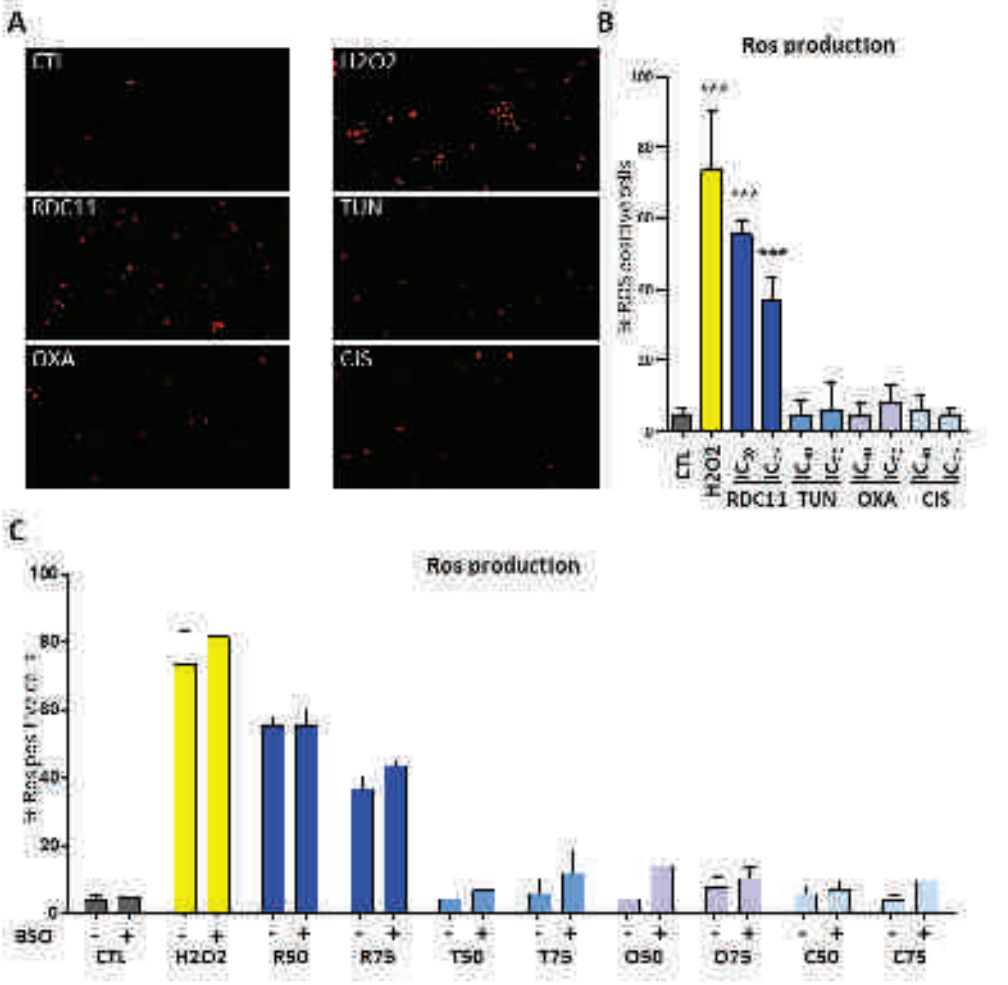

Oxidative stress induced by RDC11: (A&B) A549 cells were treated with H_2O_2 at 100µM, RDC11, tunicamycin (TUN), oxaliplatin (OXA) and cisplatin (CIS) at the IC_{50} or the IC_{75} for 6h or non treated (CTL) and Ros production was assessed by dihydroethidine. (A) Fluorescence microscopic photos of these cells are shown, and Ros positive cells were counted (B). (C) A549 cells were treated with the same conditions and a co-treatment with buthionine sulfoximide (BSO) and Ros production was assessed and counted following the same method. Biological replicates are represented and statistics were performed on technical replicates. Student t test are considered as significative with $\alpha = 0.05$: *=0.05, **=0.01, ***=0.001

Figure 7

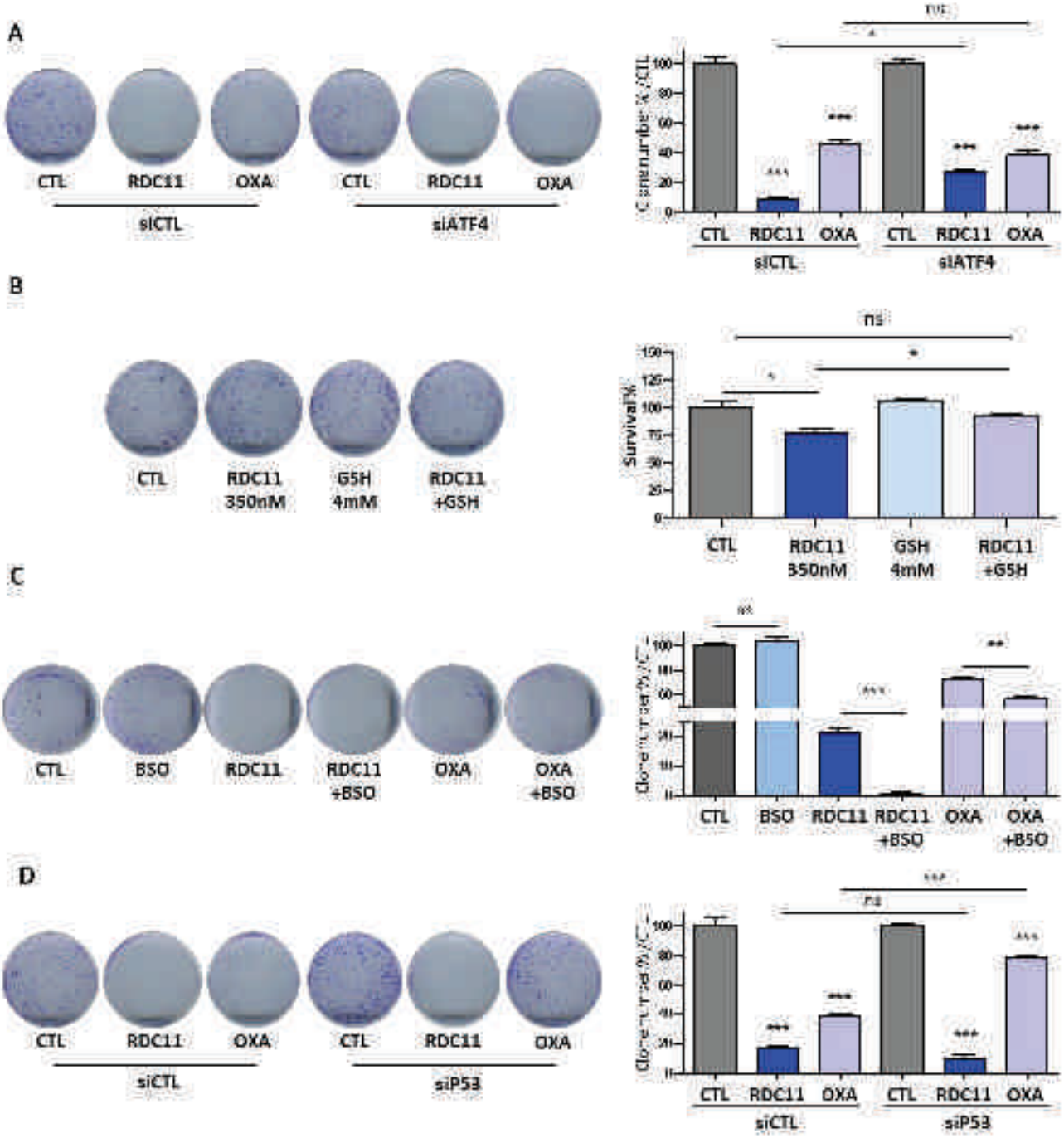

(A-D) Clonogenic assays were performed on AGS cells. (A&D) AGS cells were transfected with a silencer RNA control (siCTL) or a specific siRNA against ATF4 (siATF4) or P53 (siP53) for 24h and treated with RDC11 and oxaliplatin (OXA) at 250nM for 24h. (B) AGS cells were treated with RDC11 at 350nM, Glutathione at 4mM (GSH) and RDC11 combined with Glutathione for 24h. (C) AGS cells were treated with RDC11 and Oxaliplatin (OXA) at the IC_{50} or BSO at 1mM or in combination with BSO for 24h. The number of colonie is counted manually 8 days after platingt. Representative experiments are shown and statistics were performed on technical replicates. Student t-test are considered as significative with ns>0.5, *=0.05, **=0.01, ***=0.001

Figure 8

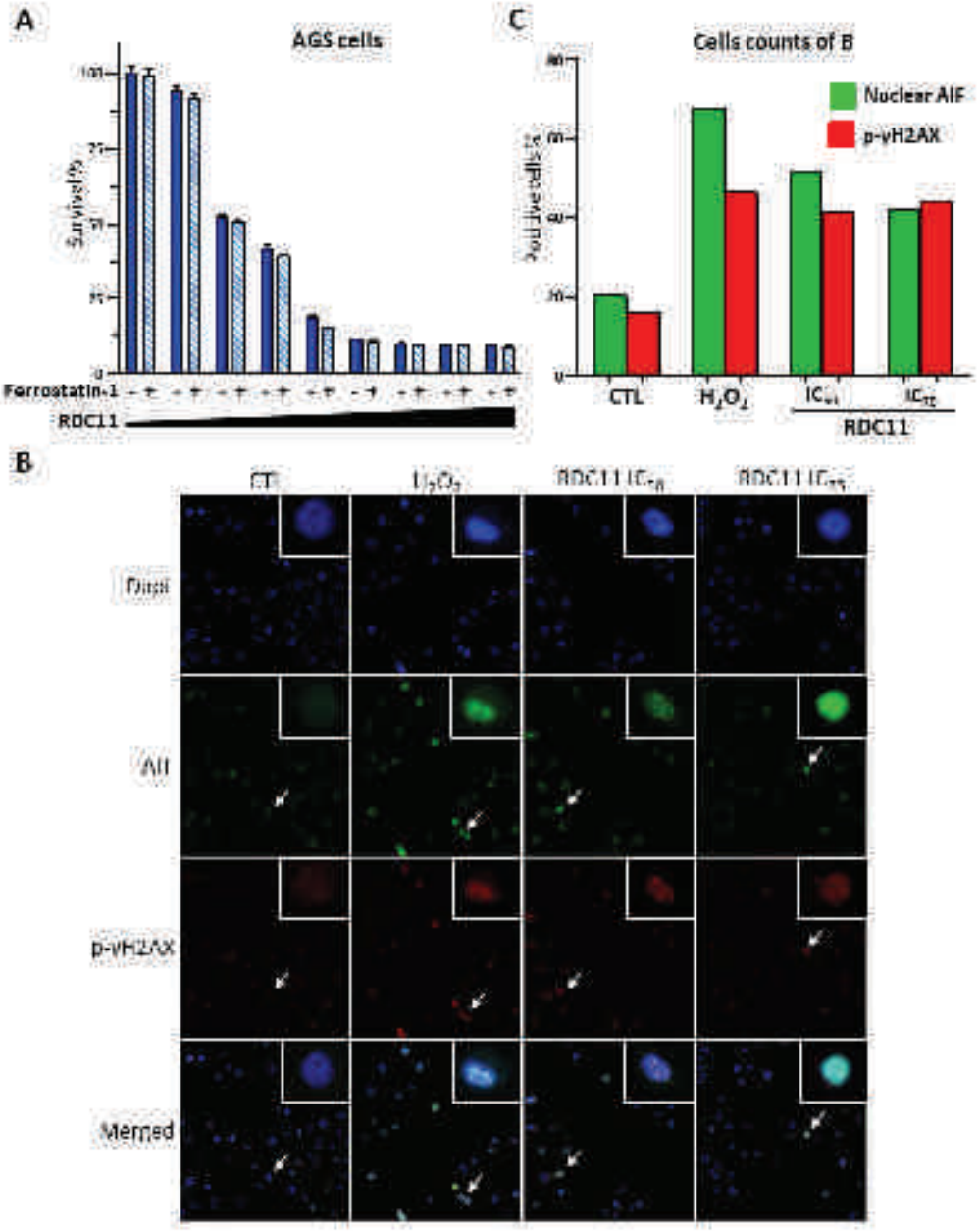

(A) AGS cells were treated with growing concentrations of RDC11 with or without ferrostatin-1 for 18h and cell survival was assessed by MTT survival assay. (B) Fluorescence microscopic photos of AGS cells treated with H_2O_2 at 100µM, RDC11 at the IC_{20} and IC_{75} for 6h or non treated (CTL) are shown. (C) AGS cells treated with the same conditions and positive cells for nuclear AIF and p-γH2AX expression were counted.

Figure 9

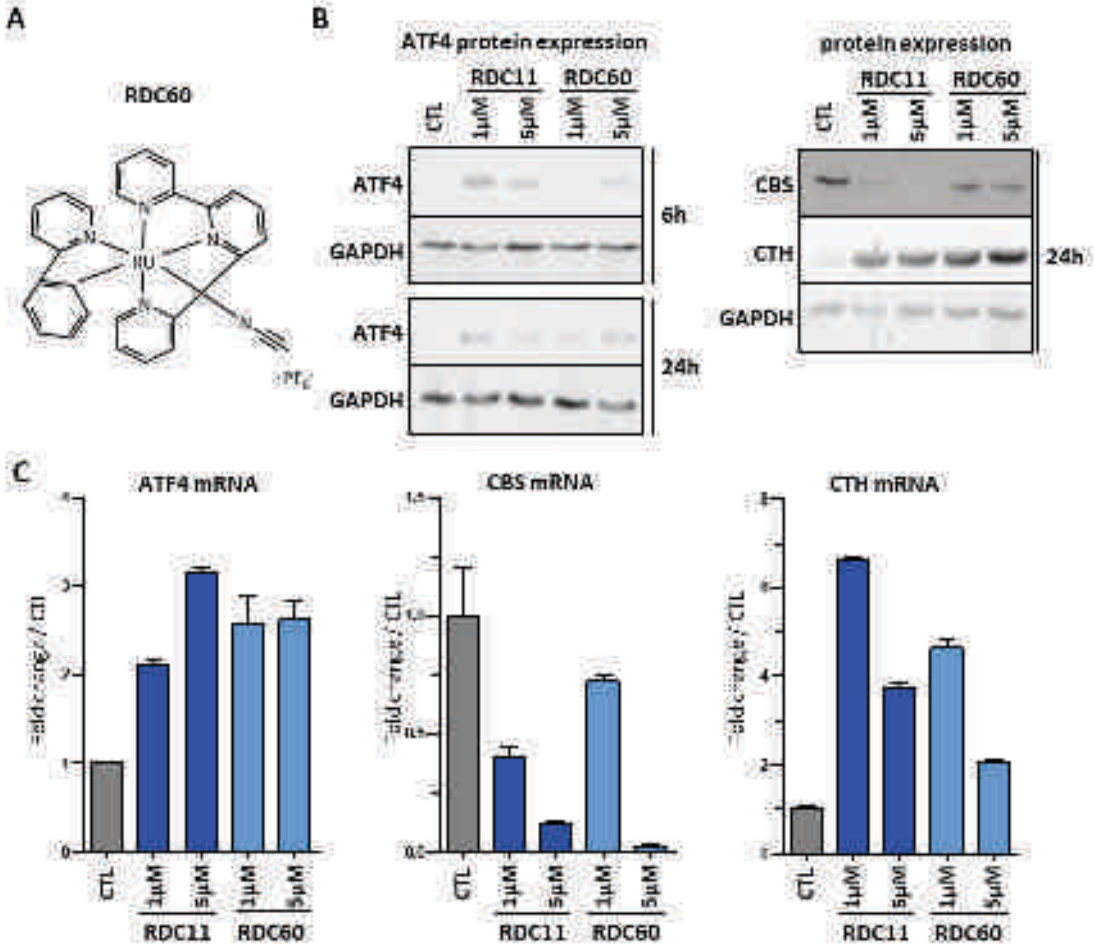

(A) Chemical structure of RDC60. (B) AGS cells were treated with RDC11 and RDC60 at 1µM or 5µM for 6h and 24h and western blot analysis showed the expression of ATF4, CBS, CTH and GAPDH. (C) AGS cells were treated with the same conditions and RT-qPCR analysis revealed the mRNA level of ATF4, CBS and CTH.

Supplemental Figure 1

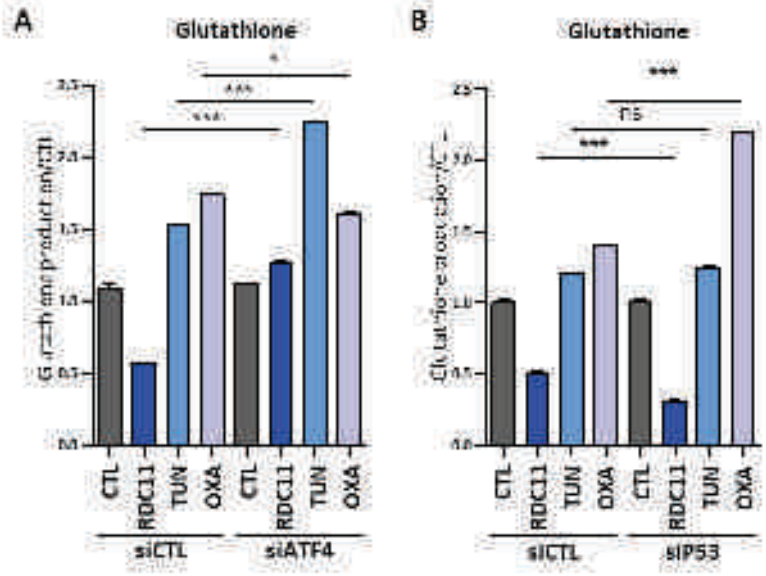

(A&B) MO5 cells were transfected with a silencer RNA control (siCTL) or a specific siRNA against ATF4 (siATF4) or P53 (siP53) for 48h and then treated with RDC11, tunicamycin (TUN) and oxaliplatin (OXA) at the IC_{50} or non treated (CTL) for 24h and glutathione production was measured using a glutathione kit (Enzo lifesciences).

Results (Objective 4)

Ruthenium and Osmium Cyclometallated drugs target the ER stress pathway in cancer cells: Identification of ABCB1 and EGFR as resistance mechanisms

Contexte et apport scientifique de l'article

De nombreux dérivés de ruthénium et d'osmium ont été intensivement étudiés pour leurs propriétés anticancéreuses. L'attrait pour ce type de composés repose sur les propriétés physico-chimiques des métaux de transition. De plus, des dérivés de ruthénium ou d'osmium possédant une grande variété de ligands ont été synthétisés conduisant à la génération de nombreux composés organométalliques associés à diverses structures, lipophilicités et potentiels redox. Cette diversité de composés pouvant être créée à partir de ces atomes métalliques explique en partie les nombreuses voies cellulaires impactées par ces composés, parmi lesquelles on retrouve la voie de P53 ou encore la voie du stress du réticulum.

Actuellement, l'activité biologique, la sensibilité ou la résistance à ce type de composé n'ont pas été liées aux propriétés physico-chimiques et ligands présents sur l'atome de métal. Certaines études tendent à démontrer un rôle spécifique de certains ligands sur les voies biologiques régulées. Par exemple, le RM175, un complexe en « piano stool » a été démontré capable d'induire des dommages à l'ADN et induire une réponse dépendante de P53 (Hayward et al., 2005). D'autre part, au laboratoire, nous avons démontré que certains complexes de ruthénium de la famille des RDC (comme le RDC11) sont capables d'induire la voie du stress du réticulum (Meng et al., 2009). Cependant, aucune étude n'a réellement démontré le lien entre la structure des composés et la fonction de ceux-ci, ce qui représente un obstacle au développement de composés plus spécifiques de certaines voies cellulaires.

C'est pourquoi cette étude vise à mettre en évidence un lien structure-fonction en s'intéressant plus spécifiquement à l'effet d'un changement de métal du ruthénium vers l'osmium. Par ailleurs, nous nous sommes intéressés aux facteurs cellulaires permettant d'expliquer ces différences de sensibilité/résistance envers les dérivés de ruthénium et d'osmium.

Pour répondre à cette question, nous avons comparé deux paires de composés cyclométallés. Chaque paire est constituée d'un composé organométallique possédant les mêmes ligands et les mêmes structures spatiales, à l'exception de l'atome central qui peut être un atome de ruthénium ou un atome d'osmium. Chaque composé diffère par leur potentiel redox et leur charge ce qui nous a permis d'étudier le rôle de ces caractéristiques physico-chimiques dans leur activité biologique.

Cette étude est la première à démontrer que le changement d'atome de ruthénium par un atome d'osmium augmente l'activité cytotoxique de ces composés. Par ailleurs, pour la première fois, nous avons pu mettre en évidence le rôle du transporteur ABCB1 dans l'efflux

de dérivés organométalliques à base de ruthénium et d'osmium. Ceci élargit nos connaissances sur la pharmacodynamique de ces composés. De façon intéressante, j'ai pu démontrer que l'inhibition pharmacologique des transporteurs ABC par le vérapamil conduit à une amélioration de la cytotoxicité de ces composés ce qui pourrait à terme être une option thérapeutique visant à améliorer l'efficacité des traitements à base de ruthénium ou d'osmium chez les patients.

Ruthenium and Osmium Cyclometallated drugs target the ER stress pathway in cancer cells: Identification of ABCB1 and EGFR as resistance mechanisms

Cynthia Licona,[a] Jean-Baptiste Delhorme,[a] Gilles Riegel,[a] Vania Vidimar,[a] Ricardo Cerón-Camacho,[b] Bastien Boff,[c] Aina Venkatasamy,[a] Catherine Tomasetto,[d] Priscila da Silva Figueiredo Celestino Gomese,[e] Didier Rognan,[e] Jean-Noel Freund,[a] Ronan Le Lagadec,[b] Michel Pfeffer,[c] Isabelle Gross,[a] Georg Mellitzer,[a] and Christian Gaiddon[a]*

[a] Interface Recherche Fondamentale en Cancérologie, Université de Strasbourg, Inserm UMR_S 1113, 3 av. Molière, 67200, Strasbourg, France

[b] Instituto de Química, UNAM, Circuito Exterior s/n, Ciudad Universitaria, Ciudad de México, 04510, Mexico.

[c] Institut de Chimie, UMR7177, Laboratoire de Synthèses Métallo-Induites, 4 rue Blaise Pascal, 67000, France

[d] IGBMC, Université de Strasbourg, U1258 INSERM UMR-7104 CNRS, Ilkirch, France

[e] Laboratoire d'Innovation Thérapeutique, UMR7200 CNRS-Université de Strasbourg, F-67400 Illkirch, France.

Keywords: ruthenium; osmium; anticancer drugs; resistance; genomics; ABCB1; EGFR; ER stress; p53.

ABSTRACT:

Background and purpose: Ruthenium (Ru) and osmium (Os) complexes have been shown to bypass some of the resistance mechanisms of platinum anticancer drugs, suggesting that they might represent therapeutic alternatives and are now tested in clinic. However, the resistance mechanisms that may alter the cytotoxicity of Ruthenium and Osmium complexes have not been identified yet. Here we investigated the mechanisms governing the variability in cytotoxicity of two ruthenium cyclometallated compounds and their osmium equivalents.

Experimental approach: We characterized in vitro and in vivo the anticancer properties on various cancer cell lines of the 4 cyclometallated compounds. We also developed a 4-steps approach based on the correlation between cytotoxicity measures and transcriptomic data of 60 cancer lines to identify genes involved in the sensibility/resistance towards Ru and Os complexes.

Keys results: We showed that the compounds target the endoplasmic reticulum stress pathway and that their activity was not hindered by mutation in the tumor suppressor gene TP53. Then, we identify multiple sensibility/resistance genes that correlated with cyclometallated compounds cytotoxicity. Docking and functional studies demonstrated that inhibition of some of these resistance mechanisms, namely ABCB1 export and EGFR expression, improved cyclometallated complexes activity. Interestingly, switching from Ruthenium to Osmium favors cytotoxicity while reducing sensibility to ABCB1 export mechanism.

Conclusion and implications: In summary, this study represents the first comprehensive investigation of the resistance mechanisms that alter the biological activity of ruthenium or osmium complexes and identifies some of the chemical determinant that are important for their activity.

Abbreviations:

Ru: Ruthenium

Os: Osmium

ER: Endoplasmic reticulum

MTT: 3-(4,5-dimethylthiazol-2-yl)-2,5-diphenyltetrazolium bromide

GO: glucose oxidase

Introduction

Ruthenium (Ru) - and osmium (Os)-based compounds are being intensively investigated as potential anticancer drugs encouraged by the long-lasting successes of platinum-based drugs and the intrinsic physico-chemical properties of transition metals.[1-3] Although being relatively advanced into the clinical trial process, the development of Ru-based compounds towards patients is handicapped by the diverse and controversial hypotheses on the physico-chemical determinant(s) relevant for their biological activity.[4] Indeed, multiple Ru- and Os-based compounds have been designed with different ligands, such as half-sandwich “piano-stool” structures, and different types of bonds between the metal and the ligands (O, N, C, Cl).[3, 5] This variety leads to a wide range of spatial structures, lipophilicities, metal charges (0 to IV) and redox potentials. These various physico-chemical properties may explain also the diversity of possible direct biological targets (DNA, Kinase, redox proteins) and regulated signaling pathways, such as p53 and endoplasmic reticulum (ER) stress).[6-18] However, the relative contribution of a specific physico-chemical property to a given effect on a direct target or signaling pathway remains often enigmatic. It is difficult to comprehend the exact contribution of each physico-chemical determinant taken individually (ie. redox potential, lipophilicity, presence of specific ligands), as by changing a given ligand, several of these characteristics are being modified simultaneously.

In addition, as the mode of action remains often enigmatic, the biological determinants that drives the sensitivity or resistance of the cancer cells towards these compounds has never been investigated. For instance, original work done on the “piano stool like” Ru complex RM175 showed the requirement of the DNA damage response factor and tumor suppressor gene TP53 for its cytotoxicity [10]. In contrast, we showed that the organoruthenium complex, RDC11, acts via the endoplasmic reticulum (ER) stress effector CHOP [12]. More recently, it was shown that two Os structures discriminate between the necessity for TP53 or for ER stress pathway for their cytotoxicity [14]. Importantly, no studies have yet described resistance mechanisms for Ru or Os complexes. In the era of personalized medicine, such information is critical for the development of optimized compounds and for their translation towards the clinic.

In an attempt to address these issues, we search for the potential resistance mechanisms that might impact on the cytotoxicity of Ru and Os complexes by investigating potential candidates, such as TP53, and by using an unbiased transcriptomic approach on 60 different cancer cell lines. For this study we chose 2 pairs of cyclo-organometallic compounds bearing bidentate ligands that were previously described [19, 20]. Within each pair, the complexes have similar ligands but differ by the metal, either Ru or Os, which changes the redox potential of the complex. Both pairs differ by the lipophilicity of the ligands (one phenanthroline vs two). This allowed us to investigate the relative contribution of redox potential (based on the metal) and the lipophilicity in their biological activity. A comprehensive physico-chemical, molecular, cellular and in vivo study was performed on these 4 complexes. We report that a switch from Ru to Os that modifies only the redox potential evokes a strong increase in cytotoxicity, which increased activation of ER stress pathway. However, mutations in TP53 does not represent a resistance mechanism for these complexes. However, we identified genes that correlates with the sensibility of the cancer cells towards our Ru of Os complexes. For instance, we showed that the ABCB1 export mechanism and EGFR high expression reduce the activity of our complexes. Interestingly, the Os complex appears less sensible towards ABCB1 expression.

Results

Exchange of ruthenium to osmium in organometallic complexes favors anticancer properties

Scheme 1 shows the structure of the cyclometalated complexes investigated in this study: the related compounds RDC11/ODC2 and RDC34/ODC3 whose synthesis have been previously described.[19, 20] Cytotoxicities of RDC11 and RDC34 have been investigated earlier.[12, 13, 18, 21, 22] All the compounds were stable at room temperature in PBS at least for more than 24 hours (Figure S1a). The replacement of Ru in RDC11 by Os in ODC2 did not significantly affect the spatial structure or the lipophilicity measured by phase separation assay (Log(Po/w). However, introduction of Os caused a significant drop in the redox potential (E°1/2 M(III/II) value) (Table 1).

The measurement of oxygen consumption via a Clark electrode showed that the redox potential of the compound modified

its ability to alter in vitro the activity of the purified redox enzymes, glucose oxidase and horseradish peroxidase (Table 1). The addition of a second phenanthroline in RDC34 and ODC3 did not modify substantially the redox potential but improved the lipophilicity and changed the spatial structure, which also impacted on the ability to alter redox enzyme function (Table1).

The cytotoxicity was tested on a panel of human cancer cell lines. The replacement of Ru by Os decreases the IC_{50} values (concentrations reducing viability by 50%) of ODC2 and ODC3 in HCT116 cells measured by MTT [3-(4,5-dimethylthiazol-2-yl)-2,5-diphenyltetrazolium bromide] assay (Table 1, Figure 1b, Figure S2a, b). The increase in activity was confirmed on the data obtained from the NCI on 8 types of cancers present in the NCI panel of cancer cell lines, both on the GI_{50} (50% of growth inhibition, Figure 1c, d, Figure S2c, d, e) and the LC_{50} (dose inducing 50% of lethality, Figure S2f). ODC3 displayed a strong anti-proliferative activity in the nanomolar range on cell lines of several types of cancers, suggesting that improving the lipophilicity favors the cytotoxicity.

We then investigated the mechanisms of cytotoxicity on HCT116 cells using flow cytometry. Treatment of HCT116 cells with RDC11, RDC34, ODC2 and ODC3 increased the number of cells in sub-G1, as well as the number of cells in G0/G1 (Figure 1e, f). This suggested that ODC2 and ODC3 can induce both cell cycle arrest in G0/G1 and apoptosis. In addition, ODC2 and ODC3 led to a sub-G1 phase slightly more important than their ruthenium counterparts. Induction of apoptosis was confirmed using Western blot for a marker, cleaved PARP1 (Figure S2h). Of note, quantification of cleaved products indicated that ODC3 was more potent than RDC34 to induce apoptosis, which is consistent with the survival assays. Similarly, ODC3 induced higher expression of the pro-apoptotic gene NOXA (Figure S2i). Finally, in vivo experiments performed on 3LL lung cancer cells in mice showed that ODC2 and ODC3 were slightly more efficient to reduce tumor growth although the differences were not statistically significant (Table 1, Figure S2j).

Osmium cyclometallated complexes induce ER stress pathway markers and are insensitive towards TP53 mutations.

We previously showed that cyclometallated RDC11 and RDC34, bearing one or two phenanthrolines respectively, induced the ER stress pathway.[12]·[13] However, an osmium compound (indicated as CL2 in this study) that also contains a phenanthroline was unable to induce ER stress.[14] Therefore, we evaluated the ability of ODC2 and ODC3 to regulate the expression of ER stress markers. ODC2 and ODC3 induced the pro-apoptotic ER stress transcription factor CHOP, while neither the coordinated phenanthroline complex (CL2) nor oxaliplatin displayed any significant effect (Figure 2a, Figure S3a). Similarly, ODC2, but not cisplatin, induced the phosphorylation of Elf2a, one of the early steps in the ER stress pathway (Figure 2b). Interestingly, ODC2 displayed a stronger ability to induce these markers compared to RDC11, further supporting the higher cytotoxicity of osmium complexes over their ruthenium counterparts, likely mediated by the redox potential difference. These results indicate also that the presence of the cyclometallated 2-phenylpyridine ligand onto the osmium atom is important to tune osmium complexes' biological activity. Similar results were obtained with ODC3 and RDC34 on CHOP and its target gene CHAC1 (Figure S3a, b). To further understand the role of the ER stress in the biological activity of ODC2, we inhibited two effectors of the ER stress pathway, EIF2a and CHOP. Inhibition of EIF2a by salubrinal did not reduce the biological activity of ODC2 (Figure 2c). In contrast, the silencing of CHOP expression diminished the cytotoxicity of ODC2 (Figure 2d). These results suggest that ODC2 does not require for its activity the PERK1-EIF2a branch of the ER stress pathway but needs the expression of the downstream effector CHOP. However, it is likely that the ODC2- regulated expression of CHOP might involve one of the two other components of the ER stress pathway, ATF6 or XBP1s. [23]

Genomic approach to identify ABCB1 and EGFR as resistance mechanisms for cyclometallated ruthenium and osmium complexes.

We then investigated why the 60 cell lines of the NCI panel showed different sensibility towards RDCs and ODCs (Figure 1a). Based on the frequent mutation of the tumor suppressor gene p53 and its role in the activity of some osmium complexes, such as CL2[14], we investigated whether mutations in this gene might represent a resistance factor for ODC2 and ODC3 activity. We first observed that mutation of the p53 tumor suppressor gene in the cancer cell lines did not diminish

the cytotoxicity of ODCs, and rather increases it, suggesting that TP53 is not necessary for their activities (Figure 2e).

This was further supported by the fact that ODC2 did not increase p53 protein level (Figure 2a), in contrast to the previously described osmium complex CL2[14], and that p53 inhibition using pifithrin did not reduce the cytotoxicity of ODC2 (Figure S3c). Hence to identify potential resistance mechanisms of cyclometallated complexes we used a strategy based on 4 successive steps that integrated the cytotoxicity data obtained from the NCI, the gene expression levels from Cell Express (http:// cellexpress.cgm.ntu.edu.tw), and TGCA (http:// www.cbioportal. org).

In the first step, we defined two groups of cell lines. The first group contained the 4 most resistant cell lines towards RDC11 and ODC2, namely NCI ADR, CAKI1, HCT15, UO3, showing a high GI_{50} for RDC11 (around 10^{-4}M) or ODC2 (close to 10^{-5}M).

The second group contained the most sensitive cell lines, namely HOP92, OVCAR3, NCI H522, SKMEL5, with a low GI_{50} close to or below 10^{-6}M. Then, we analyzed the gene signatures that might differentiate these two groups of cells using Cell Express (http://cellexpress. cgm.ntu.edu.tw). Amongst them, 1356 genes presented a p value < 10^{-3}, indicating that the biological response of cancer cells towards the complexes might involve numerous pathways (Figure 3a, b S4a).

In the second step, we selected to the 100 most significantly differently expressed ($p<10^{-6}$) genes for a first validation by correlating their expression with 4 couples of sensitive and resistant cell lines spanning 4 different cancer types: HOP92 and NCI ADR for lung cancer, HCT15 and KM12 for colon cancer, BT549 and HS578T for breast cancer, OVCAR3 and OVCAR8 for ovarian cancer. This step was used to limit inter-cancer type bias. Out of the initial 100 genes only 20 maintained a p value bellow 0.01, such as ABCB1, EGFR or NRF2F (Figure 3c). In the third step, these genes were further validated by correlating their expression to the IG50 of the 60 cell lines of the NCI panel (Figure 3d). Out of 20 genes only 10 correlated with the GI_{50} with a r >0.3 and a p value <0.01.

Amongst them, the expression level of two genes, ABCB1 and EGFR, correlated particularly well with the IG50. This strategy allowed us to identify genes that have the most robust correlation between their expression and the toxicity on cancer cell lines of different origins. In addition, both are targets of pharmacological inhibitors that have already FDA approval to be used on patients. The final fourth step was to further validate their importance in RDC11 cytotoxicity using functional experiments. For instance, we investigated the importance of EGFR that is overexpressed in various cancers and that can be inhibited by Cetuximab. Cell lines with low (OVCAR3; z-score 0.16) and high (OVCAR5; z-score 1.8) expression of EGFR were treated with RDC11 alone or RDC11 with Cetuximab (Figure 3e). Cetuximab inhibition of EGFR signaling was verified by following AREG and EREG expression, known downstream genes of EGFR signaling. Cetuximab increased by two-fold the cytotoxicity of RDC11 in the OVCAR5 cells but had no significant effect on OVCAR3 cells. Hence, elevated expression of EGFR reduces RDC11 cytotoxicity.

ABCB1 as carrier of cyclometallated complexes.

Then, we focused on ABCB1 (MDR1, P-gp), encoding a membrane protein that exports compounds outside the cells and whose expression correlated the most with the cytotoxic activity of RDC11 and ODC2 (Figure 3b, 5a, S4b). Besides the report that import of these compounds into cells is mediated by passive and active mechanisms, so far no one has ever investigated whether cyclometallated complexes are or not expelled and subjected to such resistance mechanisms.[21] Therefore, identification of ABCB1 as the most correlated gene is interesting as no information exists yet on the role of ABC transporters in the biological activity of ruthenium or osmium cyclometallated complexes.

First, we analyzed whether RDC11 could be transported by ABCB1. Flexible docking of RDC11 into the inner hydrophobic cavity of inward-facing ABCB1 unambiguously proposes two adjacent binding modes to transporter residues known to host several ABCB1 ligands (Figure 4a).

Site 1 corresponds to the location where absolute lowest binding free energy pose (-7.52 $kcal.mol^{-1}$) of the ligand is found (Figure 4b). RDC11 is docked in a hydrophobic environment lined by several aromatic residues (Phe72, Phe336, Tyr950, Phe951) that exhibit either edge-to-face or face-to-face interactions with the two aromatic groups of the RDC11 ligand. No

polar interactions with the ligand could be detected, the Ru atom being just used as a tether to optimally orient the 2-phenylpyridine and the 1,10-phenanthroline rings with respect to their aromatic environment. As with most ABCB1 ligands, a second binding site (Site2), adjacent to the first one is found on the upper part of the inner cavity (Figure 4c) that is particularly rich in aromatic residues.[24-26] The second site corresponds to the preferred location of most docking poses (Figure 4b) with a slightly lower binding free energy (from -5.18 to -6.76 kcal.mol^{-1}). As for site 1, site 2 is lined by a majority of aromatic amino acids (Phe303, Tyr307, Phe335, Phe336, Phe343, Phe978) exhibiting aromatic interactions to the ligand. Again, no apolar interactions to the transporter are detected in this second binding site. These current docking data clearly suggests that binding of this RDC11 ligand to a nucleotide-free inward-facing conformation of the ABCB1 protein is feasible. As for many existing substrates, we cannot rule out the possibility of a simultaneous occupation of both sites by two copies of the RDC11 ligand. The structural close resemblance between RDC11 and ODC2 indicate that both complexes are fitting ABCB1. However, the existing modeling tools do not allow us to differentiate possible fitting differences caused by changes in the electronic clouds surrounding the metal ion that caused the difference in term of redox potential.

Inhibition of ABCB1 activity increased cyclometallated complexes cytotoxicity

Having established that our RDC and ODC complexes can be transported by ABCB1, we investigated the impact of its expression on their cytotoxic activity. For this, we selected two colon cancer cell lines with either low (HCT116) or high (SW480) expression for ABCB1 (Figure 5b). Importantly, the expression of ABCB1 or other ABC transporters was not significantly impacted by the treatment with RDCs or ODCs (Figure S4b, c). Inhibition of ABC transporters, including ABCB1, was achieved by using verapamil. Verapamil treatment increased by about 270% RDC11's cytotoxic activity in SW480 cells (Figure 5c, d), but did not change it in HCT116 cells (Figure S4d).

Verapamil increased slightly less (255%) the cytotoxic activity of ODC2 in SW480 cells (Figure 5d). These results confirm that ABCB1 expression and activity account, at least partially, for the sensitivity of cancer cells towards RDC11 and ODC2, and that RDC11 might be more sensitive to ABCB1 expression level. This represents the first evidence that the biological activity of cyclometallated drugs is modulated by ABC transporters. In addition, these results suggest that the efficacy of organometallic complexes on patients might be improved by combining them with an inhibitor of ABC transporters like verapamil. To further investigate the role of ABCB1 in the activity of our complexes on a larger scale, NCI cell lines were separated into two groups based on ABCB1 expression as measured by the z-score: the first group with high expression (ABCB1 expression with a z score > 2) and the second group with low expression (z score < 2). All 4 compounds displayed low cytotoxicity in the high ABCB1-expressing group, and higher cytotoxicity in the low ABCB1-expressing group.

Interestingly, the difference of cytotoxicity between the two groups of cell lines was higher with the ruthenium-containing complexes compared to osmium-containing complexes (GI_{50} ratio of 1480-fold for RDC11 and 770-fold for ODC2; GI_{50} ratio of 4.75 10^5 -fold for RDC34 and 1980-fold for ODC3) (Figure 5e). This suggested that in average the change of ruthenium for osmium limits ABCB1 resistance mechanisms. Therefore, ABCB1 might contribute to the balance of import and export mechanisms governing organometallic drugs concentration in cells.

Discussion and Conclusion

Ruthenium and osmium complexes are being intensively investigated as potential anticancer drugs.[1-3] Multiple Ru- and Os-based compounds have been designed and this variety leads to a diversity of possible direct biological targets, including (DNA, Kinase, redox proteins) and regulated signaling pathways, such as p53.[6-18] Several of these metal complexes are tested on patients in clinical trials. However, the relative contribution of a specific physico-chemical characteristic to a given effect on a direct target or signaling pathway remains often enigmatic for osmium or ruthenium complexes. In addition, the biological determinants that drives the sensitivity or resistance of the cancer cells towards these compounds has never been investigated. To address these questions, we used 2 pairs of cyclo-organometallic compounds bearing bidentate ligands that were previously described and that differs either by the metal (Os versus Ru) or the number of phenanthroline (1 versus 2)[19, 20]. We expected the metal exchange to modify the redox potential and the number to phenanthrolines to

modify the lipophilicity. Using these complexes, we compared in vitro and in vivo their anticancer properties and we investigated the potential resistance mechanisms that impaired their activity by developing a 4-step strategy that implemented correlations between the cytotoxicity and the genetic signatures of 60 different cancer cell lines.

Osmium and ruthenium cyclometallated complex as anticancer drugs: Role of redox potential and lipophilicity

The 4 complexes exhibited high cytotoxicity on all the 60 cell lines tested. At least part of the cytotoxicity can be linked to apoptosis as several markers were induced, such as cleavage of PARP or induction of NOXA. The exchange of ruthenium to osmium in the mono or di-phenanthroline compounds increased the cytotoxicity and the in vivo anticancer activity. As the exchange only modifies the redox potential of the complexes, this observation demonstrated the importance of the redox potential in the biological activity of cyclometallated complexes. The role of the redox potential might be linked to the ability of the metal complexes to alter the activity of redox enzymes, as metal exchange also modified the impact of the compounds on glucose oxidase or HRP. The addition of a second phenanthroline increased also significantly the activity of the metal-based complexes, both with ruthenium and osmium. This effect is likely due to the change in lipophilicity brought by the second phenanthroline, but it might also be attributed in part to structural changes.

Osmium cyclometallated complexes induces ER stress effectors.

Both ODC2 and ODC3 induced the expression of the ER stress pathway effector CHOP, as well as one of its target gene, CHAC1. Interestingly, the osmium complex with one phenanthroline and no Os-C bond did not induce these markers, as previously reported [14]. Hence, the ability of inducing ER stress markers seems to be rather a characteristic of cyclometallated ruthenium and osmium and not a general feature. However, we previously reported that ruthenium complexes with piano-stool structures can also have similar properties on ER stress markers [27]. Importantly, activation of the ER stress pathway, or at least these effectors, can account for the cell death induced by these cyclometallated complexes. Indeed, silencing of CHOP reduced ODC2 cytotoxicity. The exact mechanistic processes that allow cyclometallated compounds to induce the ER stress pathway remains to establish. Interestingly, the ER stress pathway has been shown to be induced by intracellular redox imbalance and abnormal protein oxidation, which may both be altered by the redox properties of cyclometallated compounds, including via deregulation of redox enzyme activities.

ABCB1 and EGFR expression as resistance mechanisms against cyclometallated compounds

No resistance mechanisms have yet been identified against ruthenium or osmium compounds, despite the fact that their anticancer activity is tested in human. The 4-step process we developed showed that multiple genes may account for the sensibility of a given cell line towards cyclometallated compounds. The difficulty encountered to validate on the 60 cell lines some of the genes identified as sensibility markers in the first step (8 cell lines) highlights the number and the cell-to-cell variabilities of the resistance mechanisms that may be involved. The genes initially identified and that may, at least in part and in some cell lines, account for the sensibility towards ruthenium and osmium compounds span multiple cellular processes. Similarly, resistance mechanisms are complexes and how cancer cells respond to a given drugs depends on multiple factors, such as the availability of given direct targets, number of off-targets, and expression of generic anti- and pro-apoptotic proteins. Taking advantage of the existence of inactivating drugs, we demonstrated that overexpression of ABCB1 or EFGR reduced the cytotoxicity of cyclometallated drugs. For instance, ABCB1 may account for an elevated export of the cyclometallated compounds towards the outside of the cell. Besides the use of an inhibitor of ABCB1 transporter to demonstrate its role, docking and modelling analyses support that ABCB1 may export cyclometallated complexes. Hence, by reducing cyclometallated drugs concentration in the cell, cytotoxicity is reduced. EGFR, as the receptor for the growth factor EGF, induces proliferative and pro-survival pathways, such as MAPK and AKT. EGFR over-expression or activating driver mutations are frequent events in several cancer types [28]. Hence, elevated expression of EGFR may counterbalance the cytotoxicity activity of the cyclometallated complexes.

In conclusion, this study may be the first report, to the best of our knowledge, that identifies resistance mechanisms against cyclometallated osmium or ruthenium complexes. In particular, we demonstrated that the cytotoxic activity of cyclometallated complexes is reduced by high expression of ABCB1 and that exchange of ruthenium by osmium reduces this effect. Hence, the efficacy of ruthenium and osmium complexes in patients might be improved by cotreatment with inhibitors of ABC transporters, like as verapamil. Furthermore, the insight gained into the role of the redox potential in the biological activity of these compounds constitute a significant step towards the design of more efficient and less expensive small molecules that could target cancers cells more efficiently.

Methods

Chemicals

Ruthenium and osmium derived compounds were synthesized and characterized as previously described [19, 20]. Oxaliplatin, Verapamil were purchased from Sigma-Aldrich® and Cetuximab was provided by Merk.

Cell culture, MTT (3-(4,5-Dimethylthiazol-2-yl)-2,5-diphenyltetrazolium bromide) test, **IC_{50}** and NCI **IG_{50}**

Human colorectal HCT116 and SW480 cells, ovarian OVCAR3 and OVCAR5 were obtained from ATCC and maintained at 37°C at 20% O_2, 5% CO_2 in DMEM, 1 g/L glucose (Dulbecco's modified Eagle's medium; Life Technology), supplemented with 10% fetal calf serum (Life Technology), penicillin/streptomycin (100 UI/mL – 100 µg/ml) and gentamycin (50mg/mL). MTT test was performed using 96-well culture plates (Costar) [29]. IC_{50} were calculated on extrapolated fit curves based on concentration/effect data analyzed by GraphPad Prism using the equation: Y=Bottom + (Top-Bottom)/(1+10^((LogIC50-X)*HillSlope)). NCI renamed the IC_{50} into the GI_{50}, the concentration that causes 50% growth inhibition, to emphasize the correction for the cell count at time zero; thus, GI_{50} is the concentration of test drug where 100×(T-T0)/(C-T0) = 50 (dtp.cancer.gov/databases_tools/docs/ compare /compare_methodology.htm#specon).

Transfection of siRNA

SiRNA transfection was performed using RNAiMAX protocol as described by the provider (Life Technology, Saint Aubin, France). Sequences of siRNA for CHOP were previously described [12].

Kinetics of enzymatic O2 uptake

The measurements were made using a homemade Clark electrode with a mylar surface (YSI Yellow springs) equipped with a probe YSI 5331 in a 1.5 mL cell, at the controlled temperature of 25 °C. The calibration was performed as follows. The cell was filled with distilled water at 25 °C with stirring and a voltage was recorded. Then the cell was cleaned and filled with the previously deoxygenated water (in vacuum and bubbled with argon) and a lower voltage was recorded. A drop in 0.06 V was referred to 1.21×10-3 M of O2 ([O2] in water at 25 °C). The buffer was first added into the cell followed by the ruthenium complex in solution and glucose oxidase (GO). The solution was stirred and the recording device was turned on. The reaction was initiated by the addition of a solution of D-glucose after 20 s and the cell was immediately sealed. Time intervals between readings were in the range of from 3 to 10 min depending on the concentration of D-glucose, which was varied in the range of from 0.0025 M to 0.1 M. The concentrations of ruthenium complexes are indicated in legends to Figures. Each measurement was made at least in duplicate.

Quantitative reverse transcription-PCR (RT-qPCR)

Gene expression was assessed by qPCR using 18S as the normalizing gene [30]. Total RNA was isolated with TRIzol

reagent (Invitrogen). RNA was quantified using a Nanodrop 2000 Spectrophotometer (Thermo Scientific) and cDNA synthesized from 1µg total RNA using the iScript cDNA synthesis kit (Bio-Rad Laboratories). qPCR was performed in Bio-Rad iCycler thermal cycler using iQ SYBR Green supermix (Bio-Rad Laboratories). Specificity of the amplification was assessed by performing a melting curve analysis. Nucleotide sequences of the primers are indicated in supplementary material and methods.

Western Blot

Cells were lysed in Laemmli Sample Buffer 1X (125 mM Tris–HCl, pH 6.7, containing 3.3% SDS, 0.7 M 2-mercaptoethanol, 10% glycerol and 0.02% Bromophenol Blue) and then boiled for 5 minutes before loading. Equal amounts of total-protein extracts were separated on 12% PAGE and then electro- transferred to nitrocellulose membranes (Bio-Rad Laboratories). Equal loading was ensured by using an antibody directed against actin (1/2000; Sigma). Immunoprobing was performed with p53 (1/500; BD Transduction Labs), CHOP (1/1000; Novus Biologicals), Eif2a (1/1000, Abcam). Membranes were then probed with secondary horseradish-peroxidase-conjugated antibody (anti-rabbit, 1/5000 or- mouse 1/1000, SantaCruz). Antibody reaction was revealed with chemiluminescence detection procedures (Immun-StarTM HRP Chemiluminescence Kits, Bio-Rad Laboratories) and using the Molecular Imager® ChemiDocTM XRS+ System (Bio-Rad Laboratories).

In vivo tumor growth

C57BL/6 mice (8-weeks old) were injected subcutaneously with 5 x 10^{-5} 3LL cells. Injections of RDC (RDC34 and ODC3 at 4 mmol/kg; RDC11 and ODC2 at 13.3 mmol/kg) started when tumors were palpable (100 mm3) and were performed intraperitoneally twice a week. Tumor volumes were measured using caliper. Solutions were prepared in PBS/5% Cremophore. Data are representative of two independent experiments (n = 7 animal per group). Control group were injected only with vehicule (PBS/5% Cremophore). Drugs effect were statistically different ($p < 0.01$) compared to control, as calculated by a one-way ANOVA test followed by a Tukey test. Animal experiments have been approved by the regional ethic and animal welfare committee, are performed by authorized and trained personnel, and hosted in an animal facility with the necessary mandatory administrative authorizations.

Flow cytometry

Hypodiploid DNA was measured as described [9]. Briefly, 5X10^6 cells were centrifuged and fixed in 1 ml of ice-cold 70% ethanol at 4°C for 1h, washed once in PBS, 2mM EDTA, and resuspended in 1 ml of PBS containing 0.25mg of RNase A, 2mM EDTA, and 0.1mg of propidium iodide. After incubation at 37°C for 30 min, cells were analyzed. The fluorescence of 10,000 cells was analyzed using a FACScan flow cytometer and CellQuest software (BD Biosciences, San Jose, CA).

ASSOCIATED CONTENT

Supporting Information

The Supporting Information is available free of charge on the ACS Publications website.

PDF file containing Supplementary figure S1, S2, S3 and S4 are provided.

AUTHOR INFORMATION

Corresponding Author

* Dr. Christian Gaiddon; Email: Gaiddon@unistra.fr; Ph: +33 683525356.

Author Contributions

The manuscript was written through contributions of all authors. All authors have given approval to the final version of the manuscript.

Funding Sources

This work is supported by CNRS, Ligue contre le cancer, ARC, COST CM1105, DGAPA-UNAM (PAPIIT Project IN-207316) and CONACyT E-COS Nord 279063.

Competing Interests' Statement: The authors declare no potential conflicts of interest

ACKNOWLEDGMENT

We are thanking E. Martin for all her help with her cell culture expertise and support. We also acknowledge L. Mathern for her administrative support.

REFERENCES

[1] M.A. Jakupec, M. Galanski, V.B. Arion, C.G. Hartinger, B.K. Keppler, Antitumour metal compounds: more than theme and variations, Dalton Trans, (2008) 183-194.

[2] L. Kelland, The resurgence of platinum-based cancer chemotherapy, Nat Rev Cancer, 7 (2007) 573-584.

[3] G. Gasser, I. Ott, N. Metzler-Nolte, Organometallic anticancer compounds, Journal of medicinal chemistry, 54 (2011) 3-25.

[4] A. Bergamo, C. Gaiddon, J.H. Schellens, J.H. Beijnen, G. Sava, Approaching tumour therapy beyond platinum drugs Status of the art and perspectives of ruthenium drug candidates, J Inorg Biochem, 106 (2012) 90-99.

[5] M. Hanif, M.V. Babak, C.G. Hartinger, Development of anticancer agents: wizardry with osmium, Drug Discov Today, (2014).

[6] H.Y. Mei, J.K. Barton, Tris(tetramethylphenanthroline)ruthenium(II): a chiral probe that cleaves A-DNA conformations, Proc Natl Acad Sci U S A, 85 (1988) 1339-1343.

[7] V. Brabec, DNA modifications by antitumor platinum and ruthenium compounds: their recognition and repair, Prog Nucleic Acid Res Mol Biol, 71 (2002) 1-68.

[8] B.M. Zeglis, V.C. Pierre, J.K. Barton, Metallo-intercalators and metallo-insertors, Chem Commun (Camb), (2007) 4565-4579.

[9] C. Gaiddon, P. Jeannequin, P. Bischoff, M. Pfeffer, C. Sirlin, J.P. Loeffler, Ruthenium (II)-derived organometallic compounds induce cytostatic and cytotoxic effects on mammalian cancer cell lines through p53-dependent and p53- independent mechanisms, J Pharmacol Exp Ther, 315 (2005) 1403-1411.

[10] R.L. Hayward, Q.C. Schornagel, R. Tente, J.S. Macpherson, R.E. Aird, S. Guichard, A. Habtemariam, P. Sadler, D.I. Jodrell, Investigation of the role of Bax, p21/Waf1 and p53 as determinants of cellular responses in HCT116 colorectal cancer cells exposed to the novel cytotoxic ruthenium(II) organometallic agent, RM175, Cancer Chemother Pharmacol, 55 (2005) 577-583.

[11] K.S. Smalley, R. Contractor, N.K. Haass, A.N. Kulp, G.E. Atilla-Gokcumen, D.S. Williams, H. Bregman, K.T. Flaherty, M.S. Soengas, E. Meggers, M. Herlyn, An organometallic protein kinase inhibitor pharmacologically activates p53 and induces apoptosis in human melanoma cells, Cancer Res, 67 (2007) 209-217.

[12] X. Meng, M.L. Leyva, M. Jenny, I. Gross, S. Benosman, B. Fricker, S. Harlepp, P. Hebraud, A. Boos, P. Wlosik, P. Bischoff, C. Sirlin, M. Pfeffer, J.P. Loeffler, C. Gaiddon, A Ruthenium-Containing Organometallic Compound Reduces Tumor Growth through Induction of the Endoplasmic Reticulum Stress Gene CHOP, Cancer Res, 1;69(13) (2009) 5458-

5466.
[13] V. Vidimar, X. Meng, M. Klajner, C. Licona, L. Fetzer, S. Harlepp, P. Hebraud, M. Sidhoum, C. Sirlin, J.P. Loeffler, G. Mellitzer, G. Sava, M. Pfeffer, C. Gaiddon, Induction of caspase 8 and reactive oxygen species by ruthenium-derived anticancer compounds with improved water solubility and cytotoxicity, Biochem Pharmacol, 84 (2012) 1428-1436.
[14] K. Suntharalingam, T.C. Johnstone, P.M. Bruno, W. Lin, M.T. Hemann, S.J. Lippard, Bidentate ligands on osmium(VI) nitrido complexes control intracellular targeting and cell death pathways, J Am Chem Soc, 135 (2013) 14060-14063.
[15] W.H. Ang, A. De Luca, C. Chapuis-Bernasconi, L. Juillerat-Jeanneret, M. Lo Bello, P.J. Dyson, Organometallic Ruthenium Inhibitors of Glutathione-S-Transferase P1-1 as Anticancer Drugs, ChemMedChem, (2007).
[16] S.J. Dougan, A. Habtemariam, S.E. McHale, S. Parsons, P.J. Sadler, Catalytic organometallic anticancer complexes, Proc Natl Acad Sci U S A, 105 (2008) 11628-11633.
[17] B. Gava, S. Zorzet, P. Spessotto, M. Cocchietto, G. Sava, Inhibition of B16 melanoma metastases with the ruthenium complex imidazolium trans-imidazoledimethylsulfoxide-tetrachlororuthenate and down-regulation of tumor cell invasion, J Pharmacol Exp Ther, 317 (2006) 284-291.
[18] M. Klajner, P. Hebraud, C. Sirlin, C. Gaiddon, S. Harlepp, DNA binding to an anticancer organo-ruthenium complex, J Phys Chem B, 114 (2010) 14041-14047.
[19] B. Boff, C. Gaiddon, M. Pfeffer, Cancer cell cytotoxicity of cyclometalated compounds obtained with osmium(II) complexes, Inorganic chemistry, 52 (2013) 2705-2715.
[20] R. Ceron-Camacho, D. Morales-Morales, S. Hernandez, R. Le Lagadec, A.D. Ryabov, Easy access to bio-inspired osmium(II) complexes through electrophilic intramolecular C(sp2)-H bond cyclometalation, Inorganic chemistry, 47 (2008) 4988-4995.
[21] M. Klajner, C. Licona, L. Fetzer, P. Hebraud, G. Mellitzer, M. Pfeffer, S. Harlepp, C. Gaiddon, Subcellular localization and transport kinetics of ruthenium organometallic anticancer compounds in living cells: a dose-dependent role for amino Acid and iron transporters, Inorganic chemistry, 53 (2014) 5150-5158.
[22] V. Vidimar, C. Licona, R. Ceron-Camacho, E. Guerin, P. Coliat, A. Venkatasamy, M. Ali, D. Guenot, R. Le Lagadec, A.C. Jung, J.N. Freund, M. Pfeffer, G. Mellitzer, G. Sava, C. Gaiddon, A redox ruthenium compound directly targets PHD2 and inhibits the HIF1 pathway to reduce tumor angiogenesis independently of p53, Cancer Lett, 440-441 (2019) 145-155. [23] A. Nagelkerke, J. Bussink, F.C. Sweep, P.N. Span, The unfolded protein response as a target for cancer therapy, Biochim Biophys Acta, 1846 (2014) 277-284.
[24] S.G. Aller, J. Yu, A. Ward, Y. Weng, S. Chittaboina, R. Zhuo, P.M. Harrell, Y.T. Trinh, Q. Zhang, I.L. Urbatsch, G. Chang, Structure of P-glycoprotein reveals a molecular basis for poly-specific drug binding, Science, 323 (2009) 1718-1722.
[25] P. Szewczyk, H. Tao, A.P. McGrath, M. Villaluz, S.D. Rees, S.C. Lee, R. Doshi, I.L. Urbatsch, Q. Zhang, G. Chang, Snapshots of ligand entry, malleable binding and induced helical movement in P-glycoprotein, Acta Crystallogr D Biol Crystallogr, 71 (2015) 732-741.
[26] P.H. Palestro, L. Gavernet, G.L. Estiu, L.E. Bruno Blanch, Docking applied to the prediction of the affinity of compounds to P-glycoprotein, Biomed Res Int, 2014 (2014) 358425.
[27] M.J. Chow, C. Licona, G. Pastorin, G. Mellitzer, W.H. Ang, C. Gaiddon, Structural tuning of organoruthenium compounds allows oxidative switch to control ER stress pathways and bypass multidrug resistance, CHEMICAL SCIENCE, 7 (2016) 4117-4124.
[28] R. Roskoski, Jr., Small molecule inhibitors targeting the EGFR/ErbB family of protein-tyrosine kinases in human cancers, Pharmacol Res, 139 (2019) 395-411.
[29] C. Gaiddon, M. de Tapia, J.P. Loeffler, The tissue-specific transcription factor Pit-1/GHF-1 binds to the c-fos serum response element and activates c-fos transcription, Mol Endocrinol, 13 (1999) 742-751.
[30] S. Benosman, I. Gross, N. Clarke, A.G. Jochemsen, K. Okamoto, J.P. Loeffler, C. Gaiddon, Multiple neurotoxic stresses converge on MDMX proteolysis to cause neuronal apoptosis, Cell Death Differ, (2007).

Figure Legends

Figure 1: Growth inhibition and cytotoxic activity of the Ru and Os complexes. **A.** Structures of the Ru and Os complexes employed in this study. **B.** Survival of HCT116 treated with RDC11 and ODC2 for 48 hours and measured by MTT assay. **C.** NCI data of Growth Inhibition 50 (IG_{50}) for the 60 NCI cell lines treated by RDC11, ODC2, RDC34, and ODC3 obtained by SRB were analysed using GraphPad Prism. **D.** Mean of IG_{50} for each of the 8 types of cancer of the NCI panel. **E. F.** Identification of the cell cycle and sub-G1 populations by Flow Cytometry Analysis (FACS) in HCT116 cells treated by RDC11 and ODC2 (E), or RDC34 and ODC3 (F). *, **, *** indicate statistical differences of 0.05, 0.01 and 0.001 respectively as determined by anova followed by Tukey post-test using GraphPad Prism software.

Figure 2. Role of p53 and ER stress markers in the cytotoxic activity of the Ru and Os complexes. **A.** Western blot of p53 and CHOP in HCT116 cells treated for 24h with the indicated compounds at the $IC_{25,\ 50,\ 75}$. Ox = oxaliplatin (IC_{50} = 1µM; IC_{75} = 5µM); ODC2 (0,25; 1; 2;5µM) CL2 (IC_{25}= 2µM; IC_{50} = 5; IC_{75} = 10µM); Ct, DMSO 1%. **B.** Western blot of eiF2a phosphorylated (eif2a*) in HCT116 cells treated for 24h with the indicated compounds. Cisplatin (cisp; IC_{50} = 1µM, IC_{75} = 5µM), RDC11 (IC_{50} = 1µM; IC_{75}; 2.5µM) **C. D.** Survival of HCT116 cells treated with ODC2 at the IC_{50} of IC_{75} and with salubrinal (C; 10µM) or transfected with siRNA directed against CHOP (D). Cells were transfected for 48h with the siRNA before treatment for 48h. Graph shows mean and standard deviation of % of surviving cells compared to the control condition (Ct) **E.** IG50 of ODC2 and ODC3 in NCI 60 cancer cell line panel as distributed in two groups, cell lines with wild type p53 (n=15) or and cell lines with mutated p53 (p53µt; n=30). *** indicate statistical differences of 0.001 as determined by anova followed by Tukey post-test using GraphPad Prism software.

Figure 3. **A.** Multistep selection process for resistance genes against Ru/Os complexes. **B.** Heatmap of gene signature identification step using 8 cell lines for CellExpress analysis. 4 sensitive cell lines (HOP92, SKMEL5, H522, OVCAR3) and 4 resistant cell lines (NCI AR, CAKI1, HCT15, UO31) for RDC11 were chosen and the genes commonly expressed in each group were identified using the CellExpress website. **C.** First validation step on 16 cell lines using cBioPortal transcriptomic data. Data of indicated genes for 16 cell lines segregated in two groups (resistant versus sensible to RDC11 based on the IG_{50} from the NIC data) obtained from cBioPortal were analyzed using GraphPad Prism. In each group a cell line from the same type of cancer is present. HOP92 and NCI ADR for lung cancer, HCT15 and KM12 for colon cancer, BT549 and HS578T for breast cancer, OVCAR3 and OVCAR8 for ovarian cancer. Graph represent mean and standard deviation of relative mRNA level (z score) for the groups of sensitive (Sens) and resistant (Res) cell lines. **D.** Second validation step for EFGR expression on the 60 cell lines of the NCI and using cBioPortal transcriptomic data. EGFR expression is indicated in relative level (z score). **E.** Functional validation step for EGFR using cetuximab (Cet, 0.5µM), a selective inhibitor of EGFR, on 2 cell lines, with low (OVCAR3) and high (OVCAR5) expression of EGFR. Cetuximab was added 1h before treatment with RDC11. Cell survival was evaluation by MTT after 48 hours of treatment. Graph indicates mean (n = 3) and standard deviation of IC_{50} obtained in each condition. ** indicate statistical differences of 0.01 as determined by anova followed by Tukey post-test using GraphPad Prism software.

Figure 4. Binding modes of RDC11 to the human ABCB1 transporter. **A.** Overall view of the two adjacent binding modes of RDC11 (green and cyan sticks) to the ABCB1 protein (white ribbons). **B.** Close-up to binding site 1. The RDC11 ligands are shown as green sticks, with the Ru atom displayed as a pink sphere. ABCB1 residues lining the binding site are represented by tan sticks and are labelled at their Cα-atom. **C.** Close-up to binding site 2. The RDC11 ligands are shown as cyan sticks, with the Ru atom displayed as a pink sphere. ABCB1 residues lining the binding site are represented by tan sticks and are labelled at their Cα-atom.

Figure 5. Impact of ABCB1 expression and inhibition on ruthenium- and osmium-based organometallic complexes. **A.** Correlation of *ABCB1* expression level (z score) with the cytotoxicity (GI_{50}) of RDC11 in the whole NCI cancer cell line panel. Correlation coefficient is indicated as calculated by Pearson test and p value (n=60). **B.** mRNA levels of *abcb1* in HCT116 and SW480 colon cancer cells measured by RT-qPCR after 24h of treatment at the IC_{50} (see figure 1). mRNA level of *ABCB1* were normalized to the housekeeping gene *tpb*. **C.** To test for the impact of the ABC transporter inhibitor verapamil

(50µM), cells were treated only 1h with RDC11, and the MTT assay was performed after 48h. Verapamil was present during the whole experiement. Curves are means of three independent experiments. **D.** ABC sensitivity represented as % of IC_{50} difference between cells treated only with RDC11 or ODC2 (CT) and cells co-treated with verapamil. $p<0.01$ (t-test) (d). **E.** Shift of IG_{50} in the NCI 60 cancer cell lines depending on the expression level (high, n=4; low, n=56) of ABCB1. *** indicate statistical differences of 0.001 as determined by anova followed by Tukey post-test using GraphPad Prism software.

SYNOPSIS

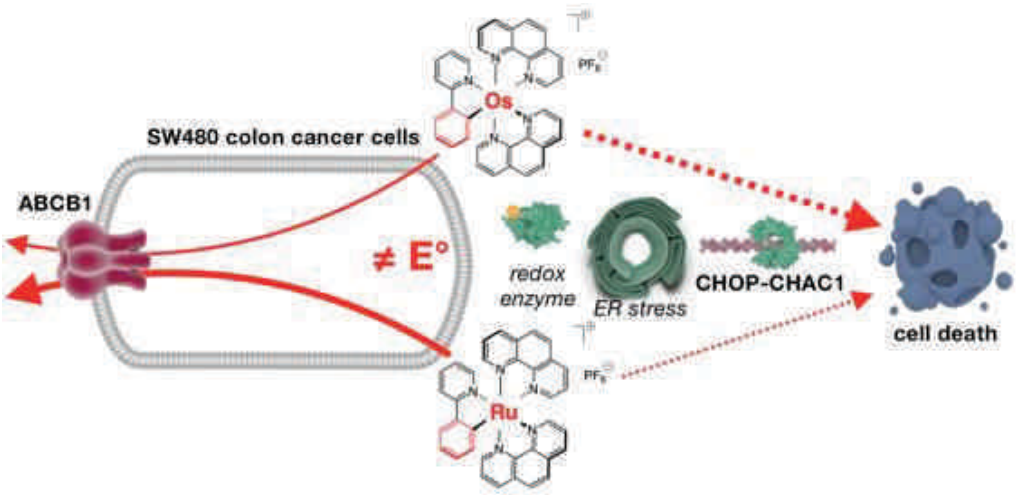

Tables

Complexes	E°'V (Ag/AgCl)	Log(Po/w)	k_3 (M^{-1} s^{-1}) x10^6 Glucose Ox.	HRP	IC50 µM	Tumor %Ct
ODC2	0.12	1.15 ± 0.05	2.9 ± 0.3	2.7	1.2 ± 0.1	55 ± 12
RDC11	0.43	1.2 ± 0.05	1.7 ± 0.2	0.1	1.8 ± 0.1	60 ± 11
ODC3	0.1	2.34 ± 0.04	1.8 ± 0.2	58	0.09 ± 0.01	58 ± 8
RDC34	0.33	2.35 ± 0.05	7.5 ± 0.4	2.3	0.15 ± 0.01	62 ± 9

Table 1. Physico-chemical and biological properties of Ru and Os organometallics.

Figure 1

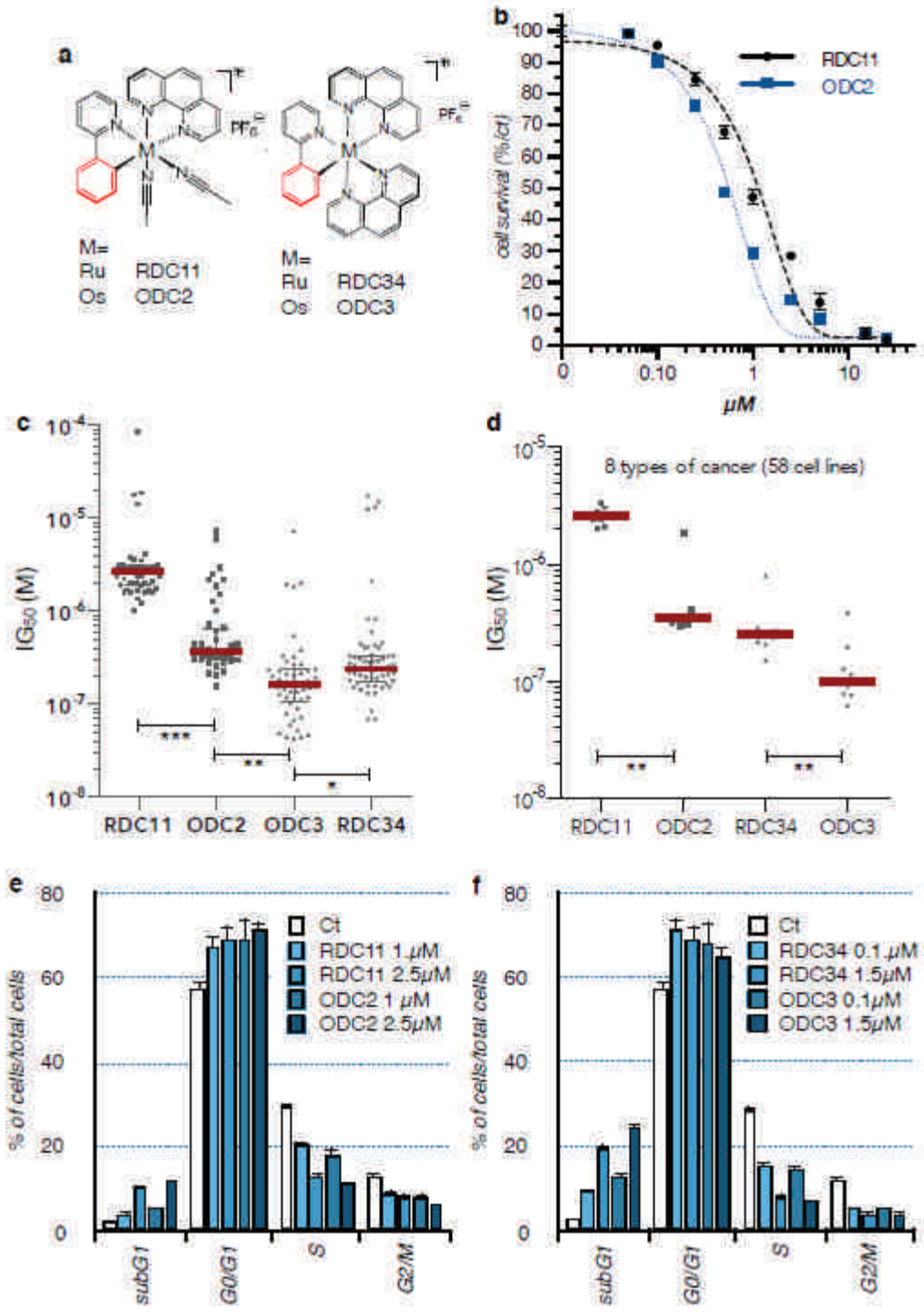
a
M=
Ru RDC11
Os ODC2
M=
Ru RDC34
Os ODC3
b
RDC11
ODC2
cell survival (%ctl)
μM
c
IG50 (M)
RDC11 ODC2 ODC3 RDC34
d
8 types of cancer (58 cell lines)
IG50 (M)
RDC11 ODC2 RDC34 ODC3
e
% of cells/total cells
Ct
RDC11 1 μM
RDC11 2.5μM
ODC2 1 μM
ODC2 2.5μM
subG1 G0/G1 S G2/M
f
% of cells/total cells
Ct
RDC34 0.1 μM
RDC34 1.5μM
ODC3 0.1μM
ODC3 1.5μM
subG1 G0/G1 S G2/M

Figure 2

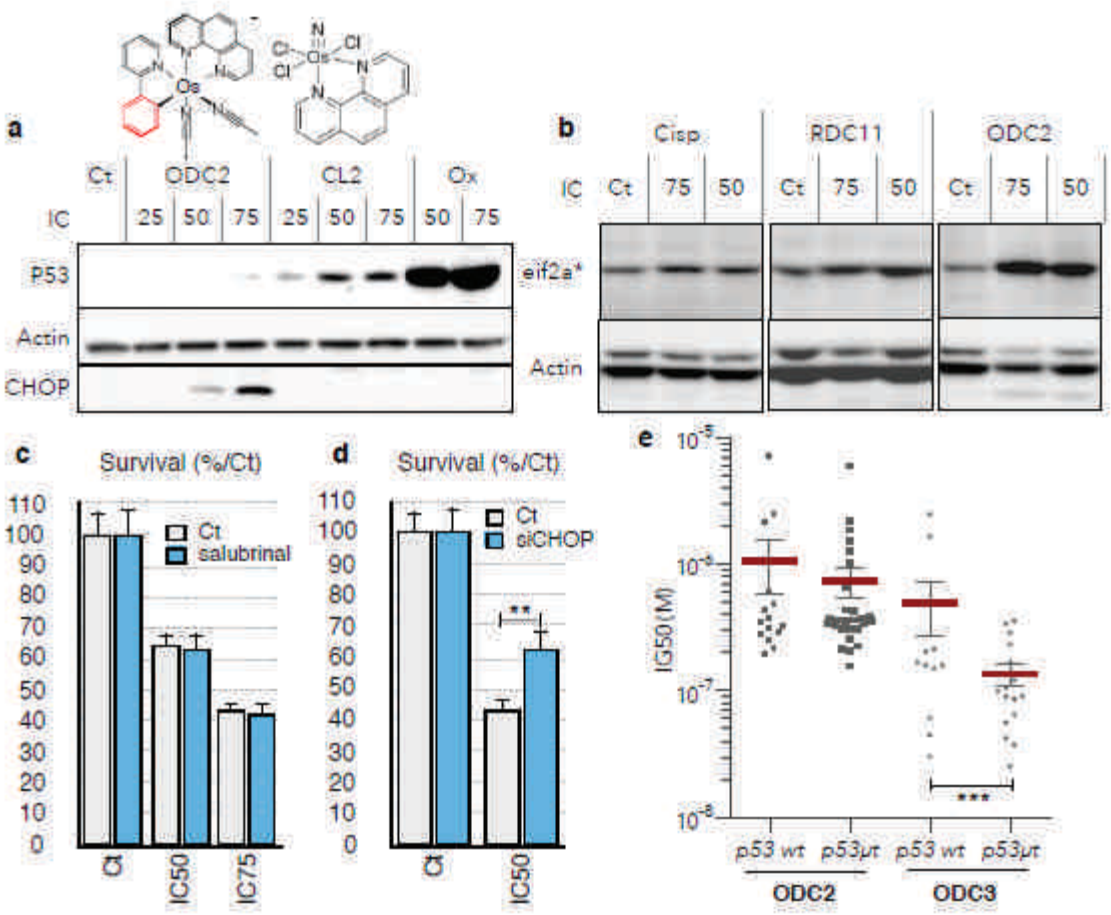
a
Ct
ODC2
CL2
Ox
IC
25
50
75
25
50
75
50
75
P53
Actin
CHOP
eif2a*
Actin
b
Cisp
RDC11
ODC2
IC
Ct
75
50
Ct
75
50
Ct
75
50
c
Survival (%/Ct)
Ct
salubrinal
110
100
90
80
70
60
50
40
30
20
10
0
Ct
IC50
IC75
d
Survival (%/Ct)
Ct
siCHOP
**
Ct
IC50
e
IG50 (M)
p53 wt
p53μt
p53 wt
p53μt
***
ODC2
ODC3

Figure 3

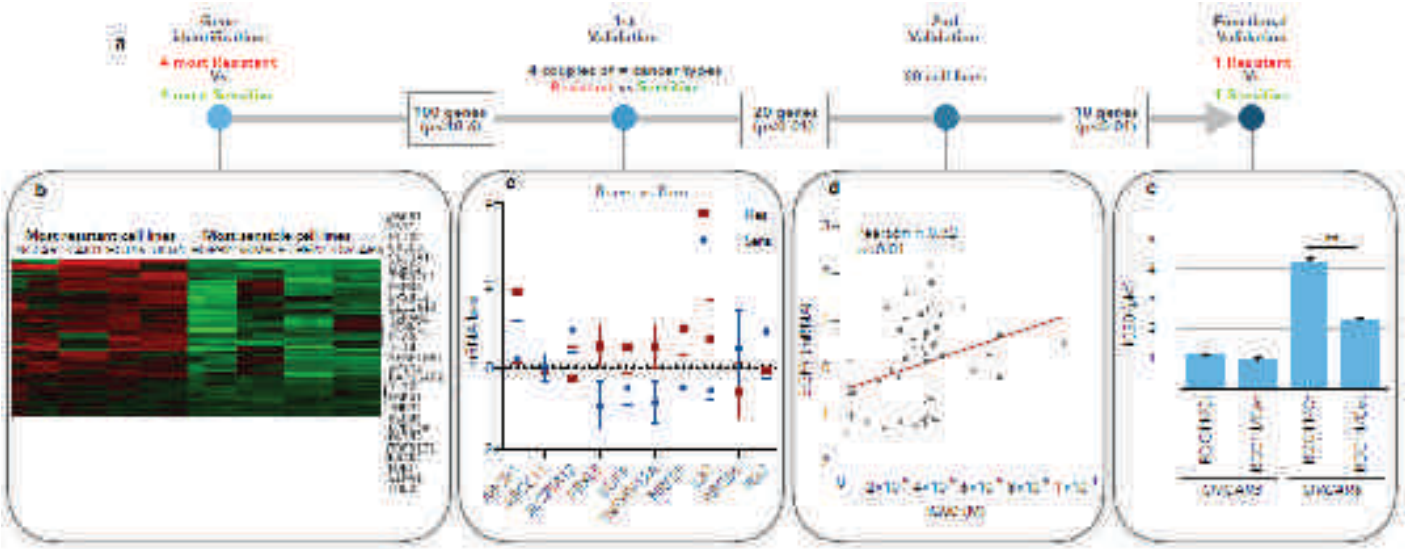

Figure 4

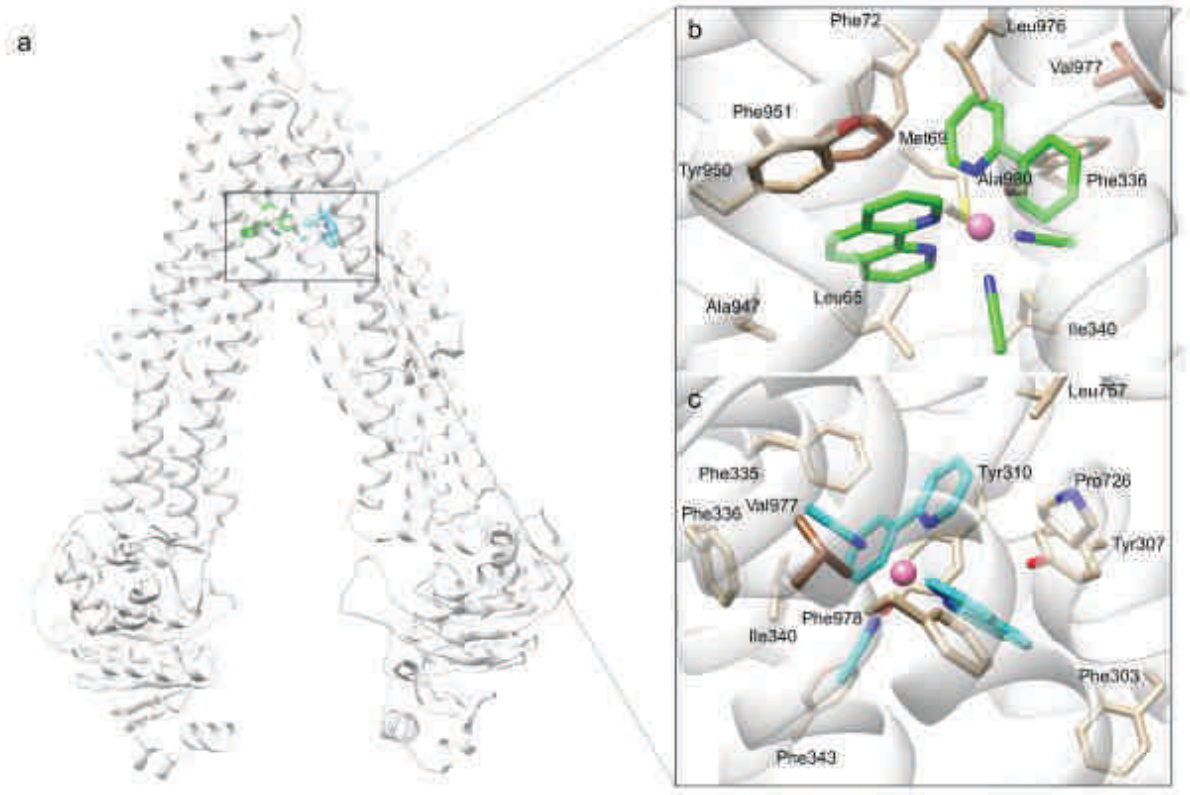
a
b
Phe72
Leu976
Val977
Phe951
Met69
Tyr950
Ala980
Phe336
Ala947
Leu65
Ile340
c
Leu757
Phe335
Tyr310
Pro726
Phe336
Val977
Tyr307
Phe978
Ile340
Phe303
Phe343

Figure 5

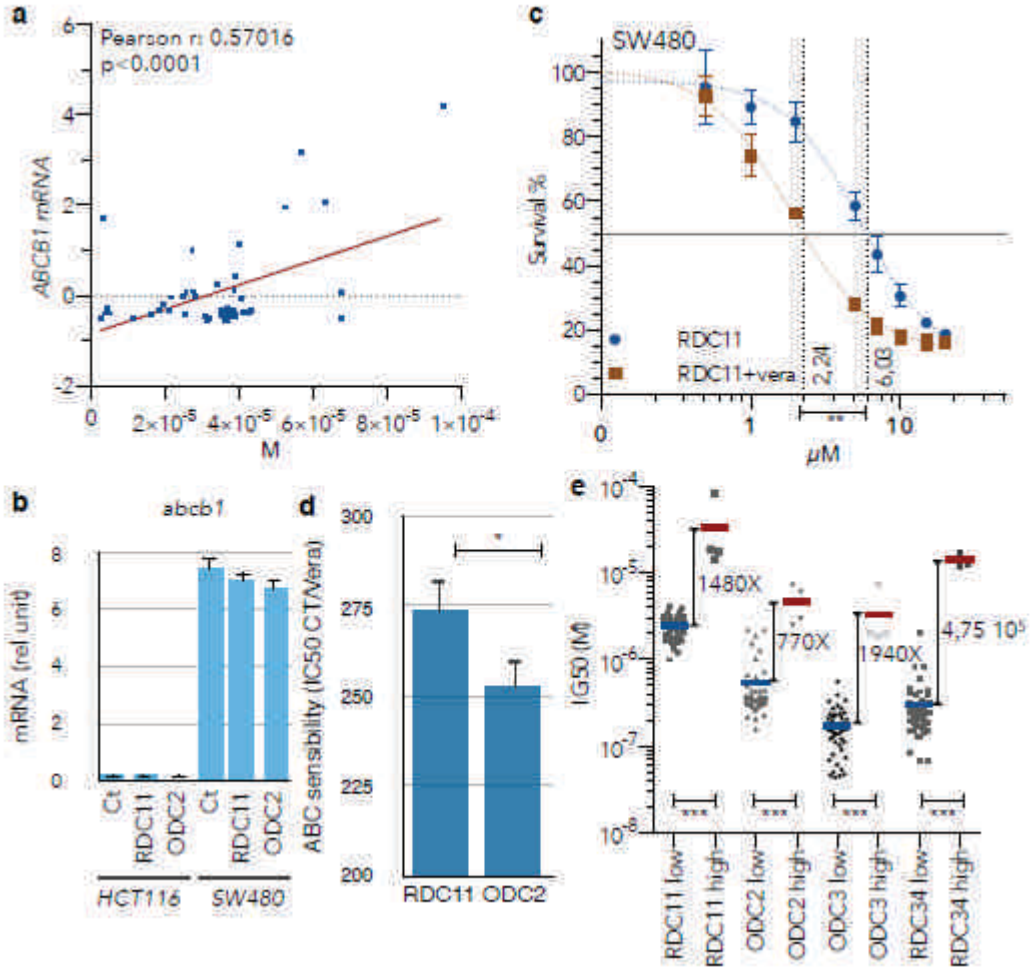
a
Pearson r: 0.57016
p<0.0001
ABCB1 mRNA
M
b
abcb1
mRNA (rel unit)
Ct
RDC11
ODC2
HCT116
SW480
d
ABC sensibility (IC50 CT/Vera)
RDC11 ODC2
c
SW480
Survival %
RDC11
RDC11+vera
2,24
6,08
μM
e
IG50 (M)
1480X
770X
1940X
4,75 10⁵
RDC11 low
RDC11 high
ODC2 low
ODC2 high
ODC3 low
ODC3 high
RDC34 low
RDC34 high

Figure S1

a

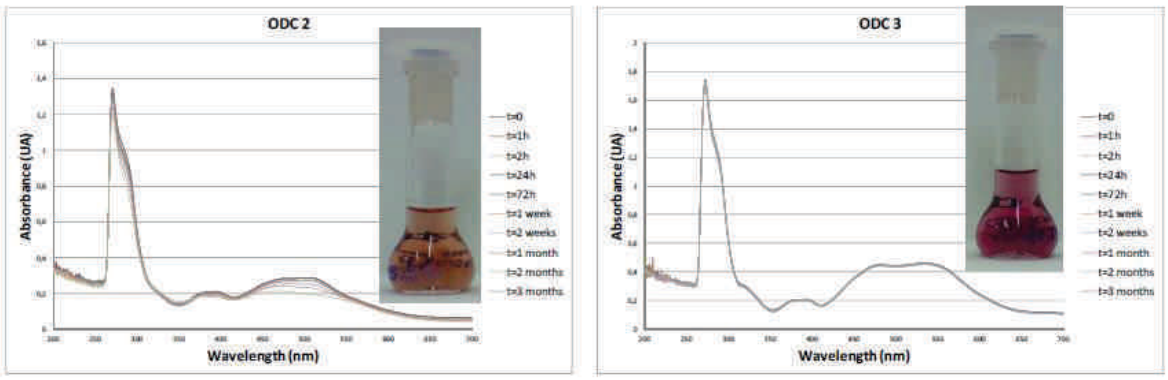

Figure S1: Stability and structure data of ODC2 and ODC3
a, Evolution of ODC2 and ODC3 stability over the time as measured by spectrometry

Figure S2

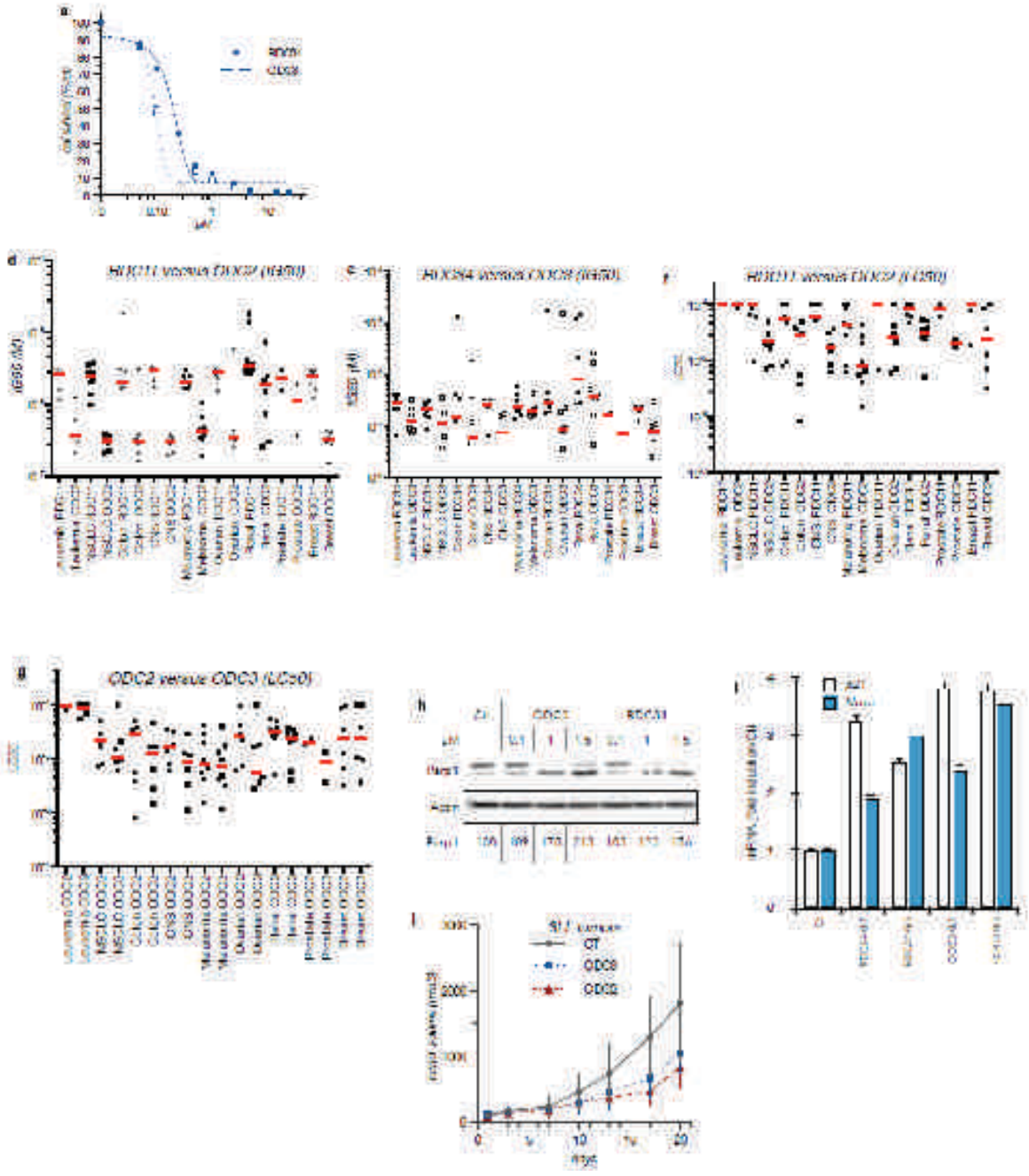

Figure S2: Cell growth and cytotoxicity of ODC2 and ODC3 compared to RDC11 and RDC34, on the 60 cancer cell lines of the National Cancer Institute

a., MTT test on HCT116 cells treated for 48h.

d, e, Diagrams representing the concentration for 50% of cell growth inhibition (IG50). NCI cancer cell lines (60) were grouped by cancer origins. Each point indicate a cell line. Red line indicate the median.

f, g, Diagrams representing the concentration for 50% of cell lethality (LC50). NCI cancer cell lines were grouped by cancer origins. Each point indicate a cell line. Red line indicate the median.

h, Parp1 cleaved visualized by Western blot from extract of HCT116 cells treated with the indicated drugs. Actin serves as internal control for protein concentration and loading.

i. mRNA levels of two known p53 target genes (p21 and noxa, f.) in the HCT116 treated with RDC34 or ODC3 at the indicated concentrations (µM). mRNA levels were assessed by RT-qPCR. Graph indicated means and standard devieation relative to the control (Ct, DMSO1%)

j. 3LL tumor growth folowing treatment with OD2 or ODC3. C57BL/6 mice (8-weeks old) were injected subcutaneously with 5 x e-5 3LL cells. Injections of RDC (RDC34 and ODC3 at 4 mmol/kg; RDC11 and ODC2 at 13.3 mmol/kg) started when tumors were palpable (100 mm3) and were performed twice a week. Solutions were prepared in PBS/5% Cremophore. Data are representative of two independent experiments (n = 7). Drugs effect were statistically different ($p < 0.01$) compared to control, as calculated by a one-way ANOVA test followed by a Tukey test.

Figure S3

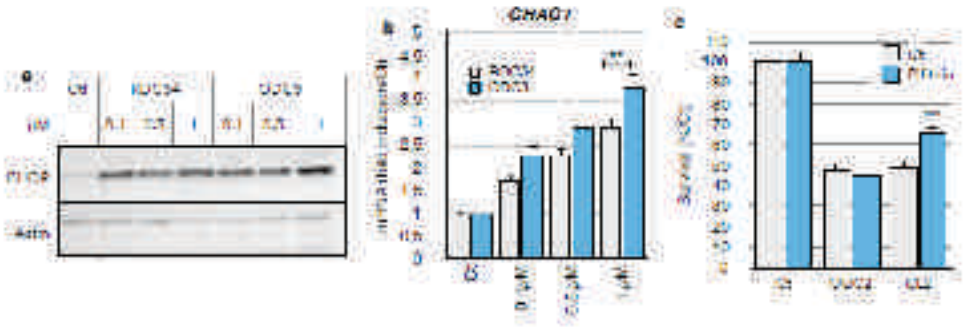

Figure S3: Expression of ER stress markers.

a, CHOP Western blot from extract of HCT116 cells treated with the indicated drugs. Actin serves as internal control for protein concentration and loading.
b. mRNA levels of the known CHOP target gene CHAC1 in the HCT116 colon cancer cell line treated with RDC34 or ODC3 at the indicated concentrations. mRNA levels were assessed by RT-qPCR.
c. Impact of the p53 inhibitor pifithrin on ODC2 and CL2 cytotoxicity. Pifithrin (10µM) was added 1h prior ODC2 and CL2. IC50 for ODC2 and CL2 were used (see figure 1). Cell survival was assessed using MTT test after 48h of treatment. Graph represents mean and standard deviation in % of surviving cells to the control (Ct, DMSO 1%).

** indicate statistical differences of 0.01 as determined by anova followed by Tukey post-test using GraphPad Prism software

Figure S4

a

Gene differently regulated Res/Sens cell lines (top 20/1000 genes with p>10-6)

Gene	p-value
FBXL5	3.277488E-11
EFR3A	1.856141E-10
PGK1	5.168053E-08
P3H1	7.970327E-08
ABCB1	1.648344E-07
WWC1	2.005928E-07
LPAR1	2.076520E-07
DOK4	4.771678E-07
SLC25A12	6.001617E-07
PLCB4	7.295562E-07
DOK4	8.615423E-07
NA	1.053210E-06
STEAP1	1.111157E-06
PLCB4	1.283180E-06
NA	1.373833E-06
GALNS	1.584826E-06
MCTS1	1.596777E-06
EGFR	1.665328E-06
NT5DC2	2.178898E-06

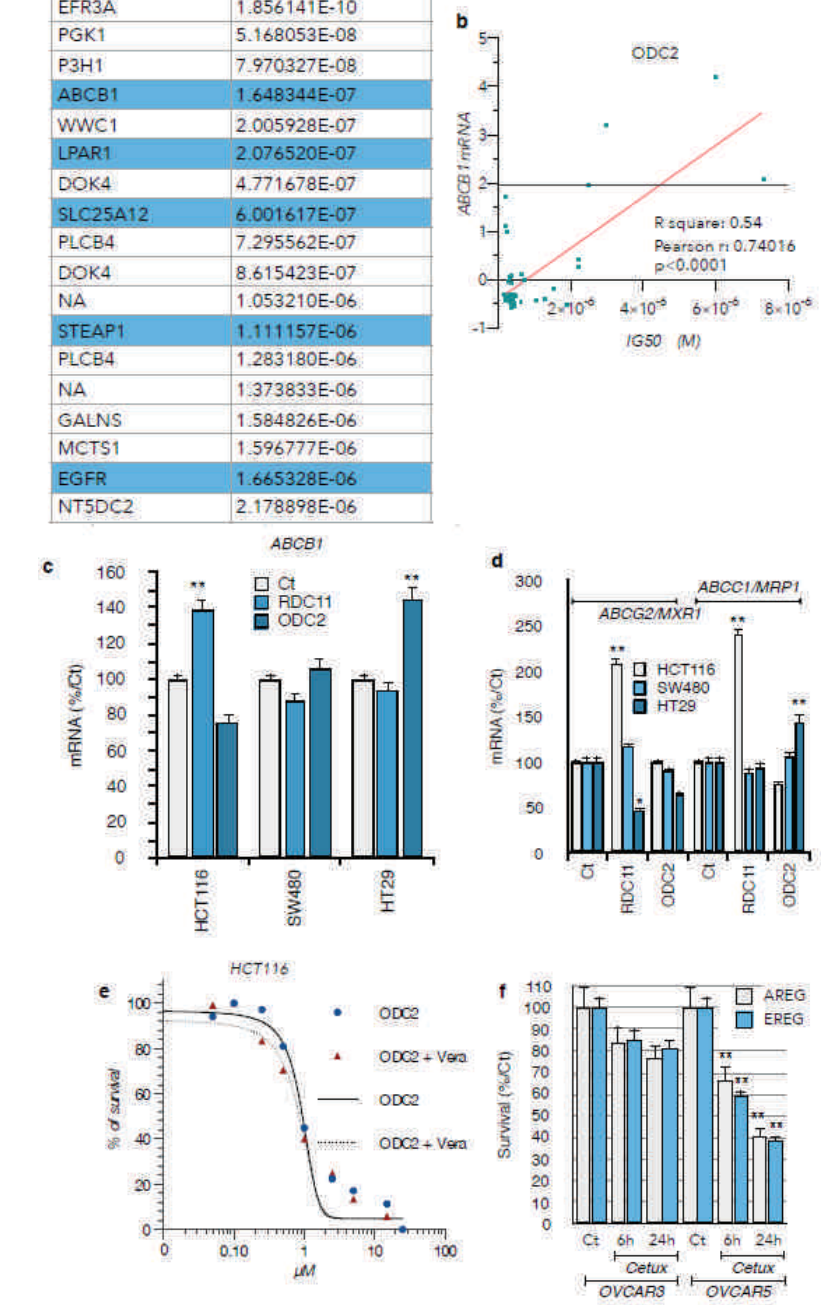

Figure S4:
a, List of the 20 most relevant gene differentially expressed between the two groups of cell lines with low and high sensibility towards RDC11. 4 sensitive cell lines (HOP92, SKMEL5, H522, OVCAR3) and 4 resistant cell lines (NCI AR, CAKI1, HCT15, UO31) for RDC11 were chosen and the genes commonly expressed in each group were identified using the CellExpress website.
b. Correlation of ABCB1 expression with the IG50 of the 60 different cancer cell lines of the NCI panel**.** mRNA are indicated as z score.
c, mRNA level of ABCB1 in response to RDC11 and ODC2. mRNA level are shown as % relative to the Ct.
d. Gene expression of export proteins (ABCG2, ABCC1). mRNA levels of two known drug export proteins (ABCG2 and ABCC1) in the indicated colon cancer cell lines treated with ODC2 or RDC11 at their IC50. mRNA levels were assessed by RT-qPCR.
e, MTT assay in HCT116 cells treated with ODC2, or ODC2 and verapamil (50μM). Cells were treated for 1h with ODC2 and MTT was performed 48h later. Verapamil was left during the whole experiment.
f. Gene expression of EGFR regulated genes (AREG, EREG) in OVCAR3 and OVCAR5 cells treated with Cetuximab (cetux, 0.5μM. mRNA levels were assessed by RT-qPCR.

** indicate statistical differences of 0.01 as determined by anova followed by Tukey post-test using GraphPad Prism software

Discussion & Perspectives

Development of new types of anticancer agents represents a major challenge in oncology. For several types of cancers, including gastric cancer, the use of platinum-based compounds does not completely fulfill the needs of patients due to their strong side effects and frequent resistance of the tumor to the treatment. However, in many cases platinum-based compounds are efficient, which encourages researchers to develop novel metal-based anticancer drugs being not sensitive to resistance mechanisms and/or the induction of side effects. In this respect, osmium- and ruthenium-based compounds were intensively studied for their anticancer properties and the variety of compounds that can be synthetized. Despite the clinical development of several ruthenium compounds like NAMI-A and KP1019 (Bergamo et al., 2012; Zeng et al., 2017), the development of others is not advancing mainly due to the lack of knowledge about their mode of action.

During my PhD, my project was focusing on two main aspects, which were the investigation of the mode of action of ruthenium-based compounds, more precisely RDC11, and the implication of efflux pumps in the sensibility towards ruthenium- and osmium-based organometallic compounds.

I) RDC11: Investigating the mode of action.

In the present work, I demonstrate that RDC11, like other ruthenium-based drugs, displays a higher cytotoxic activity on gastric cancer cells when compared to platinum compounds in vitro and in vivo. More precisely, I demonstrate that RDC11 displays its cytotoxic activity through oxidative and ER stress induction similarly to what has been shown by our group for other types of cancer (Meng et al., 2009; Vidimar et al., 2019). However, further investigations are needed in order to fully understand the mode of action of RDCs and promote their entry in clinical trials. With my PhD work, I could demonstrate the induction of a new interesting pathway by RDC11 linking ER stress induction to the repression of the transsulfuration pathway. Firstly, I could show that RDC11 induces the expression of several markers of the ER stress pathway including CHOP and XBP1s in gastric cancer cells, which is in accordance with

previous studies (Licona et al., 2017; Meng et al., 2009). Secondly, in addition to the activation of CHOP and XBP1s, I found that RDC11 also induces the expression of the transcription factor ATF4, an upstream regulator of CHOP expression. Importantly, ATF4 is also known to regulate several genes implicated in amino acids import and synthesis including cystathionine gamma-lyase (CTH), a central actor of the transsulfuration pathway (Dickhout et al., 2012; Mistry et al., 2016). Therefore, I investigated the role of RDC11 on the transsulfuration pathway known to be the only way of cysteine de novo synthesis. I demonstrate that, in gastric cancer cells, RDC11 treatment can increase CTH expression in an ATF4 dependent manner and further to repress CBS expression suggesting that ATF4 acts as a repressor on CBS expression. Interestingly, CBS is known to be the "rate limiting" step of the transsulfuration (Zhu et al., 2018) and repression of its activity suggest that RDC11 lowers the flux through the transsulfuration pathway resulting in lower cysteine production. Interestingly, I could demonstrate that RDC11 induces the expression of the antiporter xCT which might therefore lead to increased glutamate efflux in order to replenish cysteine content, further enhancing the dramatic decrease of glutamate levels. Like glutamate is a precursor for glutathione (GSH) synthesis (Liu et al., 2014), this strong decrease results in the important reduction of glutathione production suggesting a lower antioxidant capacity for RDC11 treated cells. RDC11 was demonstrated to induce high levels of ROS similar to the known ROS inducer H_2O_2. Furthermore, high ROS production correlated with low GSH content are known to be associate with cellular weakening suggesting that those regulations are implicated in the cytotoxic activity of RDC11. Importantly, further decreasing GSH levels by buthionine sulfoximine (BSO) treatment, a glutamate-cysteine ligase inhibitor, resulted in a more pronounced cell death induction by RDC11. In contrast, supplementing cells with GSH resulted in a rescue of RDC11 induced cell death. Taken together, those results demonstrate that the decrease in GSH levels participate actively in the mode of action of RDC11. In addition, I demonstrate by flow cytometry that RDC11 induces apoptosis, without inducing caspase-3 cleavage. Together, my observation that RDC11 induces ER stress, ROS production and low glutathione levels led us to hypothesis that RDC11 might induce either ferroptosis or caspase independent cell death.

I.1) Ferroptosis

Ferroptosis is an iron dependent cell death induced by low GSH and high ROS production (Yang et al., 2014). For this I analyzed the induction of ferroptosis markers by RDC11 and the effect of ferrostatin-1, which inhibits ferroptosis, on the cytotoxicity of RDC11. Firstly, I compared the effect of RDC11 to the effect of a known inducer of ferroptosis, Erastin on the mRNA expression of GPx4 and PTGS2 (encoding for the cyclooxygenase-2 (COX-2)) (Jiang et al., 2009; Yang et al., 2014). At the transcriptional level, RDC11, like Erastin, was able to decrease GPx4 expression. However, no induction of PTGS2 was observed with RDC11 suggesting that ferroptosis might only be partially induced by RDC11. However, analysis of the effect of RDC11 on those ferroptosis markers should be performed at the protein level as its activity is mostly regulated at the post-translational level. Secondly, in order to assess the functionality of ferroptosis induction, I used the ferroptosis inhibitor, ferrostatin-1. If ferroptosis would play a role in RDC11 cytotoxicity, co-treatment of RDC11 with ferrostatin-1 should enhance the survival of treated cells, in other words partially block its cytotoxicity. Co-treatment of AGS cells with ferrostatin-1 and RDC11 did not affect cell survival further confirming an absence of ferroptosis induction.

Despite the fact that ferrostatin-1 did not change the cytotoxicity of RDC11, RDC11 partially induced the expression of ferroptosis markers. This suggests that RDC11 might only lead to an uncomplete induction of ferroptosis. However, in order to synthetize new ruthenium-based compounds able to induce this pathway, it remains to be further investigated why RDC11 did not induce a complete ferroptosis. For example, the iron metabolism should be analyzed focusing on enzymes like DMT1 (Divalent Metal Transporter 1) or transferrin, which plays a central role in iron homeostasis and which could help us to uncover why in the case of RDC11, ferroptosis is not induced.

I.2) Caspase independent apoptosis

Another cell death pathway that can explain the cytotoxicity of RDC11 and which is totally independent of caspase-3 cleavage is the induction of caspase independent cell death (Elmore, 2007), which would be in accordance with my observation that, in

contrast to oxaliplatin, RDC11 does not induce cleaved caspase 3 expression. Caspase independent cell death is mediated by the translocation of AIF from the mitochondria to the nucleus (Bano and Prehn, 2018). According to the literature, PARP-1 is a major actor of the induction of caspase independent cell death, which plays a role in dissipating mitochondrial membranes facilitating the release of AIF (Bano et al., 2018). Furthermore, PARPs activity leads to the synthesis of poly(ADP-ribose) (PAR) polymers interacting with the C-terminal domain of membrane bound AIF, controlling AIF release leading to AIF dependent chromatinolysis. With my work, I could demonstrate through immunofluorescence that AGS cells treated with RDC11 present high levels of nuclear AIF suggesting an induction of caspase independent cell death. Interestingly, in the case of RDC11, it seems that inhibiting PARP activity by olaparib did not decrease the number of positive cells but lowered the intensity of AIF nuclear signal suggesting a less important AIF translocation in absence of PARP activity. This suggests that RDC11 induces caspase independent cell death but the precise role of AIF and PARP in the cytotoxicity of RDC11 still need some further investigations. Therefore, the role of PARP and AIF in RDC11 mediated caspase independent apoptosis should be investigated by analyzing the effect of PARPs inhibition or the loss of AIF expression using olaparib or specific siRNAs respectively.

I.3) How does RDC11 induce ER stress?

Published data clearly suggest that ruthenium-based compounds might, in general, be able to induce the ER stress pathway (Chow et al., 2016, 2018; Meng et al., 2009; Xu et al., 2019). However, one of the major challenges is to understand how those compounds induce this pathway. In order to better identify RDC11 cellular targets, we performed an affinity chromatography approach by using a matrix bound RDC11 (matrix: HypoGel 400-COOH). Protein extract from RDC11 treated AGS cells were loaded onto matrix bound RDC11 and RDC11 interacting proteins were then eluted with an excess of free RDC11 and analyzed by mass spectrometry (Licona et al., 2017). This analysis revealed an interaction between RDC11 and two PDIs, namely DNAJC10 and PDIA3. PDIs are proteins responsible for disulphide bonds formation and rearrangement within the ER (Figure 14) (Jordan and Gibbins, 2006) and their inhibition can induce misfolded protein aggregation. Furthermore, it is well known that

protein aggregation can induce ER stress pathway (Lee and Lee, 2017). For this reason, our hypothesis is that RDC11 is able to induce ER stress pathway through PDI inhibition. With my work I already could show that RDC11 represses the expression of DNAJC10 and PDIA3 suggesting lower cellular protein folding capacity maybe causing ER stress activation. Moreover, I obtained similar results for other PDI family members including PDIA4, 5 and 6 suggesting an ER stress induction due to lower PDIs expression. However, a more precise analysis of the interaction between RDC11 and these PDIs should be performed in gastric cancer cells in order to confirm the mass spectrometry analysis and further determine RDC11 effects on PDIs activity.

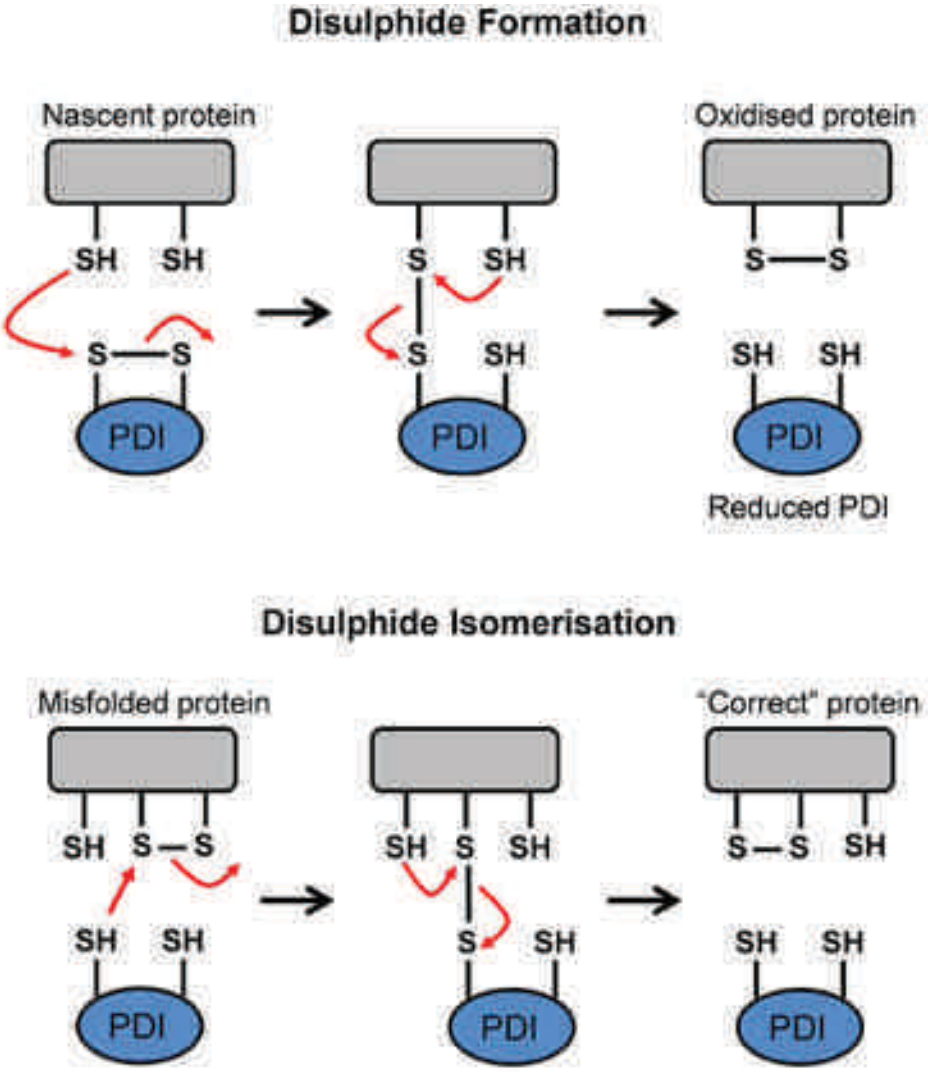

Figure 14: Schematic representation of disulphide bond formation and isomerisation and the implication of protein disulphide isomerase
Source Emma R et *al.*, 2016 Front Cell Dev

Interestingly, in contrary to RDC11, the classical inducer of ER stress tunicamycin was shown to induce the expression of those PDIs, highlighting an important difference in the type of ER stress induced by those two compounds. It would be interesting to determine more precisely if this difference accounts for the differences observed in the cytotoxic activity and ER stress pathway induction by those two drugs. On one hand, RDC11 was shown to induce ER stress pathway and ATF4 expression, leading to repression of the transsulfuration pathway and glutathione production participating in its cytotoxic activity. On the other hand, even if tunicamycin is able to induce ATF4, it did not decrease glutathione production highlighting the therapeutic potential of RDC11 in contrast to classical ER stress inducers.

I.4) Do different metals induce the same or different ER stress pathways?

In the lab, we are investigating ruthenium- but also osmium-based compounds for their anticancer potentials. For several members of those families (RDC and ODC), we have generated osmium counterparts of ruthenium-based drugs, for example in the case of RDC11 and ODC2. This means that RDC11 and ODC2 have the same ligands attached and only differ in the core-metal, ruthenium versus osmium respectively. Importantly, investigating compounds with the same ligands but different metals allows us to determine the role of the metal in the cytotoxic activity of the compound and further determine if we can link metals with the induction of specific pathways. With my work, I have provided the evidence that ruthenium and osmium compounds with the same ligands are equally able to induce ER stress pathway. However, the ER stress sensors that are activated and the kinetic of their induction by RDCs and ODCs are not identical and also differ from tunicamycin, a well-known ER stress pathway inducer, suggesting the induction of another type of ER stress. Furthermore, this suggests a dynamic regulation of the different ER stress branches, IRE1α, ATF6 and PERK respectively, induced by RDC11 and ODC2. For example, in our laboratory, we provided the evidence that the cytotoxic activity of ODC2 requires the induction of CHOP but did not require the PERK-ATF4 axis, which is not the case for its ruthenium counterpart, RDC11. Understanding specifically how and which ER stress sensor is induced by organometallic compounds still remain of great interest for the scientific

community. Therefore, investigating in more details whether IRE1α, ATF6 or PERK is activated in response to those compounds and determine if their induction play a pro-survival or pro-apoptotic role would enable the development of new classes of organometallic compounds. Those new compounds would be designed to induce specifically the pro-apoptotic side while inhibiting the pro-survival one of ER stress. That is why silencing specific branches of ER stress pathway and understanding their role in the cytotoxic activity of our compounds would be important in order to understand the functionality of ER stress induction.

II) Sensibility to efflux

II.1) Investigating the implication of the ABC family in the activity of RDC11

The difference observed in the cytotoxic activity of RDC11 and its osmium counterpart ODC2 led us to investigate genes or pathways playing a role in the transmembrane transport of platinum-based anti-cancer drugs. Firstly, the clustering of the NCI cancer cell lines into 2 groups: sensible (with a low GI_{50}) or resistant (with a high GI_{50}) to RDC11 and ODC2. Then, we identify the top 100 most significantly differently expressed genes between the sensible and resistant groups. Furthermore, we correlate their expression with 4 couples of sensitive and resistant cell lines spanning different cancer types in order to avoid inter-cancer type bias. This led to the selection of 20 genes including ABCB1, a member of the ATP-binding cassette (ABC) transporter superfamily known to regulate cytotoxic potential of platinum-based anticancer drugs (Martinez-Balibrea et al., 2015). The aim of this part of my PhD project was to understand if ABCB1 can give account for the different cytotoxic potential of RDC11 and ODC2. More precisely, I wanted to determine if inhibiting ABC mediated efflux using verapamil, an ABC transporter inhibitor, enhances the cytotoxic activity of our compounds by inducing higher intracellular drug contents. To do so, I co-treated colon cancer cells with verapamil and RDC11 or ODC2 in order to determine if cell survival is impacted by the inhibition of the drug efflux. This showed that inhibition of ABC mediated efflux increases the cytotoxic activity of RDC11 and ODC2 suggesting that ABCB1 is implicated in the efflux of ruthenium- and osmium-based drugs.

Importantly, this study presents the first evidence of organometallic drugs efflux and its contribution in their cytotoxicity. However, verapamil is not a specific inhibitor of ABCB1 inhibiting also other ABC family members. Therefore, I cannot exclude that the effect observed on cell survival is specific to the inhibition of ABCB1 or might be due to the inhibition of additional ABC transporter family members. For this reason, further investigations focusing on specific inhibition of ABCB1, with for example silencer RNAs, should be performed in order to specifically analyze the role of ABCB1 in organometallic drug efflux.

Conclusion

The present work gives a new insight about how osmium- and ruthenium-based compounds act on cancer cell. More precisely, I showed during my PhD that one main mode of action of RDC11 is the metabolic regulation of the transsulfuration pathway enabling a glutathione shut down and induction of caspase independent cell death. Furthermore, I provided for the first time the evidence that ABC mediated efflux of osmium- and ruthenium-based compounds regulate the cytotoxicity of these compounds.

Altogether, these studies demonstrate for the first time the implication of metabolic pathways and drug efflux mechanisms in the cytotoxic activity of organometallic compounds. These new targets should be incorporated in the study of new generations organometallic drugs in order to determine more precisely their biological activities and also if we can extrapolate the here presented results to other organometallic drugs.

Conclusion scheme

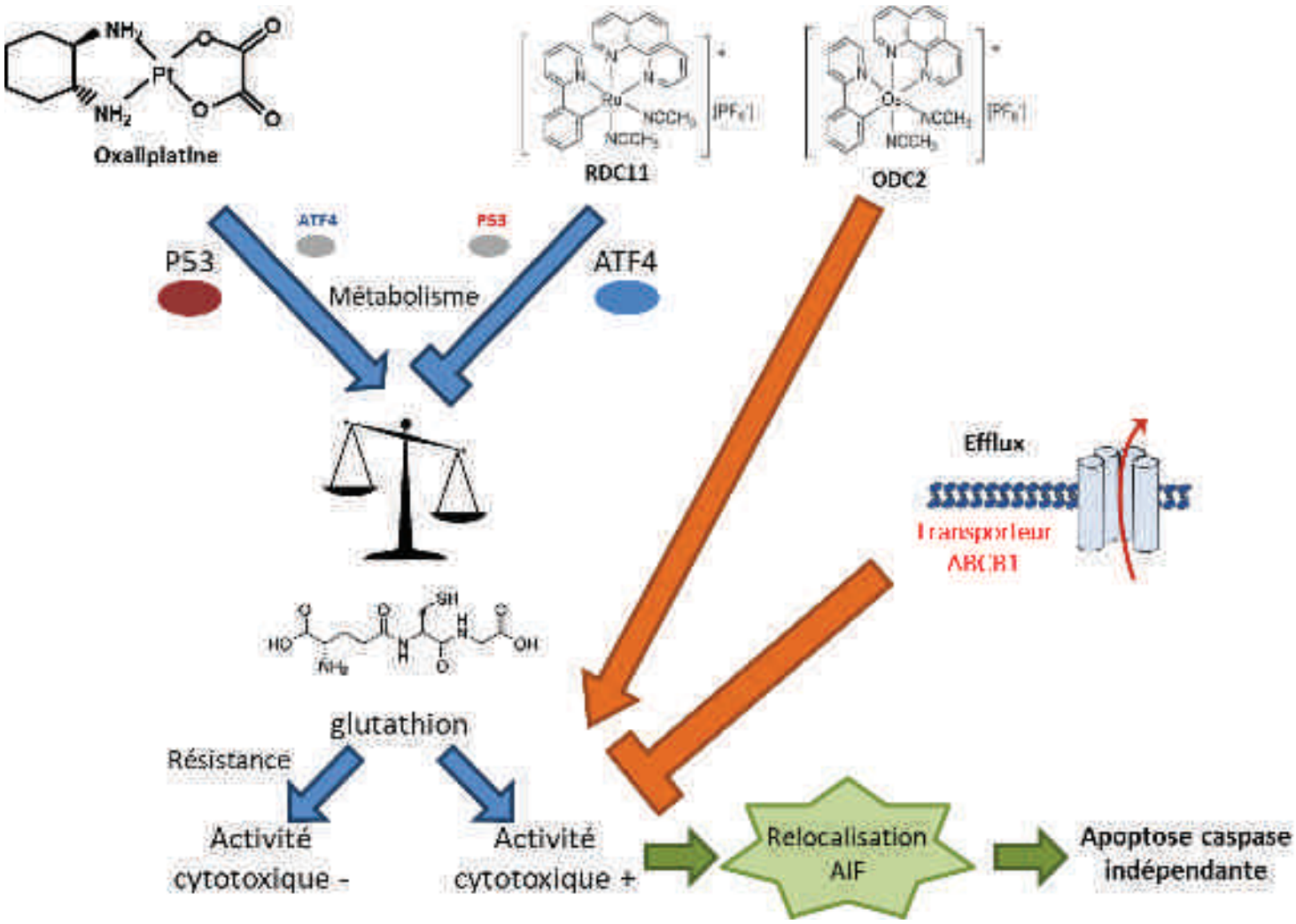

Bibliography

Alasiri, G., Fan, L.Y.-N., Zona, S., Goldsbrough, I.G., Ke, H.-L., Auner, H.W., and Lam, E.W.-F. (2018). ER stress and cancer: The FOXO forkhead transcription factor link. Mol. Cell. Endocrinol. *462*, 67–81.

Alcindor, T., and Beauger, N. (2011). Oxaliplatin: a review in the era of molecularly targeted therapy. Curr. Oncol. Tor. Ont *18*, 18–25.

Ameri, K., and Harris, A.L. (2008). Activating transcription factor 4. Int. J. Biochem. Cell Biol. *40*, 14–21.

Balendiran, G.K., Dabur, R., and Fraser, D. (2004). The role of glutathione in cancer. Cell Biochem. Funct. *22*, 343–352.

Bano, D., and Prehn, J.H.M. (2018). Apoptosis-Inducing Factor (AIF) in Physiology and Disease: The Tale of a Repented Natural Born Killer. EBioMedicine *30*, 29–37.

Bergamo, A., Gaiddon, C., Schellens, J.H.M., Beijnen, J.H., and Sava, G. (2012). Approaching tumour therapy beyond platinum drugs: status of the art and perspectives of ruthenium drug candidates. J. Inorg. Biochem. *106*, 90–99.

Binet, F., and Sapieha, P. (2015). ER Stress and Angiogenesis. Cell Metab. *22*, 560–575.

Boff, B., Gaiddon, C., and Pfeffer, M. (2013). Cancer cell cytotoxicity of cyclometalated compounds obtained with osmium(II) complexes. Inorg. Chem. *52*, 2705–2715.

Chen, W., Zou, P., Zhao, Z., Weng, Q., Chen, X., Ying, S., Ye, Q., Wang, Z., Ji, J., and Liang, G. (2016). Selective killing of gastric cancer cells by a small molecule via targeting TrxR1 and ROS-mediated ER stress activation. Oncotarget *7*, 16593–16609.

Chow, M.J., Licona, C., Yuan Qiang Wong, D., Pastorin, G., Gaiddon, C., and Ang, W.H. (2014). Discovery and investigation of anticancer ruthenium-arene Schiff-base complexes via water-promoted combinatorial three-component assembly. J. Med. Chem. *57*, 6043–6059.

Chow, M.J., Licona, C., Pastorin, G., Mellitzer, G., Ang, W.H., and Gaiddon, C. (2016). Structural tuning of organoruthenium compounds allows oxidative switch to control ER stress pathways and bypass multidrug resistance. Chem. Sci. *7*, 4117–4124.

Chow, M.J., Babak, M.V., Tan, K.W., Cheong, M.C., Pastorin, G., Gaiddon, C., and Ang, W.H. (2018). Induction of the Endoplasmic Reticulum Stress Pathway by Highly Cytotoxic Organoruthenium Schiff-Base Complexes. Mol. Pharm. *15*, 3020–3031.

Cloonan, S.M., Elmes, R.B.P., Erby, M., Bright, S.A., Poynton, F.E., Nolan, D.E., Quinn, S.J., Gunnlaugsson, T., and Williams, D.C. (2015). Detailed Biological Profiling of a Photoactivated and Apoptosis Inducing pdppz Ruthenium(II) Polypyridyl Complex in Cancer Cells. J. Med. Chem. *58*, 4494–4505.

Combs, J.A., and DeNicola, G.M. (2019). The Non-Essential Amino Acid Cysteine Becomes Essential for Tumor Proliferation and Survival. Cancers *11*.

Dasari, S., and Tchounwou, P.B. (2014). Cisplatin in cancer therapy: molecular mechanisms of action. Eur. J. Pharmacol. *740*, 364–378.

Deeley, R.G., and Cole, S.P. (1997). Function, evolution and structure of multidrug resistance protein (MRP). Semin. Cancer Biol. *8*, 193–204.

Dickhout, J.G., Carlisle, R.E., Jerome, D.E., Mohammed-Ali, Z., Jiang, H., Yang, G., Mani, S., Garg, S.K., Banerjee, R., Kaufman, R.J., et al. (2012). Integrated stress response modulates cellular redox state via induction of cystathionine γ-lyase: cross-talk between integrated stress response and thiol metabolism. J. Biol. Chem. *287*, 7603–7614.

Elmore, S. (2007). Apoptosis: a review of programmed cell death. Toxicol. Pathol. *35*, 495–516.

Feng, R., Zhai, W.L., Yang, H.Y., Jin, H., and Zhang, Q.X. (2011). Induction of ER stress protects gastric cancer cells against apoptosis induced by cisplatin and doxorubicin through activation of p38 MAPK. Biochem. Biophys. Res. Commun. *406*, 299–304.

Flocke, L.S., Trondl, R., Jakupec, M.A., and Keppler, B.K. (2016). Molecular mode of action of NKP-1339 - a clinically investigated ruthenium-based drug - involves ER- and ROS-related effects in colon carcinoma cell lines. Invest. New Drugs *34*, 261–268.

Galluzzi, L., Senovilla, L., Vitale, I., Michels, J., Martins, I., Kepp, O., Castedo, M., and Kroemer, G. (2012). Molecular mechanisms of cisplatin resistance. Oncogene *31*, 1869–1883.

Garattini, S.K., Basile, D., Cattaneo, M., Fanotto, V., Ongaro, E., Bonotto, M., Negri, F.V., Berenato, R., Ermacora, P., Cardellino, G.G., et al. (2017). Molecular classifications of gastric cancers: Novel insights and possible future applications. World J. Gastrointest. Oncol. *9*, 194–208.

Hanif, M., Babak, M.V., and Hartinger, C.G. (2014). Development of anticancer agents: wizardry with osmium. Drug Discov. Today *19*, 1640–1648.

Harding, H.P., Novoa, I., Zhang, Y., Zeng, H., Wek, R., Schapira, M., and Ron, D. (2000a). Regulated translation initiation controls stress-induced gene expression in mammalian cells. Mol. Cell *6*, 1099–1108.

Harding, H.P., Zhang, Y., Bertolotti, A., Zeng, H., and Ron, D. (2000b). Perk is essential for translational regulation and cell survival during the unfolded protein response. Mol. Cell *5*, 897–904.

Harding, H.P., Zhang, Y., Zeng, H., Novoa, I., Lu, P.D., Calfon, M., Sadri, N., Yun, C., Popko, B., Paules, R., et al. (2003). An integrated stress response regulates amino acid metabolism and resistance to oxidative stress. Mol. Cell *11*, 619–633.

Hartinger, C.G., Phillips, A.D., and Nazarov, A.A. (2011). Polynuclear ruthenium, osmium and gold complexes. The quest for innovative anticancer chemotherapeutics. Curr. Top. Med. Chem. *11*, 2688–2702.

Hatem, E., El Banna, N., and Huang, M.-E. (2017). Multifaceted Roles of Glutathione and Glutathione-Based Systems in Carcinogenesis and Anticancer Drug Resistance. Antioxid. Redox Signal. *27*, 1217–1234.

Hellmich, M.R., and Szabo, C. (2015). Hydrogen Sulfide and Cancer. Handb. Exp. Pharmacol. *230*, 233–241.

Hernández-Breijo, B., Monserrat, J., Ramírez-Rubio, S., Cuevas, E.P., Vara, D., Díaz-Laviada, I., Fernández-Moreno, M.D., Román, I.D., Gisbert, J.P., and Guijarro, L.G. (2011). Preclinical evaluation of azathioprine plus buthionine sulfoximine in the treatment of human hepatocarcinoma and colon carcinoma. World J. Gastroenterol. *17*, 3899–3911.

Hetz, C. (2012). The unfolded protein response: controlling cell fate decisions under ER stress and beyond. Nat. Rev. Mol. Cell Biol. *13*, 89–102.

Hetz, C., Chevet, E., and Harding, H.P. (2013). Targeting the unfolded protein response in disease. Nat. Rev. Drug Discov. *12*, 703–719.

Hishiki, T., Yamamoto, T., Morikawa, T., Kubo, A., Kajimura, M., and Suematsu, M. (2012). Carbon monoxide: impact on remethylation/transsulfuration metabolism and its pathophysiologic implications. J. Mol. Med. Berl. Ger. *90*, 245–254.

Işeri, S., Ercan, F., Gedik, N., Yüksel, M., and Alican, I. (2007). Simvastatin attenuates cisplatin-induced kidney and liver damage in rats. Toxicology *230*, 256–264.

Jakubowski, H. (2006). Pathophysiological consequences of homocysteine excess. J. Nutr. *136*, 1741S-1749S.

Jefferies, H., Coster, J., Khalil, A., Bot, J., McCauley, R.D., and Hall, J.C. (2003). Glutathione. ANZ J. Surg. *73*, 517–522.

Jiang, C.C., Mao, Z.G., Avery-Kiejda, K.A., Wade, M., Hersey, P., and Zhang, X.D. (2009). Glucose-regulated protein 78 antagonizes cisplatin and adriamycin in human melanoma cells. Carcinogenesis *30*, 197–204.

Johnstone, T.C., Suntharalingam, K., and Lippard, S.J. (2015). Third row transition metals for the treatment of cancer. Philos. Transact. A Math. Phys. Eng. Sci. *373*.

Jordan, P.A., and Gibbins, J.M. (2006). Extracellular disulfide exchange and the regulation of cellular function. Antioxid. Redox Signal. *8*, 312–324.

Kabil, O., Yadav, V., and Banerjee, R. (2016). Heme-dependent Metabolite Switching Regulates H2S Synthesis in Response to Endoplasmic Reticulum (ER) Stress. J. Biol. Chem. *291*, 16418–16423.

Kania, E., Pająk, B., and Orzechowski, A. (2015). Calcium homeostasis and ER stress in control of autophagy in cancer cells. BioMed Res. Int. *2015*, 352794.

Karimi, P., Islami, F., Anandasabapathy, S., Freedman, N.D., and Kamangar, F. (2014). Gastric cancer: descriptive epidemiology, risk factors, screening, and prevention. Cancer Epidemiol. Biomark. Prev. Publ. Am. Assoc. Cancer Res. Cosponsored Am. Soc. Prev. Oncol. *23*, 700–713.

Kauvar, L.M., Morgan, A.S., Sanderson, P.E., and Henner, W.D. (1998). Glutathione based approaches to improving cancer treatment. Chem. Biol. Interact. *111–112*, 225–238.

Kilari, D., Guancial, E., and Kim, E.S. (2016). Role of copper transporters in platinum resistance. World J. Clin. Oncol. *7*, 106–113.

Kim, J., Kim, H., Roh, H., and Kwon, Y. (2018). Causes of hyperhomocysteinemia and its pathological significance. Arch. Pharm. Res. *41*, 372–383.

Klajner, M., Licona, C., Fetzer, L., Hebraud, P., Mellitzer, G., Pfeffer, M., Harlepp, S., and Gaiddon, C. (2014). Subcellular localization and transport kinetics of ruthenium organometallic anticancer compounds in living cells: a dose-dependent role for amino acid and iron transporters. Inorg. Chem. *53*, 5150–5158.

Konkankit, C.C., Marker, S.C., Knopf, K.M., and Wilson, J.J. (2018). Anticancer activity of complexes of the third row transition metals, rhenium, osmium, and iridium. Dalton Trans. Camb. Engl. 2003 *47*, 9934–9974.

Lai, W.K.C., and Kan, M.Y. (2015). Homocysteine-Induced Endothelial Dysfunction. Ann. Nutr. Metab. *67*, 1–12.

Lee, E., and Lee, D.H. (2017). Emerging roles of protein disulfide isomerase in cancer. BMB Rep. *50*, 401–410.

Li, C., Ip, K.-W., Man, W.-L., Song, D., He, M.-L., Yiu, S.-M., Lau, T.-C., and Zhu, G. (2017). Cytotoxic (salen)ruthenium(iii) anticancer complexes exhibit different modes of cell death directed by axial ligands. Chem. Sci. *8*, 6865–6870.

Licona, C., Spaety, M.-E., Capuozzo, A., Ali, M., Santamaria, R., Armant, O., Delalande, F., Van Dorsselaer, A., Cianferani, S., Spencer, J., et al. (2017). A ruthenium anticancer compound interacts with histones and impacts differently on epigenetic and death pathways compared to cisplatin. Oncotarget *8*, 2568–2584.

Lin, Y., Wang, Z., Liu, L., and Chen, L. (2011). Akt is the downstream target of GRP78 in mediating cisplatin resistance in ER stress-tolerant human lung cancer cells. Lung Cancer Amst. Neth. *71*, 291–297.

Liu, Y., Hyde, A.S., Simpson, M.A., and Barycki, J.J. (2014). Emerging regulatory paradigms in glutathione metabolism. Adv. Cancer Res. *122*, 69–101.

Lu, H., Blunden, B.M., Scarano, W., Lu, M., and Stenzel, M.H. (2016). Anti-metastatic effects of RAPTA-C conjugated polymeric micelles on two-dimensional (2D) breast tumor cells and three-dimensional (3D) multicellular tumor spheroids. Acta Biomater. *32*, 68–76.

Maclean, K.N., Greiner, L.S., Evans, J.R., Sood, S.K., Lhotak, S., Markham, N.E., Stabler, S.P., Allen, R.H., Austin, R.C., Balasubramaniam, V., et al. (2012). Cystathionine protects against endoplasmic reticulum stress-induced lipid accumulation, tissue injury, and apoptotic cell death. J. Biol. Chem. *287*, 31994–32005.

Mandic, A., Hansson, J., Linder, S., and Shoshan, M.C. (2003). Cisplatin induces endoplasmic reticulum stress and nucleus-independent apoptotic signaling. J. Biol. Chem. *278*, 9100–9106.

Martinez-Balibrea, E., Martínez-Cardús, A., Ginés, A., Ruiz de Porras, V., Moutinho, C., Layos, L., Manzano, J.L., Bugés, C., Bystrup, S., Esteller, M., et al. (2015). Tumor-Related Molecular Mechanisms of Oxaliplatin Resistance. Mol. Cancer Ther. *14*, 1767–1776.

Massai, L., Fernández-Gallardo, J., Guerri, A., Arcangeli, A., Pillozzi, S., Contel, M., and Messori, L. (2015). Design, synthesis and characterisation of new chimeric ruthenium(II)-gold(I) complexes as improved cytotoxic agents. Dalton Trans. Camb. Engl. 2003 *44*, 11067–11076.

McConkey, D.J. (2017). The integrated stress response and proteotoxicity in cancer therapy. Biochem. Biophys. Res. Commun. *482*, 450–453.

Meng, X., Leyva, M.L., Jenny, M., Gross, I., Benosman, S., Fricker, B., Harlepp, S., Hébraud, P., Boos, A., Wlosik, P., et al. (2009). A ruthenium-containing organometallic compound reduces tumor growth through induction of the endoplasmic reticulum stress gene CHOP. Cancer Res. *69*, 5458–5466.

Mistry, R.K., Murray, T.V.A., Prysyazhna, O., Martin, D., Burgoyne, J.R., Santos, C., Eaton, P., Shah, A.M., and Brewer, A.C. (2016). Transcriptional Regulation of Cystathionine-γ-Lyase in Endothelial Cells by NADPH Oxidase 4-Dependent Signaling. J. Biol. Chem. *291*, 1774–1788.

Moenner, M., Pluquet, O., Bouchecareilh, M., and Chevet, E. (2007). Integrated endoplasmic reticulum stress responses in cancer. Cancer Res. *67*, 10631–10634.

Mosharov, E., Cranford, M.R., and Banerjee, R. (2000). The quantitatively important relationship between homocysteine metabolism and glutathione synthesis by the transsulfuration pathway and its regulation by redox changes. Biochemistry *39*, 13005–13011.

Mungrue, I.N., Pagnon, J., Kohannim, O., Gargalovic, P.S., and Lusis, A.J. (2009). CHAC1/MGC4504 is a novel proapoptotic component of the unfolded protein response, downstream of the ATF4-ATF3-CHOP cascade. J. Immunol. Baltim. Md 1950 *182*, 466–476.

Novak, M.S., Büchel, G.E., Keppler, B.K., and Jakupec, M.A. (2016). Biological properties of novel ruthenium- and osmium-nitrosyl complexes with azole heterocycles. J. Biol. Inorg. Chem. JBIC Publ. Soc. Biol. Inorg. Chem. *21*, 347–356.

Oakes, S.A. (2017). Endoplasmic reticulum proteostasis: a key checkpoint in cancer. Am. J. Physiol. Cell Physiol. *312*, C93–C102.

Ojha, R., and Amaravadi, R.K. (2017). Targeting the unfolded protein response in cancer. Pharmacol. Res. *120*, 258–266.

Oun, R., Moussa, Y.E., and Wheate, N.J. (2018). The side effects of platinum-based chemotherapy drugs: a review for chemists. Dalton Trans. Camb. Engl. 2003 *47*, 6645–6653.

Peng, F., Zhang, H., Du, Y., and Tan, P. (2018). Cetuximab enhances cisplatin-induced endoplasmic reticulum stress-associated apoptosis in laryngeal squamous cell carcinoma cells by inhibiting expression of TXNDC5. Mol. Med. Rep. *17*, 4767–4776.

Perek, N., and Denoyer, D. (2002). The multidrug resistance mechanisms and their interactions with the radiopharmaceutical probes used for an in vivo detection. Curr. Drug Metab. *3*, 97–113.

Philippe, C., Dubrac, A., Quelen, C., Desquesnes, A., Van Den Berghe, L., Ségura, C., Filleron, T., Pyronnet, S., Prats, H., Brousset, P., et al. (2016). PERK mediates the IRES-dependent translational activation of mRNAs encoding angiogenic growth factors after ischemic stress. Sci. Signal. *9*, ra44.

Rabik, C.A., Fishel, M.L., Holleran, J.L., Kasza, K., Kelley, M.R., Egorin, M.J., and Dolan, M.E. (2008). Enhancement of Cisplatin [cis-Diammine Dichloroplatinum (II)] Cytotoxicity by O6-Benzylguanine Involves Endoplasmic Reticulum Stress. J. Pharmacol. Exp. Ther. *327*, 442–452.

Röcken, C. (2017). Molecular classification of gastric cancer. Expert Rev. Mol. Diagn. *17*, 293–301.

Rosenberg, B., Vancamp, L., and Krigas, T. (1965). INHIBITION OF CELL DIVISION IN ESCHERICHIA COLI BY ELECTROLYSIS PRODUCTS FROM A PLATINUM ELECTRODE. Nature *205*, 698–699.

Rosenberg, B., Vancamp, L., Trosko, J.E., and Mansour, V.H. (1969). Platinum Compounds: a New Class of Potent Antitumour Agents. Nature *222*, 385.

Ryu, C.S., Kwak, H.C., Lee, K.S., Kang, K.W., Oh, S.J., Lee, K.H., Kim, H.M., Ma, J.Y., and Kim, S.K. (2011). Sulfur amino acid metabolism in doxorubicin-resistant breast cancer cells. Toxicol. Appl. Pharmacol. *255*, 94–102.

Ryu, C.S., Kwak, H.C., Lee, J.-Y., Oh, S.J., Phuong, N.T.T., Kang, K.W., and Kim, S.K. (2013). Elevation of cysteine consumption in tamoxifen-resistant MCF-7 cells. Biochem. Pharmacol. *85*, 197–206.

Sainuddin, T., Pinto, M., Yin, H., Hetu, M., Colpitts, J., and McFarland, S.A. (2016). Strained ruthenium metal-organic dyads as photocisplatin agents with dual action. J. Inorg. Biochem. *158*, 45–54.

Sbodio, J.I., Snyder, S.H., and Paul, B.D. (2019). Regulators of the transsulfuration pathway. Br. J. Pharmacol. *176*, 583–593.

Scheeff, E.D., Briggs, J.M., and Howell, S.B. (1999). Molecular modeling of the intrastrand guanine-guanine DNA adducts produced by cisplatin and oxaliplatin. Mol. Pharmacol. *56*, 633–643.

Schoenhacker-Alte, B., Mohr, T., Pirker, C., Kryeziu, K., Kuhn, P.-S., Buck, A., Hofmann, T., Gerner, C., Hermann, G., Koellensperger, G., et al. (2017). Sensitivity towards the GRP78 inhibitor KP1339/IT-139 is characterized by apoptosis induction via caspase 8 upon disruption of ER homeostasis. Cancer Lett. *404*, 79–88.

Sharma, A., Houshyar, R., Bhosale, P., Choi, J.-I., Gulati, R., and Lall, C. (2014). Chemotherapy induced liver abnormalities: an imaging perspective. Clin. Mol. Hepatol. *20*, 317–326.

Shen, L., Wen, N., Xia, M., Zhang, Y., Liu, W., Xu, Y., and Sun, L. (2016). Calcium efflux from the endoplasmic reticulum regulates cisplatin-induced apoptosis in human cervical cancer HeLa cells. Oncol. Lett. *11*, 2411–2419.

Shi, S., Tan, P., Yan, B., Gao, R., Zhao, J., Wang, J., Guo, J., Li, N., and Ma, Z. (2016). ER stress and autophagy are involved in the apoptosis induced by cisplatin in human lung cancer cells. Oncol. Rep. *35*, 2606–2614.

Sun, H., Lin, D.-C., Guo, X., Masouleh, B.K., Gery, S., Cao, Q., Alkan, S., Ikezoe, T., Akiba, C., Paquette, R., et al. (2016). Inhibition of IRE1α-driven pro-survival pathways is a promising therapeutic application in acute myeloid leukemia. Oncotarget *7*, 18736–18749.

Suntharalingam, K., Johnstone, T.C., Bruno, P.M., Lin, W., Hemann, M.T., and Lippard, S.J. (2013). Bidentate ligands on osmium(VI) nitrido complexes control intracellular targeting and cell death pathways. J. Am. Chem. Soc. *135*, 14060–14063.

Tew, K.D. (2016). Glutathione-Associated Enzymes In Anticancer Drug Resistance. Cancer Res. *76*, 7–9.

Tew, K.D., Manevich, Y., Grek, C., Xiong, Y., Uys, J., and Townsend, D.M. (2011). The role of glutathione S-transferase P in signaling pathways and S-glutathionylation in cancer. Free Radic. Biol. Med. *51*, 299–313.

Tian, J., Liu, R., and Qu, Q. (2017). Role of endoplasmic reticulum stress on cisplatin resistance in ovarian carcinoma. Oncol. Lett. *13*, 1437–1443.

Townsend, D.M., Findlay, V.L., and Tew, K.D. (2005). Glutathione S-transferases as regulators of kinase pathways and anticancer drug targets. Methods Enzymol. *401*, 287–307.

Traverso, N., Ricciarelli, R., Nitti, M., Marengo, B., Furfaro, A.L., Pronzato, M.A., Marinari, U.M., and Domenicotti, C. (2013). Role of glutathione in cancer progression and chemoresistance. Oxid. Med. Cell. Longev. *2013*, 972913.

Velu, C.S., Niture, S.K., Doneanu, C.E., Pattabiraman, N., and Srivenugopal, K.S. (2007). Human p53 is inhibited by glutathionylation of cysteines present in the proximal DNA-binding domain during oxidative stress. Biochemistry *46*, 7765–7780.

Verfaillie, T., Garg, A.D., and Agostinis, P. (2013). Targeting ER stress induced apoptosis and inflammation in cancer. Cancer Lett. *332*, 249–264.

Vidimar, V., Meng, X., Klajner, M., Licona, C., Fetzer, L., Harlepp, S., Hébraud, P., Sidhoum, M., Sirlin, C., Loeffler, J.-P., et al. (2012). Induction of caspase 8 and reactive oxygen species by ruthenium-derived anticancer compounds with improved water solubility and cytotoxicity. Biochem. Pharmacol. *84*, 1428–1436.

Vidimar, V., Licona, C., Cerón-Camacho, R., Guerin, E., Coliat, P., Venkatasamy, A., Ali, M., Guenot, D., Le Lagadec, R., Jung, A.C., et al. (2019). A redox ruthenium compound directly targets PHD2 and inhibits the HIF1 pathway to reduce tumor angiogenesis independently of p53. Cancer Lett. *440–441*, 145–155.

Wang, F.-Y., Tang, X.-M., Wang, X., Huang, K.-B., Feng, H.-W., Chen, Z.-F., Liu, Y.-N., and Liang, H. (2018a). Mitochondria-targeted platinum(II) complexes induce apoptosis-dependent autophagic cell death mediated by ER-stress in A549 cancer cells. Eur. J. Med. Chem. *155*, 639–650.

Wang, L., Cai, H., Hu, Y., Liu, F., Huang, S., Zhou, Y., Yu, J., Xu, J., and Wu, F. (2018b). A pharmacological probe identifies cystathionine β-synthase as a new negative regulator for ferroptosis. Cell Death Dis. *9*, 1–17.

Xu, L., Zhang, P.-P., Fang, X.-Q., Liu, Y., Wang, J.-Q., Zhou, H.-Z., Chen, S.-T., and Chao, H. (2019). A ruthenium(II) complex containing a p-cresol group induces apoptosis in human cervical carcinoma cells through endoplasmic reticulum stress and reactive oxygen species production. J. Inorg. Biochem. *191*, 126–134.

Xu, Y., Wang, C., Su, J., Xie, Q., Ma, L., Zeng, L., Yu, Y., Liu, S., Li, S., Li, Z., et al. (2015). Tolerance to endoplasmic reticulum stress mediates cisplatin resistance in human ovarian cancer cells by maintaining endoplasmic reticulum and mitochondrial homeostasis. Oncol. Rep. *34*, 3051–3060.

Yang, W.S., SriRamaratnam, R., Welsch, M.E., Shimada, K., Skouta, R., Viswanathan, V.S., Cheah, J.H., Clemons, P.A., Shamji, A.F., Clish, C.B., et al. (2014). Regulation of Ferroptotic Cancer Cell Death by GPX4. Cell *156*, 317–331.

Zeng, L., Gupta, P., Chen, Y., Wang, E., Ji, L., Chao, H., and Chen, Z.-S. (2017). The development of anticancer ruthenium(ii) complexes: from single molecule compounds to nanomaterials. Chem. Soc. Rev. *46*, 5771–5804.

Zhang, L., Qi, Q., Yang, J., Sun, D., Li, C., Xue, Y., Jiang, Q., Tian, Y., Xu, C., and Wang, R. (2015). An Anticancer Role of Hydrogen Sulfide in Human Gastric Cancer Cells. Oxid. Med. Cell. Longev. *2015*, 636410.

Zhao, H., Li, Q., Wang, J., Su, X., Ng, K.M., Qiu, T., Shan, L., Ling, Y., Wang, L., Cai, J., et al. (2012). Frequent Epigenetic Silencing of the Folate-Metabolising Gene Cystathionine-Beta-Synthase in Gastrointestinal Cancer. PLOS ONE *7*, e49683.

Zhu, H., Blake, S., Chan, K.T., Pearson, R.B., and Kang, J. (2018). Cystathionine β-Synthase in Physiology and Cancer. BioMed Res. Int. *2018*, 3205125.

Annexes

During my PhD, I could participate to several studies in collaboration with other labs. This work allows me to have a greater overview about the mode of action of other metal-based drugs and one of this work led to a publication published in Metallomics:

Reactivity of Cu(ii)-, Zn(ii)- and Fe(ii)-thiosemicarbazone complexes with glutathione and metallothionein: from stability to dissociation to transmetallation.

Metallomics

PAPER

Reactivity of Cu(II)–, Zn(II)– and Fe(II)–thiosemicarbazone complexes with glutathione and metallothionein: from stability to dissociation to transmetallation†

Cite this: DOI: 10.1039/c9mt00061e

Alice Santoro,[a] Bertrand Vileno,[ab] Òscar Palacios,[c] Manuel David Peris-Díaz,[d] Gilles Riegel,[e] Christian Gaiddon,[e] Artur Krężel[d] and Peter Faller *[af]

Received 15th March 2019,
Accepted 4th April 2019

DOI: 10.1039/c9mt00061e

rsc.li/metallomics

Thiosemicarbazones (TSCs) are a class of strong metal ion ligands, which are currently being investigated for several applications, such as anticancer treatment. In addition to these ligands only, which exert their activity upon interaction with metal ions in cells, preformed metal–TSC complexes are also widely studied, predominantly with the essential metal ions iron, copper and zinc. Currently, it is unclear what the active species are, which complexes are present and what are their biological targets. Herein, we study the complexes of copper(II), zinc(II) and iron(II) with three TSCs, PT, 3-AP (triapine) and Dp44mT, (latter two are currently in clinical trials), concerning their reactivity with glutathione (GSH) and Zn_7-metallothionein (Zn_7MT-1, 2 and 3). These two cysteine-containing molecules can have a major impact on metal–TSC complexes because they are abundant in the cytosol and nucleus, they are strong metal ligands and have the potential to reduce Cu(II) and Fe(III). Our results indicate that Fe(II)–TSC is stable in the presence of typical cytosolic concentrations of GSH and Zn_7MT. In contrast, all three Cu(II)–TSCs react rapidly due to the reduction of Cu(II) to Cu(I), which is then transferred to MT. This suggests that Cu(II)–TSCs are rapidly dissociated in a cytosolic-type environment and the catalytic generation of reactive oxygen species by Cu(II)–TSCs is stopped. Moreover, in the case Cu(II)–Dp44mT, transmetallation with Zn(II) from MT occurs. The reaction of Zn(II)–TSCs is ligand dependent, from predominant dissociation for PT and 3-AP, to very little dissociation of Zn(II)–$Dp44mT_2$. These results indicate that GSH and Zn_7MT may be important factors in the fate of Cu(II)– and Zn(II)–TSCs. In particular, for Cu, its chemistry is complex, and these reactions may also occur for other families of Cu-complexes used in cancer treatment or for other applications.

Significance to metallomics

Thiosemicarbazone (TSC) ligands have been widely investigated for their anticancer activity. Even though their mechanism of action is still unclear, the essential metals Cu, Zn and Fe seem to play a pivotal role in their antitumor activity. In our contribution, we explore a neglected aspect of their anticancer activity with Cu, Zn and Fe, which deals with their stability in the cytosol and nucleus against two abundant thiol rich molecules, metallothionein (MT) and glutathione (GSH). Our results show that MT/GSH may be very important modulators of metallo-drugs since disruption or transmetallation can occur, which in turn impacts metal-dependent ROS production.

[a] *Institut de Chimie, UMR 7177, CNRS-Université de Strasbourg, 4 rue Blaise Pascal, 67000, Strasbourg, France. E-mail: pfaller@unistra.fr*
[b] *French EPR Federation of Research (REseau NAtional de Rpe interDisciplinaire (RENARD), Fédération IR-RPE CNRS #3443), Strasbourg, France*
[c] *Departament de Química, Universitat Autònoma de Barcelona, E-08193 Cerdanyola del Vallès, Barcelona, Spain*
[d] *Department of Chemical Biology, Faculty of Biotechnology, University of Wrocław, F. Joliot-Curie 14a, 50-383, Wrocław, Poland*
[e] *Inserm UMR_S 1113, Université de Strasbourg, 3 avenue Molière, 67200, Strasbourg, France*
[f] *University of Strasbourg Institute for Advanced Study (USIAS), Strasbourg, France*

† Electronic supplementary information (ESI) available. See DOI: 10.1039/c9mt00061e

Introduction

Metal-based drugs are a class of drugs that either contain metals or metal ions (metallodrugs) when they are applied such as metal–ligand complexes and nanoparticles or are compounds applied without metals but interact with metal ions in the body (mostly chelators). Metal–ligand complexes, mostly with small ligands, have been widely investigated, with different metal ions and a large variety of ligand families. They

have been evaluated for different applications such as cancer therapy, antimicrobials, antiparasitic agents, diagnosis and imaging, and treatment of arthritis.[1–3]

Several metallodrugs have been approved and used clinically, with the most well-known being the platinum compounds *cis*-Pt, carbo-Pt and oxali-Pt.[4] Thus far, these used metallodrugs contain non-essential metals, such as Pt, Ag, and Ga. However, metallodrugs containing essential metals, *i.e.* for humans Fe, Zn, Cu, Mn, Mo, and W, have not made it to clinical use yet. Nevertheless, there is strong research activity on metallodrugs composed of essential metals. A potential advantage is that they will be less toxic since essential metal ions are tightly regulated by transporters, carriers, binding-proteins, *etc.*, and hence able to deal with fluctuating amounts of these metal ions.[5–7]

For metallodrugs in the form of a metal–ligand complex, which are administered as a complex, the following non-exclusive conceptually different mechanism can be considered: (i) it is the metal complex that has the therapeutic activity, *e.g.* by catalysing a reaction, (ii) the complex dissociates into ligand and metal ion and there is an additive or synergistic effect of both separated entities, (iii) the complex is a prodrug, and only one part is active (either the metal or the ligand itself), but the complex is needed to reach the target, and (iv) the complex is a prodrug and the ligand has to be transformed and the transformed metal–ligand complex has an activity like in (i)–(iii).

Chelators that gain their activity upon metal binding in organism are prodrugs and obviously are limited to the present metal, *i.e.* almost exclusively essential metals. An FDA approved example is bleomycin with iron.[8] However, for chelators, it is often unclear which metal ions they interact with, if they form ternary complexes with metalloproteins or if their activity is not directly dependent on metal ligation. Chelators can also function as shuttles or ionophores, *i.e.* their action is to transport metal ions, which then exert further activity.

Thiosemicarbazones (TSCs) are a class of ligands clinically investigated for a variety of biological activities, such as antimicrobial, antimalarial and anticancer.[9–11] They are basically bidentate ligands, but are often equipped with a further coordinating moiety to improve stability *via* tridentate ligation (Fig. 1). A variation, the 1,2-bis(thiosemicarbazone) ligands (bTSCs), which serve mostly as tetradentate ligands with a N_2S_2 donor set, are also under investigation for different types of applications.[12–14] The anticancer activity of TSCs is not fully understood and different derivatives may have different types of action. In some cases the TSC alone was found to be as active as the metal complex, and in other cases metal complexes showed higher activity.[15,16] Mostly, the activity of TSCs has been attributed to the inhibition of ribonucleotide reductase, but whether this involves chelation of the iron in this enzyme or chelation of Fe beforehand and inhibition *via* the preformed Fe–TSC complex remains unclear.[17–20] Also a non-Fe dependent mechanism has been suggested, involving quenching of the tyrosine radical in ribonucleotide reductase by the non-metallated-TSC.[21] Moreover other targets have been suggested, such as the thioredoxin system.[20,22]

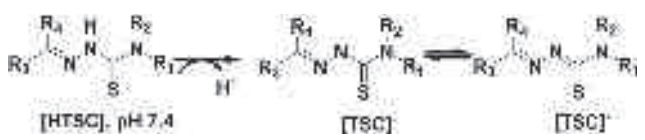

Fig. 1 Scheme of the deprotonation step of thiosemicarbazone (TSC)-like ligands from their neutral form at physiological pH. The resulting negative charge is mainly localized on the S atom *via* thione–thiol tautomeric equilibrium.

Due to their relatively strong metal-chelating properties, other metal–TSC complexes and their anticancer activities have been studied, mostly with Cu(II) and Zn(II).[23–26] Also the possibility that metal-free TSCs may be able to bind Zn(II) or Cu(II) ions and these complexes then exerting their activity has been discussed. To illustrate the complexity of this issue, in the case of di-2-pyridylketone 4-cyclohexyl-4-methyl-3-thiosemicarbazone (DpC) and some di-2-pyridylketone thiosemicarbazone (DpT) types, the Zn(II)-complex showed generally higher antitumor activity, but its toxicity was attributed to the Cu(II)-complex after the Zn(II)-complex crossed the cytosol and underwent transmetallation in the lysosomal compartment.[24,27,28] This shows that metal–TSCs can be transformed into apo-TSCs or transmetallated. As discussed above, apo-TSC can potentially pick up metals, depending on the availability of different metal ions, which is compartment dependent.

Two important molecules in this regard are glutathione (GSH) and metallothionein (MT). GSH has two important features: (i) it is a reducing agent, and thus can potentially reduce Cu(II) to Cu(I) and Fe(III) to Fe(II). This can have a major impact on the stability of the complex, and hence its fate. (ii) GSH is a metal chelator, having different ligands (O, N and S).[29] Although the stability and nature of the Cu(I)–, Zn(II)– and Fe(II)–GSH complexes formed under biological relevant conditions are not clear (Cu(I), Zn(II) and Fe(II) seem to form preferentially $Cu(I)_4(GS)_6$, $Zn(II)(GSH)_2$ and Fe(II)(GSH) complexes, respectively[30–32]), their affinity is generally lower compared to the respective metalloproteins. However, GSH is present at very high concentrations, often reported in the range of 1–10 mM in the cytosol or nucleus.[33–35] Thus, it can become a serious competitor for metal-binding of exogenous metal-complexes. Indeed, GSH was suggested to contribute the Cu(I)-, Zn(II)- and Fe(II)-metabolism.[31,36,37] For instance, Cu(I)–GSH complexes have been proposed to mediate Cu(I) transport to or from proteins, such as from copper transporter 1 (Ctr1) and MT,[38,39] as confirmed by *in vitro* studies.[40,41]

MTs are less concentrated than GSH, but reported concentrations for cytosol and nucleus span from about 3 μM to almost 1 mM.[42] However, MT is a better reducing agent than GSH ($E^{\circ}_{MT} = -366$ mV and $E^{\circ}_{GSH} = -240$ mV)[43] and a much stronger chelator for Cu(I) ions than GSH (K_d(MT) $\sim 10^{-19}$ M and K_d(GSH) $\sim 10^{-15-17}$ M).[30,44,45] Noteworthy, Cu(I) bound to MT is quite stable under aerobic conditions and does not generate ROS.[46] Moreover, MTs are mainly loaded with Zn(II) ions, which are released upon Cu(II) or Cu(I)-binding. Additionally, GSH and GSSG have been shown to be critical modulators of the rate of Zn(II) transfer reactions from MTs.[47] Thus, MTs

have the potential to perform a metal swap with a Cu-chelator, leading to the transmetallation of the latter.[44,48,49]

Metal-complexes of TSCs have not been investigated for their reactivity with MT, with or without GSH, in a test tube, despite its potential importance. However, Petering and co-workers showed the formation of Cu(I)–MT in cells exposed to the related bisTCS called kts (3-ethoxy-2-oxobutyraldehyde bis-thiosemicarbazone).[50] This shows clearly that MT can also be an important player in the reactivity of metal–TSCs. The reactivity of Cu(II)–(b)TSCs with GSH has been studied for different (b)TSC ligands.[52–54] It has generally been observed that GSH can reduce Cu(II)–(b)TSCs and often Cu(I) is then released when an excess of GSH is present (or a strong chelator such as bathocuproine disulfonate).[53,54] During this process Cu(II)–(b)TSCs can produce reactive oxygen species (ROS).[53,55,56]

In the present work, we investigated three α-N-heterocyclic TSCs, 2-pyridinecarboxaldehyde thiosemicarbazone (PT), 3-amino-pyridine-2-carbaldehyde thiosemicarbazone (3-AP; triapine),[23,57] and di-2-pyrydylketone 4,4-dymethyl-3-thiosemicarbazone (Dp44mT).[58] Among them, 3-AP and Dp44mT have been clinically investigated in multiple clinical trials (phase I and II) as anticancer drugs.[9,57] We studied the reactivity of their Cu(II), Zn(II) and Fe(II) complexes in the presence of physiological relevant GSH and/or Zn_7MT concentrations (for the cytosol and nucleus) to evaluate their stability against dissociation and potential transmetallation reactions (Fig. 2).

There are two different schemes to consider: (i) a preformed metal–TSC complex existing extracellularly enters the cell. In this case, the oxidized form, Cu(II) and Fe(III) will be the relevant oxidation states. (ii) TSC is applied as a ligand only and enters the cell and is then able to pick up a metal ion. Here, Cu(I) and Fe(II) will be the more relevant forms since they are the most prevalent intracellularly. Generally, Fe(III)–TSCs have a much lower affinity compared to the main extracellular Fe(III)-binding protein transferrin.[58,59] Transferrin is only partially loaded with Fe(III); thus, it is expected to withdraw Fe(III) from TSCs. Similarly, TSCs are very poor Cu(I)-ligands (ref. 60 and see below). Thus, we investigated the more likely existing Fe(II) and Cu(II)–TSC complexes, which are also the better characterized forms.

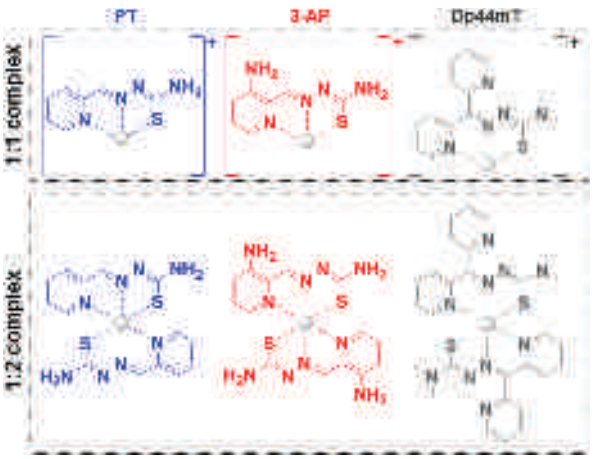

Fig. 2 Chemical structure of the thiosemicarbazone (TSC) metal complexes studied herein (TSCs: PT, 3-AP and Dp44mT) with a 1 : 1 and/or 1 : 2 stoichiometry. The metals considered are Cu, Zn and Fe.

We chose the Zn_7MT-1 isoform of MT since it is the one ubiquitously expressed in all cell tissues. Besides, we used the Zn_7MT-2a and Zn_7MT-3 isoforms to evaluate potential differences in their behaviour.

Our results indicate that Fe(II)–TSCs resist against demetallation by GSH and Zn_7MT-1; whereas, Cu(II)–TSCs are rapidly deactivated by reduction and dissociation, and for Dp44mT a Cu/Zn transmetallation occurred. In the case of zinc, only Zn(II)–Dp44mT_2 resisted GSH, not the two others (PT and 3-AP). These results indicate that GSH and MT have a major impact on the fate of Cu(II)/Zn(II)–TSC complexes, which may be true for other types of Cu(II)/Zn(II)-complexes.

Results and discussion

Reactivity of Cu(II)–TSC complexes with GSH

The mode of action of Cu(II)–TSC complexes as anticancer metal compounds has been related to their ability to generate intracellular ROS in the presence of biological reducing agents, such as the intracellular thiol GSH.[61–63] Indeed, the conversion of Cu(II) to Cu(I) is the first step to start ROS production *via* Cu-dependent chemistry.

Thus, we started our study by evaluating the reactivity of the Cu(II)–TSC complexes with GSH. The interactions of Cu(II)–TSCs and –bTSCs with GSH have been studied in the past for different molecules (see introduction); thus, the aim was to repeat the reactions to confirm and compare the following experiments with Zn_7MT-1. Besides using its thiol function to reduce Cu(II) to Cu(I), GSH itself is known to bind Cu(I) quite strongly. Hence, GSH itself could sequester Cu(I) from the Cu(I)–TSCs, leading to the dissociation of the Cu(II)-complexes.

The reactivity of each Cu(II)–TSC complex (Cu(II)–PT/3-AP/Dp44mT) with GSH was initially studied by absorbance spectroscopy through the corresponding characteristic CT and d–d bands. First, to elucidate the stoichiometry of the metal-complexes formed under our experimental conditions, Cu(II)-titration experiments were carried out (see Fig. S1 for PT, Fig. S2 for 3-AP and Fig. S3 for Dp44mT, ESI†). For the three ligands, the formation of Cu(II)-complexes with a 1 : 1 stoichiometry was observed. Hence Cu(II)–TSC complexes were generated in HEPES buffer with a Cu(II) to ligand ratio of 0.9 : 1 to avoid the presence of free Cu(II). GSH in 3 mM concentration was then added to the preformed Cu(II)-complexes and the reaction was monitored over time. For all three Cu(II)–TSCs exposed to 3 mM GSH, the instantaneous formation of a ternary adduct [TSC–Cu(II)–GSH] was detected (Fig. 3B–D), based on a blue shift of ~80 nm of the d–d band (insets in Fig. 3B–D and Table 1) together with a small red shift of the corresponding CT band. A similar shift in the CT band has been observed for a pyridoxal-TSC upon binding of GSH.[56]

The formation of ternary adducts was confirmed by continuous wave-electron paramagnetic resonance (EPR) at low temperature (100 K). Indeed, it has been shown for Cu(II)–PT that

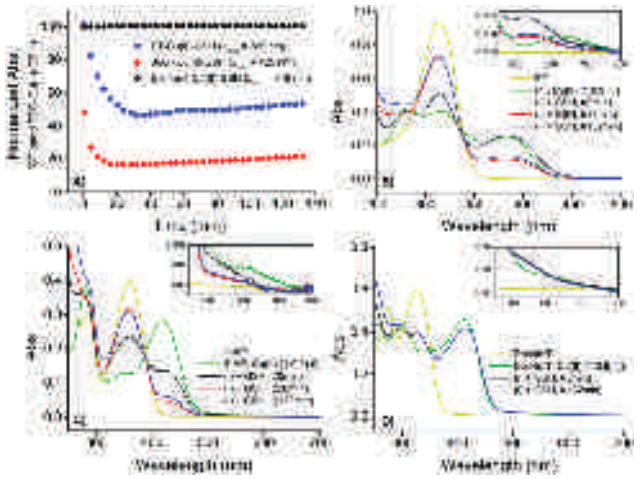

Fig. 3 Reaction of the Cu(II)–TSC complexes with GSH monitored over time by absorbance spectroscopy. (A) Data are expressed as normalized absorbance of the λ_{max} of the CT bands of the [TSC–Cu(II)–GSH] ternary adducts as a function of time. Intermediate spectra were collected at 4 min intervals. (B–D) UV-Vis spectra for the reaction of GSH with Cu(II)–PT, Cu(II)–3-AP, and Cu(II)–Dp44mT, respectively. Insets refer to the Vis region of the spectra (450–800 nm), in which the d–d bands are present. Upon the addiction of GSH to the preformed Cu(II)–TSCs, the following changes were observed in the spectra: (1) blue and red shift of the d–d and CT bands (formation of the ternary adduct [TSC–Cu(II)–GSH]), (2) decrease in intensity of the d–d and CT bands of [TSC–Cu(II)–GSH] (Cu(II) reduction and dissociation from [TSC–Cu(II)–GSH]), (3) increase in intensity of the d–d and CT bands of [TSC–Cu(II)–GSH] (re-formation of [TSC–Cu(II)–GSH]), for PT (B) and 3-AP (C). Experimental conditions: 30 μM TSC, 27 μM Cu(II) (ratio TSC : Cu(II), 1 : 0.9), 3 mM GSH, 100 mM HEPES buffer, pH 7.4. μM TSC, 27 μM Cu(II) (ratio TSC : Cu(II), 1 : 0.9), 3 mM GSH, 100 mM HEPES buffer, pH 7.4.

Table 1 Table summarizing the λ_{max} values (UV-Vis absorbance) of the different species observed in the reaction of Cu(II)–PT/3-AP/Dp44mT with GSH (TSC, Cu(II)–TSC, [TSC–Cu(II)–GSH])

	λ_{max} values (nm)				
		Cu(II)–TSC		TSC–Cu(II)–GSH	
	TSC	d–d band	CT band	d–d band	CT band
PT	313	628	382	530	386
3-AP	359	606	418	528	425
Dp44mT	328	608	411	536	416

GSH binding to the Cu(II) center affects its EPR fingerprint.[61,64] Therefore, we probed the reaction with the complex Cu(II)–PT (Fig. 4). Cu(II)–PT showed a typical axial Cu(II) EPR spectrum (blue line, Fig. 4). Upon the addition of GSH, a significant shift in the g parallel values was observed from *ca.* 2.205 to 2.142 together with a noticeable change within the superhyperfine structure (red line, Fig. 4 and Fig. S4, Table S1 for the EPR simulation parameters, ESI†). These changes are consistent with the substitution of an equatorial ligand (likely H_2O or buffer molecule) by a thiolate from GSH.[65]

However, after the fast formation of a ternary adduct of GSH with all three Cu(II)–TSCs, very marked differences in terms of further reactivity could be observed (Fig. 3). The addition of GSH to the preformed Cu(II)–Dp44mT complex resulted in the immediate binding of GSH to the complex, but no changes in the spectrum of the ternary adduct [Dp44mt–Cu(II)–GSH] could be detected over a period of 132 min. Hence, the Cu(II)–Dp44mT complex did not dissociate in the presence of GSH.

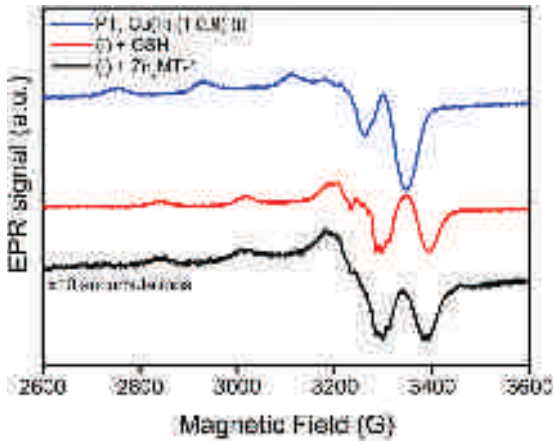

Fig. 4 Detection of ternary adducts [TSC–Cu(II)–GSH/Zn_7MT-1]. EPR spectra of snap-frozen solutions of the Cu(II)–PT complex (blue line), after the addiction of GSH (red line) and after the addiction of Zn_7MT-1 (black line). Experimental conditions: 1 mM PT, 900 μM Cu(II), 3 mM GSH or 200 μM Zn_7MT-1 (ratio PT/Cu(II)/Zn_7MT-1 1 : 0.9 : 0.2), HEPES buffer 100 mM, pH 7.4 and T = 100 K. All samples were supplemented by 10% v/v glycerol.

On the contrary, the addition of GSH to the preformed Cu(II)–PT and Cu(II)–3-AP complexes resulted in the immediate formation of the ternary adduct [TSC–Cu(II)–GSH], from which Cu(II) was rapidly reductively dissociated to form the Cu(I)–GSH species.

Indeed, a decrease in intensity of the CT and d–d bands of the ternary adducts [PT–Cu(II)–GSH] and [3-AP–Cu(II)–GSH] was observed over time together with an increase in the intensity of the band of the free ligands. The Cu(II) reduction and dissociation of the ternary adducts [PT/3-AP–Cu(II)–GSH] with consequent Cu(I) binding to GSH was confirmed based on the appearance of the characteristic CT absorption band of the Cu(I)–GSH species at 265 nm under a saturated argon atmosphere (Fig. S5A and C, ESI†) and on the disappearance of the EPR signature of the [PT–Cu(II)–GSH] species after 30 min from the addition of GSH to the preformed Cu(II)–PT complex at RT (Fig. S6, ESI†).

Under an oxygen atmosphere, after around 36 min (PT) and 20 min (3-AP) the slow re-oxidation of Cu(I) to Cu(II) and re-formation of the Cu(II)-complex started to be observed (Fig. 3B and C). This was not detected in the absence of O_2 (Fig. S5A and C, ESI†), but when O_2 was vigorously bubbled through the sample, the oxidation was faster with the re-generation of the ternary adducts, [PT/3-AP–Cu(II)–GSH].

It is worth noting that the reduction of Cu(II) and release of Cu(I) from the ternary adduct with 3-AP was faster compared to that with PT. The reason for this is not known. The assumed limiting step is the reduction of Cu(II) to Cu(I). The redox potentials reported for Cu(II)–3-AP and Cu(II)–PT are −0.19 and −0.14 mV respectively; thus, Cu(II)–PT should be easier to

reduce.[19] However, these potentials were obtained in 66% organic solvent and in the absence of the relevant ternary complexes with GSH.

The classical concentration of GSH in cells is between 1–10 mM. Thus, we tested also other GSH concentrations. As expected, at higher concentrations of GSH (6 and 9 mM), a faster release of Cu(I) from the Cu(II)–PT complex was observed (Fig. S7, ESI†). Again, in line with the higher amount of reduced GSH available in solution, the re-oxidation of Cu(I) to Cu(II) and consequently the re-formation of the Cu(II)–PT complex was slower and hence it was not observed over a period of 120 min.

The data obtained led to the proposition of Reactions (1) and (2) (x is likely 1.5 due to the formation of $Cu(I)_4$–S_6 clusters in GSH[30]):

$$[Cu(II)\text{–}TSC]^+ + GSH \rightarrow [TSC\text{–}Cu(II)\text{–}GS^-] + H^+ \quad (1)$$

$$[TSC\text{–}Cu(II)\text{–}GS^-] + xGSH \rightarrow Cu(I)\text{–}GS_x^- + TSC + 1/2GSSG + xH^+ \quad (2)$$

PT and 3-AP undergo reactions (1) and (2), where (1) is faster than (2). Cu(II)–Dp44mT seems to perform reaction (2) much slower than PT and 3-AP.

Overall, this suggests that the fate of Cu(II)–TSCs with mM GSH concentrations, as encountered in the cytosol of cells, is quite different. Cu(II)–Dp44mT does not dissociate, and undergoes only a very slow redox cycle with GSH and O_2. In contrast, the Cu(II)-complexes of PT and 3-AP dissociate with Cu(I)-bound to GSH. This makes Cu(I) available for its sequestration by other copper binding proteins. Among them, MTs, well-known for being excellent metal-chelators and present in high concentrations (3 μM–1 mM) can be a possible binding site for the released Cu(I).

Reactivity of Cu(II)–TSC complexes with Zn_7MT-1

Before investigating the effect of both GSH and Zn_7MT-1, we evaluated the reactivity of the Cu(II)-complexes of PT, 3-AP and Dp44mT, with Zn_7MT-1 alone since MT is Cys-rich and can reduce Cu(II) from Cu(II)–TSCs and form ternary adducts with the complexes. Thus, Cu(II)–TSCs were exposed to 6 μM Zn_7MT-1. The used MT concentration is at the lower range for the values reported in the cytosol and nucleus.

The reactions were followed by absorbance spectroscopy (Fig. 5), which suggested that all the Cu(II)–TSCs reacted with Zn_7MT-1 *via* the formation of a ternary complex, [TSC–Cu(II)–Zn_7MT-1], by binding of a thiolate from Zn_7MT-1 to Cu(II)–TSCs. This was supported by the immediate blue shift in the d–d bands (insets Fig. 5A–C), the changes in the EPR spectra, *i.e.* shift in the g parallel values from *ca.* 2.205 to 2.147 and changes within the superhyperfine structure, and the loss in the EPR intensity (black line, Fig. 4 and Fig. S4, Table S1 for the EPR simulation parameters, ESI†) shown for PT. Hence, Zn_7MT-1 was able to reduce Cu(II) to Cu(I) *via* its cysteines and to chelate Cu(I) finally. This was supported by the typical circular dichroism spectrum of $Cu(I)_4Zn(II)_4$MT-1 (CD bands at about (+) 255 and (−) 285 nm) (Fig. 6) shown for 3-AP. This CD spectrum has been observed in the past after reaction of MTs with Cu(II) and Cu(II)-compounds.[40,48,66,67]

Cu(I) binding to MT-1 was also confirmed by ESI-MS for the reaction of Zn_7MT-1 with Cu(II)–3-AP (Fig. 7 and Fig. S8, ESI†)

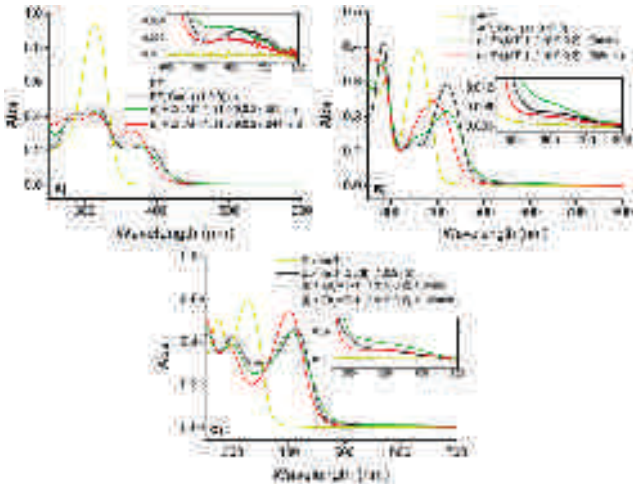

Fig. 5 UV-Vis spectra of the Zn_7MT-1 reaction with Cu(II)–PT (A), Cu(II)–3-AP (B), and Cu(II)–Dp44mT (C) monitored over time after Zn_7MT-1 added to the preformed Cu(II)–TSC complex. Intermediate spectra were collected at 4 min intervals. Insets in (A–C) refer to the Vis region of the spectra (450–800 nm) for the corresponding reaction. Upon the addiction of Zn_7MT-1 to the preformed Cu(II)–TSCs, the following changes were observed in the spectra: (1) blue shift of the d–d band of Cu(II)–TSC (formation of the ternary adduct [TSC–Cu(II)–Zn_7MT-1]), (2) decrease in intensity of the d–d band (Cu(II)) reduction and dissociation from [TSC–Cu(II)–Zn_7MT-1] and (3) disappearance of the CT band of the Cu(II)-complex and appearance of a new band at higher energy (formation of the Zn(II)–TSC complex). Experimental conditions: 30 μM TSC, 27 μM Cu(II), 6 μM Zn_7MT-1 (ratio TSC : Cu(II) : Zn_7MT-1, 1 : 0.9 : 0.2), 100 mM HEPES buffer, and pH 7.4.

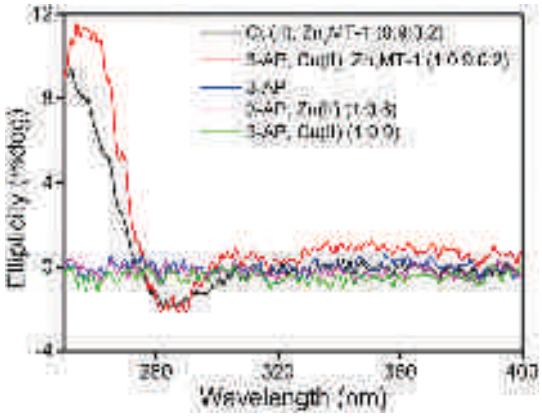

Fig. 6 Copper binding to MT-1 and formation of the $Cu(I)_4Zn(II)_4$MT-1 species from the mixture Cu(II)–3-AP/Zn_7MT-1. CD spectra of 3-AP (blue line); 3-AP/Cu(II), 1 : 0.9 (green line); 3-AP/Zn(II), 1 : 0.6 (purple line); 3-AP/Cu(II)/Zn_7MT-1, 1 : 0.9 : 0.2 (red line, spectrum registered after 120 min from the addition of Zn_7MT-1 to the preformed Cu(II)–3-AP complex), and Cu(II)/Zn_7MT-1, 0.9 : 0.2 (black line). Experimental conditions: 100 μM PT, 90 μM Cu(II), 20 μM Zn_7MT-1 (ratio 3-AP : Cu(II) : Zn_7MT-1, 1 : 0.9 : 0.2), 100 mM HEPES buffer, and pH 7.4.

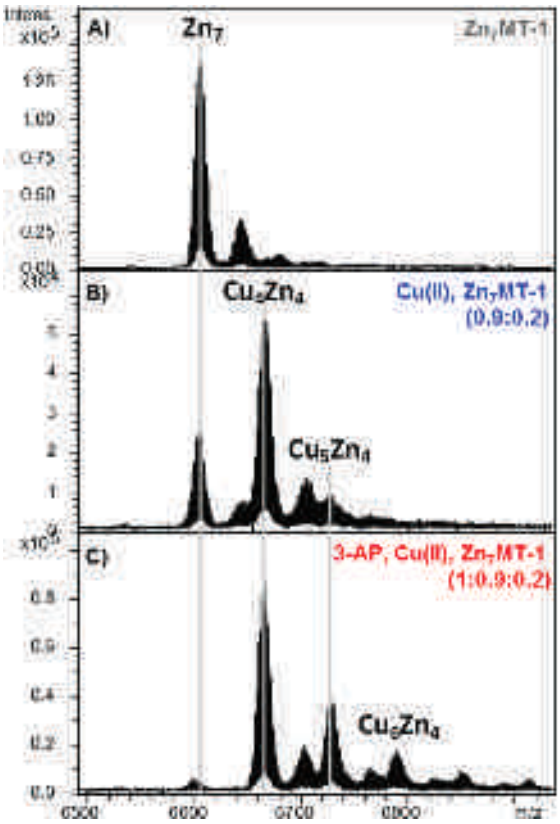

Fig. 7 Deconvoluted ESI-MS spectra (A) of Zn_7MT-1, (B) Cu(II)/Zn_7MT-1, 0.9 : 0.2, and (C) 3-AP/Cu(II)/Zn_7MT-1, 1 : 0.9 : 0.2 (spectrum registered after 120 min from the addition of Zn_7MT-1 to the preformed Cu(II)–3-AP complex). Experimental conditions: 50 μM 3-AP, 45 μM Cu(II), 10 μM Zn_7MT-1 (ratio 3-AP : Cu(II) : Zn_7MT-1, 1 : 0.9 : 0.2), 50 mM ammonium acetate, and pH 7.4. The main peak in (A) of $m/z \sim 6610$ has the mass expected for Zn_7MT-1 at neutral pH; the main peak in (B and C) at $m/z \sim 6671$ corresponds to the substitution of three Zn(II) ions with four Cu(I) ions, and the peaks at $m/z \sim 6732$ and 6792 correspond to the substitution of three Zn(II) ions with five and six Cu(I) ions, respectively.

and Cu(II)–Dp44mT (Fig. S9, ESI†). The immediate appearance of the main peak at $m/z \sim 6671$ (after deconvolution of the spectra), which corresponds to the substitution of three Zn(II) ions with four Cu(I) ions ($Cu(I)_4Zn(II)_4$MT-1), was observed upon the addition of Zn_7MT-1 to the preformed Cu(II)–3-AP/Dp44mT complexes.

It is also well documented that Cu(I)-binding to Zn_7MT results in the release of Zn(II). Indeed, in the present experiments, a band in the region of 360–400 nm was formed during the reactions, which is typical for the Zn(II)–TSC complexes (Fig. 5A–C). Thus, overall the following reaction occurs:

$$4\text{Cu(II)–TSC} + \text{Zn}_7\text{MT-1} \rightarrow \text{Cu(I)}_4\text{Zn(II)}_4\text{MT-1} + 3\text{Zn(II)–TSC} + \text{TSC} \quad (3)$$

It is important to highlight that with Zn_7MT-1, Cu(II)–Dp44mT also reacted, not only Cu(II)–PT and Cu(II)–3-AP. This is in contrast to GSH, which was not able to withdraw Cu(II) from Dp44mT. The reason for this is not known, but may be due to the more reducing potential of MT.[43]

Reactivity of Cu(II)–TSC complexes with GSH and Zn_7MT-1

Finally, the reactivity of the Cu(II)–TSC complexes with GSH and Zn_7MT-1 was investigated, two compounds likely to be encountered by a Cu(II)-complex in the cytosol or nucleus. The results shown in Fig. 8 are consistent with the previous results (for GSH and Zn_7MT-1 only), which show that GSH/Zn_7MT-1 can reduce Cu(II) to Cu(I) from Cu(II)–TSCs and that Cu(I) is transferred to Zn_7MT-1, where it is stabilized in the form of Cu(I) by the formation of the $Cu(I)_4Zn(II)_4$MT-1 species. These reactions have a half-time of about 5 and 10 min for 3-AP and PT, respectively (Table S2, ESI†), and for Dp44mT of about 4 min. In the latter case, due to the simultaneous generation of the corresponding Zn(II)–$Dp44mT_2$ complex, the $t_{1/2}$ could not be accurately determined.

Also in this case, the Cu(I) binding to MT-1 was confirmed by ESI-MS for the reaction of Zn_7MT-1/GSH with Cu(II)–3-AP (Fig. S10, ESI†) and Cu(II)–Dp44mT (Fig. S11, ESI†).

The same reactivity was observed for the Zn_7MT-2a and Zn_7MT-3 isoforms (Fig. S13–S15, ESI†), which only differ in their kinetics. The half-times for the reactions with Zn_7MT-3 were generally more rapid than that for Zn_7MT-1/2 (3 min for PT and 2 min for 3-AP). This is consistent with the faster kinetics of Cu(I)/Zn(II) exchange for MT-3 already reported.[68]

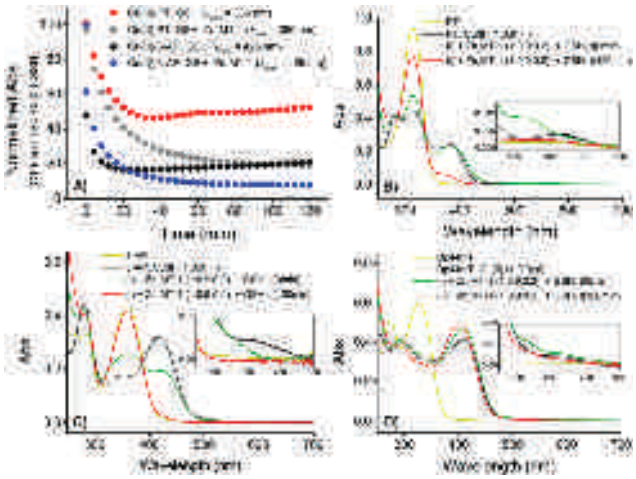

Fig. 8 Reaction of Cu(II)–TSCs with GSH and Zn_7MT-1 monitored by absorbance spectroscopy. (A) Kinetics for Cu(II) release from Cu(II)–PT/3-AP with GSH in the presence (PT: grey; 3-AP: blue) and absence (PT: red; 3-AP: black) of Zn_7MT-1. Data are expressed as normalized absorbance of the λ_{max} of the CT bands of [PT/3-AP–Cu(II)–GSH] ternary adducts as a function of time. Intermediate spectra were collected at 4 min intervals. UV-Vis spectra of the reaction of (B) Cu(II)–PT, (C) Cu(II)–3-AP, and (D) Cu(II)–Dp44mT with GSH/Zn_7MT-1 monitored over time after GSH and Zn_7MT-1 additions to the preformed Cu(II)–TSC complex. Insets refer to the Vis region of the spectra (450–800 nm) for the corresponding reactions. Upon the addition of GSH/Zn_7MT-1 to the preformed Cu(II)–TSCs, the following changes were observed in the spectra: (1) blue and red shift of the d–d and CT bands (formation of the ternary adduct [TSC–Cu(II)–SH(GSH/Zn_7MT-1)]), (2) decrease in intensity of the d–d and CT bands of [TSC–Cu(II)–SH(GSH/Zn_7MT-1)] (Cu(II) reduction and dissociation from [TSC–Cu(II)–GSH/Zn_7MT-1], (3) and appearance of a new band at higher energy in D) (formation of Zn(II)–Dp44mT). Experimental conditions: 30 μM PT, 27 μM Cu(II), 6 μM Zn_7MT-1 (ratio TSC : Cu(II) : Zn_7MT-1, 1 : 0.9 : 0.2), 3 mM GSH, 100 mM HEPES buffer, and pH 7.4.

For PT and 3-AP, when comparing the kinetics of the reduction of Cu(II) to Cu(I) *via* the CT band (Fig. 8A) with (PT: grey; 3-AP: blue) and without Zn_7MT-1 (PT: red; 3-AP: black), it can be observed that the kinetics at the beginning of the reactions are very similar. This implies that GSH reduces Cu(II) to Cu(I) from Cu(II)–PT/3-AP and then shuttles the latter to Zn_7MT-1. Moreover, the Cu(II)–PT/3-AP complexes are not re-formed over time. Hence, when Zn_7MT-1 is present in solution, the reaction is not reversible, confirming the Cu(I) binding to MT-1 and consequent formation of the $Cu(I)_4Zn(II)_4$MT-1 species, which is stable towards oxidation.[46,48]

No spectrum of the Zn(II)–PT/3-AP complex was observed under these conditions, suggesting that the Zn(II) released from Zn_7MT-1 was not bound to PT or 3-AP, but to GSH. Indeed, further experiments showed that 3 mM GSH can withdraw Zn(II) from Zn(II)–PT/3-AP (Fig. S19 (ESI†) and Fig. 9). Thus, the overall reaction is as follows:

$$4\text{Cu(II)–PT/3-AP} + x\text{GSH} + \text{Zn}_7\text{MT-1} \rightarrow \text{Cu(I)}_4\text{Zn(II)}_4\text{MT-1} + 4\text{PT/3-AP} + 2\text{GSSG} + 3\text{Zn–GS}_{(x-4)/3}{}^{-} + x\text{H}^{+} \quad (4)$$

In contrast, for Cu(II)–Dp44mT the reactivity was different from PT/3-AP. First, the overall reaction leads to the binding of Zn(II) to Dp44mT, *i.e.* transmetallation occurs as follows (reaction (5)):

$$4\text{Cu(II)–Dp44mT} + 4\text{GSH} + \text{Zn}_7\text{MT-1} \rightarrow \text{Cu(I)}_4\text{Zn(II)}_4\text{MT-1} + 3\text{Zn(II)–Dp44mT}_2 + \text{Dp44mT}_2 + 2\text{GSSG} + 4\text{H}^{+} \quad (5)$$

The higher affinity of Dp44mT for Zn(II) with respect to GSH was confirmed by a direct competition experiment (Fig. 9 and Fig. S20, ESI†).

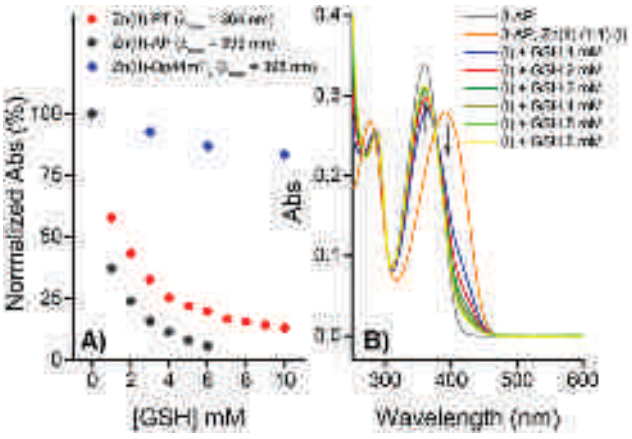

Fig. 9 Reaction of Zn(II)–TSC complexes with GSH monitored by absorbance spectroscopy. A concentrated stock solution of GSH was titrated into the preformed Zn(II)–TSC complexes ([GSH] = 1–10 mm). (A) Data are expressed as normalized absorbance (Abs) of the λ_{max} of the Zn(II)–PT, Zn(II)–3-AP, and Zn(II)–$Dp44mT_2$ complexes (at 364 nm, 395 nm, 398 nm, respectively) as a function of GSH concentration (mM). (B) UV-Vis spectra for the reaction of Zn(II)–3-AP with GSH. Experimental conditions: 30 μM TSC, 30 μM Zn(II), HEPES buffer 100 mM, and pH 7.4. 1 μL aliquots of a 100 mM stock solution of GSH were added to obtain the desired GSH concentration (from 1 to 10 mM).

Since Cu(II)–Dp44mT does not dissociate in the presence of GSH (see above), but does with the addition of Zn_7MT-1, questions arise concerning the mechanism. There are two possibilities: (i) Zn_7MT-1 plays the role of reducing agent and not GSH, even though it is present at much a lower concentration (6 μM Zn_7MT-1 against 3 mM GSH) (Fig. S12, ESI†) and (ii) GSH can reduce, likely slowly, Cu(II) in Dp44mT, but Cu(I) binds stronger to Dp44mT than to GSH or it is immediately re-oxidized before dissociation. In the presence of Zn_7MT-1, Zn_7MT-1 can pull out Cu(I) from Dp44mT since it is a stronger ligand than GSH, and/or trap Cu(I) before re-oxidation to Cu(II) occurs.

In summary, in the presence of physiological relevant GSH and Zn_7MT-1 concentrations, all three Cu(II)–TSC complexes dissociate relatively fast and Cu(I) in turn is bound to Zn_7MT-1. A difference is that only Dp44mT, not 3-AP and PT, can coordinate the Zn(II) released from Zn_7MT-1 in the presence of GSH.

This means that Cu(II)–TSC complexes can rapidly undergo changes when entering the cytosol/nucleus. Cu(II)–PT and Cu(II)–3-AP dissociate rapidly; thus, PT and 3-AP only exist as free ligands. For Cu(II)–Dp44mT, fast transmetallation with Zn(II) is possible by a metal swap with Zn_7MT-1 with the formation of Zn(II)–$Dp44mT_2$.

Reactivity of the Zn(II)–TSC complexes with GSH

As mentioned above, the three TSCs differed in their capacity to bind Zn(II) released from Zn_7MT-1 in the presence of GSH. To confirm these results and also because different Zn(II)–TSC complexes have been considered as anticancer drugs, the reactivity of the Zn(II)–TSC complexes with GHS was investigated.[27] The Zn(II) binding behaviour to the ligands under our experimental conditions was initially characterized *via* absorbance spectroscopy with titration experiments (Fig. S16–S18, ESI†). Only for Dp44mT the formation of a complex Zn(II)–$Dp44mT_2$ with a distinct 1 : 2 stoichiometry was detected (Fig. S18, ESI†).

As shown in Fig. 9A, B and Fig. S16, S17 (ESI†), the competition of GSH for Zn(II) was concentration and complex dependent. Zn(II)–$Dp44mT_2$ did not dissociate even at 10 mM GSH. In contrast, 1 mM GSH was enough to retrieve more than 50% of Zn(II) bound to 3-AP and almost half from PT. The reaction was very rapid (<1 min, the mixing time). This indicates that only Zn(II)–$Dp44mT_2$ is stable against GSH in the cytosol; whereas, Zn(II)–PT and Zn(II)–3-AP rapidly dissociate.

$$\text{Zn(II)–PT/3-AP} + 2\text{GSH} \rightarrow \text{Zn(II)–(GS}^{-})_2 + \text{PT/3-AP} + 2\text{H}^{+} \quad (6)$$

$$\text{Zn(II)–Dp44mT}_2 + 2\text{GSH} \rightarrow \text{Zn(II)–Dp44mT}_2 + 2\text{GSH} \quad (7)$$

Reactivity of the Fe(II)–TSC_2 complexes with Zn_7MT-1 and GSH

TSCs were originally developed to target the higher demand of cancer cells for iron. Hence, the activity of TSCs was initially ascribed only to Fe chelation and later on to the redox cycling of

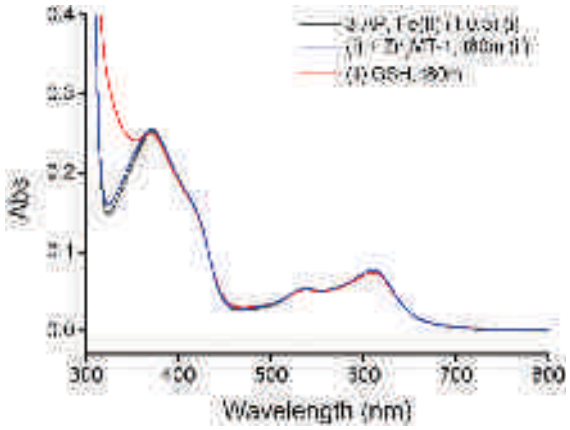

Fig. 10 Reaction of the Fe(II)–3-AP$_2$ complex with Zn$_7$MT-1 and GSH monitored by absorbance spectroscopy. To the preformed Fe(II)–3-AP$_2$ complex, Zn$_7$MT-1 was added and the reaction was monitored over time for 60 min at 4 min intervals. To the mixture Fe(II)–3-AP$_2$/Zn$_7$MT-1, GSH was added and the reaction was monitored for 80 min at 4 min intervals. Blue line: UV-Vis spectrum for the reaction between Fe(II)–3-AP$_2$ and Zn$_7$MT-1 at *t* 60 min and red line: UV-Vis spectrum for the reaction after the addition of GSH to the mixture Fe(II)3–AP$_2$/Zn$_7$MT-1. Experimental conditions: 30 μM 3-AP, 15 μM Fe(III), AscH$^-$ 5 mM (formation of the Fe(II)–3-AP$_2$ complex with a ratio 3-AP : Fe(II), 2 : 1), 100 mM HEPES buffer, and pH 7.4. Addiction of Zn$_7$MT-1 6 μM and GSH 3 mM.

the Fe-complex generated.[9] Therefore, the Fe(II)–TSC$_2$ complexes were also investigated for their reactivity with Zn$_7$MT-1 and GSH. To the preformed Fe(II)–PT$_2$, Fe(II)–3-AP$_2$, Fe(II)–Dp44mT$_2$ complexes, Zn$_7$MT-1 was added and the reaction monitored over time. Then to the Fe(II)–TSC$_2$/Zn$_7$MT-1 mixture, GSH was added (Fig. 10 for 3-AP/S21 for PT and Dp44mT).

Fe(II)–TSC$_2$ did not dissociate over time both in the presence of Zn$_7$MT-1 alone and after the addition of GSH. The absence of reactivity with Zn$_7$MT-1 is consistent with the biologically non-relevant Fe binding of the protein. The inability of GSH to dissociate Fe(II)–TSC$_2$ may be ascribed to the inability of GSH to form ternary adducts with the complex and to the lower stability of the Fe(II)–GSH complex compared to Fe(II)–TSC$_2$.

ROS production catalysed by Cu–TSC and Fe–TSC$_2$ complexes in the presence of Zn$_7$MT-1

As previously introduced, one of the proposed mechanisms for the anticancer activity of Cu(II/I)–TSCs and Fe(III/II)–TSCs$_2$ is the intracellular production of ROS. Hence, we investigated the ROS production catalysed by Cu(I)–PT and Fe(II)–PT$_2$ (as representative of the three Cu(I)/Fe(II)–TSCs) with EPR through spin-trapping investigation (Fig. 11).

This confirmed that Cu(II)–PT was able to produce HO$^\bullet$ in the presence of only GSH, concomitant with a significant loss in the Cu(II)–PT background (baseline Fig. 11A). Both features indicate the reduction of Cu(II) to Cu(I) by GSH followed by the reduction of dioxygen to ROS by Cu(I)–PT (Reactions (1) and (2)). Similarly, Fe(III)–PT was also able to produce HO$^\bullet$ (Fig. 11C).

Zn$_7$MT-1 can suppress the metal-catalysed ROS production *via* two mechanisms: (i) by ROS scavenging (destruction of the product)[69] and (ii) by metal-binding with concomitant redox-silencing of the complex (neutralisation of the catalyst), and hence complete suppression of the ROS production.[46]

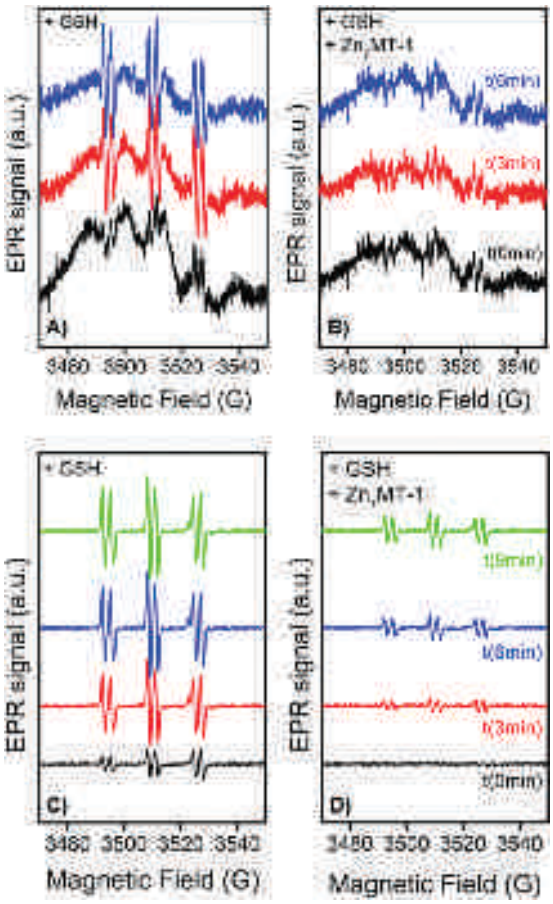

Fig. 11 EPR spin-trap experiments for the reactions of Cu–PT and Fe–PT$_2$ with GSH (A and C), and with GSH and Zn$_7$MT-1 (B and D). 4-POBN (α-[4-pyridyl-1-oxide]-*N*-*tert*-butylnitrone) was used as the primary spin-trap and DMSO (from the ligand stock solution, ~5%) as the secondary spin-trap. Both Cu–PT and Fe–PT$_2$ catalysed the formation of HO$^\bullet$ in the presence of GSH (A and C), which is fully ceased by Zn$_7$MT-1 in the case of the Cu–PT complex (B). The POBN–CH$_3$ spin adduct (g = 2.0056, AH = 2.7 G and AN = 16 G) is formed *via* the reaction of HO$^\bullet$ with DMSO in the presence of POBN. Experimental conditions (A and B): 1 mM PT (stock solution in DMSO), 900 μM Cu(II), ± 200 μM Zn$_7$MT-1 (ratio PT : Cu(II) : Zn$_7$MT-1 (1 : 0.9 : 0.2)), GSH 3 mM, HEPES buffer 50 mM, pH 7.4, and POBN 50 mM. (C and D) 1 mM PT (stock solution in DMSO), 500 μM Fe(III), ± 100 μM Zn$_7$MT-1, GSH 3 mM, TRIS buffer 50 mM, pH 7.4, and POBN 50 mM. Experiments were performed at room temperature.

The ESR spectra upon the addition of Zn$_7$MT-1 to Cu(II)–PT and Fe(III)–PT is shown in Fig. 11B and D, respectively. For Cu–PT, no signal originating from HO$^\bullet$ above the background was observed, indicating that Cu-transfer to MT-1 completely abolished the Cu(II)–TSC-mediated ROS production (mechanism ii). In contrast, Zn$_7$MT-1 was only able to partially reduce the Fe(II)–TSC$_2$-mediated ROS production (Fig. 11D). This is consistent with scavenging activity *via* mechanism (i).

Thus, Zn$_7$MT-1 is able to completely suppress the production of HO$^\bullet$ by Cu–PT by binding and redox-silencing Cu(I), but it is only able to inhibit the ROS produced by Fe–PT because it cannot withdraw Fe, but is able to scavenge HO$^\bullet$.

This indicates that Zn_7MT-1 is a more efficient ROS scavenger for Cu–TSCs compared to Fe–TSCs.

Conclusions and remarks

In the present work, we investigated the reactivity of several M^{2+}–TSC complexes with GSH and Zn_7MT-1 at concentrations found in the cytosol and nucleus. The results are summarized in Table 2 and in Fig. 12 with a schematic representation. The reactivity depends on the type of ligand and on the type of metal ion. All three Fe(II)–TSC complexes were: (i) stable, indicating that a Fe(II)–TSC complex could exist for a longer time in the cytosol and (ii) able to catalyse the production of ROS. Zn_7MT-1 could only partially suppress the ROS production catalysed by Fe–PT *via* HO$^{\bullet}$ scavenging. This supports the notion that Fe may be the most important metal complex in the biological activity of TSCs, at least with respect to the cytosol.

Table 2 Reactivity of the Cu(II)/Zn(II)/Fe(II)–TSC complexes studied in this work with GSH (i), Zn_7MT-1 (ii) and GSH in the presence of Zn_7MT-1 (iii). Cytosol/nucleus stability refers to the metal complexes existing in the cytosol after reaction with GSH and Zn_7MT-1 under physiological-like conditions

		Resistance to			
Me complex		GSH	Zn_7MT	Zn_7MT GSH	Stability with GSH&Zn_7MT (cytosol/nucleus)
PT	Cu(II)	✘	✘	✘	$Fe(II)–PT_2$
	Zn(II)	✘	—	—	
	Fe(II)	✔	✔	✔	
3-AP	Cu(II)	✘	✘	✘	$Fe(II)–3\text{-}AP_2$
	Zn(II)	✘	—	—	
	Fe(II)	✔	✔	✔	
Dp44mT	Cu(II)	✔	✘	✘	$Zn(II)–Dp44mT_2$ $Fe(II)–Dp44mT_2$
	Zn(II)	✔	—	—	
	Fe(II)	✔	✔	✔	

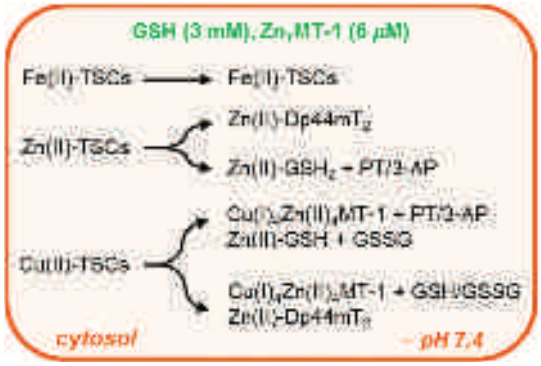

Fig. 12 Schematic representation of the reactivity of Cu(II)/Zn(II)/Fe(II)–TSC complexes in the presence of physiological relevant concentrations of GSH and Zn7MT-1 found inside the cytosol and nucleus (pH 7.4). As a consequence of this reactivity, the three TSCs studied may not be able to acquire Cu ions from the cytosol/nucleus. Acquiring Fe(II) may be possible for all three TSCs, but in the case of Zn(II), only for Dp44mT. Hence, MTs together with GSH are key players that can strongly impact the fate of Cu/Zn metal-based drugs.

In the case of Zn, Zn(II)–3-AP and –PT dissociate partially within seconds in the presence of mM GSH, although not totally from Zn(II)–PT. However, considering that other zinc sites exist in a cell, which are often unoccupied, it is well possible that Zn dissociates almost completely and rapidly from Zn(II)–PT, entering the cytosol.[70] In contrast, Zn(II)–$Dp44mT_2$ does dissociate, even at 10 mM GSH concentration. However, this dissociation is very rapid if stronger (than Dp44mT) Zn-binding sites are available in the cell, and Zn(II) can be rapidly transferred to them.

The most complex behaviour was observed for Cu(II)–TSCs. Overall, Cu(II)–3-AP and PT have very similar behaviours, where they only differ slightly by their kinetics, with 3-AP reacting faster than PT. Cu(II)–3-AP and –PT react within a few minutes with GSH and/or Zn_7MT-1. A ternary complex with a thiolate is first formed (*via* the cysteine of GSH or MT-1), then Cu(II) is reduced and dissociated from 3-AP/PT. If Zn_7MT-1 is present, Cu(I) ends up in MT-1, and if only GSH is present, Cu(I) binds to GSH. Nevertheless, this indicates that the lifetime of Cu(II)–3-AP/PT in the cytosol may be quite short (couple of minutes), which quite significantly limits the time to produce ROS in a cytosol-type environment. Thus, the question arises if it is really the complex Cu(II)–3-AP/PT that is responsible for the biological activity or the combination of Cu(II)/Cu(I) on one side and free ligand TSC on the other side. Of course, this is only valid under the conditions in the cytosol and nucleus, where high concentrations of GSH and Zn_7MT-1 are present. In other compartments, with less GSH and/or Zn_7MT-1, Cu(II)–3-AP/PT may be stable and exhibit activity.

Cu(II)–Dp44mT reacts differently. Although GSH rapidly forms a ternary complex [Dp44mT–Cu(II)–GSH], this complex is stable and no transfer of Cu(I) to GSH is observed. This can be explained by the expected lower redox potential of Cu(II)–Dp44mT compared to 3-AP and PT due to the additional electron donating groups (3 methyls and one pyridine), stabilizing Cu(II), compared to Cu(I). Reduction to Cu(I) is a prerequisite for Cu transfer to GSH.

However, Zn_7MT-1 can react rapidly with Cu(II)–Dp44mT, also *via* first (i) formation of a ternary complex [Dp444mT–Cu(II)–Zn_7MT-1], (ii) reduction of Cu(II) to Cu(I) and (iii) its transfer to MT-1. This indicates that with the GSH and Zn_7MT-1 concentrations typically found in cytosol and nucleus, Cu(II)–Dp44mT dissociates quite rapidly, and then the same question for PT/3-AP arises (see above).

The reason why Zn_7MT-1 at only 6 μM concentration but not GSH at 3 mM can extract Cu(II) from Cu(II)–Dp44mT may be related to the lower reduction potential of MT, its greater efficiency to reduce Cu(II) to Cu(I) from Cu(II)–Dp44mT, and the stronger affinity of MT-1 for Cu(I) compared to GSH.

Another remarkable point is that after the reaction of Cu(II)–Dp44mT with Zn_7MT-1, the released Zn(II) from Zn_7MT-1 can bind to Dp44mT even when GSH is present. Hence, it is possible that in the case of Cu(II)–Dp44mT transmetallation occurs when entering the cytosol or nucleus, with Cu(II)–Dp44mT being

transformed into Zn(II)–Dp44mT$_2$. Of course the stability of the Zn(II)–Dp44mT$_2$ complex also depends on other competitors, as discussed above.

The anticancer activity of some Zn(II)–TSCs and bTSCs has been attributed to the localization of the Zn(II)–TSC to the lysosome and subsequent transmetallation with Cu(II). From our data, the existence of Zn(II)–TSC in the cytosol is possible for Dp44mT, but less likely for Zn(II)–3-AP and –PT, which will more likely enter the lysosome without Zn(II). To the best of our knowledge, the GSH and MT concentrations in the lysosome are not well known. However, it is clear that the affinity of GSH and MT for Cu(I) and Zn(II) ions at lower pH $\sim$ 5, as found in lysosomes, will dramatically decrease. Also the metal affinities of TSCs decrease with a decrease in pH, but to a lesser extent because metal-binding to TSCs is possible for protonated TSCs since the protonated nitrogen is not involved directly in the Cu(II)-coordination.[9] Thus our data does not contradict the proposed mechanism of formation of Cu(II)–TCS complexes in the lysosome and its induced lysosomal membrane permeabilization and cytotoxicity.[27] It rather supports this view. Moreover, our data is consistent with the study by Kraker *et al.*, who showed the transfer of Cu(II) to MT from the Cu(II)-complex of 3-ethoxy-2-oxobutyraldehyde bis(thiosemicarbazonato) after being taken up by cells.[50]

In summary, GSH and MTs are two of the most important reducing agents found within the cytosol and nucleus. GSH is normally the most concentrated peptide-like compound in a cell, but MTs can also exist at high concentrations and have a high load of cysteines and metal-binding sites. They can be considered as important modulators and partners of metal-drugs. Indeed, the above results for the three TSCs show that the chemistry of these compounds with GSH and Zn$_7$MT-1 should be considered, in particular for Cu- and Zn(II)-drugs. Also, the fast decomposition of Cu(II) and Zn(II)-complexes in the cytosol and nucleus can occur *via* sulphur chemistry. Our results also imply that that PT, 3-AP and Dp44mT cannot chelate copper in the cytosol or nucleus. Moreover, reactions of transmetallation are also possible. For instance, for Cu(II)- and Zn(II)-metallodrugs that have DNA as a target, GSH/MT can change the drug rapidly on the way from entering the cell to the DNA in the nucleus. Thus, we think that Cu(II) and Zn(II)-metallodrugs, which have targets in the cytosol or nucleus, should be tested for their reactivity against (at least) GSH since this is an easily available compound. However better characterization also requires additional tests with the more reducing MT.

Conflicts of interest

There are no conflicts to declare.

Acknowledgements

We acknowledge the support from: IDEX program, University of Strasbourg (AS); the Frontier Research in Chemistry Foundation (Strasbourg), Installation grant (PF); the Reseau NAtional deRpe interDisciplinaire (RENARD, Fédération IR-RPE CNRS #3443) (VB); the Spanish Ministerio de Ciencia e Innovación and FEDER for the project BIO2015-67358-C2-2-P, as well as the Servei d'Anàlisi Química at the UAB for allocating instrument time (OP, member of the ''Grup de Recerca de la Generalitat de Catalunya'' ref. 2017SGR-864); National Science Center of Poland (NCN) under Opus grant no. 2016/21/B/NZ1/02847. We also thank Dr Milan Vašák (University of Zürich) for providing the mouse Zn$_7$-MT-1 protein batch.

Notes and references

1 Z. Guo and P. J. Sadler, *Angew. Chem., Int. Ed.*, 1999, **38**, 1512.
2 K. D. Mjos and C. Orvig, *Chem. Rev.*, 2014, **114**, 4540.
3 D. S. Kalinowski, C. Stefani, S. Toyokuni, T. Ganz, G. J. Anderson, N. V. Subramaniam, D. Trinder, J. K. Olynyk, A. Chua, P. J. Jansson, S. Sahni, D. J. R. Lane, A. M. Merlot, Z. Kovacevic, M. L. H. Huang, C. S. Lee and D. R. Richardson, *Biochim. Biophys. Acta, Mol. Cell Res.*, 2016, **1863**, 727.
4 T. C. Johnstone, K. Suntharalingam and S. J. Lippard, *Chem. Rev.*, 2016, **116**, 3436.
5 W. A. Wani, U. Baig, S. Shreaz, R. A. Shiekh, P. F. Iqbal, E. Jameel, A. Ahmad, S. H. Mohd-Setapar, M. Mushtaque and L. Ting Hun, *New J. Chem.*, 2016, **40**, 1063.
6 C. Santini, M. Pellei, V. Gandin, M. Porchia, F. Tisato and C. Marzano, *Chem. Rev.*, 2014, **114**, 815.
7 U. Jungwirth, C. R. Kowol, B. K. Keppler and G. Christian, *Antioxid. Redox Signaling*, 2012, **15**, 1085.
8 V. Murray, J. K. Chen and L. H. Chung, *Int. J. Mol. Sci.*, 2018, **19**, E1372.
9 P. Heffeter, V. F. S. Pape, E. A. Enyedy, B. K. Keppler, G. Szakas and C. R. Kowol, *Antioxid. Redox Signaling*, 2018, **15**, 1085.
10 K. C. Park, L. Fouani, P. J. Jansson, D. Wooi, S. Sahni, D. J. R. Lane, D. Palanimuthu, H. C. Lok, Z. Kovačević, M. L. H. Huang, D. S. Kalinowski and D. R. Richardson, *Metallomics*, 2016, **8**, 874.
11 H. Beraldo and D. Gambino, *Mini-Rev. Med. Chem.*, 2004, **4**, 31.
12 B. M. Paterson and P. S. Donnelly, *Chem. Soc. Rev.*, 2011, **40**, 3005.
13 K. Y. Djoko, B. M. Paterson, P. S. Donnelly and A. G. McEwan, *Metallomics*, 2014, **6**, 854.
14 P. J. Crouch, L. W. Hung, P. A. Adlard, M. Cortes, V. Lal, G. Filiz, K. A. Perez, M. Nurjono, A. Caragounis, T. Du, K. Laughton, I. Volitakis, A. I. Bush, Q.-X. Li, C. L. Masters, R. Cappai, R. A. Cherny, P. S. Donnelly, A. R. White and K. J. Barnham, *Proc. Natl. Acad. Sci. U. S. A.*, 2009, **106**, 381.
15 C. R. Kowol, W. Miklos, S. Pfaff, S. Hager, S. Kallus, K. Pelivan, M. Kubanik, É. A. Enyedy, W. Berger, P. Heffeter and B. K. Keppler, *J. Med. Chem.*, 2016, **59**, 6739.
16 K. Ishiguro, Z. P. Lin, P. G. Penketh, K. Shyam, R. Zhu, R. P. Baumann, Y. L. Zhu, A. C. Sartorelli, T. J. Rutherford and E. S. Ratner, *Biochem. Pharmacol.*, 2014, **91**, 312.

17 J. Shao, *Mol. Cancer Ther.*, 2006, **5**, 586.
18 R. A. Finch, M. C. Liu, A. H. Cory, J. G. Cory and A. C. Sartorelli, *Adv. Enzyme Regul.*, 1999, **39**, 3.
19 C. R. Kowol, P. Heffeter, W. Miklos, L. Gille, R. Trondl, L. Cappellacci, W. Berger and B. K. Keppler, *J. Biol. Inorg. Chem.*, 2012, **17**, 409.
20 Y. Yu, Y. S. Rahmanto, C. L. Hawkins and D. R. Richardson, *Mol. Pharmacol.*, 2011, **79**, 921.
21 Y. Aye, M. J. C. Long and J. Stubbe, *J. Biol. Chem.*, 2012, **287**, 35768.
22 Y. Yu and D. R. Richardson, *J. Biol. Chem.*, 2011, **286**, 15413.
23 É. A. Enyedy, N. V. Nagy, É. Zsigó, C. R. Kowol, V. B. Arion, B. K. Keppler and T. Kiss, *Eur. J. Inorg. Chem.*, 2010, 1717.
24 E. M. Gutierrez, N. A. Seebacher, L. Arzuman, Z. Kovacevic, D. J. R. Lane, V. Richardson, A. M. Merlot, H. Lok, D. S. Kalinowski, S. Sahni, P. J. Jansson and D. R. Richardson, *Biochim. Biophys. Acta, Mol. Cell Res.*, 2016, **1863**, 1665.
25 D. Denoyer, S. A. S. Clatworthy and M. A. Cater, *Met. Ions Life Sci.*, 2018, **18**, 469.
26 X. Yu, A. Blanden, A. T. Tsang, S. Zaman, Y. Liu, J. Gilleran, A. F. Bencivenga, S. D. Kimball, S. N. Loh and D. R. Carpizo, *Mol. Pharmacol.*, 2017, **91**, 567.
27 A. E. Stacy, D. Palanimuthu, P. V. Bernhardt, D. S. Kalinowski, P. J. Jansson and D. R. Richardson, *J. Med. Chem.*, 2016, **59**, 4965.
28 P. J. Jansson, T. Yamagishi, A. Arvind, N. Seebacher, E. Gutierrez, A. Stacy, S. Maleki, D. Sharp, S. Sahni and D. R. Richardson, *J. Biol. Chem.*, 2015, **290**, 9588.
29 A. Krezel and W. Bal, *Acta Biochim. Pol.*, 1999, **46**, 567.
30 M. T. Morgan, L. A. H. Nguyen, H. L. Hancock and C. J. Fahrni, *J. Biol. Chem.*, 2017, **292**, 21558.
31 A. Krezel and W. Bal, *Bioinorg. Chem. Appl.*, 2004, **2**, 293.
32 R. C. Hider and X. L. Kong, *Biometals*, 2011, **24**, 1179.
33 J. Forshammar, L. Block, C. Lundborg, B. Biber and E. Hansson, *J. Biol. Chem.*, 2011, **286**, 649.
34 D. Ralph, *Prog. Neurobiol.*, 2000, **62**, 649.
35 M. Deponte, *Antioxid. Redox Signaling*, 2017, **27**, 1130.
36 A. Bhattacharjee, K. Chakraborty and A. Shukla, *Metallomics*, 2017, **9**, 1376.
37 A. Krezel, J. Wójcik, M. Maciejczyk and W. Bal, *Chem. Commun.*, 2003, 704.
38 E. B. Maryon, S. A. Molloy and J. H. Kaplan, *Am. J. Physiol.: Cell Physiol.*, 2013, **304**, C768.
39 J. H. Kaplan and E. B. Maryon, *Biophys. J.*, 2016, **110**, 7.
40 A. Santoro, N. Wezynfeld, M. Vašák, W. Bal and P. Faller, *Chem. Commun.*, 2017, **53**, 11634.
41 E. B. Maryon, S. A. Molloy and J. H. Kaplan, *Am. J. Physiol.: Cell Physiol.*, 2013, **304**, C768.
42 E. S. Woo, A. Monks, S. C. Watkins, A. S. Wang and J. S. Lazo, *Cancer Chemother. Pharmacol.*, 1997, **41**, 61.
43 W. Maret and B. L. Vallee, *Proc. Natl. Acad. Sci. U. S. A.*, 1998, **95**, 3478.
44 E. Atrián-Blasco, A. Santoro, D. L. Pountney, G. Meloni, C. Hureau and P. Faller, *Chem. Soc. Rev.*, 2017, **46**, 7683.
45 L. Banci, I. Bertini, S. Ciofi-Baffoni, T. Kozyreva, K. Zovo and P. Palumaa, *Nature*, 2010, **465**, 645.
46 G. Meloni, P. Faller and M. Vašák, *J. Biol. Inorg. Chem.*, 2011, **16**, 1067.
47 L. J. Jiang, W. Maret and B. L. Vallee, *Proc. Natl. Acad. Sci. U. S. A.*, 1998, **95**, 3483.
48 G. Meloni, V. Sonois, T. Delaine, L. Guilloreau, A. Gillet, J. Teissié, P. Faller and M. Vašák, *Nat. Chem. Biol.*, 2008, **4**, 366.
49 A. Krężel and W. Maret, *Int. J. Mol. Sci.*, 2017, **18**, 1.
50 A. Kraker, S. Krezoski, J. Schneider, D. Minkel and H. Petering, *J. Biol. Chem.*, 1985, **260**, 137.
51 D. H. Petering, *Bioinorg. Chem.*, 1972, **1**, 273.
52 D. H. Petering, *Bioinorg. Chem.*, 1972, **1**, 255.
53 J. García-Tojal, R. Gil-García, V. I. Fouz, G. Madariaga, L. Lezama, M. S. Galletero, J. Borrás, F. I. Nollmann, C. García-Girón, R. Alcaraz, M. Cavia-Saiz, P. Muñiz, Ò. Palacios, K. G. Samper and T. Rojo, *J. Inorg. Biochem.*, 2018, **180**, 69.
54 Z. Xiao, P. S. Donnelly, M. Zimmermann and A. G. Wedd, *Inorg. Chem.*, 2008, **47**, 4338.
55 J. García-Tojal, A. García-Orad, A. A. Díaz, J. L. Serra, M. K. Urtiaga, M. I. Arriortua and T. Rojo, *J. Inorg. Biochem.*, 2001, **84**, 271.
56 R. W. Byrnes, M. Mohan, W. E. Antholine, R. X. Xu and D. H. Petering, *Biochemistry*, 1990, **29**, 7046.
57 C. M. Nutting, C. M. L. van Herpen, A. B. Miah, S. A. Bhide, J.-P. Machiels, J. Buter, C. Kelly, D. de Raucourt and K. J. Harrington, *Ann. Oncol.*, 2009, **20**, 1275.
58 A. Gaál, G. Orgován, Z. Polgári, A. Réti, V. G. Mihucz, S. Bosze, N. Szoboszlai and C. Streli, *J. Inorg. Biochem.*, 2014, **130**, 52.
59 É. Enyedy, M. F. Primik, C. R. Kowol, V. B. Arion, T. Kiss and B. K. Keppler, *Dalton Trans.*, 2011, **40**, 5895.
60 D. Mahendiran, N. Pravin, N. S. P. Bhuvanesh, R. S. Kumar, V. Viswanathan, D. Velmurugan and A. K. Rahiman, *ChemistrySelect*, 2018, **3**, 7100.
61 W. E. Antholine and F. Taketa, *J. Inorg. Biochem.*, 1984, **20**, 69.
62 P. J. Jansson, P. C. Sharpe, P. V. Bernhardt and D. R. Richardson, *J. Med. Chem.*, 2010, **53**, 5759.
63 D. P. J. Narasimhan, W. Antholine and C. R. Chitambar, , 1991, **289**, 393.
64 W. E. Antholine, B. Kalyanaraman and D. H. Petering, *Environ. Health Perspect.*, 1985, **64**, 19.
65 J. Peisach and W. E. Blumberg, *Arch. Biochem. Biophys.*, 1974, **165**, 691.
66 G. Meloni, P. Faller and M. Vašák, *J. Biol. Chem.*, 2007, **282**, 16068.
67 R. S. Chung, C. Howells, E. D. Eaton, L. Shabala, K. Zovo, P. Palumaa, R. Sillard, A. Woodhouse, W. R. Bennett, S. Ray, J. C. Vickers and A. K. West, *PLoS One*, 2010, **5**, e12030.
68 J. S. Calvo, V. M. Lopez and G. Meloni, *Metallomics*, 2018, **10**, 1777.
69 M. Sato and I. Bremner, *Free Radical Biol. Med.*, 1993, **14**, 325.
70 W. Maret, *Metallomics*, 2015, **7**, 202.

Gilles RIEGEL

Rôle de la voie du stress du réticulum et de la biosynthèse du glutathion dans l'activité anticancéreuse de composés organométalliques à base de ruthénium dans le cancer gastrique.

Résumé

Résumé

Le traitement du cancer repose sur une résection chirurgical associée à une chimiothérapie péri-opératoire à base de platine. Ces drogues provoquent des effets secondaires et sont sensibles à des mécanismes de résistances, soulignant la nécessité de développer de nouvelles thérapies parmi lesquelles les dérivés de ruthénium démontrent des propriétés prometteuses.

Ce travail démontre le rôle du métabolisme, notamment des voies de transsulfuration et de la biosynthèse de glutathion dans l'activité du RDC11 (ruthenium derived compounds). Ces dérégulations métaboliques sont médiées par l'effet du RDC11 sur la voie du stress du réticulum. En outre, j'ai caractérisé le rôle de l'atome métallique dans la sensibilité des cellules cancéreuses face à ces composés. Le remplacement d'un atome de ruthénium par un atome d'osmium réduit significativement l'efflux de ces composés, augmentant leur concentration intracellulaire et leur efficacité.

Ces travaux caractérisent le rôle du métabolisme pour l'activité des dérivés organométalliques, ouvrant de nouvelles perspectives pour l'étude de leur mode d'action, visant à favoriser l'entrée de ceux-ci en essai clinique.

Mots clés : Stress du réticulum, transsulfuration, biosynthèse du glutathion, composés organométalliques, efflux, métabolisme.

Résumé en anglais

Summary

Cancer treatment is still based on surgery associated with platinum-based chemotherapy. These drugs induce side effects and are sensitive to resistance mechanisms. This shows the need to develop new anticancer therapies among which ruthenium compounds display promising properties.

This study demonstrates the implication of metabolism, namely, the transsulfuration pathway and glutathione biosynthesis in the activity of the RDC11 (ruthenium derived compounds). These metabolic regulations are mediated by the effect of RDC11 on the ER stress pathway. Furthermore, I characterized the role of the metallic atoms in the sensitivity of cancer cells towards these drugs. More precisely, replacement of ruthenium by osmium reduces strongly the efflux of these drugs, increasing their intracellular concentration and efficiency.

This work characterises the role of cellular metabolism for the anticancer activity of organometallic compounds, opening the way for the investigation of these compounds mode of action looking forward entry in clinical trials.

Key words: Reticulum stress, transsulfuration, glutathione biosynthesis, organometallic compounds, efflux, metabolism